e-ISSN : 2320-0847
p-ISSN : 2320-0936

American Journal of Engineering Research (AJER)

Volume 3 Issue 12– December 2014

www.ajer.org ajer.research@gmail.com

Editorial Board

American Journal of Engineering Research (AJER)

CONTENTS

Volume-3 Issue-12

American Journal of Engineering Research (AJER)
e-ISSN: 2320-0847 p-ISSN: 2320-0936
Volume-03, Issue-12, pp-01-06
www.ajer.org

Research Paper

Analysis the opportunities and threats of Mehr Housing in Mashhad Metropolis (A case of Golbahar New Town)

Hadi Ivani*[1], Mohammad Rostami[2]
[1*] *Faculty of Art and Architecture, Payame Noor University, Iran (Corresponding author)*
[2] *MSc student of Geography & urban Planning, Payam Noor University, Iran*

ABSTRACT: *In recent years, the construction industry has been thriving due to an increase in national and international investment to the extent that it is now the largest in the Middle East region. In order to, the aim of current research is analysis the opportunities and threats of Mehr Housing in Mashhad Metropolis with point on Golbahar New Town housing project. Applied methodology is based on libraries, documents and field study. In the case of library, data were collected by studying books, articles and internet. In continuous it was used of interview and questionnaire for complete the data's. Results show that 70 percent of the Iranians own homes, with huge amounts of idle money entering the housing market and the annual turnover in the construction industry amounts to 38.4 billion US$.*

KEY WORDS: *Golbahar New Town, Mehr Housing, Mashhad Metropolis, Housing industry*

I. INTRODUCTION

The construction industry of Iran is divided into two main sections. The first is government infrastructure projects, which are central for the cement industry. The second is the housing industry (Ayse, 2013). In recent years, the construction industry has been thriving due to an increase in national and international investment to the extent that it is now the largest in the Middle East region. The Central Bank of Iran indicates that 70 percent of the Iranians own homes, with huge amounts of idle money entering the housing market. The annual turnover in the construction industry amounts to 38.4 billion US$ (Merip, 2013). The real estate sector contributed to 5% of GDP in 2008. Statistics from March 2004 to March 2005 put the number of total Iranian households at 15.1 million and the total number of dwelling units at 13.5 million, signifying a demand for at least 5.1 million dwelling units. Every year there is a need for 750,000 additional units as young couples embark on married life (Xang, 2013). At present, 2000 units are being built every day although this needs to increase to 2740 units (Wikipedia.org, 2014). Different countries for resolving the housing problem have carried out some different techniques, some have tried to rehabilitate slums around the cities, some of them gave mortgage to eligible, and some gave land with cooperation of municipalities to eligible, some taking tax on uninhabited houses, giving facilities to mass manufacturers etc. We have high inflation and high cost of housing in Iran. Demanding more than supply housing has negative effect on inflation. Demanding housing is divided in two parts in Iran: a) Real demand of housing based on household needs. b) Investment demand to maintain equity. Needing more supply to improve situation. Mass housing project is the best way for more supply. Nowadays housing problem has been one of the greatest of people's concern. The ninth and tenth government has been giving mortgage, land and mass housing to eligible to decrease or eliminate housing problem in Iran. No ownership of housing or ownership records of housing or residential lands that hasn't used governmental sources for housing and is in charge a house, are eligible for taking facilities. The government decided to implement the mass housing project called Mehr housing in all cities. Thus after passing the Mehr housing project in cabinet in 2007 and passing the official process, the government started to build housing cooperative in cities and enrolling eligible individuals who lived in desired city for 5 years (Banaei & Parvizian, 2013). Acute problems of urbanization led to new theoretical perspectives and solutions that have been reflected in national development policies. Building new towns has been proposed as one of the basic policies toward population growth and inflation in large cities. In different periods of history, new towns have been built around the world (Frank, 1972). Building new towns in Iran goes back to past times; one can count many cities that were founded in a specified period (Piran, 1989). In Iran, during the last three decades, the rapid growth of urban population has not been in proportion to the capacities of urban space facilities, and due infrastructure and

required profession were not also provided. Since, spatial distribution of cities and population has not been based on a comprehensive plan which is in congruent with regional and provincial sectors, the issues resulted from the rapid urban population growth have become multifarious and convoluted (Anabestani & et al, 2013). In this betwwen Golbahar New Town has specific situation in Mehr housing project.

II. BACKGROUND

For a decade after the revolution, the land question, especially in cities, was among the most contested issues in the Islamic Republic. The collapse of state authority, coupled with the populist convictions of the new regime and spontaneous popular land occupations labeled as "revolutionary housing," led to the dramatic expansion of cities. Tehran doubled in size within two years, and Ahvaz tripled in area from 9 to 29 square miles (75 km^2). But only a small fraction of this geographic expansion was confiscated private land. The rest, more than 90 percent of the total distributed, had been public land. From 1979 to 1993 nearly half a million hectares of predominantly public unoccupied land was converted into private and cooperative residential property. New state institutions like the Urban Land Organization and the Housing Foundation played the key role in this massive transfer of property. By the mid-1980s more than 60 percent of all urban residential land transactions were being allocated by the state (Middle East Research and Information Project, 2012). This large-scale transfer of mostly public land, coupled with the absence of enforceable regulation, transformed Iran's urban geography. Between 1979 and 1982, 75 percent of all new construction in Tehran occurred outside the formal city limits, where satellite villages were transformed into sprawling suburbs. Remarkably, by 1986 urban housing stock had doubled, as Housing Ministry surveys showed that more than half of all urban dwellings in the entire country had been built after the revolution. It was private individuals who built these 2.3 million new units. The state merely transferred the public land into private hands; its share of investment in housing construction (affordable or otherwise) was less than 2 percent of the total after the revolution. Following an extraordinary boom in the Iranian real estate market between 2004 and 2007, activity in this market suddenly slowed down from early 2008. In 2009, construction activity was at its lowest level for the past eight years. Since 2010, this sector has experienced a modest recovery (Wikipedia.org, 2014; Athari, 1993).

Study of housing issue contain, economic decisions such as mortgage amount, taxes etc. government decisions such as services, issue priority etc. applicants interests such as the design of units, size of units etc. for addressing that issue they should be examined simultaneously. There is the interaction of various factors of social, economic and political in housing issue so we are faced with a complex system. We need to know the policies feedback to understand the efficiency of policies and applicant satisfaction of Mehr housing and also proposed alternative policies. On one hand system dynamics has ability of solving complex problems of nonlinear and feedback loops. In the system dynamics approach, first, we have a description of the problem then identifying the level and the rate of problem, on the next steps simulation and alternative policies will be discussed (Jarzynka, 2005). Considering the difficulties and problems that mainly rise in continuous development of metropolitan cities that are due to high and increasing demands for housing, providing the land needed for development inside the cities has practically been a thorny problem and charges high costs. New towns as the detached extensions have largely tackled the problem, and have been able to provide appropriate conditions for mass housing, and with mass production of land and urban services, they have managed to relatively control land price, and naturally reduce the land price in metropolitan cities as demand goes up. Despite the relative success in controlling the growth and development of metropolitan cities, new towns failed to realize their goals, their major shortcoming was their inability to absorb population (Gholamiyan, 2010). Kazemi-Sefat (2011) in evaluating the success of Hashtgerd new town in absorbing the overflow population of Tehran Metropolis believes that there is a big difference between the predicted population absorption and the number of residential units between 1996 and 2006 in Hashtgerd Comprehensive urban Plan and the status quo. Ebrahim et al. (2005) in an analysis of the necessity of building the new town of Golbahar and its role in decentralization of Mashhad Metropolis concluded that this town has failed to decentralize Mashhad Metropolis, to the extent that in terms of population, employment, housing and other predictions from 1996, even up to 2001, none of the above objectives were achieved. For example, until 2001 only about 10% (2397 people) of the predicted population for 1996 (24,000 people) have been achieved. Harirchi et al. (2009) in their study of citizens' quality of life in Pardis believed that increase in social capital improves the quality of life, and there is a significant correlation between satisfaction with neighborhood and quality of life, but there was not any significant correlation between the quality of life and the marital status and age groups (Anabestani & et al, 2013). Howard believed that the theory of "garden city" is a way for dealing with population growth in large cities, organization and spatial distribution of population and industry. He claimed that the goals of building garden cities are to create a functional structure, optimize population size and area, employment and self-reliance, development of green belts, optimum density and public ownership of land. He implemented two plans of garden cities (1928) before his death (Hall, 1992). As a result of revolutionary dreams of utopianisms and

reformist ideas of Howard and their compliance with national planning policies in the UK and other countries, the notion of new town was accepted as a liberal opportunity for reform and providing a better way for urban life. However, urbanization expansion resulting from immigration from villages to cities and adjunction of surrounded villages to metropolitans in developed and developing countries has shaken the bottom of housing quality and quantity and it has changed the issue of housing into a great problem. Housing shortage, housing inacceptable quality, old textures, settlement in urban outskirts, inappropriate accesses of housings to urban services and etc are included among urbanization consequences and Iran is not an exception. Therefore, in metropolitans like Mashhad, as a second population pole of the country and commercial, historical and cultural center in national and international scale, which has always encountered with population growth rate, settlement conditions and living condition in urban neighborhoods have been inconsistent regarding urban sustainable development criteria (Zanganeh & et al., 2013).

III. CASE STUDY REGION

Mashhad City is considered as Iran's second metropolitan and World's second religious metropolitan and largest population center of Eastern Iran. The city is provincial capital of Khorasan Razawi and its population is 2766258 (Iran Statistics Center, 2011). The city is located at 36.20º North latitude and 59.35º East longitude, in the valley of the Kashaf River. The city has 13 urban districts, totally 29000 hectares. Urban population density is approximately 119.4 people per square meter. As one of the old and historical regions on the Great Khorasan Province and Old Toos, Mashhad has been developed thanks to the Shrine of Imam Reza (P.B.U.H), Eighth Shiite Imam. Metropolitan Mashhad has historical-political, economic-administrative and cultural-intellectual centrality and religious function as well as border, beyond-country situation. It accepts 10-15 million pilgrims and tourists annually in such a way that it bears the title of the second religious city of Islam world and the second national metropolitan in terms of population (Mafi & Saghayi, 2008; Zanganeh & et al., 2013). Golbahar new town with latitude of 37, 36 and longitude of 59, 14 and the average height of 1250 m above sea level, is located in the plain between the mountains of Hezar Masjid and Binalood, 45 km northwest of Mashhad at Mashhad-Quchan road. Golbahar urban area is 4,000 hectares and its design follows a linear checked organization. The planned area includes two urban zones and four regions. The first zone includes some parts of the downtown, construction of eleven neighborhoods and two region centers were anticipated, and the central core of Golbahar new town was formed in this zone, and the resettlement program have been made for one project is being carried out in 1,000 acres of land in the town. According to the conducted researches, the physical progress of the project

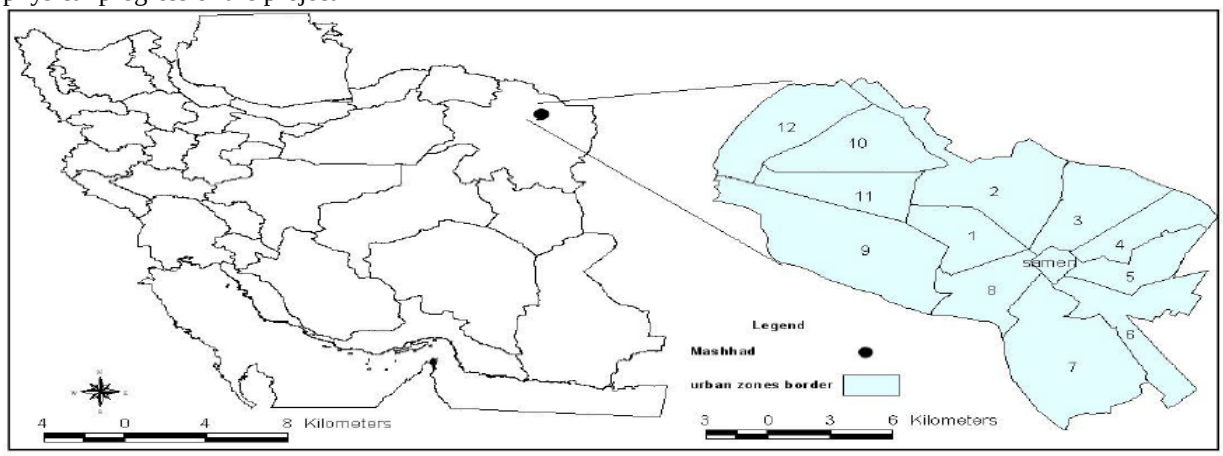

Fig. 1. Case study region map.

in 2011 were about 45%, for example in neighborhood 1 to 6, center of the first region, construction area included Golbahar recreational complex, and parts of neighborhood 7 and 22 (area for light industries) (Anabestani & et al, 2013).

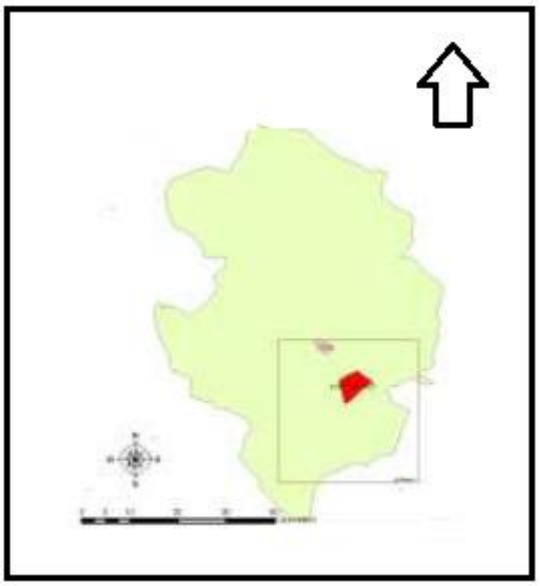

Fig. 2. A view of Golbahar new town.

IV. MATERIAL & METHODS

In present study the data were collected from libraries, documents and field study. In the case of library, data were collected by studying books, articles and internet. Then, field study was done and including observation, discussion and filling questionnaire and data were analyzed by using a qualitative range. Finally, it is presented some solve ways.

V. FINDINGS & RESULTS

Housing is one of the most important sections of development in a country and its economic importance has put it in the center of attention. It can cause rise and depression of habitation by its extended economic aspects. Mehr Housing plan is a state run housing project in most cities started 2007 in Iran to protect and provide cheap housing for poor people and young couples. Mehr housing project by its large scale and wide dimensions can affect the society's economy (Karshenasana & Beiranvand, 2013). Therefore, to investigate weaknesses and strengths of this project in terms of economic and applying necessary reformation can increase the success probability of this project. For this purpose, this study assesses the weaknesses and strengths of Mehr housing of province of Golbahar New Town in Iran. The trend of house production during current decade shows that about 600 to 800 thousands constructional permissions have been issued, annually. Therefore, 550 thousands constructional permission as Mehr housing during recent months, and increase of construction section rather than agricultural and oil groups in economic development, indicate the extension of this project. It also suggests that the trend of its implementation will lead to increase of GDP; economic prosperity in other related sectors associated with housing and will prevent from economic declination during future years (Soomelou, 2010). In Golbahar new town, a population of over 13/4 thousand people live in 3940 households, using Cochran sampling formula, a sample size of 143 households were selected from the residential units, and urban households questionnaires were filled out and the required data were obtained. Having collected and processed the data by SPSS, Data were analyzed and the subject was investigated.

Table (1): Housing Statistics in Mashhad city

Mehregan town, self-owners	Binalod New Town	Golbahar New Town
21761	3713	39785

Overall, social conditions of life in the new town from citizens' perspective with the standard deviation of 0.65 were 3.016. Among the three indices of the mentioned variable, citizens' willingness to reside in the town with a mean of 1.3 and standard deviation of 0.79 had the highest ranking, and access to social security for citizens, with a mean of 2.96 and standard deviation of 1.1 had the lowest rank.

5.1. Applicant satisfaction

Several factors are involved in the applicant satisfaction, but we can consider some important factors which are the most weight or are of the highest priorities, such as the trend of project financing and power of

host of project, supply and demand market condition, project design and the size of project are main factors that each of them have a separate weight between [0, 1] and they have been considered for the sum of 1. Mehr housing applicants are considered as low-income deciles in society along with income close to work insurance rights. According to central bank of Iran, every household can almost spend 1 out of 3 of his income on housing issues. Project financing is expressed by purchasing power. If the total monthly repayment in section 2.2 of residential units like monthly charge per unit and land rent mentioned in section 2.1.1.6, were equal or low than cost in housing section for applicant, the related weight would be given them. As it is mentioned in section 1 in accordance with high inflation and high cost of housing in Iran, increase into housing demand instead of housing supply have negative effect on inflation. Thus, if housing supply and demand were equal or supply was more than demand, the weight of supply and demand market condition would be submitted. Project design is total of national regulations symbol of build (Industrialization) of Iran, apartment living culture, design and project specifications. As it is mentioned in section 1, due to low rise of building and lack of individual custom of living in apartments, apartment living culture isn't conventional and it is not a part of the individual culture. In addition, in section of designing and apartment specifications, useful space of residential units were reduced which is why, they want allocate the space to design hallways and elevator, in spite of lack of modern facilities such as shooting , etc. in view of the average of 3 factors considered for project design, we can give their weight. Generally, in small town, the area of houses is large and compatible with their life style. Although living in apartment with the area of 75 meters in large cities is typical, this isn't considered desirable in small towns. Due to the area of houses, their weight can be given (Banaei & Parvizian, 2013).

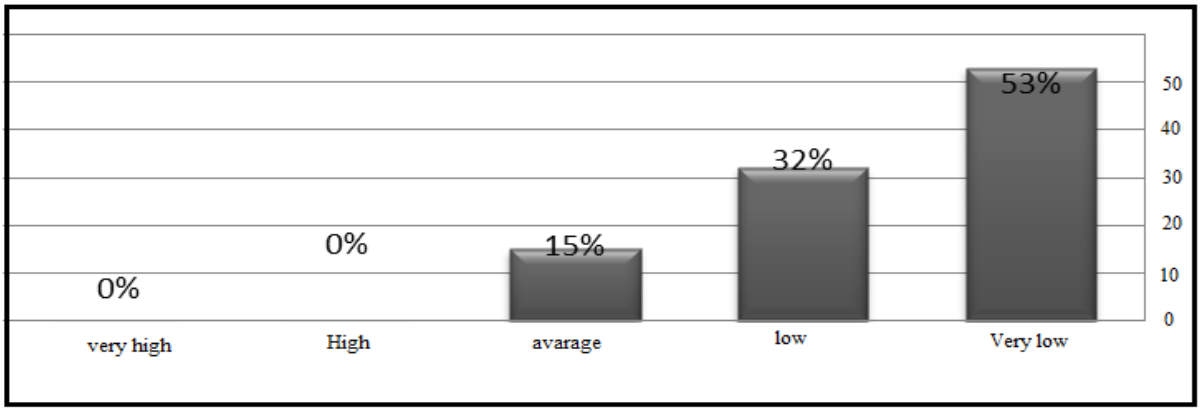

Fig. 3. properly implemented rate of Mehr housing project in Golbahar new town.

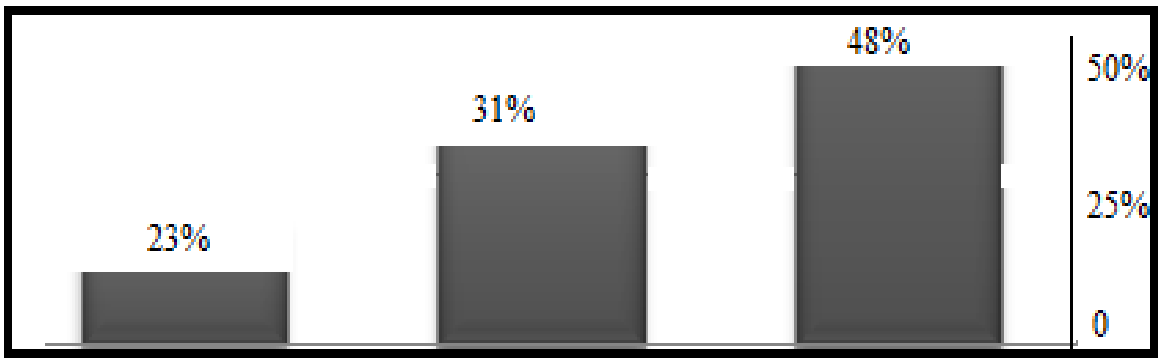

Fig. 4. properly implemented rate of Mehr housing project in Golbahar new town.

There are some advantages associated with the implementation of this project such as utilization of scale economy and low cost homes for needy and young couples faced weakness in urbanization and technical principles. In addition, quality of houses, national production and economic growth, family density, index of access to house, employment, investment, saving energy, landfill consumption pattern of reformation, use of urban rusty texture, paid facilities, role of targeting subsidies, satisfaction of applicants from payment way of facilities, and effect of low income people for providing financial resources are among other issues discussed in this paper. Therefore, by testing the main hypothesis of research, findings have indicated that Mehr housing had not achieved its economic goals. The individuals' opinion about access of Mehr housing to economic goals was estimated 3, which was medium (Karshenasana & Beiranvand, 2013).

VI. CONCLUSION

In Iran, during the last three decades, the rapid growth of urban population has not been in proportion to the capacities of urban space facilities, and due infrastructure and required profession were not also provided. Since, spatial distribution of cities and population has not been based on a comprehensive plan which is in congruent with regional and provincial sectors, the issues resulted from the rapid urban population growth have become multifarious and convoluted. In this between Golbahar New Town has specific situation in Mehr housing project. Overall, social conditions of life in the new town from citizens' perspective with the standard deviation of 0.65 were 3.016. Among the three indices of the mentioned variable, citizens' willingness to reside in the town with a mean of 1.3 and standard deviation of 0.79 had the highest ranking, and access to social security for citizens, with a mean of 2.96 and standard deviation of 1.1 had the lowest rank.

REFERENCES

[1]. **Anabestani, A. Anandestani, Z. Heydari, A.** (2013). Analysis the Satisfaction of the residents of Golbahar new town with the living conditions and its effects on Mashhad metropolis. International Journal of Management Sciences and Business Research, 2013 ISSN (2226-8235) Vol-2, Issue 11.

[2]. **Athari. K.,** (1999), development strategies, planning strategies and new towns, the new urban culture, new towns proceedings, Development Company of New Towns. (In Persian)

[3]. **Ayes, J.** (2013). "System Dynamic Approach for Analyzing Cyclic Mechanism in Land Market and Their Effect on House Market Fluctuations", Proceedings of the 29th International Conference of the System Dynamics Society.

[4]. **Banaei, M. Parizian, J.** (2013). Housing projects for the poor a plan with no aim.

[5]. **Gholamiyan. T.,** (2010), the role of New Towns in the metropolises overflows Iranian population, geography and urban planning master's thesis, University of Mazandaran. (In Persian)

[6]. **Hall, P.** (1992), Urban and regional Planning, Rutledge, London, pp21-24.

[7]. **Jarzynka, K., "U.S.** (2005) Low Income Housing Policy A Dynamic System Evaluation", Proceedings of the 23rd International Conference of the System Dynamics Society, July 17- 21, Boston.

[8]. **Karshenasana, A. Beiranvand, M.** (2013). A review on weaknesses and strengths of delivering Mehr housing project in terms of achieving economical goals. Management Science Letters 2521–2530.

[9]. **Mafi, E. Saghai, M.** (2008). Hashtgerd New Town huge overflow crowd in Tehran, Journal of Transportation and Development, No. 47, pp. 71-65.

[10]. **Merip, H.** (2013). Transformation problems of New Towns, New Towns in Iran and the Proceedings of the experience, the first book, Development Company of New Towns. (In Persian).

[11]. **Middle East Research and information project.** (2013).

[12]. **Statistical Center of Iran**, (2011).

[13]. **Wikipedia,** 2013.

[14]. **Xang, U.** (2013). "Evaluation And Ranking The factors on The Time, Cost, And Quality Mass Housing Projects in Iran With AHP", Proceedings of the 5th International Conference of Project Management, Tehran.

[15]. **Zanganeh et al,** (2006): The planning towns in Iran, AJSCSs, Vol. 23, No. 6, p. 412–422.

American Journal of Engineering Research (AJER)
e-ISSN : 2320-0847 p-ISSN : 2320-0936
Volume-03, Issue-12, pp-07-14
www.ajer.org

Research Paper Open Access

Study on MHD Free Convection Heat and Mass Transfer Flow past a Vertical Plate in the Presence of Hall Current

[1]M. S. Hossain, [2]S. K. Paul, [3]S. F. Ahmmed and [4]T. Sultana
[1,2,3]*Mathematics Discipline, Khulna University, Khulna-9208, Bangladesh.*
[4]*Dept. of Mathematics, Govt. Sundarban Adarsha College, Khulna, Bangladesh.*

ABSTRACT: *A two-dimensional MHD free convection heat and mass transfer flow of viscous, incompressible and electrically conducting fluid past a vertical flat plate embedded in porous medium in the presence of hall current under the influence of uniform magnetic field applied normal to the flow is studied analytically. In this research work, we make the governing equations dimensionless by usual non-dimensional variables and we obtained a set of ordinary differential equations. Then these obtained ordinary differential equations are solved analytically by using perturbation technique. The expressions for velocity field, temperature distribution, concentration field, skin friction, the rate of heat transfer and the rate of mass transfer are derived. Finally the results are discussed in detailed with the help of graphs and tables to observe the effect of different parameters like Magnetic parameter (M), radiation parameter (F), Grashof number (Gr), modified Grashof number (Gm), Prandtl number (Pr), permeability parameter (k), Eckert number (Ec) and the chemical reaction parameter (Kc).*

KEY WORDS: *Hall current, Chemical reaction, MHD, Radiation, Porous medium.*

I. INTRODUCTION

Magneto-hydrodynamics (MHD) is the science which deals with the motion of a highly conduction fluid in the presence of magnetic field. It is the branch of continuum mechanics which deals with the flow of electrically conducting fluids in electric and magnetic fields. Many natural phenomena and engineering problems are worth being subjected to an MHD analysis. Furthermore, Magneto-hydrodynamic (MHD) has attracted the attention of a large number of scholars due to its diverse applications. In engineering it finds its application in MHD pumps, MHD bearings etc. Workers likes Hossain and Mandal [1] have investigated the effects of magnetic field on natural convection flow past a vertical surface. Free convection flows are of great interest in a number of industrial applications such as fiber and granular insulation, geothermal systems etc. As a branch of plasma physics the field of Magneto-hydrodynamics consists of the study of a continuous, electrically conducting fluid under the influence of electromagnetic fields. Originally, MHD included only the study of strictly incompressible fluid but today the terminology is applied to studies of partially ionized gases as well. Soundalgekar and Takhar [2] first, studied the effect of radiation on the natural convection flow of a gas past a semi-infinite plate using the Cogly-Vincentine-Gilles equilibrium model. For the same gas Takhar *et al.* [3] investigated the effects of radiation on the MHD free convection flow past a semi-infinite vertical plate. Later Hossain *et al.* [4] studied the effect of radiation on free convection from a porous vertical plate. Poonia and Chaudhary [5] studied about the flows through porous media. Recently researchers like Alam and Rahman [6], Sharma and Singh [7] Chaudhary and Arpita [8] studied about MHD free convection heat and mass transfer in a vertical plate or sometimes oscillating plate. Muthucumaraswamy and Janakiraman [9] studied MHD and radiation effects on moving isothermal vertical plate with variable mass diffusion.

Therefore several authors, viz. Raptis and Soundalgekar [10], Agrawal *et al.* [11], Jha and Singh [12], Jha and Prasad [13] have paid attention to the study of MHD free convection and mass transfer flows. Abdusattar [14] and Soundalgekar *et al.* [15] also analyzed about MHD free convection through an infinite vertical plate. Acharya *et al.* [16] have presented an analysis to study MHD effects on free convection and mass transfer flow through a porous medium with constant auction and constant heat flux considering Eckert number as a small perturbation parameter. This is the extension of the work of Bejan and Khair [17] under the influence of magnetic field.

In our present work, we study about the effects of thermal radiation and chemical reaction on mass transfer on unsteady free convection flow past an exponentially accelerated infinite vertical plate through porous medium in the presence of magnetic hall current. The dimensionless governing equations are reduced to a set of ordinary differential equation. Then we solve these equations with the help of transformed boundary conditions. We have used MATHMATICA to draw graph and to find the numerical results of the equation.

II. MATHEMATICAL FORMULATION

Consider the two-dimensional flow of an electrically conducting, viscous, incompressible, radiating, fluid of density ρ through a porous medium occupying a semi-infinite region of the space bounded by a vertical infinite surface. Fig.1 shows the physical model where the $\bar{x}$-axis is taken along the vertical and $\bar{y}$ axis is horizontal perpendicular to the plate. A uniform magnetic field B_0 is applied normally to the flow region.

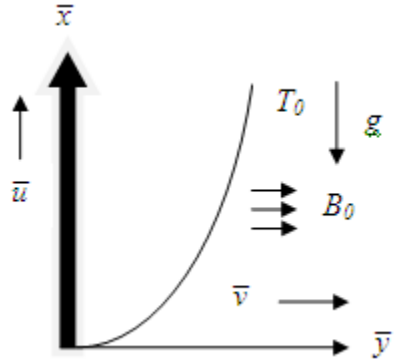

Figure 1 The Physical Co-ordinate System

$$\frac{\partial \bar{v}}{\partial \bar{y}} = 0 \tag{1}$$

$$\bar{v}\frac{\partial \bar{u}}{\partial \bar{y}} = \upsilon \frac{\partial^2 \bar{u}}{\partial \bar{y}^2} + g\beta\left(\bar{T} - \bar{T}_\infty\right) + g\bar{\beta}\left(\bar{C} - \bar{C}_\infty\right) - \frac{\sigma B_0^{\,2}}{\rho\left(1+m^2\right)}\bar{u} - \frac{\upsilon}{k}\bar{u} \tag{2}$$

$$\bar{v}\frac{\partial \bar{T}}{\partial \bar{y}} = \frac{\kappa}{\rho C_p}\frac{\partial^2 \bar{T}}{\partial \bar{y}^2} + \frac{\upsilon}{C_p}\left(\frac{\partial \bar{u}}{\partial \bar{y}}\right)^2 - \frac{1}{\rho C_p}\frac{\partial q_r}{\partial \bar{y}} \tag{3}$$

$$\bar{v}\frac{\partial \bar{C}}{\partial \bar{y}} = D\frac{\partial^2 \bar{C}}{\partial \bar{y}^2} - Kc\left(\bar{C} - \bar{C}_\infty\right) \tag{4}$$

The corresponding boundary conditions are

$$\left.\begin{aligned} \bar{y} = 0 \quad &: \bar{u} = 0, \quad \bar{T} = \bar{T}_w, \quad \bar{C} = \bar{C}_w \\ \bar{y} \to \infty \quad &: \bar{u} \to 0, \quad \bar{T} \to \bar{T}_\infty, \quad \bar{C} \to \bar{C}_\infty \end{aligned}\right\} \tag{5}$$

Here $\bar{u}$ and $\bar{v}$ are the velocity components along the $\bar{x}$ and $\bar{y}$- directions respectively where $\bar{T}$ is the fluid temperature; $\bar{T}_w$ is the temperature of the fluid at the plate, T_∞ is the fluid temperature far away from the plate, g is the acceleration due to gravity, β is the coefficient of thermal expansion, κ is the thermal conductivity, ρ is the density of the fluid, C_p is the specific heat at constant pressure, σ is the electrical conductivity, D is the molecular diffusivity, v_0 is the uniform velocity, $\bar{C}$ is the concentration of species, $\bar{C}_w$ is the mean concentration, $\bar{C}_\infty$ is the concentration of species for uniform flow, B_0 is the uniform applied magnetic field, ρ is the density, v is the kinematic viscosity, β is the coefficient of volume expansion and $\bar{\beta}$ is the coefficient of volume expansion with concentration and the other symbols have their usual meaning.

To make dimensionless the governing equations from (1) to (4) under the boundary conditions (5) we now introduce the following dimensionless quantities.

$$\left.\begin{aligned} u = \frac{1}{v_0}\bar{u},\ y = \frac{v_0}{\upsilon}\bar{y},\ \theta = \frac{\bar{T} - \bar{T}_\infty}{\bar{T}_W - \bar{T}_\infty},\ F = \frac{4I_1\upsilon^2}{\kappa v_0^{\,2}},\ Gr = \frac{g\beta\upsilon\left(\bar{T}_w - \bar{T}_\infty\right)}{v_0^{\,3}},\ Gm = \frac{g\bar{\beta}\upsilon\left(\bar{C}_W - \bar{C}_\infty\right)}{v_0^{\,3}} \\ Pr = \frac{\mu C_p}{\kappa},\ Sc = \frac{\upsilon}{D},\ Kc = \frac{\upsilon}{v_0^{\,2}}\bar{K}c,\ Ec = \frac{v_0^{\,2}}{C_P\left(\bar{T}_w - \bar{T}_\infty\right)},\ M = \frac{\sigma B_0^{\,2}\upsilon}{\rho v_0^{\,2}},\ k = \frac{v_0^{\,2}}{\upsilon^2}\bar{k},\ \phi = \frac{\bar{C} - \bar{C}_\infty}{\bar{C}_w - \bar{C}_\infty} \end{aligned}\right\} \tag{6}$$

Equation (1) implies $\bar{v} = -v_0$ (say) (7)

In the optically thick limit, the fluid does not absorb its own emitted radiation in which there is no self absorption, but it does absorb radiation emitted by the boundaries. Mahaptra *et al.* [18] showed that in the optically thick limit for a non gray near equilibrium as

$$\frac{\partial q_r}{\partial \bar{y}} = 4I_1\left(\bar{T} - \bar{T}_\infty\right) \tag{8}$$

Thus the non-dimensional form of the governing equations (1), (2) and (3) are respectively as follows:

$$u'' + u' - Nu = -Gm\phi - Gr\theta \tag{9}$$

where $N = \dfrac{M}{1+m^2} + \dfrac{1}{k}$

$$\theta'' + Pr\theta' - F\theta = -PrEcu'^2 \tag{10}$$

$$\phi'' + Sc\phi' - KcSc\phi = 0 \tag{11}$$

where dashes denote differentiation with respect to *y*.

The corresponding boundary conditions (5) in non-dimensional forms are

$$\left.\begin{aligned} y = 0 \quad &: u = 0, \quad \theta = 1, \quad \phi = 1 \\ y \to \infty \quad &: u \to 0, \quad \theta \to 0, \quad \phi \to 0 \end{aligned}\right\} \tag{12}$$

III. METHOD OF SOLUTION

To solve the equations (9), (10) and (11) with boundary conditions (12), we use the following simple perturbation. The governing equations (9), (10) and (11) are expanded in power of Eckert number *Ec*(<<1). So we consider *Ec* as a perturbation quantity. Also we consider a second order correction of it.

$$\left.\begin{aligned} u(y) &= u_0(y) + Ecu_1(y) + O\left(Ec^2\right) \\ \theta(y) &= \theta_0(y) + Ec\theta_1(y) + O\left(Ec^2\right) \\ \phi(y) &= \phi_0(y) + Ec\phi_1(y) + O\left(Ec^2\right) \end{aligned}\right\} \tag{13}$$

Substituting (13) in equations (9), (10) and (11) we get

$$u_0'' + u_0' - Nu_0 = -Gm\phi_0 - Gr\theta_0 \tag{14}$$

$$u_1'' + u_1' - Nu_1 = -Gm\phi_1 - Gr\theta_1 \tag{15}$$

$$\theta_0'' + Pr\theta_0' - F\theta_0 = 0 \tag{16}$$

$$\theta_1'' + Pr\theta_1' - F\theta_1 = -Pru_0'^2 \tag{17}$$

$$\phi_0'' + Sc\phi_0' - ScKc\phi_0 = 0 \tag{18}$$

$$\phi_1'' + Sc\phi_1' - ScKc\phi_1 = 0 \tag{19}$$

subject to the boundary conditions

$$\left.\begin{aligned} y = 0 \quad &: u_0 = 0, \quad u_1 = 0, \quad \theta_0 = 1, \quad \theta_1 = 0, \quad \phi_0 = 1, \quad \phi_1 = 0 \\ y \to \infty \quad &: u_0 \to 0, \quad u_1 \to 0, \quad \theta_0 \to 0, \quad \theta_1 \to 0, \quad \phi_0 \to 0, \quad \phi_1 \to 0 \end{aligned}\right\} \tag{20}$$

Solving equations (14) to (19) with boundary condition (20), the following results are obtained

$$\begin{aligned} u = {} & k_3 e^{-k_1 y} + \left(k_4 + Eck_{29}\right)e^{-k_2 y} + \left(k_5 + Eck_{30}\right)e^{-k_6 y} \\ & + Ec\left(k_{23}e^{-2k_1 y} + k_{24}e^{-2k_2 y} + k_{25}e^{-2k_6 y} + k_{26}e^{-k_{11} y} + k_{27}e^{-k_{13} y} + k_{28}e^{-k_{15} y}\right) \end{aligned} \tag{21}$$

$$\theta = \left(1 + Eck_{22}\right)e^{-k_2 y} + Ec\left(k_{16}e^{-2k_1 y} + k_{17}e^{-2k_2 y} + k_{18}e^{-2k_6 y} + k_{19}e^{-k_{11} y} + k_{20}e^{-k_{13} y} + k_{21}e^{-k_{15} y}\right) \tag{22}$$

$$\phi = e^{-k_1 y} \tag{23}$$

Now we want to calculate the skin friction, the rate of heat transfer (Nusselt number) and the rate of mass transfer (Sherwood number). For this purpose we differentiate *u*, θ and ϕ with respect to *y* and then for *y*=0 we can write, where *y* is the dimensionless coordinate axis normal to the plate.

$$\tau = -k_1 k_3 - k_2 k_4 - k_5 k_6 - Ec\left(2k_1 k_{23} + 2k_2 k_{24} + 2k_6 k_{25} + k_{11} k_{26} + k_{13} k_{27} + k_{15} k_{28} + k_2 k_{29} + k_6 k_{30}\right)$$

$$Nu = k_2 + Ec\left(2k_1 k_{16} + 2k_2 k_{17} + 2k_6 k_{18} + k_{11} k_{19} + k_{13} k_{20} + k_{15} k_{21} + k_2 k_{22}\right)$$

$$Sh = k_1$$

IV. RESULTS AND DISCUSSION

In order to get the physical insight into situation of the problem of our study the effects of Prandtl number (*Pr*), Schmidt number (*Sc*), magnetic parameter (*M*), Grashof number (*Gr*), modified Grashof number (*Gm*), Eckert number (*Ec*), Hall parameter (*m*), chemical reaction parameter (*Kc*), permeability parameter (*k*), radiation parameter (*F*) on velocity field, temperature field, concentration field, skin-friction, the rate of heat transfer in terms of Nusselt number (*Nu*) and the rate of mass transfer in terms of Sherwood number (*Sh*) are studied taking different numerical values. To observe the effects of these parameters, the values of Schmidt number (*Sc*) are chosen for hydrogen (*Sc*=0.22), water-vapor (*Sc*=0.60), ammonia (*Sc*=0.78) at 25ºC and one atmosphere pressure. The values of Prandtl number (*Pr*) are chosen for sodium (*Pr*=0.01), air (*Pr*=0.71) and water (*Pr*=7.0). We also choose the Grashof number for heat transfer is *Gr*=5.0, 6.0, 10.0 and modified Grashof number for mass transfer is *Gm*=2.0, 3.0, 4.0. The values of magnetic parameter are given *M*=1.0, 3.0, 5.0 arbitrarily.

The velocity profiles *u* for different values of the above parameters are illustrated in Fig.2 to Fig.11, the temperature profiles θ for different values of the parameters are described in Fig.12 to Fig.14 and the concentration profiles ϕ for different values of the above parameters are expressed in Fig.15 and Fig.16. Also the numerical values of Skin-Friction (τ), the rate of heat transfer (*Nu*) and the rate of Mass Transfer (*Sh*) are shown in the Table 1 to Table 3.

In the Fig.2 it is observed that the velocity decreases with the increase of magnetic parameter (*M*). Physically this is true as the magnetic force retards he flow, velocity decreases. Fig.3 shows the velocity distributions for different values of Hall parameter (*m*). After analysing the figure it is noticed that the velocity increases with the increase of Hall parameter (*m*). It is described in the Fig.4 that the velocity distributions for different values of chemical reaction parameter (*Kc*). In this figure we observe the velocity decreases with the increase of chemical reaction parameter (*Kc*). We see in Fig.5 that the velocity increases with the increase of permeability parameter (*k*). Fig.6 indicates that the velocity decreases with the increase of radiation parameter (*F*). From Fig.7 the velocity increases with the increase of Grashof number (*Gr*). At *y*=0 the velocity profiles are zero. In the Fig.8 it is observed that the velocity increases with the increase of modified Grashof number (*Gm*). It is clear in Fig.9 that the velocity decreases with the increase of Schmidt number (*Sc*). Also Fig.10 marks that the velocity decreases with the increase of Prandtl number (*Pr*). Physically it is true because the increase in the Prandtl number due to increasing the viscosity of the fluid which makes the fluid thick and hence decrease the velocity of fluid. The velocity distributions for different values of Eckert number (*Ec*) is shown in the Fig.11. In this figure we observe the velocity increases with the increase of Eckert number (*Ec*).

From Fig.12 it is clear that the temperature decreases with the increase of radiation parameter (*F*). At *y*=0 the temperature profiles attain the maximum value 1.0 and then decrease smoothly and attain to zero with the increase of *y*. It is observed in the Fig.13 that the temperature distributions for different values of Prandtl number (*Pr*). In this figure it is noticed that the temperature decreases with the increase of Prandtl number (*Pr*). The temperature profiles attain the maximum value 1.0 at *y*=0 and then gradually attain nearly to zero for large values of *y*. Fig.14 shows the temperature distributions for different values of Eckert number (*Ec*). After analysing the figure it is noticed that the temperature increases with the increase of Eckert number (*Ec*).

Fig.15 depicts that the concentration decreases with the increase of reaction parameter (*Kc*). In this figure maximum value of concentration profiles for *y*=0 is 1.0 the concentration profiles decrease smoothly and attain to zero for large value of *y*. In the Fig.16 it marks that the concentration decreases with the increase of Schmidt number (*Sc*). We get the maximum value of concentration profiles for *y*=0 the concentration profiles gradually attain zero with the increase of *y*.

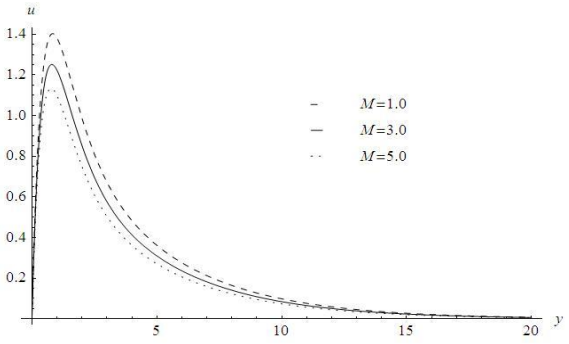

Figure 2 Velocity profiles where *Gr*=6.0, *Gm*=3.0, *F*=0.5, *Kc*=0.04, *Sc*=0.22, *Pr*=0.71, *m*=2.0, *k*=0.5 and *Ec*=0.01 against *y*.

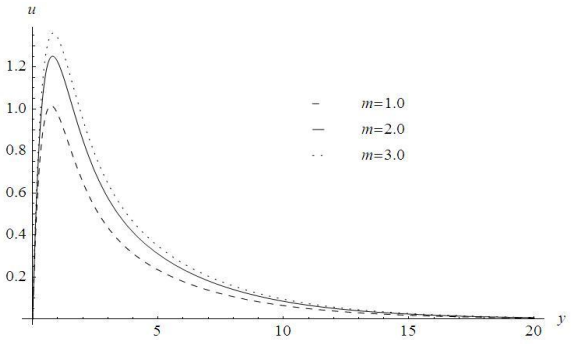

Figure 3 Velocity profiles where *M*=3.0, *Gr*=6.0, *Gm*=3.0, *F*=0.5, *Kc*=0.04, *Sc*=0.22, *Pr*=0.71, *k*=0.5 and *Ec*=0.01 against *y*.

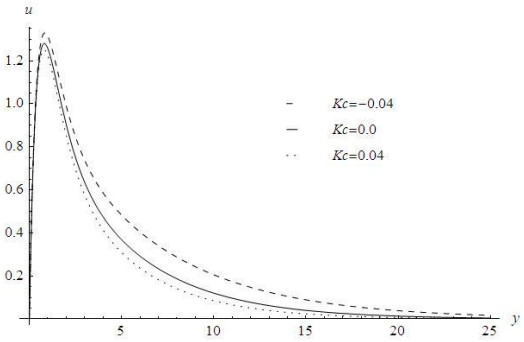

Figure 4 Velocity profiles where M=3.0, Gr=6.0, Gm=3.0, F=0.5, Kc=0.04, Sc=0.22, Pr=0.71, m=2.0, k=0.5 and Ec=0.01 against y.

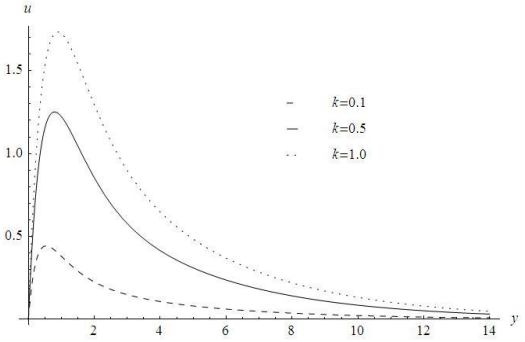

Figure 5 Velocity profiles where M=3.0, Gr=6.0, Gm=3.0, F=0.5, Kc=0.04, Sc=0.22, Pr=0.71, m=2 and Ec=0.01 against y.

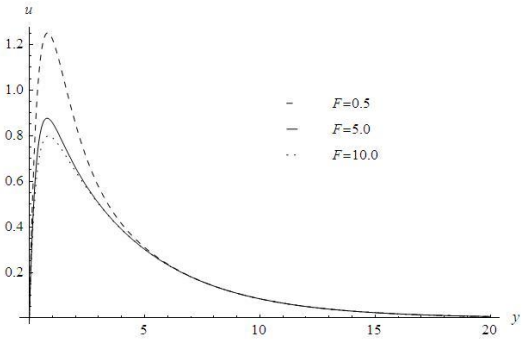

Figure 6 Velocity profiles where M=3.0, Gr=6.0, Gm=3.0, Kc=0.04, Sc=0.22, Pr=0.71, m=2, k=0.5 and Ec=0.01 against y.

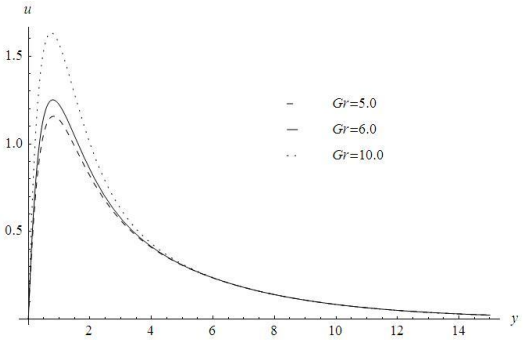

Figure 7 Velocity profiles where M=3.0, Gm=3.0, F=0.5, Kc=0.04, Sc=0.22, Pr=0.71, m=2, k=0.5 and Ec=0.01 against y.

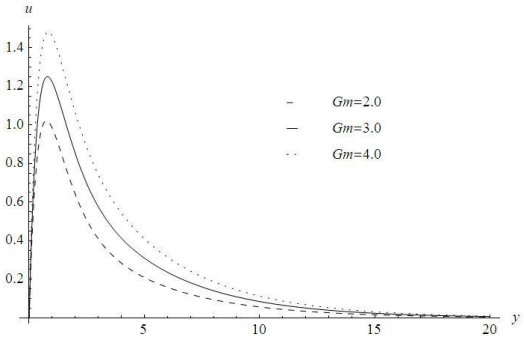

Figure 8 Velocity profiles where M=3.0, Gr=6.0, F=0.5, Kc=0.04, Sc=0.22, Pr=0.71, m=2, k=0.5 and Ec=0.01 against y.

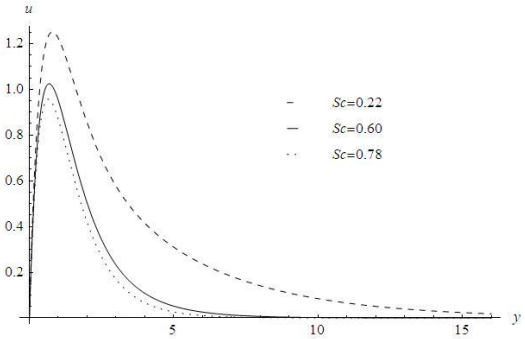

Figure 9 Velocity profiles where M=3.0, Gm =3.0, Gr=6.0, F=0.5, Kc=0.04, Pr=0.71, m=2, k=0.5 and Ec=0.01 against y.

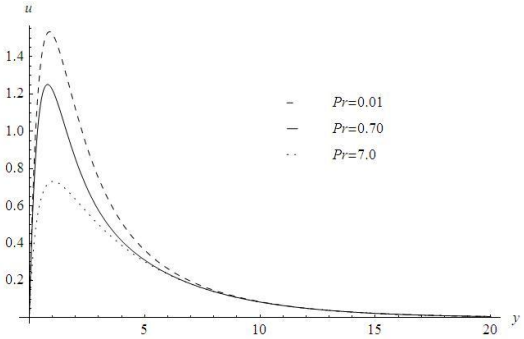

Figure 10 Velocity profiles where M=3.0, Gm=3.0, Gr=6.0, F=0.5, Kc=0.04, Sc=0.22, m=2, k=0.5 and Ec=0.01 against y.

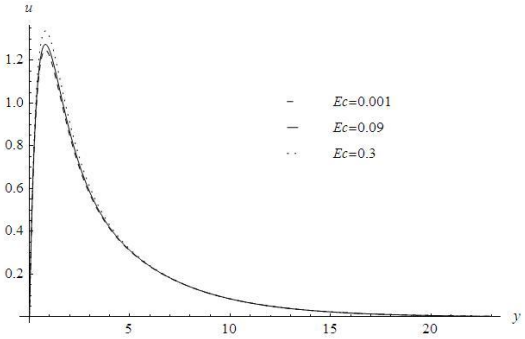

Figure 11 Velocity profiles where M=3.0, Gm=3.0, Gr=6.0, F=0.5, Kc=0.04, Sc=0.22, m=2, k=0.5 and Pr=0.71 against y.

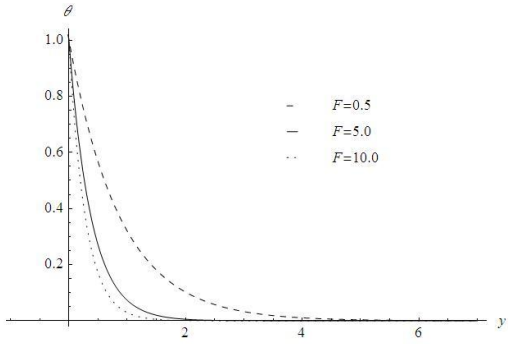

Figure 12 Temperature profiles where *M*=3.0, *Gr*=6.0, *Gm* =3.0, *Kc*=0.04, *Sc*=0.22, *Pr*=0.71, *m*=2, *k*=0.5 and *Ec*=0.01 against *y*.

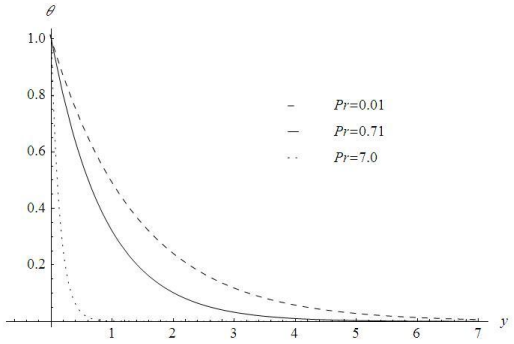

Figure 13 Temperature profiles where *M*=3.0, *Gm*=3.0, *Gr*=6.0, *F*=0.5, *Kc*=0.04, *Sc*=0.22, *m*=2, *k*=0.5 and *Ec*=0.01 against *y*.

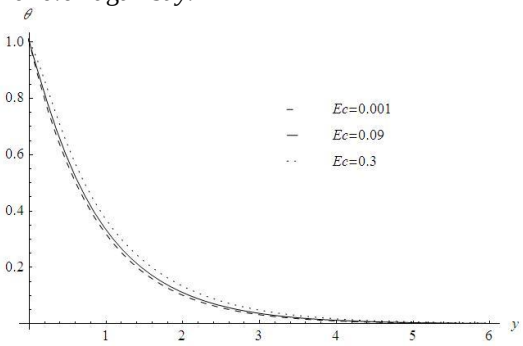

Figure 14 Temperature profiles where *M*=3.0, *Gm*=3.0, *Gr*=6.0, *F*=0.5, *Kc*=0.04, *Sc*=0.22, *m*=2, *k*=0.5 and *Pr*=0.71 against *y*.

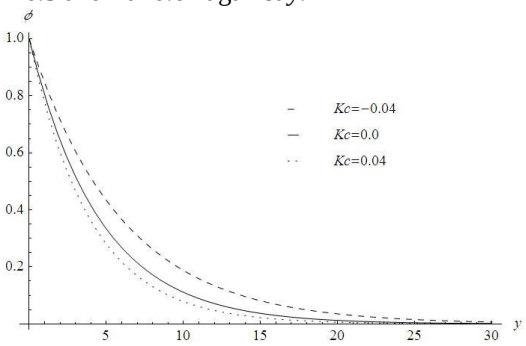

Figure 15 Concentration profiles where *M*=3.0, *Gr*=6.0, *Gm*=3.0, *F*=0.5, *Sc*=0.22, *Pr*=0.71, *m*=2, *k*=0.5 and *Ec*=0.01 against *y*.

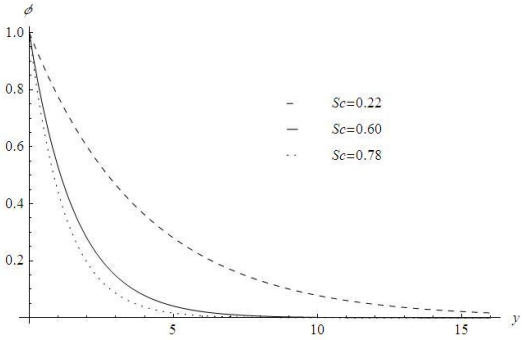

Figure 16 Concentration profiles where *M*=3.0, *Gr*=6.0, *Gm*=3.0, *F*=0.5, *Kc*=0.04, *Pr*=0.71, *m*=2, *k*=0.5 and *Ec*=0.01 against *y*.

Table 1 Numerical values of Skin-Friction (τ)

Sl. No.	*M*	*m*	*F*	*Kc*	*k*	*τ*
1	1.0	2.0	0.5	0.04	0.5	4.99799
2	3.0	2.0	0.5	0.04	0.5	4.65836
3	5.0	2.0	0.5	0.04	0.5	4.38312
4	3.0	1.0	0.5	0.04	0.5	4.10228
5	3.0	2.0	0.5	0.04	0.5	4.65836
6	3.0	3.0	0.5	0.04	0.5	4.90566
7	3.0	2.0	0.5	0.04	0.5	4.65836
8	3.0	2.0	5.0	0.04	0.5	3.65714
9	3.0	2.0	10.0	0.04	0.5	3.35018
10	3.0	2.0	0.5	−0.04	0.5	4.79238
11	3.0	2.0	0.5	0.00	0.5	4.70956
12	3.0	2.0	0.5	0.04	0.5	4.65836
13	3.0	2.0	0.5	0.04	0.1	2.50745
14	3.0	2.0	0.5	0.04	0.5	4.65836
15	3.0	2.0	0.5	0.04	1.0	5.70216

Table 2 Numerical values of the rate of Heat Transfer (*Nu*)

Sl. No.	*M*	*m*	*F*	*Kc*	*k*	*Nu*
1	1.0	2.0	0.5	0.04	0.5	1.11868
2	3.0	2.0	0.5	0.04	0.5	1.12324
3	5.0	2.0	0.5	0.04	0.5	1.12659
4	3.0	1.0	0.5	0.04	0.5	1.12970
5	3.0	2.0	0.5	0.04	0.5	1.12324
6	3.0	3.0	0.5	0.04	0.5	1.11996
7	3.0	2.0	0.5	0.04	0.5	1.12324
8	3.0	2.0	5.0	0.04	0.5	2.60881
9	3.0	2.0	10.0	0.04	0.5	3.52950
10	3.0	2.0	0.5	−0.04	0.5	1.12154
11	3.0	2.0	0.5	0.00	0.5	1.12260
12	3.0	2.0	0.5	0.04	0.5	1.12324
13	3.0	2.0	0.5	0.04	0.1	1.14178
14	3.0	2.0	0.5	0.04	0.5	1.12324
15	3.0	2.0	0.5	0.04	1.0	1.10770

Table 3 Numerical values of the rate of Mass Transfer (*Sh*)

Sl. No.	*Sc*	*Kc*	*Sh*
1	0.22	0.04	0.254568
2	0.60	0.04	0.637639
3	0.78	0.04	0.818135
4	0.22	−0.04	0.167446
5	0.22	0.0	0.220000
6	0.22	0.04	0.254568

V. CONCLUSION

In the present research work, we have studied the effects of Hall current, chemical reaction and radiation on MHD free convection flow through a vertical plate embedded in porous medium. The results are given graphically to illustrate the variation of velocity, temperature and concentration with different parameters. Also the Nusselt number, Sherwood number and skin-friction are presented in tables. From the analysis of the study the following conclusions are made:

The velocity profiles increase with the increase of Hall parameter (*m*), permeability parameter (*k*), Grashof number (*Gr*) and modified Grashof number (*Gm*). On the other hand, it decrease with the increase of magnetic parameter (*M*), chemical reaction parameter (*Kc*), radiation parameter (*F*), Schmidt number (*Sc*) and Prandtl number (*Pr*). The temperature distributions decrease with the increase of radiation parameter (*F*) and Prandtl number (*Pr*). The concentration distributions decrease with the increase of chemical reaction parameter (*Kc*) and Schmidt number (*Sc*).

The skin friction (τ) increases with the increase of Hall parameter (*m*) and permeability parameter (*k*) whereas it decreases with the increase of magnetic parameter (*M*), radiation parameter (*F*) and chemical reaction parameter (*Kc*). The heat transfer rate expressed in terms of the Nusselt number(*Nu*) increases with the increase of magnetic parameter (*M*), radiation parameter (*F*) and chemical reaction parameter (*Kc*) and decreases with the increase of Hall parameter (*m*) and permeability parameter (*k*). The mass transfer rate expressed in terms of Sherwood number (*Sh*) increases with the increase of Schmidt number (*Sc*) and chemical reaction parameter (*Kc*).

APPENDIX

$$k_1 = \frac{1}{2}\left\{Sc + \sqrt{Sc^2 + 4ScKc}\right\}, \quad k_2 = \frac{1}{2}\left\{Pr + \sqrt{Pr^2 + 4F}\right\}, \quad k_3 = -\frac{Gm}{k_1^2 - k_1 - N}, \quad k_4 = -\frac{Gr}{k_2^2 - k_2 - N}$$

$$k_5 = -k_3 - k_4, \quad k_6 = \frac{1}{2}\left\{1 + \sqrt{1 + 4N}\right\}, \quad k_7 = k_1^2 k_3^2, \quad k_8 = k_2^2 k_4^2, \quad k_9 = k_5^2 k_6^2, \quad k_{10} = 2k_1k_2k_3k_4, \quad k_{11} = k_1 + k_2$$

$$k_{12} = 2k_1k_3k_5k_6, \quad k_{13} = k_1 + k_6, \quad k_{14} = 2k_2k_4k_5k_6, \quad k_{15} = k_2 + k_6, \quad k_{16} = \frac{-Prk_7}{4k_1^2 - 2Prk_1 - F}$$

$$k_{17} = \frac{-Prk_8}{4k_2^2 - 2Prk_2 - F}, \quad k_{18} = \frac{-Prk_9}{4k_6^2 - 2Prk_6 - F}, \quad k_{19} = \frac{-Prk_{10}}{k_{11}^2 - Prk_{11} - F}, \quad k_{20} = \frac{-Prk_{12}}{k_{13}^2 - Prk_{13} - F}$$

$$k_{21} = \frac{-Prk_{14}}{k_{15}^2 - Prk_{15} - F}, \quad k_{22} = -k_{16} - k_{17} - k_{18} - k_{19} - k_{20} - k_{21}, \quad k_{23} = \frac{-Grk_{16}}{4k_1^2 - 2k_1 - N}, \quad k_{24} = \frac{-Grk_{17}}{4k_2^2 - 2k_2 - N}$$

$$k_{25} = \frac{-Grk_{18}}{4k_6^{\,2} - 2k_6 - N}, \quad k_{26} = \frac{-Grk_{19}}{k_{11}^{\,2} - k_{11} - N}, \quad k_{27} = \frac{-Grk_{20}}{k_{13}^{\,2} - k_{13} - N}, \quad k_{28} = \frac{-Grk_{21}}{k_{15}^{\,2} - k_{15} - N}, \quad k_{29} = \frac{-Grk_{22}}{k_2^{\,2} - k_2 - N}$$

$$k_{30} = -k_{23} - k_{24} - k_{25} - k_{26} - k_{27} - k_{28} - k_{29}$$

REFERENCES

[1] M. A. Hossain and A. C. Mandal, Journal of Physics D: Applied Physics, 18, 1985, 163–169.
[2] V. M. Soundalgekar, H. S. Takhar, Modelling Measure and Cont., 51, 1992, 31–40.
[3] H. S. Tahkar, S. R. Gorla, V. M. Soundalgekar, Int. J. Numerical Methods heat fluid flow, 6, 1996, 77–83.
[4] M. A. Hossain, M. A. Alim and D. A. S. Rees, Int. J. Heat Mass Transfer, 42, 1999, 181–191.
[5] H. Poonia and R. C. Chaudhary, Theoret. Applied Mechanics, 37 (4), 2010, 263–287.
[6] M. S. Alam and M. M. Rahaman, Int. J. of Science and Technology, II (4), 2006.
[7] P. R. Sharma and G. Singh, Int. J. of Appl. Math and Mech, 4(5), 2008, 1–8.
[8] R. C. Chaudhary and J. Arpita, Roman J. Phy., 52(5–7), 2007, 505–524.
[9] R. Muthucumaraswamy and Janakiraman: MHD and Radiation effects on moving isothermal vertical plate with variable mass diffusion. Theoret. Appl. Mech. 33(1): 2006, 17–29.
[10] A. A. Raptis and V. M. Soundalgekar, ZAMM, 64, 1984, 127–130.
[11] A. K. Agrawal, B. Kishor and A. Raptis, Warme und Stofubertragung, 24, 1989, 243–250.
[12] B. K. Jha and A. K. Singh, Astrophysics Space Science, pp. 251–255.
[13] B. K. Jha and R. Prasad, J. Math Physics and Science, 26, 1992, 1–8.
[14] M. D. Abdusattar, Ind. J. Pure Applied Math., 25, 1994, 259–266.
[15] V. M. Soundalgekar, S. N. Ray and U. N. Das, Proc. Math. Soc, 11, 1995, 95–98.
[16] M. Acharya, G. C. Das and L. P. Singh, Ind. J. Pure Applied Math., 31, 2000, 1–18.
[17] A. Bejan and K. R. Khair, Int. J. Heat Mass Transfer, 28, 1985, 909–918.
[18] N. Mahaptra, G. C. Das, S. Panda, M. Acharya, J.Engg. Phys. and Thermo physics, 2010, Vol. 83, No.1.

American Journal of Engineering Research (AJER)
e-ISSN : 2320-0847 p-ISSN : 2320-0936
Volume-03, Issue-12, pp-15-22
www.ajer.org

Research Paper Open Access

Effects of Radiation and Chemical Reaction on MHD Free Convection Flow past a Vertical Plate in the Porous Medium

S. Mondal[1], S. Parvin[2], S. F. Ahmmed[3]
[1]*City University, Dhaka, Bangladesh.*
[2] *Bagerhat Govt. Girls College, Bagerhat, Bangladesh.*
[3] *Khulna University, Khulna, Bangladesh.*

ABSTRACT: *The objective is to study the effects of thermal radiation and chemical reaction on mass transfer on unsteady free convection flow past an* exponentially *accelerated infinite vertical plate through porous medium in the presence of magnetic field. The fluid is considered here as absorbing/emitting radiation but a non-scattering medium. The plate temperature is raised linearly with time and the concentration level near the plate is raised to* C'_∞ *. We use proper transformations to make the governing equations dimensionless. The dimensionless governing equations are reduced to a set of ordinary differential equations. Then we solve these equations with the help of transformed boundary conditions. The effect of various parameters such as Grashof number, Modified Grashof number, Schmidt number, Prandtl number, Magnetic parameter, time, accelerating parameter, Dimensionless porous medium factor and Dimensionless chemical reaction parameter on velocity profiles, temperature profiles, concentration profiles, skin friction profiles, rate of heat transfer profiles and rate of mass transfer profiles are shown graphically.*

KEYWORDS: *Radiation, MHD, Free Convection, Grashof number and Prandtl number.*

I. INTRODUCTION

In many engineering applications, combined heat and mass transfer play an important role in fluids condensing and boiling at a solid surface. Natural convection induced by the simultaneous action of buoyancy forces from thermal and mass diffusion is of considerable interest in many industrial applications such as geophysics, oceanography, drying processes and solidification of binary alloy. The effect of the magnetic field on free convection flows is important in liquid metals, electrolytes and ionized gases. The thermal physics of MHD problems with mass transfer is of interest in power engineering and metallurgy. When free convection flows occur at high temperature, radiation effects on the flow become significant. Many processes in engineering areas occur at high temperatures and knowledge of radioactive heat transfer becomes very important for the design of the pertinent equipment. Nuclear power plants, gas turbines and the various propulsion devices for aircraft, missiles and space vehicles are examples of such engineering areas.

Murali [1] examined the thermal radiation effect on unsteady magneto hydrodynamic flow past a vertical porous plate with variable suction. Damala [2] make a study on the effect of the steady two dimensional free convection heat and mass transfer flow electrically conducting and chemically reacting fluid through a porous medium bounded by a vertical infinite surface with constant suction velocity and constant heat flux in the presence of a uniform magnetic field is presented. The effects of chemical reaction and radiation absorption have been discussed on unsteady MHD free convection heat and mass transfer flow on a viscous, incompressible, electrically conducting fluid past a semi-infinite inclined porous plate, moving with a uniform velocity are discussed in Sudersan [3]. Gupta [4] studied free convection on flow past a linearly accelerated vertical plate in the presence of viscous dissipative heat using perturbation method. Kafousias and Rapits [5] extended this problem to include mass transfer effects subjected to variable suction or injection. Free convection effects on flow past an exponentially accelerated vertical plate was studied by Singh and Kumar [6]. The skin friction for accelerated vertical plate has been studied analytically by Hossain and Shayo [7]. Jha [8] analyzed mass transfer effects on exponentially accelerated infinite vertical plate with constant heat flux and uniform mass diffusion. Muthucumaraswamy et al. [9] studied mass transfer effects on exponentially accelerated isothermal vertical plate. Soundalgerkar and Takhar [10] have considered the radiative free convective flow of an optically thin gray gas past a semi- infinite vertical plate.

Radiation effects on mixed convection along an isothermal vertical plate were studied by Hossain and Takhar [11]. Raptis and Perdikis [12] studied the effects of thermal radiation and free convection flow past a moving vertical plate and solve the governing equations analytically. Das et al. [13] have analyzed radiation effects on flow past an impulsively started infinite isothermal vertical plate. The governing equations were solved by the Laplace transform technique. Muthucumaraswamy and Janakiraman [14] studied MHD and radiation effects on moving isothermal vertical plate with variable mass diffusion. An exact solution to one dimensional unsteady natural convection flow past an infinite vertical accelerated plate, immersed in a viscous thermally stratified fluid is investigated by Rudra and Bhaben [15]. Tasawar et al. [16] investigated the influence of radiation on magneto hydrodynamic (MHD) and mass transfer flow over a porous stretching sheet. Recently the thermal radiation effects on unsteady free convective flow of a viscous incompressible flow past an exponentially accelerated infinite vertical plate with variable temperature and uniform mass diffusion has been studies by Muthucummaraswamy and Vislakshi [17]. An analytical study is performed to examine the effects of temperature dependent heat source on the unsteady free convection and Amass transfer flow of an elasto-viscous fluid past an exponentially accelerated infinite vertical plate in the presence of magnetic field through porous medium by Rajesh [18]. Suneetha et al. [19] investigated thermal radiation effects on MHD flow past an impulsively started vertical plate in the presence of heat source/ sink by taking into account the heat due to viscous dissipation. In S.F Ahmmed et al. [20] have analyzed the numerical study on MHD free convection and mass transfer flow past a vertical flat plate.

We study the effects of thermal radiation and chemical reaction on mass transfer on unsteady free convection flow past an exponentially accelerated infinite vertical plate with variable temperature and concentration in the presence of magnetic field in the porous medium. We use proper transformations to make the governing equations dimensionless. The dimensionless governing equations are reduced to a set of ordinary differential equation. Then we solve these equations with the help of transformed boundary conditions.

II. GOVERNING EQUATIONS

$$\frac{\partial u'}{\partial t'} = g\beta(T' - T'_\infty) + g\beta^*(C' - C'_\infty) + \nu\frac{\partial^2 u'}{\partial y'^2} - \frac{\sigma B_0^2 u'}{\rho} - \frac{\nu}{K_p}u' \tag{1}$$

$$\rho C_p \frac{\partial T'}{\partial t'} = k\frac{\partial^2 T'}{\partial y'^2} - \frac{\partial q_r}{\partial y'} \tag{2}$$

$$\frac{\partial C'}{\partial t'} = D\frac{\partial^2 C'}{\partial y'^2} - K_l(C' - C'_\infty) \tag{3}$$

with the boundary conditions

$$t' > 0,\ u' = u_0 \exp(a't'),\ T' = T'_\infty + (T'_w - T'_\infty)At',\ C' = C'_\infty + (C'_w - C'_\infty)At' \text{ at } y' = 0$$

$$u' = 0, T' \to T'_\infty, C' \to C'_\infty \text{ as } y' \to \infty \tag{4}$$

MATHEMATICAL FORMULATION

We use the following transformations to make the equations (1) to (4) dimensionless.

$$u = \frac{u'}{u_0}, t = \frac{t'u_0^2}{\nu}, y = \frac{y'u_0}{\nu}, \theta = \frac{T' - T'_\infty}{T'_w - T'_\infty}, Gr = \frac{g\beta\nu(T'_w - T'_\infty)}{u_0^3}, \phi = \frac{C' - C'_\infty}{C'_w - C'_\infty},$$

$$Gm = \frac{g\beta^*\nu(C'_w - C'_\infty)}{u_0^3}, \Pr = \frac{\mu C_p}{k}, Sc = \frac{\nu}{D}, M = \frac{\sigma B_0^2 \nu}{\rho u_0^2}, R = \frac{16a^*\nu^2\sigma T'_\infty}{ku_0^2}, \tag{5}$$

$$a = \frac{a'\nu}{u_0^2}, K = \frac{K_p u_0^2}{\nu^2}, \gamma = \frac{K_l \nu}{u_0^2}$$

We know, Gr, Gm, Pr, Sc, M, R, θ, ϕ, K and γ are Thermal Grashof number, Modified Grashof number, Prandtl number, Schmidt number, Magnetic field parameter, Radiation parameter, Dimensionless temperature, Dimensionless concentration, Dimensionless porous medium factor and Dimensionless chemical reaction parameter respectively, where $A = e^{a't'}/t$. In this case the local radiant of an optically thin gray gas is expressed by

$$\frac{\partial q_r}{\partial y'} = -4a^*\sigma(T'^4_\infty - T'^4) \tag{6}$$

By using the parameter our governing equation becomes as follows

$$\frac{\partial u}{\partial t} = Gr\theta + Gm\phi + \frac{\partial^2 u}{\partial y^2} - Mu - \frac{u}{K} \tag{7}$$

$$\frac{\partial \theta}{\partial t} = \frac{1}{\Pr}\frac{\partial^2 \theta}{\partial y^2} - \frac{R}{\Pr}\theta \tag{8}$$

$$\frac{\partial \phi}{\partial t} = \frac{1}{Sc}\frac{\partial^2 \phi}{\partial y^2} - \phi\gamma \tag{9}$$

Thus the boundary conditions becomes as follows

$$\begin{aligned} &t > 0 : u = \exp(at), \theta = \exp(at), \phi = \exp(at) \text{ at } y = 0 \\ &u = 0, \theta \to 0, \phi \to 0 \text{ as } y \to \infty \end{aligned} \tag{10}$$

Let us consider the solution of the equations (7) to (9) be of the form $u = u_0 e^{at}$, $\theta = \theta_0 e^{at}$ and $\phi = \phi_0 e^{at}$ respectively. Using the above u, θ and ϕ equations (7) to (9) become

$$u_0'' - (M + \frac{1}{K} + a)u_0 + Gr\theta_0 + Gm\phi_0 = 0 \tag{11}$$

$$\theta_0'' - \Pr(\frac{R}{\Pr} + a)\theta_0 = 0 \tag{12}$$

$$\frac{1}{Sc}\phi_0'' - (a + \gamma)\phi_0 = 0 \tag{13}$$

The boundary conditions for the equations are reduced to the following form

$$\begin{aligned} &t > 0 : u_0 = 1, \theta_0 = 1, \phi_0 = 1 \text{ at } y = 0 \\ &u_0 = 0, \theta_0 = 0, \phi_0 = 0 \text{ as } y \to \infty \end{aligned} \tag{14}$$

Finally the velocity field, temperature field and concentration field can be written as

$$u = (1 + \frac{Gr}{m_1 - m_3} + \frac{Gm}{m_2 - m_3})e^{at - \sqrt{m_3}y} - Gr\frac{1}{m_1 - m_3}e^{at - \sqrt{m_1}y} - Gm\frac{1}{m_2 - m_3}e^{at - \sqrt{m_2}y} \tag{15}$$

$$\theta = e^{at - \sqrt{m_1}y} \tag{16}$$

$$\phi = e^{at - \sqrt{m_2}y} \tag{17}$$

Now we want to calculate the skin friction, the rate of heat transfer (Nusselt number) and the rate of mass transfer (Sherwood number). For this purpose we differentiate u, θ and ϕ with respect to y and get

$$\tau = \frac{du}{dy} = -\sqrt{m_3}(1 + \frac{Gr}{m_1 - m_3} + \frac{Gm}{m_2 - m_3})e^{at - \sqrt{m_3}y} + \frac{Gr.\sqrt{m_1}}{m_1 - m_3}e^{at - \sqrt{m_1}y} + \frac{Gm.\sqrt{m_2}}{m_2 - m_3}e^{at - \sqrt{m_2}y} \tag{18}$$

$$Nu = \frac{d\theta}{dy} = -\sqrt{m_1}e^{at - \sqrt{m_1}y} \tag{19}$$

$$Sh = \frac{d\phi}{dy} = -\sqrt{m_2}e^{at - \sqrt{m_2}y} \tag{20}$$

Thus for y=0 we can write the equation (18), (19) and (20)

$$\text{The skin friction } \tau = -\sqrt{m_3}(1 + \frac{Gr}{m_1 - m_3} + \frac{Gm}{m_2 - m_3})e^{at} + \frac{Gr\sqrt{m_1}}{m_1 - m_3}e^{at} + \frac{Gm\sqrt{m_2}}{m_2 - m_3}e^{at}$$

$$\text{The rate of heat transfer } Nu = -\sqrt{m_1}e^{at}$$

$$\text{The rate of mass transfer } Sh = -\sqrt{m_2}e^{at}$$

III. RESULTS AND DISCUSSION

The numerical values for the velocity profiles, temperature distribution, concentration profiles are computed for different physical parameters like Grashof number (Gr), Magnetic parameter (M) , Modified Grashof number (Gm), Radiation parameter (R), time (t), Prandtl number (Pr), Schimidt number (Sc) and accelerating parameter (a). The purpose of the calculations is to the study on the effects of the parameters upon the nature of the velocity profiles, temperature profiles and concentration profiles.

Fig. 1 represents variation in the velocity field for different values of Magnetic parameter (M) in case of cooling (Gr = 10, Gm = 5) and heating (Gr = -10, Gm = -5) of the plates with Pr = 0.71, R = 4, a = 0.5, Sc = 2.01, γ = 2, K = 4 and t = 0.2. It is observed that for an externally cooled plate an increase in Magnetic parameter (M), the velocity field decreases. For an externally heated plate the results are observed in reverse order. The variation of velocity field for various values of Schmidt number (Sc) in case of cooling (Gr = 10, Gm = 5) and heating (Gr = -10, Gm = -5) of the plate with M = 1, Pr =0.71, a = 0.5, R = 4, γ = 2, K = 4 and t = 0.2 are given in Fig. 2. Here we choose Sc = 0.22 (Hydrogen), Sc = 0.30 (Helium), Sc = 0.60 (water vapor) and Sc = 0.78 (Ammonia). It is noted from the figure that velocity field is decreasing with the increasing values of Schmidt number (Sc) in the cooling plate. But in the heating plate the velocity profile is increasing for the increasing values of Sc. Fig..3 depicts the variation of velocity field with respect to the increasing values of Grashof number (Gr) and Modified Grashof number (Gm) both in the cooled and heated plate with M =1, Pr = 0.71, Sc = 3.01, a = 0.5, R = 4, t = 0.2, γ = 2 and K = 4. Here we see that velocity is increasing with an increase in Gr and Gm for the cooling plate. The reverse effects are seen in the heated plate. It is clear in the Fig. 4 that in case of cooling (Gr = 10, Gm = 5) and heating (Gr = -10, Gm = -5) of the plates M = 1, Pr = 0.71, Sc = 2.01, a = 0.5, γ = 2, K = 4 and R = 4 the velocity field is increasing and decreasing respectively with respect to the increasing values of t. The influence of Gr on the velocity field is represented in Fig. 5. The velocity fields are increasing with the increasing values of Gr in the cooled plate. It is noted that the reverse effects are shown in the heated plate.

Fig. 6 depicts the temperature profiles against y for different values of the parameters. The magnitude of the temperature is maximum near the plate. But when we increase the values of t the magnitude of temperature is maximum at the plate and then decays to zero. Temperature profiles increase with an increase in t. In Fig..7 we observe that an increase in R decreases the temperature field and then goes to zero for large values of y. In the Fig. 8 we observe that temperature field is increasing at the plate with an increase in a and finally goes to zero.

The numerical values of the concentration are computed for different physical parameters like Schmidt number (Sc), time (t), accelerating parameter (a) and Dimensionless chemical reaction parameter (γ). The purpose of the calculations given here is to study the effects of the parameters Sc, a and t upon the nature of the concentration. In the Fig. 9 we see that concentration field is decreasing with an increasing value of Sc. The maximum values of concentration are found at the plate. The influence of t on the concentration field is presented in the Fig. 10. It is clear from the behavior of t that the concentration field increases for increasing values of t whose effect is significant at the plate but negligible far away from the plate i.e, $y \to \infty$.

The numerical values of the skin frictions are computed for different physical parameters like Magnetic field parameter (M), Radiation parameter (R), Schmidt number (Sc), Dimensionless porous medium factor (K), Dimensionless chemical reaction parameter (γ) and accelerating parameter (a). The purpose of the calculations given here is to study the effects of the parameters M, R, Sc, Gr, Gm, K, γ and a upon the nature of the rate of flow and transport. The heating and cooling take place by setting up free convection current due to temperature and concentration gradient. Fig.11 shows the influence of accelerating parameter (a) on the skin friction. Skin frictions are increased in the case of cooling (Gr = 10, Gm = 5) of the plate with the increasing values of a. The reverse effects are shown in the heating plate (Gr = -10, Gm = -5). In Fig. 12 it is shown that skin friction is decreasing with the increasing values of M. These effects are shown in the cooling plate (Gr = 10, Gm = 5) with the increasing values of M. But no effects are shown in the heating plate (Gr = -10, Gm = -5) with the increasing values of M.

The numerical values of the rate of heat transfer are computed for different physical parameters like Radiation parameter (R), Prandtl number (Pr) and accelerating parameter (a). The purpose of the calculations given here is to study the effects of the parameters R, Pr and a upon the nature of the rate of heat transfer. In the Fig. 13 we see that for increasing values of R, Pr and a the rate of heat transfer profiles are decreased and gradually goes to infinity as $t \to \infty$. Also in the Fig. 14 represents that an increase in a decreases the rate of heat transfer profiles.

IV. FIGURES

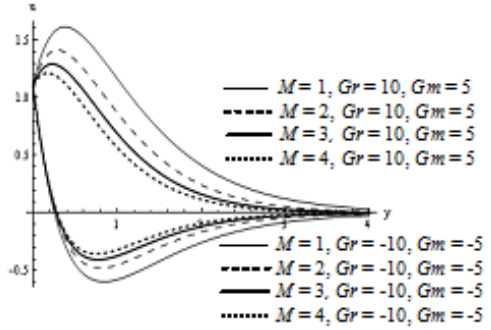

Fig. 1- Velocity profile u for different values of M With $R = 4$, $Pr = 0.71$, $a = 0.5$, $Sc = 2.01$, $K = 4$, $\gamma = 2$ and $t = 0.2$ against y.

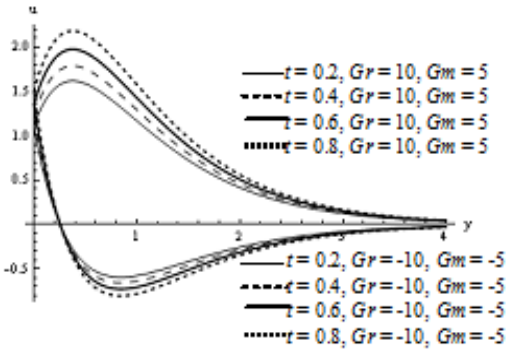

Fig. 4- Velocity profile u for different values of t with $M = 1$, $Pr = 0.71$, $Sc = 2.01$, $a = 0.5$, $K = 4$, $\gamma = 2$ and $R = 4$ against y.

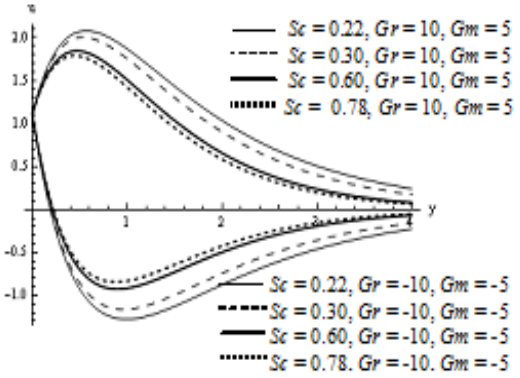

Fig. 2- Velocity profile u for different values of Sc with $M = 1$, $Pr = 0.71$, $a = 0.5$, $R = 4$, $K = 4$, $\gamma = 2$ and $t = 0.2$ against y.

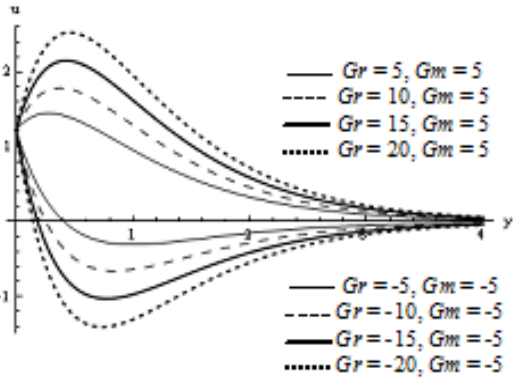

Fig. 5- Velocity profile u for different values of Gr with $M = 1$, $Pr = 0.71$, $Sc = 2.01$, $a = 0.5$ and $R = 4$ against y.

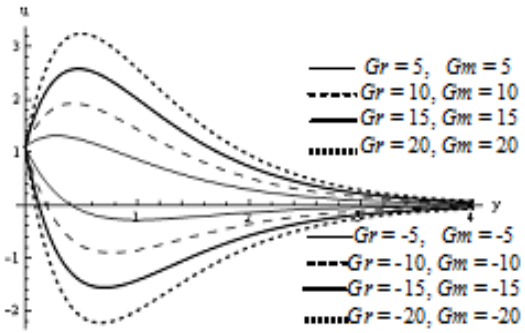

Fig. 3- Velocity profile u for different values of Gr and Gm with $M = 1$, $Pr = 0.71$, $Sc = 2.01$, $a = 0.5$, $R = 4$, $K = 4$, $\gamma = 2$ and $t = 0.2$ against y.

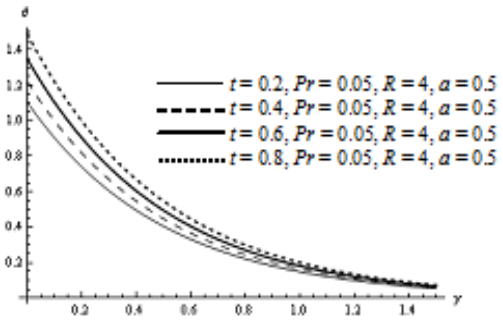

Fig. 6- Dimensionless temperature profiles Θ for different values of t against y.

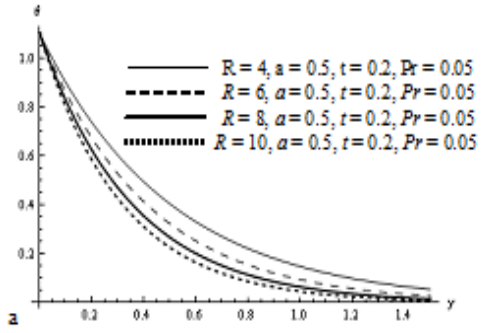

Fig. 7-Dimensionless temperature profiles Θ for different values of R against y.

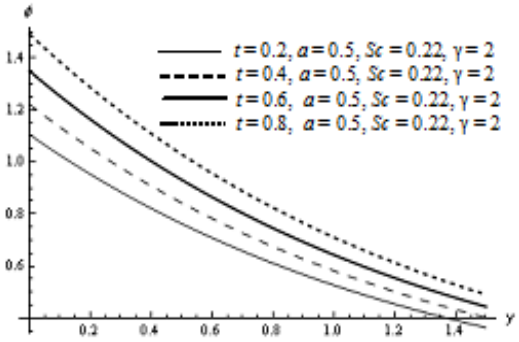

Fig. 10- Dimensionless concentration profiles φ for different values of t against y.

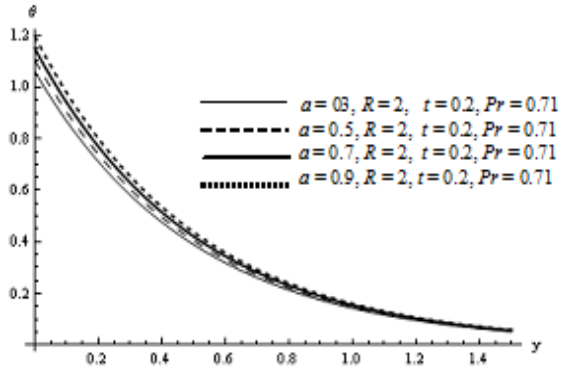

Fig. 8- Dimensionless temperature profiles Θ for different values of a against y

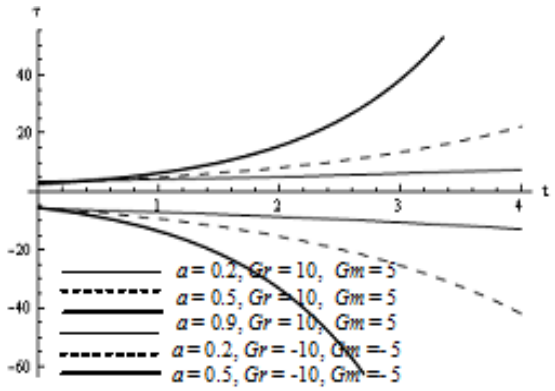

Fig. 11- The skin friction profile τ for different values of a with R = 4, M = 1, Sc = 0.22, γ = 2, K = 4 and Pr = 0.71 against t.

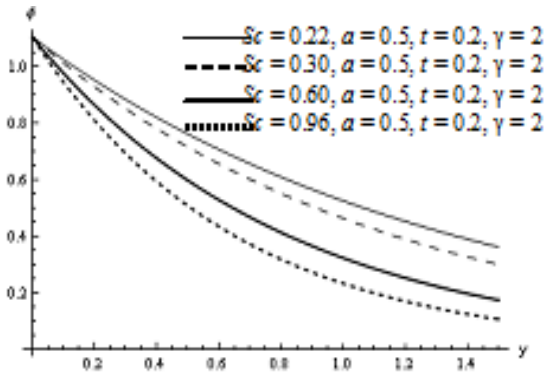

Fig. 9- Dimensionless concentration profiles φ for different values of Sc against y.

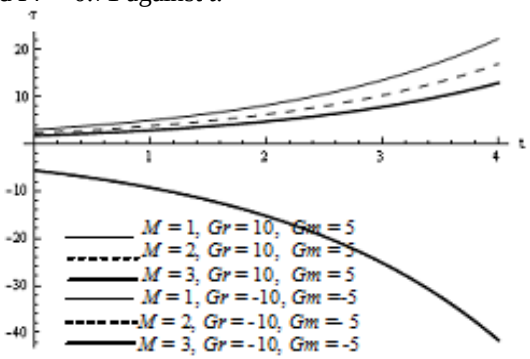

Fig. 12- The skin friction profile τ for different values of M with R = 4,a = 0.5,Sc = 0.22,γ = 2,K =4 and Pr = 0.71 against t.

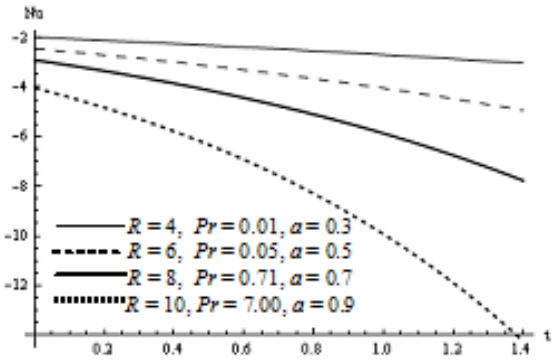

Fig. 13- Rate of heat transfer profiles *Nu* for different values of *R*, *Pr* and *a* against *t*.

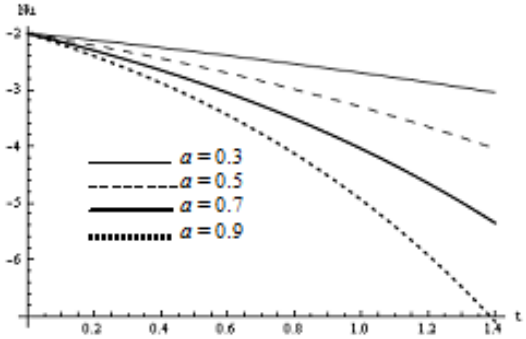

Fig. 14- Rate of heat transfer profiles *Nu* for different values of *a* with *Pr* = 0.05 and *R* = 4 against *t*.

V. CONCLUSION

From the study of the paper we conclued that the velocity are incrising with the incrising value of Grashof number (Gr), Soret number (S_0) and modified Grashof number (Gm) on the other hand it is decrising with the incrising value of magnetic parameter (M), Prandtl number (Pr), Schmidt number (Sc). We see that if the time is increasing then the velocity is incrising. The temperature increase with increase of heat source parameter (S) and decrease with increase of Prandtl number (Pr). Also we see that the concentration is increase with the increase of Soret number (S_0) and decrease with the increase of Schmidt number (Sc).

REFERENCES

[1]. R. Murali Gundagani, S. Sivaiah, NVN Babu and M.C.K Reddy, Finite element solution of thermal radiation effect on unsteady MHD flow past a vertical porous plate with variable suction. American Academic & Scholarly Research Journal. 4(3): 2012

[2]. Damala Ch. Kesavaiah, P. V. Satyanarayana, S. Venkataramana: Radiation absorption, chemical reaction and magnetic filed effects on the free convection and mass transfer flow through porous medium with constant suction and constant heat flux. International Journal of Scientific Engineering and Technology (ISSN : 2277-1581). 1(6): 274-284. 2012

[3]. Sudersan reddy, G.V.Ramana Reddy, K.Jayarami Reddy: Radiation and chemical reaction effects on MHD heat and mass transfer flow inclined porous heated plate. Asian Journal of Current Engineering and Maths. 1(3): 115– 119. 2012

[4]. Gupta A. S, Pop I. and Soundalgekar V. M. Free convection effects on the flow past an accelerated vertical plate in an incompressible dissipative fluid. Rev. Roum. Sci. Techn. -Mec. Apl. 24: 561-568. 1979

[5]. Kafousias N. G. and Raptis A. A. Mass transfer and free convection effects on the flow past an accelerated vertical infinite plate with variable suction or injection. Rev. Roum. Sci. Techn. - Mec. Apl. 26: 11-22. 1981.

[6]. Singh A.K. and Kumar N. Free convection flow past an exponentially accelerated vertical plate. Astrophysics and Space science. 98: 245-258. 1984.

[7]. Hossain M.A. and Shayo L. K. The Skin friction in the unsteady free convection flow past an accelerated plate. Astrophysics and Space Science. 125: 315-324. 1986

[8]. Jha B. K, Prasad R. and Rai S. Mass transfer effects on the flow past an exponentially accelerated vertical plate with constant heat flux. Astrophysics and Space Science. 181: 125-134. 1991

[9]. Muthucumaraswamy R, Sathappan K. E. and Natarajan R. Mass transfer effects on exponentially accelerated isothermal vertical plate. Int. J. of Appl. Math. and Mech. 4(6): 19-25. 2008

[10]. Soundalgekar V. M. and Takhar H. S. Radiation effects on free convection flow past a semi-infinite vertical plate. Modeling, Measurement and control. B51: 31-40. 1993.

[11]. Hossain M. A. and Takhar H. S. Radiation effects on mixed convection along a vertical plate with uniform surface temperature. Heat and Mass Transfer. 31: 243-248. 1996.

[12]. Raptis A. and Perdikis C. Radiation and free convection flow past a moving plate. Int. J. of App. Mech. and Engg. 4: 817-821. 1999

[13]. Das U. N, Deka R. K. and Soundalgekar V. M., Radiation effects on flow past an impulsively started vertical infinite plate. J. Theo. Mech. 1: 111-115. 1996

[14]. Muthucumaraswamy R. and Janakiraman, MHD and Radiation effects on moving isothermal vertical plate with variable mass diffusion. Theoret. Appl. Mech. 33(1): 17-29. 2006

[15]. Rudra Kt. Deka, Bhaben Ch. Neog, Unsteady natural convection flow past an accelerated vertical plate in a thermally stratfied fluid. Theoret. Appl. Mech., 36(4): 261-274, Belgrade. 2009

[16]. Tasawar Hayat, Muhammad Qasim, and Zaheer Abbas, Radiation and Mass Transfer Effects on the Magnetohydrodynamic Unsteady Flow Induced by a Stretching Sheet. Z. Naturforsch. 65a: 231 – 239. 2010
[17]. R. Muthucumaraswamy, V. Visalakshi, Radiative Flow Past an Exponentially Accelerated Vertical Plate with Variable Temperature and Mass Diffusion. Annals of Faculty Engineering Hunedoara-International Journal of Engineering Tome IX, Fascicule2 (ISSN 1584-2665): 137-140. 2011
[18]. V. Rajesh: Heat Source and Mass Transfer Effects on MHD Flow of an Elasto-Viscous Fluid Through a Porous Medium. Annals of Faculty Engineering Hunedoara-International Journal of Engineering Tome IX, Fascicule2 (ISSN 1584-2665): 205-212. 2011
[19]. S. Suneetha, N. Bhaskar Reddy and V. Ramachandra Prasad, Radiation and Mass Transfer Effects on MHD Free Convective Dissipative Fluid in the Presence of Heat Source/Sink. Journal of Applied Fluid Mechanics, 4 (1): 107-113. 2011
[20]. S. F. Ahmmed, S. Mondal and A. Ray, Numerical Study on MHD Free Convection and Mass Transfer Flow Past a Vertical Flat Plate. IOSR Journal of Engineering (IOSRJEN) e-ISSN: 2250-3021, p-ISSN: 2278-8719 Vol. 3, Issue 5 (May. 2013), ||V4 || PP 41-47

American Journal of Engineering Research (AJER)
e-ISSN : 2320-0847 p-ISSN : 2320-0936
Volume-03, Issue-12, pp-23-33
www.ajer.org
Research Paper Open Access

THE SOUL OF THOLKAPPIAM (A New theory on "VALLUVAM")

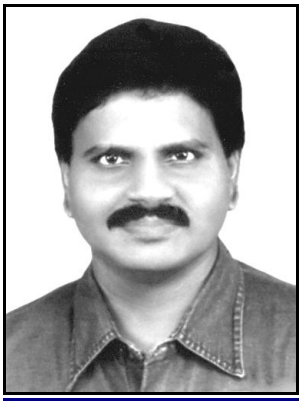

M.Arulmani,
B.E.
(Engineer)

V.R.Hema Latha,
M.A., M.Sc., M.Phil.
(Biologist)

1. Abstract:

"THOLKAPPIAR" is a Great philosopher?... **No….. No…. No…. "AKATHIAR"** shall be considered as a Great philosopher. **"THOLKAPPIAR"** shall be called as great "**POET**" **(Kaviperarasu**) elaborating various **Predefined** ancient philosophies in his **poems** written in high **grammatical** form during **post Vedic period.**

This scientific research focus that the population of **"AKATHIAR**" race (also called as Akkanna population) shall be considered as Ancient population lived in **"KACHCHA THEEVU**" during **pre-vedic period** (Say 5,00,000years ago) who written many philosophy of **planet system, medicines Ethics in "PALM LEAF MANUSCRIPT".**

It is further focused that the philosophy related to various subjects shall be considered derived from **"stone culvert"** (Tablet) scatterly available here and there. Alternatively it shall be stipulated that **"Akathiar race**" consider simply "**TRANSLATING"** the matter available in the Prehistoric stone culvert and wrote in the form of **'palm leaf manuscript'.**

It is speculated that the **human ancestor** populations shall be considered lived in **'WHITE PLANET'** (white mars) in the **early universe** who were expert in various field like **Astrophysics, Astronomy, Medicines, Ethics,** etc. written in single alphabet script called **"TRIPHTHONG SCRIPT"** written in a **super solid stone matter**. In proto Indo Europe language the Triphthong script shall be called as **"VALLUVAM**". Valluvam shall mean "**Divine language Script"** or **e-Logic.**

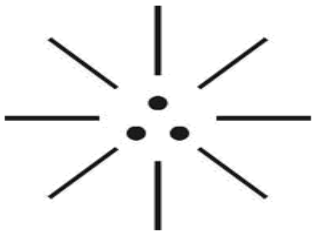

TRIPHTHONG SCRIPT
(வள்ளுவம்)

i) Right dot indicates **'vowel'**
ii) Left dot indicates **'consonant'**
iii) Centre dot indicates **'vibration'**

Millions of philosophies written in a single script shall be described as below:

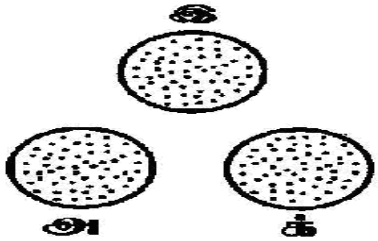

(VALLUVAM PHILOSOPHIES)

It is further focused that the prehistoric human populations lived in white planet shall be considered having distinguished genetic characteristics compared to so called modern human and called as **'ALIEN POPULATION' (or) 'AKKILEN RACE"** who belong to **'Angel Family** and capable of **'FLYING".**

*"**VALLUVAM** shall be considered as Divine Script of **Alien** Population of white planet and subsequently descended to Earth planet which was translated by **Akathiar Population in PALM LEAF MANUSCRIPT**"*

…M. Arulmani, Tamil Based Indian

2. Key Words:

a) Philosophy of "**VALLUVAM**" (e-Logic)?...
b) Philosophy of "**AKATHIAM**" (Philosophy)?...
c) Philosophy of "**KAPPIAM**" (Epic poem)?...
d) Philosophy of "**AVVAI**" (White planet)?...

3. Introduction:

Case study shows that the **origin and evolution** of various language, grammar, script across the world have many concepts and theories. In Tamil language **"Tholkappiam**" is considered as one of the five great epics which focus the high grammar value of Tamil language. **"Thirukkural"** is considered focus about **"Ethic value and morals"** about human life system which was translated in various global level languages. Further **LLIAD, ODYSSEY** in Greek, **LUSIADS** in Portuguese also considered as ancient famous epics. Further various religious texts like **BIBLE, QURAN, RAMAYANAM, MAHABHARATHAM, BHAGAVAT GITA** etc. shall also be considered as focusing Planetary system, Ethical, moral values of Ancient human life system. **If so…..**

i) **What was the first language script?....**
ii) **What was the first Ethical Text?...**

In **Tamil language research** some scholar debates that **Tholkappiam** is not the most ancient text and it may belong to the period between **3rd to 10th century AD.** Some scholar even debate that **"Tholkappiam itself was not written by Tholkappiar"** and probably a **Translated Version** by eminent scholar**.**

This research focus that the **language, script** on the Earth planet shall be considered **descended** from the **AKKILEN RACE** of White planet which shall be considered translated from **Super Solid Stone culvert** (Tablet) into **Palm leaf and other scripts** in various occasions in various languages.

4. Hypothesis and Narrations

a) Philosophy of Valluvam?...

It is hypothesized that **"Valluvam"** shall be considered as the Divine Script written by **Akkilen Populations**. The Divine script shall be considered as **"SOUL**" of language script derived from supernatural **"SPIRIT**". In proto Indo Europe language the supernatural spirit, Divine script shall be called as **"CHITTAM" "VALLUVAM**" as described below:

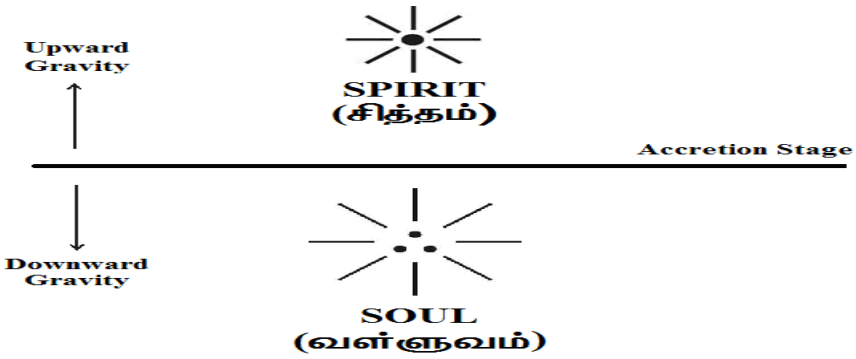

Further the **divine script** Valluvam shall be considered as exist in "**three-in-one"** form called as science of **Ethics**, Science of **Logics**, having distinguished characteristics like **photon, Electron, Proton** of fundamental particles.

i) Right dot is like **proton (**Functional property)
ii) Left dot is like **Electron** (Structural property)
iii) Centre dot is like **photon** (Control property)

It is further focused that the **three-in-one** script shall be considered focusing three-in-one personality traits of human life system (i.e.) **MORAL, CHARACTER, CONDUCT.**

b) Philosophy of AKATHIAM?...

It is hypothesized that **"AKATHIAM**" shall be considered as **"Transformed soul**" of white planet to Earth planet during pre-vedic period (say 5,00,000 years ago) as described below. In Proto Indo Europe language AKATHIAM shall mean **"AKKARATHI".** Akkarathi shall mean "**ETHICS**".

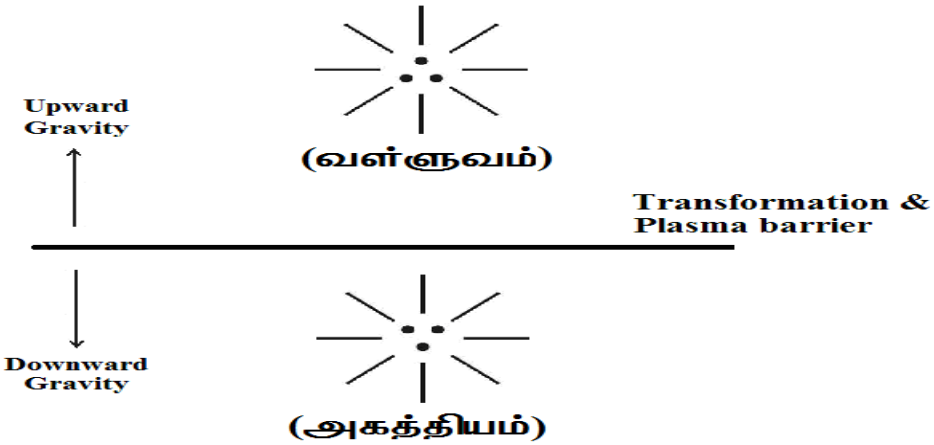

"Akathiam shall be considered as the transformed script translated in the form of Palm Leaf Script. The transformed script shall be considered as available only part and many missing scripts are yet to be traced and translated'.

…Author

c) Philosophy of Alien population?...

It is hypothesized that **Akkilen race** shall be considered as Divine population (or) Godly persons evolved due to impact of **'J-RADIATION'** (Zero hour radiation). The **Akkilen population** shall also be called as **"Thiri Valluvar"**, having exorbitant strength and high moral values. Thiri Valluvar shall mean born of **"Virgin light".**

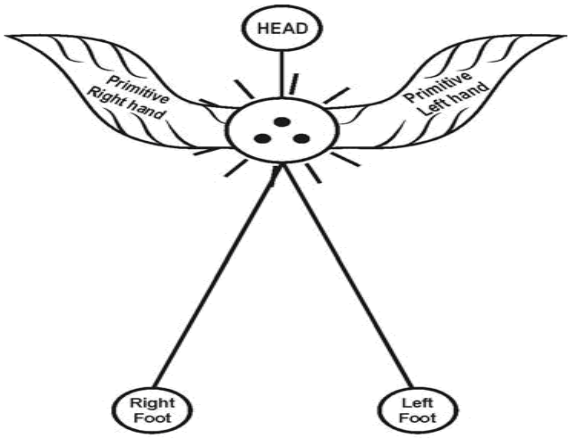

It is further hypothesized that **"KACHCHA THEEVU"** shall be considered as the **first land origin** (virgin land) on the earth planet and the **Akathiar race** populations (also called as Akkanna populations) shall be considered as **species** to Akkilen populations race of white planet.

d) Philosophy of Kappiam?...

It is hypothesized that various global level poems, epics, religious texts might have been written based on philosophy of **VALLUVAM, AKATHIAM** during the course of time.

> *"The philosophy of Thokappiam, Thirukkural, odyssey might belong to post Vedic period of about 2500 years ago. The philosophy of Valluvam might belong to period about 5,00,000 years ago"*
>
> ***…Author***

e) Philosophy of 12th Tamil Alphabet?...

It is hypothesized that 12th **Sentamil Alphabet "AUV"** might dialectically indicate the prehistoric divine script **"VALLUVAM".**

Further the etymology of English word **"Oh", "Vow", "Ah"** used in various poems for emotional expressions might be derived from the philosophy of 12th Tamil Alphabet **"AUV"**.

(i)

(oh)

(ii)

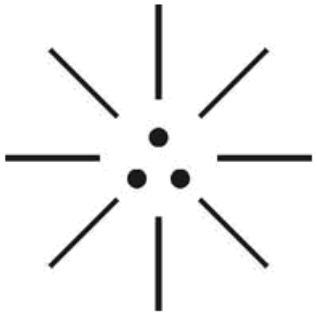

(vow)

It is focused that the Philosophy of word **vow** means solemn promise, pledge, sacred covenant, affirmation associated with moral, character, conduct shall be considered derived from the THREE-IN-ONE Philosophy of "**VALLUVAM**".

f) Tholkappiar is senior to Thiruvalluvar?...

Case study shows that Thiruvalluvar lived during third century BC in Chennai (Mylapore). Tholkappiar is believed to have lived in Kanyakumari District before the period of Thiruvalluvar. Many scholars including **Robert Caldwell** argue that Tholkappiar might have lived around **5th to 10th Centure AD.**

Further Case Study shows that epics of Tholkappiar written in **high grammatical form** further in Tholkappiam it indicates both **Sentamil** and **Kodum Tamil** which means Tholkappiam might have been written after evolution of Tamil language to the state of Sentamil.

It is hypothesized by the Author that Tholkappiar can not be senior to Thiruvalluvar and probably lived during **post vedic period** (After 5th Century) after evolution of more value in grammar in Tamil Language. Whereas the Thirukkural written by Thiruvalluvar has more **ethical, moral value** rather than grammatical value. Hence it is emphasized that Thiruvalluvar might have lived prior to Tholkappiar (say 3rd Century BC).

g) Philosophy of AVVAI?...

In Tamil history case study shows that there were three ancient female poets exist in the name of **"AVVAIYAR"** one belong to Sangam period, (2nd Century) 2nd belong to chola king period (13th Century) and another one is not exactly known.

It is hypothesized that **'AVVAI**" shall be considered belong to Divine population of **Akkilan race** lived in white planet. In proto Indo Europe language "**Avvai"** shall mean **white planet**. **"POOVAI**" shall mean **Earth planet**. The philosophy of **"Avvaiyar"** might be derived from the philosophy of "AVVAI".

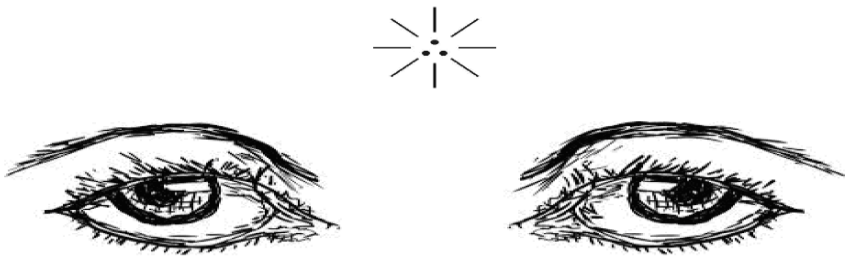

அவ்வை

(VALLUVAM)

It is speculated that after eating "NELLIKANI" Akkilen populations of white planet might be descended to Earth planet subsequently. The philosophy of **transformed populations** shall be hypothetically described as below:

(i)

DIVINE SCRIPT
(வள்ளுவம்)

(ii)

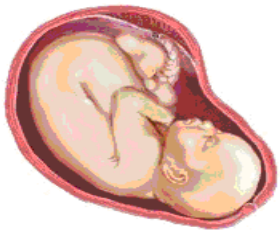

TRANSFORMATION
(அகத்தியம்)

(iii)

THOLKAPPIAR
(காப்பியம்)

h) Case Study on Thiruvalluvar?...

It is hypothesized that the Tamil Scholar **Thiruvalluvar** lived around 3rd Century BC might might have translated the predefined philosophies in three sections **ARAM** (Virtues), **PORUL (**Wealth), **INBAM (Love)** based on "**VALLUVAM".** Thirukkural has only 1330 couplets?... No… No… No… It is hypothesized that Thiruvalluvar might have translated only 1330 philosophies during his period and many more millions of philosophies missing are yet to be identified and translated.

i) Case study on palm leaf manuscript?...

Case study shows that U.V.Swaminatha Iyer (1885-1942) has given much contributions to Tamil in translating ancient **palm leaf manuscript** into reprint in Text book form.

Further **UNESCO** has a project to preserve the palm leaf manuscript of Asia called **"Memory of Asia**". A recent survey says that there are hundred thousands unpublished palm leaf manuscript of Traditional Indian knowledge in Tamil in various fields such as **Astrology, Astronomy, Medicine, Human Anatomy** etc.

(i)

(ii)

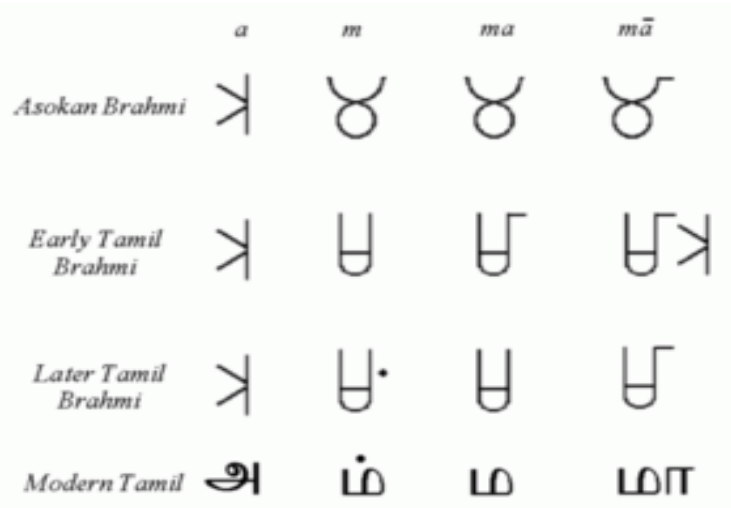

(iii)

V .CONCLUSION:

The philosophy of "**Valluvam**" shall be considered as Divine Script engraved in **super solid stone** (Tablet) about various philosophies of Astronomy, Human life system, medicine etc. Valluvam shall alternatively mean **"SOUL"** or **"THAMIL".**

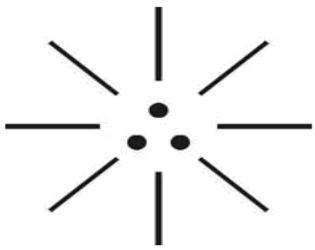

(தமிழ்)

"Tholkappiar does not mean the poet who copied the predefined philosophies. He shall be considered as ***a great poet*** *(Kaviperarasu) who translated the philosophies in high grammatical way in* ***three books*** *for the benefit of younger generations".*

…Author

5. Previous Publication:

The philosophy of origin of first life and human, the philosophy of model Cosmo Universe, the philosophy of fundamental neutrino particles have already been published in various international journals mentioned below. Hence this article shall be considered as **extended version** of the previous articles already published by the same author.

[1] Cosmo Super Star – IJSRP, April issue, 2013

[2] Super Scientist of Climate control – IJSER, May issue, 2013
[3] AKKIE MARS CODE – IJSER, June issue, 2013
[4] KARITHIRI (Dark flame) The Centromere of Cosmo Universe – IJIRD, May issue, 2013
[5] MA-AYYAN of MARS – IJIRD, June issue, 2013
[6] MARS TRIBE – IJSER, June issue, 2013
[7] MARS MATHEMATICS – IJERD, June issue, 2013
[8] MARS (EZHEM) The mother of All Planets – IJSER, June issue, 2013
[9] The Mystery of Crop Circle – IJOART, May issue, 2013
[10] Origin of First Language – IJIRD, June issue, 2013
[11] MARS TRISOMY HUMAN – IJOART, June issue, 2013
[12] MARS ANGEL – IJSTR, June issue, 2013
[13] Three principles of Akkie Management (AJIBM, August issue, 2013)
[14] Prehistoric Triphthong Alphabet (IJIRD, July issue, 2013)
[15] Prehistoric Akkie Music (IJST, July issue, 2013)
[16] Barack Obama is Tamil Based Indian? (IJSER, August issue, 2013)
[17] Philosophy of MARS Radiation (IJSER, August 2013)
[18] Etymology of word **"J"** (IJSER, September 2013)
[19] NOAH is Dravidian? (IJOART, August 2013)
[20] Philosophy of Dark Cell (Soul)? (IJSER, September 2013)
[21] Darwin Sir is Wrong?! (IJSER, October issue, 2013)
[22] Prehistoric Pyramids are RF Antenna?!... (IJSER, October issue, 2013)
[23] HUMAN IS A ROAM FREE CELL PHONE?!... (IJIRD, September issue, 2013)
[24] NEUTRINOS EXIST IN EARTH ATMOSPHERE?!... (IJERD, October issue, 2013)
[25] EARLY UNIVERSE WAS HIGHLY FROZEN?!... (IJOART, October issue, 2013)
[26] UNIVERSE IS LIKE SPACE SHIP?!... (AJER, October issue, 2013)
[27] ANCIENT EGYPT IS DRAVIDA NAD?!... (IJSER, November issue, 2013)
[28] ROSETTA STONE IS PREHISTORIC "THAMEE STONE" ?!... (IJSER, November issue, 2013)
[29] The Supernatural "CNO" HUMAN?... (IJOART, December issue, 2013)
[30] 3G HUMAN ANCESTOR?... (AJER, December issue, 2013)
[31] 3G Evolution?... (IJIRD, December issue, 2013)
[32] God Created Human?... (IJERD, December issue, 2013)
[33] Prehistoric "J" – Element?... (IJSER, January issue, 2014)
[34] 3G Mobile phone Induces Cancer?... (IJERD, December issue, 2013)
[35] "J" Shall Mean "JOULE"?... (IRJES, December issue, 2013)
[36] "J"- HOUSE IS A HEAVEN?... (IJIRD, January issue, 2014)
[37] The Supersonic JET FLIGHT-2014?... (IJSER, January issue, 2014)
[38] "J"-RADIATION IS MOTHER OF HYDROGEN?... (AJER, January issue, 2014)
[39] PEACE BEGINS WITH "J"?... (IJERD, January issue, 2014)
[40] THE VIRGIN LIGHT?... (IJCRAR, January issue 2014)

[41] THE VEILED MOTHER?... (IJERD, January issue 2014)
[42] GOD HAS NO LUNGS?... (IJERD, February issue 2014)
[43] Matters are made of Light or Atom?!... (IJERD, February issue 2014)
[44] THE NUCLEAR "MUKKULAM"?... (IJSER, February issue 2014)
[45] WHITE REVOLUTION 2014-15?... (IJERD, February issue 2014)
[46] STAR TWINKLES!?... (IJERD, March issue 2014)
[47] "E-LANKA" THE TAMIL CONTINENT?... (IJERD, March issue 2014)
[48] HELLO NAMESTE?... (IJSER, March issue 2014)
[49] MOTHERHOOD MEANS DELIVERING CHILD?... (AJER, March issue 2014)
[50] E–ACHI, IAS?... (AJER, March issue 2014)
[51] THE ALTERNATIVE MEDICINE?... (AJER, April issue 2014)
[52] GANJA IS ILLEGAL PLANT?... (IJERD, April issue 2014)
[53] THE ENDOS?... (IJERD, April issue 2014)
[54] THE "TRI-TRONIC" UNIVERSE?... (AJER, May issue 2014)
[55] Varied Plasma Level have impact on "GENETIC VALUE"?... (AJER, May issue 2014)
[56] JALLIKATTU IS DRAVIDIAN VETERAN SPORT?... (AJER, May issue 2014)
[57] Human Equivalent of Cosmo?... (IJSER, May issue 2014)
[58] THAI-e ETHIA!... (AJER, May issue 2014)
[59] THE PHILOSOPHY OF "DALIT"?... (AJER, June issue 2014)
[60] THE IMPACT OF HIGHER QUALIFICATION?... (AJER, June issue 2014)
[61] THE CRYSTAL UNIVERSE?... (AJER July 2014 issue)
[62] THE GLOBAL POLITICS?... (AJER July 2014 issue)
[63] THE KACHCHA THEEVU?... (AJER July 2014 issue)
[64] THE RADIANT MANAGER?... (AJER July 2014 issue)
[65] THE UNIVERSAL LAMP?... (IJOART July 2014 issue)
[66] THE MUSIC RAIN?... (IJERD July 2014 issue)
[67] THIRI KURAL?... (AJER August 2014 issue)
[68] THE SIXTH SENSE OF HUMAN?... (AJER August 2014 issue)
[69] THEE… DARK BOMB?... (IJSER August 2014 issue)
[70] RAKSHA BANDHAN CULTURE?... (IJERD August 2014 issue)
[71] THE WHITE BLOOD ANCESTOR?... (AJER August 2014 issue)
[72] THE PHILOSOPHY OF "ZERO HOUR"?... (IJERD August 2014 issue)
[73] RAMAR PALAM?... (AJER September 2014 issue)
[74] THE UNIVERSAL TERRORIST?... (AJER September 2014 issue)
[75] THE "J-CLOCK"!... (AJER September 2014 issue)
[76] "STUDENTS" AND "POLITICS"?... (IJERD October 2014 issue)
[77] THE PREGNANT MAN?... (AJER September 2014 issue)
[78] PERIAR IS ATHEIST?... (IJSER September 2014 issue)
[79] A JOURNEY TO "WHITE PLANET"?... (AJER October 2014 issue)
[80] Coming Soon!... (AJER October 2014 issue)

[81] THE PREJUDICED JUSTICE?... (IJERD October 2014 issue)

[82] BRITISH INDIA?... (IJSER October 2014 issue)

[83] THE PHILOSOPHY OF "HUMAN RIGHTS"?... (IJERD October 2014 issue)

[84] THE FOSTER CHILD?... (AJER October 2014 issue)

[85] WHAT DOES MEAN "CRIMINAL"?... (IJSER October 2014 issue)

[86] 1000 YEARS RULE?... (AJER November 2014 issue)

[87] AM I CORRUPT?... (IJSER November 2014 issue)

[88] BLACK MONEY?... (AJER November 2014 issue)

[89] DEAD PARENTS ARE LIVING ANGELS?... (IJERD November 2014 issue)

[90] MICHAEL IS CHIEF ANGEL?... (AJER November 2014 issue)

[91] LONG LIVE!... (IJERD November 2014 issue)

REFERENCE

[1]. Intensive Internet "e-book" study through, Google search and wikipedia
[2]. M.Arulmani, "3G Akkanna Man", Annai Publications, Cholapuram, 2011
[3]. M. Arulmani; V.R. Hemalatha, "Tamil the Law of Universe", Annai Publications, Cholapuram, 2012
[4]. Harold Koontz, Heinz Weihriah, "Essentials of management", Tata McGraw-Hill publications, 2005
[5]. M. Arulmani; V.R. Hemalatha, "First Music and First Music Alphabet", Annai Publications, Cholapuram, 2012
[6]. King James Version, "Holy Bible"
[7]. S.A. Perumal, "Human Evolution History"
[8]. "English Dictionary", Oxford Publications
[9]. Sho. Devaneyapavanar, "Tamil first mother language", Chennai, 2009
[10]. Tamilannal, "Tholkoppiar", Chennai, 2007
[11]. "Tamil to English Dictionary", Suravin Publication, 2009
[12]. "Text Material for E5 to E6 upgradaton", BSNL Publication, 2012
[13]. A. Nakkiran, "Dravidian mother", Chennai, 2007
[14]. Dr. M. Karunanidhi, "Thirukkural Translation", 2010
[15]. "Manorama Tell me why periodicals", M.M. Publication Ltd., Kottayam, 2009
[16]. V.R. Hemalatha, "A Global level peace tourism to Veilankanni", Annai Publications, Cholapuram, 2007
[17]. Prof. Ganapathi Pillai, "Sri Lankan Tamil History", 2004
[18]. Dr. K.K. Pillai, "South Indian History", 2006
[19]. M. Varadharajan, "Language History", Chennai, 2009
[20]. Fr. Y.S. Yagoo, "Western Sun", 2008
[21]. Gopal Chettiar, "Adi Dravidian Origin History", 2004
[22]. M. Arulmani; V.R. Hemalatha, "Ezhem Nadu My Dream" - (2 Parts), Annai Publications, Cholapuram, 2010
[23]. M. Arulmani; V.R. Hemalatha, "The Super Scientist of Climate Control", Annai Publications, Cholapuram, 2013, pp 1-3

American Journal of Engineering Research (AJER) ***2014***
American Journal of Engineering Research (AJER)
e-ISSN : 2320-0847 p-ISSN : 2320-0936
Volume-03, Issue-12, pp-34-40
www.ajer.org

Research Paper Open Access

Investigation on Thermal Properties of Composite of Rice Husk, Corncob and Baggasse for Building Thermal Insulation

Kyauta E.E. Dauda D.M. and Justin E
Deparment of Mechanical/Production Engineering
Abubakar Tafawa Balewa University, Bauchi. Nigeria/

ABSTRACT: *The thermal properties of some Agricultural waste (Rice Husk, Bagasse and Corncob) was investigated with the purpose of determining their use as insulators. Using varied composite percentages of each sample wastes at increasing and decreasing quantities to determine best mixtures has assisted in accurate recommendation. The work has explored the potentials for using composite samples of Rice Husk, Bagasse and Corncob as materials for thermal insulation, a solution which offers a reduction in resource use, promote recycle of the wastes, less dependent on toxic chemical types in wood/cellulose based insulators, in addition to reducing energy consumed by altering internal air conditions.The criteria for evaluation includes experimental determination of Thermal Conductivities and Specific Heat Capacities for composites samples and other dependable properties.The results from evaluations have identified that sample G with 0.231Wm^{-1}k^{-1}and 22.114m^{-1} is the best mixed with more rice husk and considerable percentage of bagasse to less percentage of corncob.*

Keywords. *Agricultural Waste, Thermal properties, composites, insulation.*

I. INTRODUCTION

. .For quite some time many buildings seems not to be habitable due to the uncontrollable environmental conditions. Hence the use of artificial air conditioning and the need for cheaper, faster cooling condition around oneself has becomes a necessity. Energy demand in building can be significantly reduced with the use of thermal insulation. The use of thermal insulation in walls and roofs can reduce the demand for air conditioning thereby reducing the cost of cooling and pollution of the environment.(Panyakaew and Fotios 2008, Radhi 2008,)

Municipal and Rural Affairs Minister of Saudi kingdom Prince Mansour bin Miteb announced on 22 october 2014 at the opening of the Saudi Energy Efficiency Forum and Exhibition 2014, being held at the Riyadh International Convention and Exhibition Center. that the government would soon make it mandatory for buildings to have thermal insulation in 24 major cities to save on rising energy costs. According to him about 70 percent of residential buildings in the country lack thermal insulation."Thermal insulation will rationalize the consumption of energy and bring many benefits to the country and its citizens. but the development of new thermal insulation material requires knowledge of the thermo-physical properties of materials.

The use of inorganic insulating materials may be harmful to human health and body and causes environmental pollution. (Liang and Ho, 2007). The production of these materials will require high energy consumption and the eventual disposal can cause environmental hazard (Panyakaew and Fotios, 2008).

Common thermal insulators are fiberglass, rock wool and mineral wool, but they are environmentally hazardous. The small particles from fiber glass and glass wool insulation can cause health hazard and respiratory or skin irritant (OSHA, 2003) most thermal insulation baths contain formaldehyde resin that can cause asthma (US EPA 2000) cellulose insulation with toxic, fire-retarding chemicals like boric acid have been identified as having the potential for significant health effects (OSHA,1999).

Thermal insulation materials must contain the following physical properties, low thermal conductivity, moisture protection and mould and fire resistance. In addition to these environmental and health impact must also be considered. Since current popular insulation materials have negative side effects from the production stage until the end of their useful lifetime (Papadopoulos, A.M., 2005) the search for alternative insulation materials become necessary. Therefore the alternatives materials with same or better properties as the conventional materials need to be exploded as it can offer lower cost (Moh'd Yakama et al 2011), one of the alternative materials that is being widely investigated is natural fiber which is cheap and easy to get (Guilbert et al 2011). Renewable fibrous thermal insulation from trees, plant or animals has the ability to regenerate itself and it requires less energy for production and biodegrade easily when disposed as waste hence have low environmental impact. (Mamohar, 2012). Using agricultural by products as thermal insulation also generates economical development for farming in rural areas. (Panyakaew and Fotios 2008).A cheap reliable and abundant supply of biodegradable fibrous materials can be obtained as waste by-products from many commercial agricultural processing industries (Rodriguez et al 2011). Materials such as coconut and sugarcane fiber, cotton, wheat straw, palm leaves, oil palm fiber and others consist of lignocelluloses fibers which are alternatives. They are biodegradable, renewable, environmentally friendly building thermal insulators. (Zhou et al 2010).

Agricultural wastes such as rice hulls, sugarcane stalks, coconut husk, corn cob or stalk oil palm shell and leaves or straw from cereal crops have high degree of fibrous content (lingo-cellulosic compound) and can serve as the main ingredient for composite materials making them suitable for manufacturing boards or panels. Baggase can be made into soft bearch, medium density hardboard or particle boards as well as high density hardboards (26) The aim of this research is to investigate the potential of agricultural waste as thermal insulation materials.

II. MATERIALS AND METHODS

2.1. Apparatus

The HILTON Thermal Conductivity Apparatus at Thermodynamics Laboratory of Abubakar Tafawa Balewa University Bauchi was used. The linear section was used to determine thermal conductivity of the samples under investigation. Cooling water was feed into one side of the apparatus to maintain a steady gradient.

The instrumentation provided permits accurate measurement of temperature and power supply. Quick response temperature probes, with a resolution of 0.1^{o} C gives an accurate digital readout in degrees centigrade. On the apparatus, a power control to provide continuous variable electrical output of 0-100 watts with direct readout was made available

2.2. Materials and Sample Production

The materials were collected at the Muda Lawal market and Yelwa metropolis. They were screened for dirt (sands and grease) and other impurities. They were cleaned and grinded to smaller particle sizes of 0.075mm Larger unmeshed particles were re-grinded and sieved again until uniform sizes were obtained. Sample mixed in various percentages were also combined with 5% binder (starch)/water) to ensure proper compaction. The total mixtures were filled into the mould and compacted and allowed to dry for some hours and was cured under the sun for 2 to 5 days (depending on atmospheric condition). A total of nine samples were produced in different percentage composition as shown in Table 1. Below.

Plate A. P.A Hilton Thermal Conductivity Apparatus

Plate B. Pictorial Views of Sample after Curing.

Table 1: Composition of Samples Mixture in Percentages

Samples	Rice husk %	Corncob %	Bagasse %
Sample A:	40	30	30
Sample B:	30	30	40
Sample C:	30	40	30
Sample D:	50	25	25
Sample E:	25	25	50
Sample F:	25	50	25
Sample G:	60	20	20
Sample H:	20	20	60
Sample I:	20	60	20

2.3. Determination of Thermal Conductivity

The HILTON Heat Conduction apparatus was used to measure Heat across a circular sample linearly under various temperatures; it was also used to carry out the Thermal Conductivity measurement across our composite samples,

The temperature displayed on the apparatus in conduction experiments were read from six sensor point as named T_1,T_2,T_3,T_7,T_8 and T_9. These describe temperature profile across heater, sample and cold section. The Power from heater was kept at 15W.

Thermal Conductivity was computed by running a script on MATLAB using the six sensor readings Tabulated on Table 2. Extrapolation between T_4 and T_6 was done to obtain accurate results. Using MATLAB (scripted code), it generated corresponding polynomials to match T_1,T_2 and T3 for hot section to the right above and T_7,T_8 and T_9 cool section below the graph to the left.

III. RESULTS

Table 2. Thermal Properties of Composite Sample of Rice Husk, Bagasse and Corncob

Sample	Thermal Conductivity (k) $Wm^{-1}K^{-1}$	Specific heat Capacity (c) $Jkg^{-1}K^{-1} \times 10^{3}$	Thermal Resistivity (r) $W^{-1}mk$
Standard Error	**±0.002**	**±0.006**	**±0.1367**
Sample A	0.2749	1.7393	3.6377
	0.3188	1.8610	3.1368
Mean value	**0.29685**	**1.8002**	**3.38725**
Sample B	0.3058	1.1644	3.2701
	0.3142	1.2847	3.1827
Mean value	**0.31**	**1.22455**	**3.2264**
Sample C	0.3768	1.9853	2.6539
	0.3741	1.9162	2.6731
Mean value	**0.37545**	**1.95075**	**2.6635**
Sample D	0.3059	1.1510	3.2690
	0.3363	1.2076	2.9735
Mean value	**0.3211**	**1.1793**	**3.12125**
Sample E	0.2461	0.5775	4.0634
	0.2566	0.7758	3.8971
Mean value	**0.25135**	**0.67665**	**3.98025**
Sample F	0.4445	0.9336	2.2497
	0.5440	0.8877	1.8382
Mean value	**0.49425**	**0.91065**	**2.04395**
Sample G	0.1961	1.1569	5.0994
	0.2660	1.3138	3.7594
Mean value	**0.23105**	**1.23535**	**4.4294**
Sample H	0.3045	0.6613	3.2841
	0.2729	0.8427	3.6644
Mean value	**0.2887**	**0.752**	**3.47425**
Sample I	0.3415	0.6833	2.9283
	0.3085	0.4522	3.2415
Mean value	**0.325**	**0.56775**	**3.0849**

Table 3: Table of Samples Parameters as Determine after Production

Sample	Specimen	Weight kg (10^{-3})	Thickness m (10^{-2})	Diameter m (10^{-2})	Area m^2 (10^{-3})	Volume m^3 (10^{-6})	Density Kg/m^3
Sample A	1	3.0	0.39	4.3	2.904	5.663	529.76
	2	3.6	0.40	4.1	2.641	5.280	681.82
Sample B	1	3.5	0.40	4.1	2.641	5.280	662.88
	2	3.5	0.40	4.1	2.641	5.280	662.88
Sample C	1	4.6	0.50	4.1	2.641	6.600	696.96
	2	4.5	0.50	4.1	2.641	6.60	681.82
Sample D	1	4.3	0.50	4.1	2.641	6.60	651.52
	2	4.3	0.50	4.1	2.641	6.60	651.52
Sample E	1	4.3	0.40	4.6	3.324	6.65	646.62
	2	4.5	0.40	4.5	3.181	6.36	707.55
Sample F	1	5.5	0.40	4.4	3.041	6.08	904.61
	2	5.7	0.40	4.4	3.041	6.08	937.50
Sample G	1	5.8	0.45	5.0	3.927	8.84	656.11
	2	5.8	0.50	4.5	3.181	7.95	729.55
Sample H	1	7.3	0.50	4.6	3.324	8.31	878.46
	2	7.3	0.45	4.5	3.181	7.16	1019.55
Sample I	1	8.0	0.50	4.3	2.904	7.26	1101.93
	2	6.6	0.50	4.5	3.181	7.95	830.19

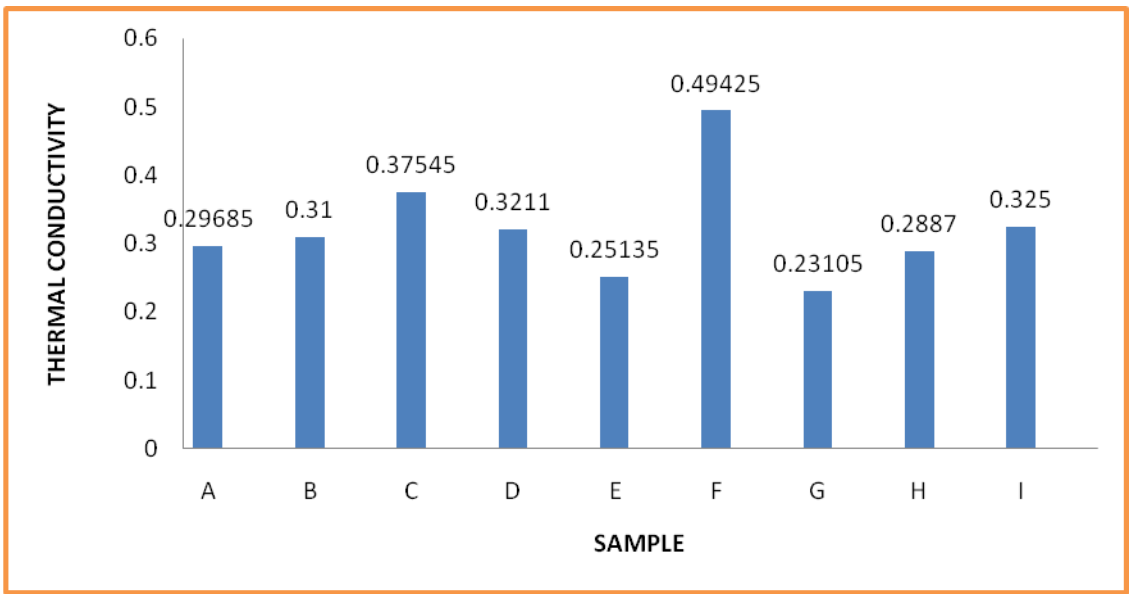

Fig.1. Distribution of Sample's Thermal Conductivity

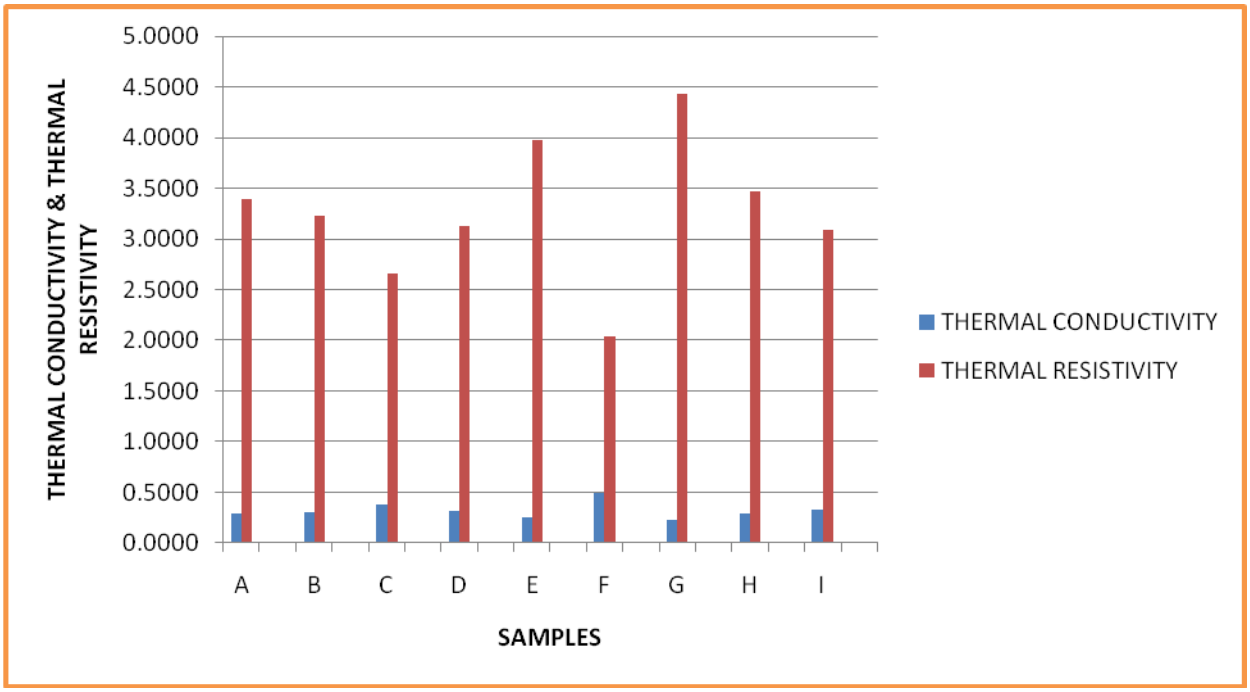

Fig. 4. A Bar chart comparing Thermal conductivity and Thermal resistivity.

IV. DISCUSSION OF RESULTS.

The three key qualities of a thermal insulation material derived from agricultural waste are resource availability, physical properties and environmental impact. Critical physical properties include resistance to fire, mould growth, insect damage and biodegradable. Baggasse has low thermal conductivity and it is environmentally friendly it can be made into boards or panels without using any chemical resin.

Comparing Table 2 and Fig 1. results with the documented values for common wood- based/cellulose insulating material as given by J. Twidell and T.Weir which shows the following thermal conductivity, Asbestos cement sheet 0.319 $W^{-1}mK$ brick building 0.600 $W^{-1}mK$ pine wood 0.138 $W^{-1}mK$ and oak wood 0.160 $W^{-1}mK$. It proofs that our samples fall within the same range. Similarly comparing the computed values on Table 2 with those given for wood-based insulating materials, we have the required ranges as 0.735-8.130 $W^{-1}mK$ which is satisfied by all our sample values. Samples B and E shows bagasse stops at 50% and shows no improvement at high quantity 60% sample H while sample C, F and I with corncob increasing is seen dangling up and downwards.

Fig 4. Shows the results of thermal conductivity and thermal resistivity. It proofs that an increase in thermal resistivity reduces thermal conductivity. Hence increasing the thermal resistivity of a material will lower its thermal conductivity thereby making it a suitable insulation material.

V. CONCLUSION

The bases for recommendation as substitute or replacement are considered under these three key qualities. They are resources availability, physical properties, and environmental impacts when using these waste considered (Rice husk, Bagasse and Corncob). The used of these material cals reduces the risk of environmental pollution. Also we have been able to show that these wastes can be used for the production of panels or broad sheet of required thickness for used as walling materials or thermal resistant materials.

In proving that all samples passed each tests and recommended ranges, it shows that it favors insulation materials for naturally cooled design in sub/tropical region.

Recommendation

In establishing conclusion based on values in this research, a temperature of 120^{o}C was set as optimum; in that regard further studies could be based on sample breaking point instead of getting samples to meet required ranges for acceptance as class A products. These studies could check other life cycle analysis (LCA) method apart from those used in this research work. Also considering Damages Impact approach over various samples to it life cycle. Furthermore the threshold point when all samples fails in each individual properties due to their percentage mixture composition.

REFERENCES

[1]. J. Twidell and T. Weir, "Renewable Energy Resources". London: E. and F. N. Sponse, 1990, pp. 418.

[2]. Panyawai, S. Chaikin D and Boonsong A. (2006). The Thermal Insulators Fabricated from natural agricultural waste. Power engineering Technology Bongkok, king Mongkut's institute of technology.

[3]. Zhou X, Zheng P.Z. Li. H. Lu. C. (2010) An environmentally friendly insulation material from cotton stalk fibers energy and building 42 1070-1074.

[4]. Rodriguez N.J. Yawez Limon M. Guttcerrez Micella, F.A. Gomez – Guzman O. Matadamas-Otiz T.P (2011) assessments of cocoa nut fibre insulation characteristics and its use to modulate temperatures in concrete slabs with the aid of finite element methodology energy and building 43, 1264 – 1272.

[5]. Guilbert, S., Guillaume, C., Gontard, N. (2011). New packaging materials based on renewable resources: properties, applications and prospects. Food Engineering Interfaces. Food Engineering Series, Springer, Part 5, 619-630.

[6]. Liang, H.H., Ho, M.C. (2007). Toxicity characteristics of commercially manufactured insulation materials for building applications in Taiwan. Construction Building Materials, 21, 1254-1261.

[7]. Manohar, K. (2012). Renewable building thermal insulation – oil palm fibre. International Journal of Engineering and Technology, 2(3), 475-479.

[8]. Mohd Yuhazri, Y.Y., Sihombing, H., Jeefferie, A.R., Ahmad, M.A.Z., Balamurugan, A.G., Norazman, M.N., Shohaimi, A. (2011). Optimization of coconut fibers toward heat insulator applications. Global Engineers & Technologist Review, 1(1), 35-40.

[9]. Panyakaew, S., Fotios, S. (2008). Agricultural waste materials as thermal insulation for dwellings in Thailand. Preliminary Results, PLEA 2008–25th Conference on Passive and Low Energy Architecture, Dublin, 22nd to 24th October 2008.

[10]. Radhi, H. (2008). A systematic methodology for optimizing the energy performance of buildings in Bahrain. Energy Building, 40, 1297-1303.

[11]. Panyawai, S., Chaiken, D. and Boonsong, A. (2006) The Thermal Insulators Fabricated from Natural Agricultural Waste.*Power Engineering Technology*. Bangkok, King Mongkut'sInstitute of Technology

[12]. ISO 14040 (1997) Environmental management - Life cycleassessment - Principles and frame-work. *ISO/FDIS 14040(1997a).* Geneva, Switzerland.

[13]. CEPMC (2000) Guidance for the Provision of EnvironmentalInformation on Construction Products. Brussels, Council forEuropean Producers of Materials for Construction.

[14]. Barbara, C. L. (2007) Building for Environmental and Economic Sustainability (BEES 4.0). National Institute of Standards and Technology (NIST), Technology Administration,U.S. Department of Commerce.

[15]. Frenel Capital (2007) http://www.searates.com/reference/portdistance/.

[16]. Department of Highway (2007) http://www.doh.go.th/dohweb/ data/data_1.html.

[17]. Pré Consultants (2007) SimaPro 7.1.5. *SimaPro Database.*The Netherlands.

[18]. Occupational Safety and Health Administration,(2003). *Synthetic Mineral Fibers: Health Hazards*. United State Department of Labor.

[19]. U.S. Environmental Protection Agency, (2000).*Health and Environmental Effect Profile forFormaldehyde*, Office of Health and EnvironmentAssessment, Office of Research andDevelopment: Cincinnati.

[20]. The U.S. Occupational Safety and HealthAdministration (OSHA), 1999. *the Health andSafety Partnership Program*, the North AmericanInsulation Manufacturers Association.

[21]. Papadopoulos, A.M., (2005). *State of art inthermal insulation materials and aims for futuredevelopments.* Energy and Building, 37: p. 77-86.

American Journal of Engineering Research (AJER)
e-ISSN : 2320-0847 p-ISSN : 2320-0936
Volume-03, Issue-12, pp-41-53
www.ajer.org

Research Paper Open Access

Pressure Distribution of Horizontal Wells in a Layered Reservoir with Simultaneous Gas Cap and Bottom Water Drives

[1]Oloro J., [2]Adewole.E.S. And [3]Olafuyi.O.A
[1]*Delta State University, Abraka,Nigeria.*
[2,3]*University of Benin, Nigeria*

ABSTRACT : *A plot of dimensionless pressure versus dimensionless time on a log-log paper was done for the six sets of data to illustrate the pressure distribution of horizontal wells in a two layered reservoir with simultaneous gas cap and bottom water drive. From the graphs it was shown that dimensionless pressure increases with dimensionless time.We also observed that when there is crossflow, pressure distribution in such reservoir is the same as that of the homogeneous system. Pressure responses in crossflow reservoir are higher than that of without crossflow.*

We also observed that the following affects the pressure distribution:
Well location along x-axis,x_{wD} ,Wellbore radius r_{wD},Interlayer fluid mobility ratio, time Normalization factor, dimensionless Well length L_D and dimensionless height h_D.
It was also observed that the well location z_{wD} along z-axis does not affect pressure distribution for two layered reservoir.Two-layer crossflow liner with Partial Isolations well completion would be recommended This method provides limited zone isolation, which can be used for stimulation or production control along the well length.
Also two-layer reservoir without crossflow with cased hole completion is recommended because it provides a high degree of the wellbore control and reservoir management.Cased hole completions are excellent for reservoirs where the horizontal well is being drilled to minimize coning problems. Perforations may be selectively squeezed off to prevent the influx of unwanted fluid.

KEY WORDS: *Well, Pressure,Layer,Reservoir,Horizontal*

I. INTRODUCTION

Production of oil from horizontal well in a layered reservoir subject to simultaneous top gas-cap and bottom water drive poses very serious challenges. The presence of a gas-cap at initial condition indicates saturated oil in equilibrium with the gas. Hence production of gas should be minimised since gas acts as the driving force like the water behind oil production Another challenge is the problem of occasioned by a permeable (crossflow) interface. Isolating each layer through a test analysis is a challenge if the layers contain oil of different properties or layers contain oil and gas .Well completion strategy has to be specially designed to achieve optimal[1] individual layer production performance. For well test analysis of pressure data, it would be required that flow from each layer is adequately quantified and delineated.It is with a view to addressing these challenges that a model was developed by combining application of instantaneous source functions and Newman product methods. to obtain dimensionless pressure distribution of horizontal wells in a layered reservoir with simultaneous gas cap and bottom water drive for sex (6) different set of reservoir and well parameters.

All integrals was evaluated numerically.(GAUSS-LEGENDRE QUADRATURE).

II. METHODOLOGY

- Dimensionless variables for horizontal well was used with instantaneous source functions were obtained for each flow period.
- In this work we treated the effect of gas cap and bottom water drive as a constant pressure condition for both top and bottom boundaries.

- The combined application of instantaneous source functions and Newman product methods was used to obtain equation for dimensionless pressure.
- Determination of flow period (Goode and Thambynayam)[2]
- Determination of interlayer fluid Mobility ratio (M)
- Time normalization factor α ,specifying equivalent flow time in layer 2 for dimensionless flow t_D in layer 1 since the layers have different response time due to different in properties.
- Computation of A_1 and A_2 using numerical method (Gauss-Legendre Quadrature)
- Value of A_1 and A_2 are substituted into Equation for dimensionless pressure and evaluated at different value of t_D to obtain the pressure distribution for each layer .
  Note: All integrals was evaluated numerically.(GAUSS-LEGENDRE QUADRATURE)

To obtain dimensionless pressure distribution of horizontal wells in a layered reservoir with simultaneous gas cap and bottom water drive .Sex (6) different set of reservoir and well parameters were used. A physical description of the problem is illustrated in fig1.0,for horizontal well, the instantaneous source function is the product of three one-dimensional instantaneous source functions is represented by a line source horizontal well in a reservoir infinite in the x and y directions and bounded by the upper and lower boundaries in the z-direction[3].

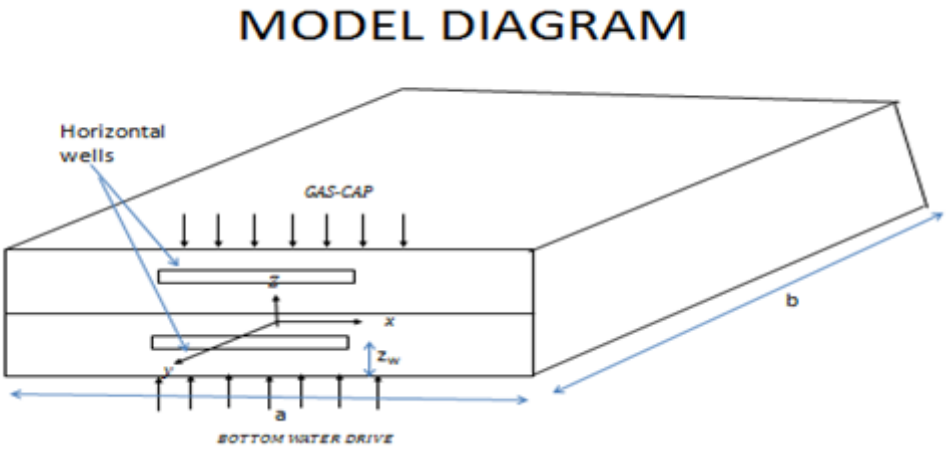

Fig.1.0 Model Diagram

Assumption

(i)Two layers reservoir (ii)Homogeneous reservoir (iii) Oil production
(iv) Negligible capillary (v) Unsteady flow of oil (vi)Slightly compressible oil production.

Dimensionless Variables

The following are dimensionless parameters used for this work.
(1)Dimensionless Pressure

$P_D = P - P(x,y,z,t)/(p - p_w)$----------1.0

(2)Dimensionless time

$$t_D = \frac{K}{\phi c_t \left(L/2\right)^2} \quad \text{----------2.0}$$

(3)Dimensionless distance in the x-direction

$$x_D = \frac{2x}{L}\sqrt{\frac{K}{k_x}} \quad \text{----------3.0}$$

(4) Dimensionless well width

$$x_y = \frac{2y}{L}\sqrt{\frac{K}{k_y}} \quad \text{----------4.0}$$

(5)Dimensionless well length

$$L_D = \frac{L}{2h}\sqrt{\frac{k_z}{k_y}} \quad \text{----------5.0}$$

(6)Dimensionless effective well bore radius

$$r_{wD} = \frac{2rw}{L}\sqrt{\frac{K}{k_X}} + \sqrt{\frac{K}{k_y}} \quad \text{----------6.0}$$

(7) Dimensionless pay thickness

$$h_D = \frac{2h}{L}\sqrt{\frac{k}{k_z}} \quad \text{----------7.0}$$

(8) Dimensionless distance in z-direction

$$z_D = \frac{2z}{L}\sqrt{\frac{K}{k_z}} \quad \text{----------8.0}$$

PRESSURE DISTRIBUTION

A general expression for dimensionless pressure for horizontal well[4].

$$P_{Dj} = 2\pi h_D \int_0^{t_D} s(x_D,\tau), s(y_D,\tau), s(z_D,\tau), \text{----9.0}$$

Mathematical Model For Layer 1

$$P_{D1} = -\frac{\beta}{4L_{D1}}\int_0^{t_D}\frac{e^{-\frac{(y_D-y_{wD1})^2+(Z_D-Z_{wD1})^2}{4\tau}}}{\tau}d\tau + 2\pi h_{D1}A_1\int_{t_{De}}^{t_{DZ}}\left[e^{-\frac{(y_{D1}-y_{wD1})^2}{4\tau}}\right]*\left[erf\frac{\left(\sqrt{\frac{K}{k_X}}-X_{D1}\right)}{2\sqrt{\tau}}+erf\frac{\left(\sqrt{\frac{K}{k_X}}-X_{D1}\right)}{2\sqrt{\tau}}\right]*$$

$$\left[1+2\sum_{n=1}^{\infty}\exp\left(\frac{n^2\pi^2\tau}{h_{D1}^2}\right)\cos n\pi\frac{Z_{D1}}{h_{D1}}\cos n\pi\frac{Z_{wD1}}{h_{D1}}\right]d\tau + 2\pi h_{D1}A_1\int_{t_{DZ}}^{t_D}\left[1+\frac{4x_{eD1}}{\pi}\sum_{n=1}^{\infty}\frac{1}{m}\exp\left(\frac{-m^2\pi^2\tau}{x_{eD1}^2}\right)\sin\frac{\pi m}{2x_{eD1}}\cos\frac{m\pi x_{eD}}{x_{eD1}}\cos\frac{m\pi x_{D1}}{x_{eD1}}\right]*$$

$$\frac{1}{y_{eD1}}\left[1+2\sum_{n=1}^{\infty}\exp\left(\frac{-m^2\pi^2\tau}{y_{eD1}^2}\right)\cos\frac{m\pi y_{wD1}}{y_{eD1}}\cos\frac{m\pi y_{D1}}{y_{D1}}*\right]*\left[\frac{2}{h_{D1}}\sum_{n=1}^{\infty}\exp\frac{\left(-(2n+1)^2\right)\pi^2\tau}{4h_{D1}^2}\cos\frac{(2n+1)\pi z_{wD1}}{h_{D1}}\cos\frac{(2n+1)\pi z_{D1}}{h_{D1}}\right]d\tau - \text{10.0.}$$

Mathematical Model For Layer 2

$$P_{D2} = -\frac{\beta}{4L_{D2}}\int_0^{t_D} e^{-\frac{(y_{D2}-y_{wD2})^2+(z_{D2}-z_{wD2})^2}{4\tau\alpha}}\frac{d\tau}{\tau} + 2\pi h_{D2}A_2\int_{t_{De}}^{t_{DZ}}\left[e^{-\frac{(y_{D2}-y_{wD2})^2}{4\tau\alpha}}\right]*\left[erf\frac{\left(\sqrt{\frac{K}{k_X}}-x_{D2}\right)}{2\sqrt{\tau\alpha}}+erf\frac{\left(\sqrt{\frac{K}{k_X}}-x_{D2}\right)}{2\sqrt{\tau\alpha}}\right]*$$

$$\left[1+2\sum_{n=1}^{\infty}\exp\left(\frac{n^2\pi^2\tau\alpha}{h_{D2}^2}\right)\cos n\pi\frac{z_{D2}}{h_{D2}}\cos n\pi\frac{z_{wD2}}{h_{D2}}\right]d\tau + 2\pi h_{D2}A_2\int_{t_{DZ}}^{t_D}\left[1+\frac{4x_{eD2}}{\pi}\sum_{n=1}^{\infty}\frac{1}{m}\exp\left(\frac{-m^2\pi^2\tau\alpha}{x_{eD2}^2}\right)\sin\frac{\pi m}{2x_{eD2}}\cos\frac{m\pi}{x_{eD2}}x_{D2}\cos\frac{\cos m\pi}{x_{eD2}}x_{D2}\right]*$$

$$\frac{1}{y_{eD2}}\left[1+2\sum_{n=1}^{\infty}\exp\left(\frac{-m^2\pi^2\tau\alpha}{y_{eD2}^2}\right)\cos\frac{m\pi}{y_{eD2}}y_{wD2}\cos\frac{m\pi}{y_{eD2}}y_{D2}\right]*\left[\frac{2}{h_{D2}}\sum_{n=1}^{\infty}\exp\frac{\left(-(2n+1)^2\right)\pi^2\tau\alpha}{4h_{D2}^2}\cos\frac{(2n+1)\pi}{h_{D2}}z_{wD2}\cos\frac{(2n+1)\pi}{h_{D2}}z_{D2}\right]d\tau \quad ---11.0$$

Constants (A_1 and A_2) at the Interface

Multiplicative factors, A_1 and A_2 are introduced such that if obtained would compensate the assumption of a constant-pressure boundary and duplicate the influence of the interface more properly.

To obtain expression for the above constant (A1 and A2), boundary conditions come to play at the interface. That is,

$P_{D1}=P_{D2}$----------12.0

$$\frac{\partial p_{D1}}{\partial z_D} = M\frac{\partial p_{D2}}{\partial z_D} \quad ----------13.0$$

From equation 3.17 and 3.18

$$A_1 = \frac{M P_{2i} V + Vd P_{2i}}{M p_i + d P_i P_{2i}} \quad ----------14.0$$

$$A_2 = \frac{V A_1 d P_i}{Md P_{2i}} \quad ----------15.0$$

Where

$$P_{2i} = 2\pi h_{D2}\int_{t_{De}}^{t_{DZ}}\left[e^{-\frac{(y_{D2}-y_{wD2})^2}{4\tau}}\right]*\left[erf\frac{\left(\sqrt{\frac{K}{k_X}}-x_{D2}\right)}{2\sqrt{\tau\alpha}}+erf\frac{\left(\sqrt{\frac{K}{k_X}}-x_{D2}\right)}{2\sqrt{\tau\alpha}}\right]*$$

$$\left[1+2\sum_{n=1}^{\infty}\exp\left(\frac{n^2\pi^2\tau\alpha}{h_{D2}^2}\right)\cos n\pi\frac{z_{D2}}{h_{D2}}\cos n\pi\frac{z_{wD2}}{h_{D2}}\right]d\tau$$

$$V = \frac{\beta}{4L_{D2}}\int_0^{t_D}\frac{(Y_D-Y_{WD2})^2+(z_{D2}-z_{WD2})^2}{4\tau}\frac{d\tau}{\tau} - \frac{\beta}{4L_{D1}}\int_0^{t_D}\frac{(Y_D-Y_{WD1})^2+(z_{D1}-z_{WD1})^2}{4\tau}\frac{d\tau}{\tau}$$

$$P_i = 2\pi h_{D1} \int_{t De}^{t DZ} \left[e^{-\frac{\left(y_{D1} - y_{wD1}\right)^2}{4\tau}} \right] * \left[erf \frac{\left(\sqrt{\frac{K}{k_X}} - X_{D1} \right)}{2\sqrt{\tau\alpha}} + erf \frac{\left(\sqrt{\frac{K}{k_X}} - X_{D1} \right)}{2\sqrt{\tau\alpha}} \right] *$$

$$\left[1 + 2 \sum_{n=1}^{\infty} \exp\left(\frac{n^2 \pi^2 \tau\alpha}{h_{D1}^2} \right) \cos n\pi \frac{Z_{D1}}{h_{D1}} \cos n\pi \frac{Z_{wD1}}{h_{D1}} \right] d\tau$$

$$dP_i = -\frac{\pi}{h_{D1}} \left[e^{-\frac{\left(Y_{D1} - Y_{WD1}\right)^2}{4\tau}} \right] * \left[erf \frac{\left(\sqrt{\frac{K}{K_x}} - x_{D1} \right)}{2\sqrt{\tau}} + erf \frac{\left(\sqrt{\frac{K}{K_x}} - x_{D1} \right)}{2\sqrt{\tau}} \right] * \left[1 + 2 \sum_{n=1}^{\infty} \exp\left(\frac{n^2 \pi^2 \tau}{h_{D1}^2} \right) \sin\left(\frac{n\pi Z_{D1}}{h_{D1}} \right) Cos\left(\frac{n\pi Z_{WD1}}{h_{D1}} \right) \right] d\tau$$

$$dP_{2i} = -\frac{\pi}{h_{D2}} \left[e^{-\frac{\left(Y_{D1} - Y_{WD1}\right)^2}{4\tau\alpha}} \right] * \left[erf \frac{\left(\sqrt{\frac{K}{K_x}} - x_{D2} \right)}{2\sqrt{\tau\alpha}} + erf \frac{\left(\sqrt{\frac{K}{K_x}} - x_{D2} \right)}{2\sqrt{\tau\alpha}} \right] * \left[1 + 2 \sum_{n=1}^{\infty} \exp\left(\frac{n^2 \pi^2 \tau\alpha}{h_{D1}^2} \right) \sin\left(\frac{n\pi Z_{D1}}{h_{D1}} \right) Cos\left(\frac{n\pi Z_{WD1}}{h_{D1}} \right) \right] d\tau$$

Interlayer Fluid Mobility Ratio:

$$M = \frac{K_1 h_1 \mu_1}{K_2 h_2 \mu_2} \quad \text{----------16.0}$$

(14) Time Normalization Factor

The term α is the time normalization factor to establish the same dimensionless time for flow in two layers of different flow behavior and is derived based on the definition of dimensionless flow times of the layers[5].The equation factor is given in equation 17.0

$$\alpha = \frac{\phi_1 c_{1t} \mu_{t1} L_1^2 K_1}{\phi_2 c_{t2} \mu_2 K_2} \quad \text{----------17.0}$$

Note:

$$t_{D2} = \alpha t_{D1}$$

Dimensionless Time Used In Horizontal Well In Terms Of L/2

$$t_D = \frac{0.0002637 \quad k \quad t}{\phi\mu \, c_t \left(\frac{L}{2} \right)^2} \quad \text{----------18.0}$$

To apply flow period equation, we substitute any of flow period in t ,in equation 1.0 above .
For example
Early-Time Radial Flow. The early-time radial flow period ends at

$$t_{e1} = \frac{190\ d_z^{2.095}\ r_w^{-0.095}\ \phi\mu\ c_t}{k_v} \quad \text{---------- 19.0}$$

Equation 18.0 is now

$$t_D = \frac{0.0002637\ k\ t_{e1}}{\phi\mu\ c_t \left(\frac{L}{2}\right)^2} \quad \text{---------- 20.0}$$

Equation 20.0 will give dimensionless value of Early-Time Radial Flow value.
Also by substituting t_{e2} and t_{e3} in equation 1.0

$$t_{e2} = \frac{20.8\phi\mu\ c_t L^2}{k_v}$$

$$t_{e3} = \frac{1230.0\phi\mu\ c_t L^2}{k_v}$$

Dimensionless values of Intermediate-time linear flow and Pseudoradial Flow can be obtained[2].

Statistical test for null significal test

The statististical test for significant differences is the t-test for two means for the results[5].

$$\sigma_{\bar{X}_1 - \bar{X}_4} = \sqrt{\frac{SS_1 + SS_4}{N_1 + N_4 - 2} * \frac{N_1 + N_4}{N_1 * N_4}} \quad \text{---------- 21.0}$$

Calculation of t-ratio

$$t = \frac{\bar{x}_1 - \bar{x}_4}{\sigma_{\bar{X}_1 - \bar{X}_4}} \quad \text{---------- 22.0}$$

Where
SS_1=Corrected sum of squares for sample 1, PD(clonts and Ramey),x1
SS_2=Corrected sum of squares for sample 2, **PD(Ozkan et al),x_2**
SS_3=Corrected sum of squares for sample 3, **PD(Malekzadeh t al)x_3**
SS_4=Corrected sum of squares for sample 4 **PD(Our Results)**,x_4
N_1=size of sample 1
N_1=size of sample 2
N_1=size of sample 3
N_1=size of sample 4
Sum of squares,SS=

$$SS_{tX} = \sum X^2 - \frac{\left(\sum X\right)^2}{N} \quad \text{---------- 23.0}$$

Hypothesis

Null hypothesis is stated: H_0: $\bar{x}_1 - \bar{x}_4 = 0$

III. RESULTS AND DISCUSSION

Table1.0: EXAMPLE 1, RESERVOIR AND WELL PROPERTIES

LD1	**LD2**	**ZWD1**	**ZWD2**	**ZD1**	**ZD2**	**DZ(ft)**
0.19764	0.194	0.995	0.788	0.005	0.004	2.5
h_{D1}	**h_{D2}**	**X_{wD1}**	**XwD2**	**YeD1**	**YeD2**	**DX(ft)**
4.785	2.5298	0.99244	0.795	0.0015	0.0215	2.00E+02
XeD2	**XeD1**	**K2(Md)**	**Kx2(Md)**	**k1(mD)**	**kx1(mD)**	**dy(ft)**
0.0215	0.14	10	10	8.94427	10	21
Ct_1(psi-1)	**ct_2(psi^{-1})**	**L1(ft)**	**L2(ft)**	**h1(ft)**	**h2(ft)**	
4.00E-06	3.00E-06	250	250	200	100	
YD1	**YD2**	**Ø1**	**Ø2**	**YWD1**	**YWD2**	
8.00E-03	6.00E-03	0.23	0.23	9.92E-01	8.94E-01	
XD1	**XD2**	**µ1(cp)**	**µ2(cp)**	**hD2**	**hd1**	
0.00757	0.0065	0.5	0.2	2.5298	4.785	

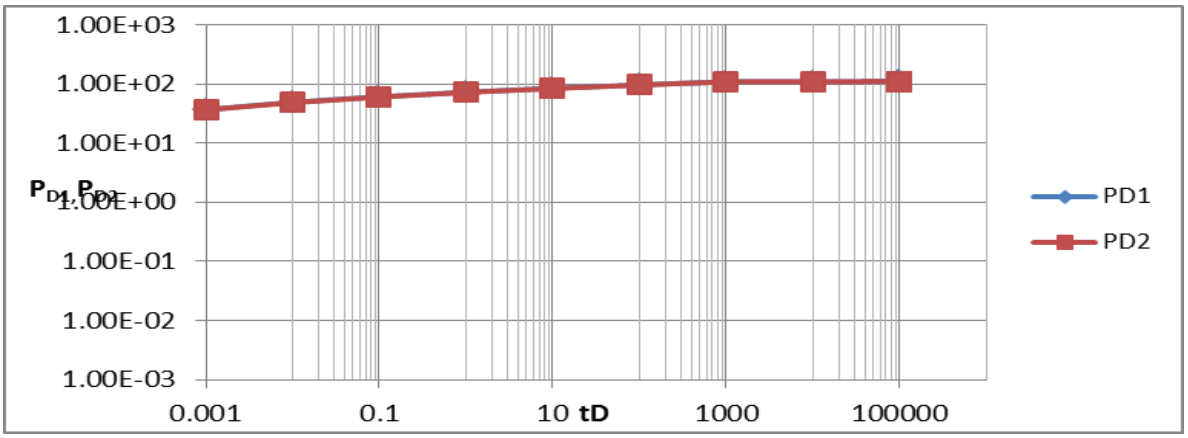

Fig. 1.0: Pressure Distribution for Two Layered Reservoir for Example 1

Pressure Distribution for Example 2: From Fig. 1.0 , it is observed that there is no significant difference between pressure response in Layer 1 and Layer 2. This could be as a result of both layers having equal permeability. In this case, possibility of having a crossflow between Layer1 and Layer 2 will not be there. Effect of layering is observed at early $t_{D,}$ and steady-state flow is observed at late $t_{D.}$ The steady-state behavior is as a result of subjection of the reservoir both up and down by a gas cap and bottom water drive.

Table2.0: EXAMPLE 2, RESERVOIR AND WELL PROPERTIES

LD1	**LD2**	**ZWD1**	**ZWD2**	**ZD1**	**ZD2**	**YD1**	**YD2**
0.1186	0.1001	0.995	0.788	0.1854	0.1793	5.93E-02	3.46E-02
hD1	**hD2**	**XwD1**	**XwD2**	**YeD1**	**YeD2**	**XD1**	**XD2**
7.495	6.43	0.992435	0.795	0.0015	0.0215	0.05925	0.04532
K_2(mD)	**K_{x2}(mD)**	**k_1(mD)**	**kx_1(mD)**	**$Ø_1$**	**$Ø_2$**	**$µ_1$(cp)**	**$µ_2$(cp)**
8	10	6.32	10	0.22	0.23	0.04	0.2
L_1(ft)	**L_2(ft)**	**h1(ft)**	**h2(ft)**	**YWD1**	**YWD2**	**XeD2**	**XeD1**
30	50	40	40	9.92E-01	8.94E-01	0.0215	0.14
r_{WD1}	**r_{WD2}**	D_x(ft)	Dx(ft)	**c_{t1}**	**c_{t2}**	k_v(mD)	D_z(ft)
0.0156	$1.11x10^{-3}$	20	8	5.00E-06	3.00E-06	0.8	30

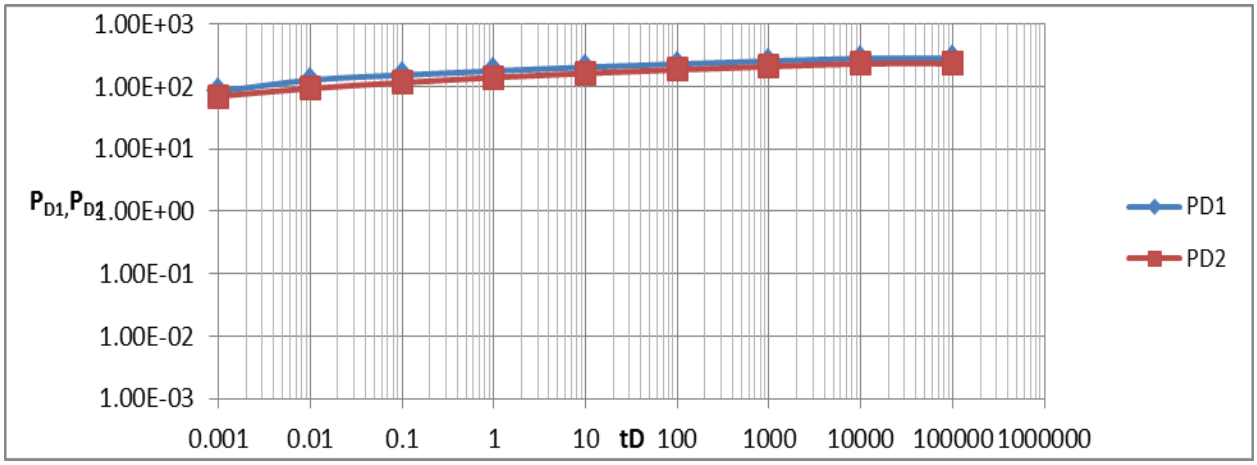

Fig. 2.0: Pressure Distribution for Two Layered Reservoir for Example 2

Pressure Distribution for Example 2 : Pressure Distribution for Two Layered Reservoir for Case Study 2 is shown in Fig. 2.0 above. The permeability of layer 2 is higher than that of layer 1 and the viscosity of Layer 1 is higher than that of Layer 2, as a result of this the pressure response in layer 2 is higher than that of Layer 1 as shown in Fig. 4.10 above. In this case study the value of α =1.51 and M=0.158. The degree of crossflow through the interface is higher toward Layer 2 as indicated by the value of M. Here completion should be carried out in Layer 2 where there is the possibility of have more recovery.

Table3.0: EXAMPLE 3, RESERVOIR AND WELL PROPERTIES

LD1	**LD2**	**ZWD1**	**ZWD2**	**ZD1**	**ZD2**	**YD1**	**YD2**
0.75293	0.7012	0.0995	0.0788	0.005	0.004	8.00E-03	6.00E-03
hD1	**hD2**	**XwD1**	**XwD2**	**K2(mD)**	**Kx2(mD)**	**k1(mD)**	**kx1(mD)**
1.32816	1.211	0.9924	0.795	10	10	10	10
YWD1	**YWD2**	**YeD1**	**YeD2**	**XD1**	**XD2**	**hd2**	**Hd1**
9.92E-01	8.94E-01	0.0015	0.0215	0.007565	0.0065	1.211	1.328157
Ø1	**Ø2**	**µ1**	**µ2**	**ct1**	**ct2**	**L1(ft)**	**L2(ft)**
0.2	0.23	1	0.2	4.00E-06	3.00E-06	1000	1500
dy(ft)	**dx(ft)**	**Dz(ft)**	**dy(ft)**	**rwD1**	**rwD2**	**XD1**	
21	200	8.05	21	0.004936	0.00221	0.008	
h2(ft)	**h1(ft)**	**XeD2**	**XeD1**	**kv(mD)**	**K_h(mD)**		
21	21	0.022	0.14	0.01	10		

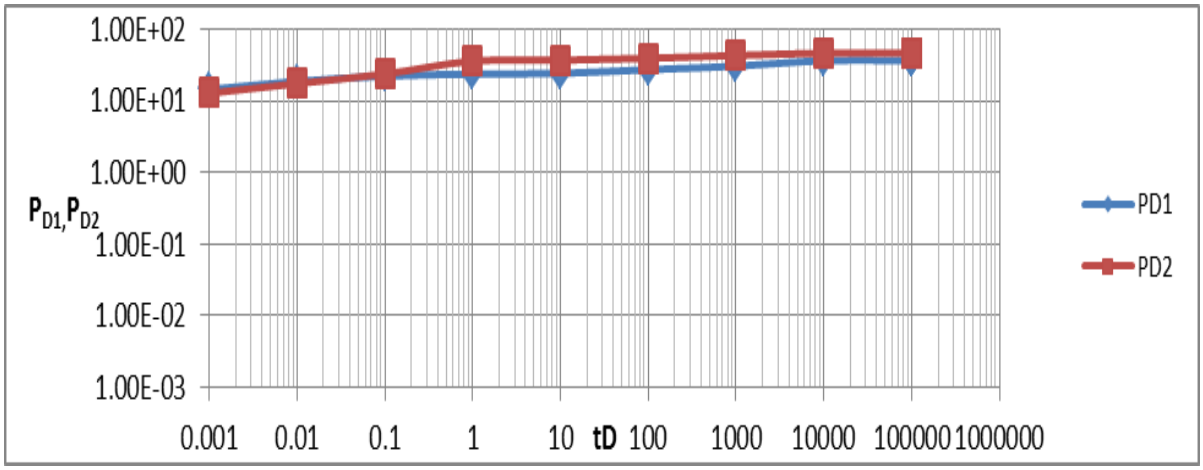

Fig. 3.0: Pressure Distribution for Two Layered Reservoir for Example 3

Pressure Distribution for Example 3 :
Pressure Distribution for Two Layered Reservoir for Case Study3 is shown in Fig.3.0 above. The permeability of the two layers equal but layer 2 has a higher porosity. This could have contributed to high productivity of Layer 2. In this case study the value of α =3.86 and M=5.0. The degree of crossflow through the interface is higher toward Layer 2 as indicated by the value of M. Here completion should be carried out in Layer 2 where there is the possibility of have more recovery.

Table4.0: EXAMPLE 4, Reservoir And Well Properties

LD1	**LD2**	**ZWD1**	**ZWD2**	**ZD1**	**ZD2**	**YD1**
0.2209	0.1109	0.995	0.788	0.005	0.004	8.00E-03
hD1	**hD2**	**XwD1**	**XwD2**	**ct2**	**L1(ft)**	**L2(ft)**
4.785	5.412	0.992435	0.795	3.00E-06	250	250
K2(mD)	**Kx2(mD)**	**k1(mD)**	**kx1(mD)**	**Ø1**	**Ø2**	**µ1(cp)**
10	10	8.94427	10	0.23	0.23	0.5
YeD1	**YeD2**	**XD1**	**XD2**	**hd2**	**Hd1**	**XeD2**
0.0015	0.0215	0.007565	0.0065	5.412	4.785	0.0215
dy(ft)	dx(ft)	YWD2	kv(mD)	dz(ft)	Dz(ft)	rwD1
21	200	8.94E-01	1	2	30	0.0160
Yw_{D1}	**ct1(psi^{-1})**	**h_1(ft)**	**h_2(ft)**	**µ2(cp)**	**XeD1**	**rwD2**
9.9E-1	5.00E-05	200	100	0.2	0.14	0.0591

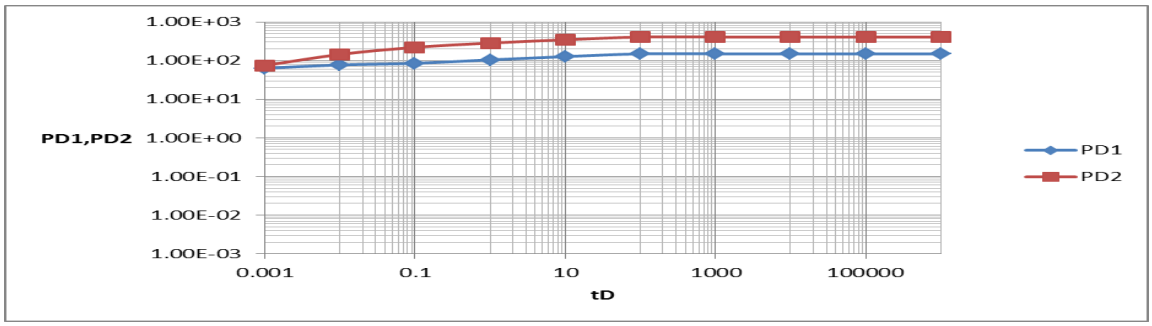

Fig. 4.0: Pressure Distribution for Two Layered Reservoir for Example 4

Pressure Distribution for Example 4
In this case study we have four numbers of flow periods . The value of time normalization factor α =37.3 and the interlayer mobility ratio M=4.47. Fig. 4.0 illustrate the pressure distribution in each layer. From the figure we observe that the pressure response is higher in Layer 2 than in Layer 1. Here the permeability is higher in Layer 2 than in Layer 1; and porosity and in both Layers are equal. The high pressure response in layer 2 could be as a result of high permeability of Layer 2 or as a result of gas cap being predominant. From the figure this reservoir experiences steady-state behavior at later $t_{D.}$

Table5.0: EXAMPLE 5, RESERVOIR AND WELL PROPERTIES

LD1	LD2	ZWD1	ZWD2	ZD1	ZD2	YD1	YD2
0.144	0.0812	0.056	0.0121	0.121	0.313	0.351	0.141
hD1	hD2	XwD1	XwD2	YeD1	YeD2	XD1	XD2
6.93	3.11	0.732	0.732	0.012	0.006	0.231	0.312
K2(mD)	Kx2(mD)	k1(mD)	kx1(mD)	Ø1	Ø2	µ1(cp)	µ2(cp)
1000	1000	1000	1000	0.2	0.21	0.3	0.3
YWD1	YWD2	XeD2	XeD1	L1(ft)	L2(ft)	h1(ft)	h2(ft)
0.00712	0.006	0.214	0.325	100	100	6	6
ct1(ft)	ct2(ft)	XD1	Dz(ft)	dx(ft)	dy(ft)	rwD1	rwD2
0.000004	0.000004	0.231	4	2	10	0.04	0.012

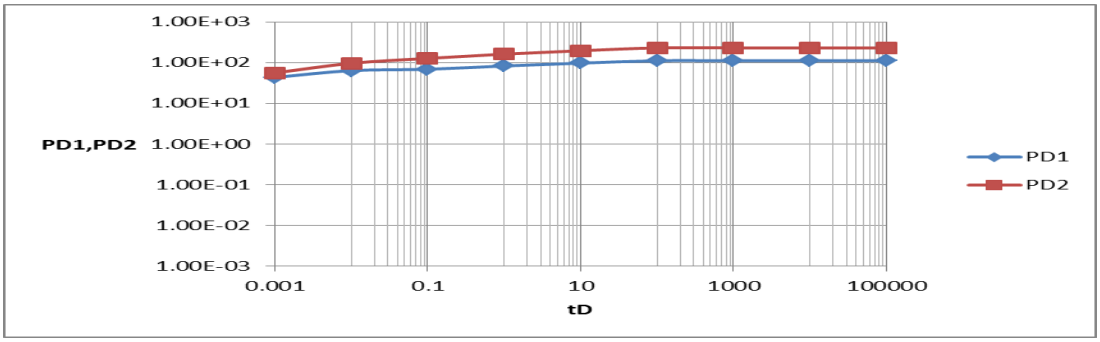

Fig. 5.0: Pressure Distribution for Two Layered Reservoir for Example 5

Pressure Distribution for Example5

In this case study we have two numbers of flow periods . The value of time normalization factor α =0.952 and interlayer mobility ratio M=1.0. Fig. 5.0 illustrates the pressure distribution of both layers. The pressure in Layer 2 is higher than that of layer 1. This could be as a result of higher porosity of Layer2 since both layers have the same permeability. It could also be as a result of as cap energy.

Table6.0: EXAMPLE 6, Reservoir and Well Properties

LD1	**LD2**	**ZWD1**	**ZWD2**	**ZD1**	**ZD2**
0.129764	6.03	0.995	0.788	0.005	0.004
hd2	**hd1**	**XwD1**	**XwD2**	**XD1**	**XD2**
4.785	2.5298	0.992435	0.795	0.007565	0.0065
K2(mD)	**Kx2(mD)**	**k1(mD)**	**kx1(mD)**	**Ø1**	**Ø2**
4	4	4	4	0.2	0.23
YWD1	**YWD2**	**YeD1**	**YeD2**	**Dz(**	**Dz(ft)**
9.92E-01	8.94E-01	0.0015	0.0215	2	0.3
XD1	**h1(ft)**	**h2(ft)**	**Dx(ft)**	**Dy(ft)**	**Dz(ft)**
0.00126	5	5	200	21	2.00E+00
rwD1	rwD2	**YD1**	**YD2**	**XeD2**	**XeD1**
$4x10^{-2}$	$1.2x10^{-2}$	8.00E-03	6.00E-03	0.0215	0.14
µ1(cp)	**µ2(cp**	**ct1psi^{-1}**	**ct2psi^{-1}**	**L1(ft)**	**L2(ft)**
0.03	0.2	4.00E-06	3.00E-06	2000	2500

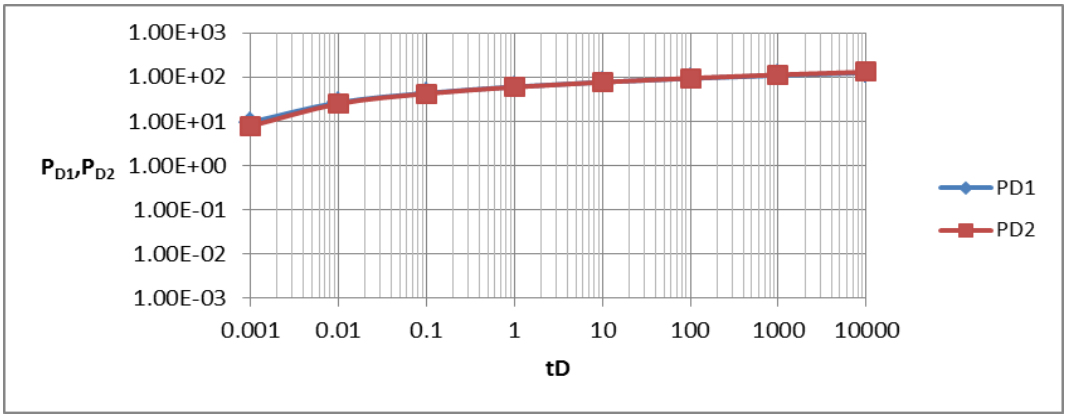

Fig. 6.0: Pressure Distribution for Two Layered Reservoir for Example 6

Pressure Distribution for Example 6

In this case study we have three numbers of flow periods . The value of time normalization factor α =0.139 and interlayered mobility ratio M=0.15. Fig. 6.0 illustrates the pressure distribution of the two Layers. Productivity is higher in Layer 1 at $t_D \leq 10$.

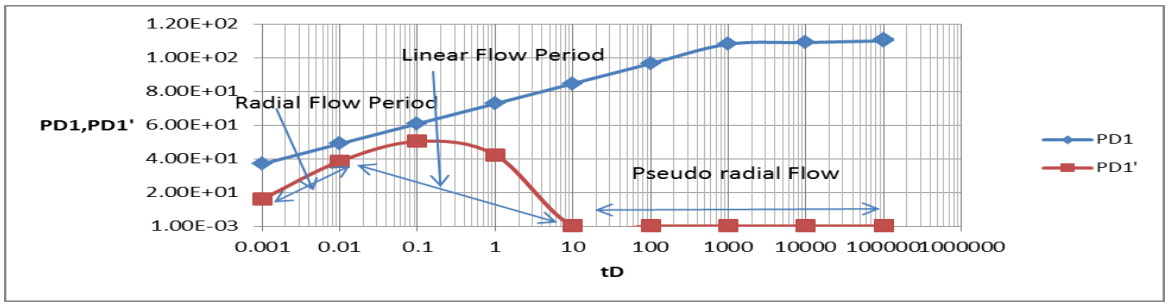

Fig. 7.0: Dimensionless Pressure and Dimensionless Pressure Derivative for Layer1 With Flow Period for Example 1.

Dimensionless Pressure and Dimensionless Pressure Derivative for Layer1 With Flow Period for Example 1.

Fig.7.0 shows pressure derivative distribution for example 1.With this figure we are able to identify the flow period. The pressure derivative enable us to identify flow period and also help in determine some Important parameters.

Table7.0:Comparison of Results

t_D	PD(clonts and Ramey),x1[6]	PD (Ozkan et al),x2[7]	PD Malekzadeh t al)x3[8]	Pd(Our Results)x4
0.0001	0.17007	0.17	0.1126	0.11033271
0.001	0.22888	0.2288	0.17098	0.356560518
0.01	0.34956	0.3495	0.29164	0.576587549
0.1	0.66767	0.6675	0.60972	0.867461538
1	1.3763	1.376	1.31828	1.339233496

VALIDATION OF RESULTS

The results of an infinite-acting reservoir have been validated as presented in Table7.0 and Fig 8.0 and also from statistic test carried out below. This implies that the numerical method used was adequate.

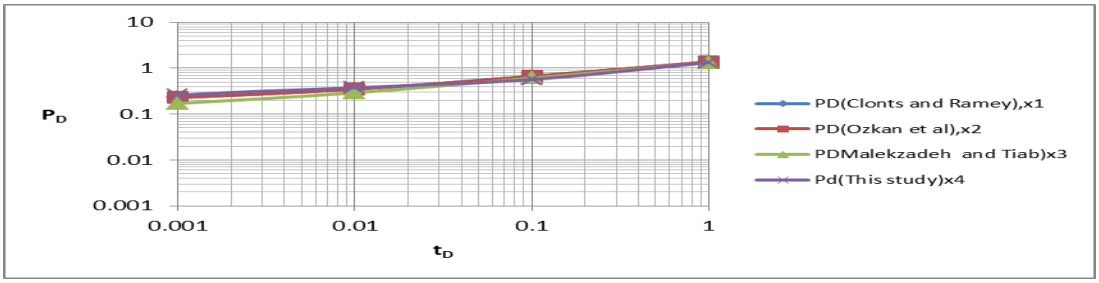

Fig 8.0: Comparison of Dimensionless Wellbore Pressure Results

From Table7.0 and equation 21.0

(i) t-Test for clonts and Ramey)x1

$$\sigma_{\bar{X}_1-\bar{X}_4} = \sqrt{\frac{0.98389062 + 0.905}{8} * \frac{10}{25}} = 0.307324526$$

Also from equation 22.0

$$t = \frac{\bar{x}_1 - \bar{x}_4}{\sigma_{\bar{X}_1-\bar{X}_4}} = \frac{0.558496 - 0.65}{0.307324526} = 0.297774389$$

=0.29777507

Similarly,
t-Test for PD(Ozkan et al),x2

t-Test for PDMalekzadeh t al)x3
=0.29778588
Degree of freedom=$N_1+N_2-2=5+5-2=8$
Choosing a significant level test H_O,$\alpha=0.05$
Therefore, the tabled t-ratio($\alpha=0.05$) for 8 degree freedom is 2.306
Since our obtained t-ratio is less than that of the tabled value H_o accepted. The conclusion drawn from the t-test carried
out, therefore there is no significant difference between our results and other Authors considered.

IV. CONCLUSION

Haven presented the problems objectives, and results of study in the previous chapters, we arrived at the following conclusion:

[1] We have been able to show behavior of pressure distribution for two layered reservoir subjected simultaneously by a Gas-cap and bottom water derive both graphical and tabular form for six examples were considered.
[2] We have been able to determine the flow regime ;(i) Radial Flow (ii) Early Linear Flow Period.

[3] We have been able to compute the multiplication factor (A_1 and A_2)using numerical method (Gauss-Legendre Quadrature)
[4] This factor decreases with dimensionless time,t_D and become zero with increase in t_D And we have seen that the time interval at which the constants maintain a zero slope marks the end of infinite-acting flow and attainment of
[5] their final values irrespective of flow time.
[6] We have also compute the dimensionless pressure and dimensionless pressure derivative using numerical

Method (Gauss-Legendre Quadrature) .The results showed that dimensionless pressure increases with dimension

time.The results show that it is possible to analyzed each layers using the conventional methods and each

layer requires properties from other layer involved.

NOMENCLATURE

C_t	Total reservoir compressibility, Psi $^{-1}$
h	Formation thickness ft
h_D	Dimensionless height
L_D	Dimensionless length
P_D	Dimensionless Pressure
P_{wD}	Dimensionless wellbore pressure
p_D	Dimensionless pressure derivative
S	Instantaneous source functions
t	Time,hrs
t_D	Dimensionless time
x,y,z	Space coordinates
x_D,y_D	Dimensionless distance in the x and y directions
x_f	Horizontal well half length
z_D	Dimension distance in the z director
k	Horizontal permeability and
k_y	Permeability in the y – direction, md
k_z	Permeability in the z direction , md
l	Horizontal well length, ft
r_D	Dimensionless radial distance in the horizontal plane
r_{wD}	Dimensionless wellbore radius
x_w	Well location in the x – direction, ft.
x_e	Distance to the boundary or reservoir length ft
x_{eD}	Dimensionless distance to the boundary
x_{WD}	Dimensionless well location in the x- direction
Z_w	Well location in the direction, ft.

z_{WD} Dimensionless well location in the Z direction
Y_w Well location in the y – direction, ft.
Dimensionless well location in the Y direction.

REFERENCES

[1] Owolabi .A.F.et al.:Pressure distribution in a layered Reservoir with gas-cap and bottom water, Nigeria Journal of Technology(NIJOTECH),Vol.31,No2 July 2012,pp189-198.
[2] Amanat .U.Chaudhry.: Oil well Testing Handbook, Advanced TWPSOM Petroleum Systems,Inc.Houston,Texas.
[3] Gringarten and Ramey.: 'The Use of Source and Green's Functions in Solving Unsteady-Flow Problems in Reservoirs'',1973.
[4] Kuchuk.F.J.et al.: Pressure Transient Behavior of Horizontal Wells with and without Gas Cap or Aquifer.SPE Formation Evaluation, March 1991.
[5] Andy Igho Joe.: Fundamental Statistics, Kraft book Ltd.
[6] Clonts.M.D., et al.:''Pressure Transient Analysis for wells with Horizontal Drainholes'',56th California Regional Meeting of the Society of Petroleum Engineers held in Oakland.C.A.April 2-4,1986.
[7] Erdal Ozkan SPE and Rajagopal Raghavan.:''Performance of Horizontal wells Subject to Bottom water Drive'', SPE Reservoir Engineering, August 1990.
[8] Malekzadeh.D.,et al.:'Interference Testing of Horizontal Wells'',SPE 1991.

American Journal of Engineering Research (AJER)
e-ISSN : 2320-0847 p-ISSN : 2320-0936
Volume-03, Issue-12, pp-54-61
www.ajer.org

Research Paper Open Access

Application Of Performance Based Seismic Design Method To Reinforced Concrete Moment Resistant Frame With Vertical Geometric Irregularity With Soft Storey

Rajkuwar Dubal[1], Gole Neha[2], Patil G. R[3], Sandip Vasanwala[4], Chetan Modhera[5]

[1](Research Scholar , Applied Mechanics Dept, SVNIT Surat,Gujrat,India , Pin395007)
[2](P.G student,Civil engg Dept, RSCOE,Pune Maharashtra India Pin411033)
[3](Assistant Professor, Civil engg Dept RSCOE,Pune Maharashtra India, Pin411033)
[4,5](Professor, Applied Mechanics Dept, SVNIT Surat,Gujrat India , Pin395007),

ABSTRACT : *A performance-based seismic design (PBSD) method is aimed at controlling the structural damage based on precise estimations of proper response parameters. PBSD method evaluates the performance of a building frame for any seismic hazard, the building may experience. Use of this method for vertical irregular buildings is verified with comparison of conventional method. Soft storey is subjected to failures due to stiffness and strength reduction. This paper deals with application of Performance based seismic design method for soft storey RC building frames(10 storeys) . Push over analysis results show significance of PBSD method in frames having soft story at lower floor level compared to higher ones.*

KEYWORDS : *RC building, , Performance based seismic design (PBSD), Response parameters, , and Push over analysis*

I. INTRODUCTION

Earthquakes have the potential for causing the greatest damages, among all the natural hazards. Since earthquake forces are random in nature & unpredictable, need of some sophisticated methods to analyze our structures for these forces. Performance based design can relate to a new dimension in the seismic design philosophy. We need to carefully understand and model the earthquake forces to study the actual behavior of structure so that structure faces a controlled damage. India has witnessed more than 690 earthquakes of Richter magnitude ('*M*') greater than 5 during 1828 to 2010. Damage survey reports show that life and property losses occur in urban and semi-urban areas. It is uneconomical to design a building so as not to suffer any damage during strong earthquake. An engineering approach aims for achieving balance in cost and performance through controlled damage. The goal of performance-based seismic design is to ensure that performance objectives are satisfied. A successful conceptual design could hopefully reduce the impact of uncertainties on the real structural behavior.

The poor performance level, and hence the high level of structural damage in the stock of building structures during the frequent earthquakes happened in India by the last decade, increased the need to the determination and evaluation of the damages in the building type of structures, so much more than ever before. The most destructive and unfortunately the most general irregularity in stock of building structures that lead to collapse is certainly the soft story irregularity. The commercial and parking areas with higher story heights reduce the stiffness of the lateral load resisting system at that story and progressive collapse becomes unavoidable in a severe earthquake for such buildings. This situation has been verified for all of the building structures with soft stories, independently from good quality of construction and design.

Current status of seismic design procedure and its weakness : Current seismic design practice around the world is carried by elastic method even though it is acknowledged that the buildings undergo large deformations in inelastic range when subjected to large earthquakes. As a result in seismic activity, there may be severe yielding and buckling of structural members and connections, can be unevenly and widely distributed in the structure designed by elastic methods. This may result in rather undesirable and unpredictable response, total collapse, or difficult and costly repair work at best.[1] There is need for more direct design methods that would fit in the framework of PBSD and produce structures that would perform as desired.

Major weaknesses of current seismic procedure:

- Increasing base shear to reduce damage is not reliable since past earthquakes have results of total collapse due to local column failure.
- Upper story failures in buildings are not justified by elastic method which assumes lateral force distribution which does not account for nonlinear behaviour of the structure.
- Earthquake changes stiffness of the members due to cracking of concrete and yielding of steel and proportioning of members according to elastic analysis leads to major failures.
- Materials like Reinforced Concrete have hysteretic (pinched) behaviour which is not accounted.
- Many studies have shown the column undergo yielding if it is designed as per capacity approach, inelastic behaviour of the column are not considered.

II. PERFORMANCE BASED SEISMIC DESIGN OF REINFORCED MOMENT RESISTANT FRAMES

Reinforced Concrete Building stock in India is mainly classified from low to medium rise buildings. Approach of I.S 1893,2002 is in tune with typical code practice followed by many other countries. In spite of knowing drawbacks of force based seismic design procedures, the practice is in vogue due to its simplicity and non-availability of the alternative. We can use guidelines given by FEMA and ATC documents by modifying them for Indian condition. An outline of the step-by-step Performance-Based Seismic Design (PBSD) procedure is given in the following.[1]

Design procedure

An outline of the step-by-step Performance-Based Seismic Design (PBSD) procedure is given in the following.

[1] Initially desired yield mechanism is selected.

[2] Fundamental period '*T*' of the structure is estimated, along with yielding drift 'θy'.[2]

[3] Determine inelastic spectral acceleration

[4] Calculate the ductility reduction factor and the structural ductility factor.

With the assumed yield drift 'θy' for different structural systems from tables in ASCE (2006)the energy modification factor, 'γ' , depends on the structural ductility factor ('μ_s') and the ductility reduction factor (' R_μ') and can be obtained from the following relationship.:[3]

$$\gamma = \frac{2\mu_s - 1}{R_\mu^2} \qquad (2.1)$$

To consider the hysteretic (degradation of strength and stiffness) behaviour, the coefficient 'C_2' (modification factor) is determined which represents the effect of pinched shape of hysteretic loops, stiffness degradation, and strength deterioration on the maximum displacement response according to FEMA 356. Ductility reduction factor 'R_μ' and energy modification factor 'γ' can be calculated as follows:

$$\theta u = \frac{\theta t}{C\,2} \qquad \mu_s = \frac{\theta u}{\theta y} \qquad \gamma = \frac{2\mu_s - 1}{R_\mu^2} \qquad (2.2)$$

5. Determine actual lateral forces

Shear distribution factor for the respective story factor for the respective story is calculated by using following equation:

$$\frac{V_i}{V_n} = \beta_i = \left(\frac{\sum_{j=1}^{n} w_j h_j}{w_n h_n}\right)^{0.75T^{-0.2}} \qquad (2.3)$$

V_i = shear force at ith level ; β_i = Shear distribution factor at ith level

w_j = Seismic weight atlevel j; h_j = height of level j from the base

w_n = Seismic weight at top level ; h_n = height of roof level from the base

Then, the lateral force at level *i*, *Fi* , can be obtained as:

$$F_i = (\beta_i - \beta_{i+1}).V_n \quad (2.4)$$

F_i = Lateral force at ith levl ; V_n = Story shear at roof level; V_y = Design base shear

Substituting the values of V_n we get following equation:

$$F_i = (\beta_i - \beta_{i+1})\left(\frac{w_n h_n}{\sum_{j=1}^{n} w_j h_j}\right)^{0.75T^{-0.2}}.V_y \quad (2.5)$$

6. Design of designated yielding and Non-designated yielding members.

For Reinforced Concrete moment frames, beams are designed as Designated Yielding members because of strength contribution from slabs and non-rectangular beam shapes (ie, T shape beam), as well as the use of different amounts of top and bottom reinforcement, plastic moments in positive and negative direction of DYM may be different:

$$\sum_{i=1}^{n} F_i h_i \theta_p = 2.M_{pc}\theta_p + \sum_{i=1}^{n} \beta_i.(M_{pb-positive} + M_{pb-negative})\gamma_i$$

$$\sum_{i=1}^{n} F_i h_i \theta_p = 2.\sum_{i=1}^{n} F_i h_i \theta_p + \sum_{i=1}^{n}(1+x)\beta_i.(M_{pb-positive})\gamma_i \quad (2.6)$$

$$\beta_i(M_{pb-positive}) = \beta_i \frac{\sum_{i=1}^{n} F_i h_i - 2M_{pc}}{(1+x)\sum_{i=1}^{n} \beta_i \frac{L}{L'_i}} \quad (2.7)$$

Where x is the ratio of the absolute value of negative Bending moment to positive Bending moment. Members that are not designated to yield (Non-DYM), such as columns in, must be designed to resist the combination of factored gravity loads and maximum expected strength of the DYM by accounting for reasonable strain-hardening and material over strength. The columns must be designed for maximum expected forces by including gravity loads on beams and columns and by considering a reasonable extent of strain-hardening and material over strength in the beam plastic hinges.

$$M_p = \xi M_{pb} = 1.25.M_{pb} \quad (2.8)$$

III. STRUCTURAL MODELLING AND IT'S RESULTS

To study the effect of soft storey we have compared 10 storey frames which was modified into 10 different models by considering soft storey in each storey with conventional and Performance based Seismic design method, we have considered 10 storey models. The basic plan and elevation for all 10 models is kept same. Frames are considered of 12mx12m area. Height of building is32m.. Basic Dimensions for the frames and general design parameters were taken commonly as .Type of frame: Moment Resistant frame, Size of Column = 500 x 500mm, Size of Beam = 300 x 600 mm, Thickness of Slab = 120mm thick Wall thickness = 150mm, Floor Finish = 1 KN/m2 ,Live load at all floor levels = 2 KN/m2,Zone IV, Medium type of soil

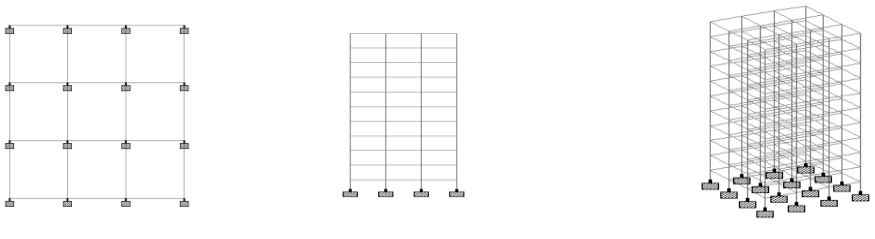

Fig 3.1 Plan and Elevation of 10 storied irregular frames with Soft Storey considered for study

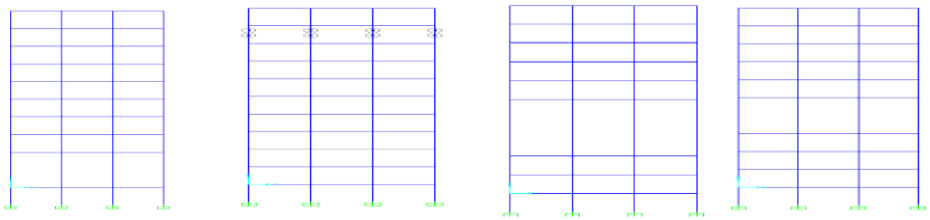

Fig 3.2 Soft Storey At First, Second, Third And Fourth Floor

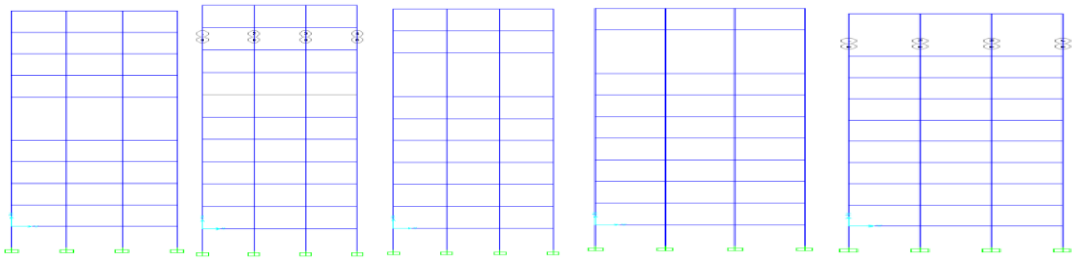

Fig 3.3 Soft Storey At Fifth, Sixth, Seventh, Eight and Nine Floor

Following Nine Soft Storey cases have been framed for analysis purpose.

Table 3.1 Soft story cases for analysis

Case I	Soft storey at first floor
Case II	Soft storey at second floor
Case III	Soft story at third floor
Case IV	Soft story at fourth floor
Case V	Soft story at fifth floor
Case VI	Soft story at sixth floor
Case VII	Soft story at seventh floor
Case VIII	Soft story at eighth floor
Case IX	Soft story at ninth floor

Table 3.2 Seismic parameters considered for design

Seismic zone factor 'Z'	0.16
Importance factor, 'I'	1
Sa Inelastic	0.1875 g
'T'	0.8s
Yield drift ratio 'θ_y'	0.5%
Target drift ratio 'θ_u'	2%
Inelastic drift ratio '$(\theta_u - \theta_y)$'	1.5%
Ductility factor	4
Reduction Factor due to Ductility '$R\mu$'	4
Energy Modification Factor 'γ'	0.43

Comparative evaluation of 10 story irregular frames (with soft storey in each storey) with respect to I.S 1893-2002 and PBSD method : Capacity spectrum curve is actual plot representing the performance point i.e. intersection point of spectral displacement and spectral acceleration. It is clear that in PBSD method performance point (intersection of demand and capacity curves) shifts due to extra confined steel which is normally incorporated in design. Hence provision for extra ductility is avoided since this care is already taken while designing.

IV. PERFORMANCE POINT COMPARISON FOR IRREGULAR FRAME WITH SOFT STOREY IN EACH STOREY

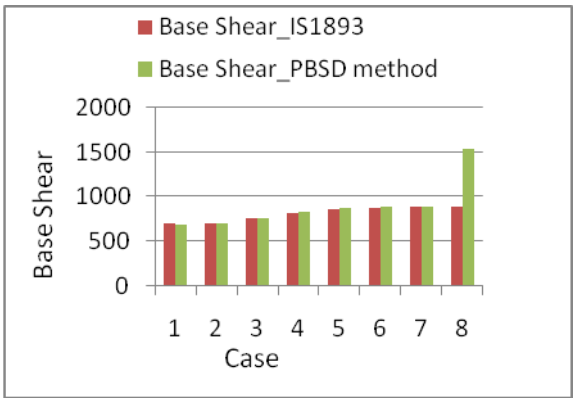

Fig 3.4 Performance point in I.S 1893-2002(force based) and PBSD method for all models with soft story (Base shear)

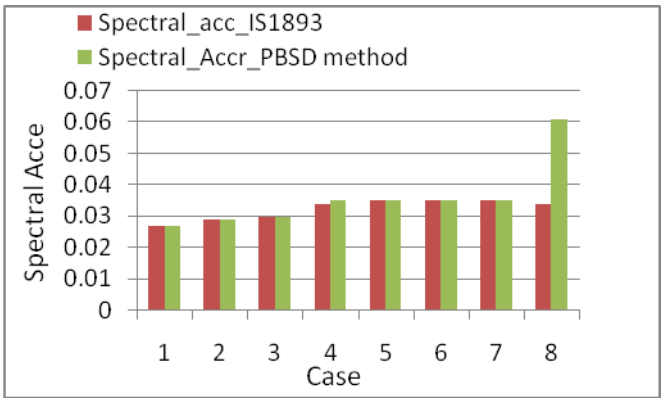

Fig 3.5 Performance point in I.S 1893-2002(force based) and PBSD method for all models with soft story (Spectral acceleration)

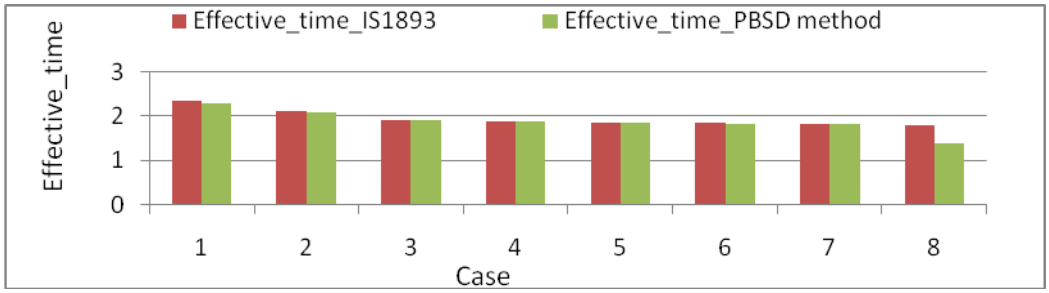

Fig 3.6 Performance point in I.S 1893-2002(force based) and PBSD method for all models with soft story (Effective time)

Some comments on push over curve nature are, in case of soft storey there is no significant achievement with respect to spectral acceleration and spectral displacement entities but with respect to displacement and effective time period performance point is enhanced.

Roof Drift Ratio : Deformed shape of any pushover curve is based on roof drift ratio. In our case normally roof drift in all soft story models designed by PBSD method are near about same or less compared to all models designed by conventional method. That means PBSD models have same deformable capacity like conventional models.

Table 3.3 Comparison Of Roof Drift Ratio W.r.t I.S. 1893 & PBSD

Case no.	Roof drift as per I.S 1893	Roof drift as per PBSD	Roof drift ratio
09	0.031	0.03	1.03
08	0.006	0.007	0.857
07	0.006	0.005	1.2
06	0.005	0.005	1
05	0.004	0.004	1
04	0.003	0.003	1
03	0.0031	0.002	0.155
02	0.002	0.002	1
01	0.058	0.066	0.878

Table 3.4 Comparison Of Base Shear w.r.t I.S. 1893 & PBSD

Case no.	Base Shear as per I.S 1893;2002	Base Shear as per PBSD
09	1083.38	2035.9325
08	1215.93	1215.93
07	1106.44	1486.10
06	840.678	1171.52
05	1255.93	986.44
04	1001.69	1093.22
03	1381.017	1290.847
02	1319.32	1309.83
01	645	840

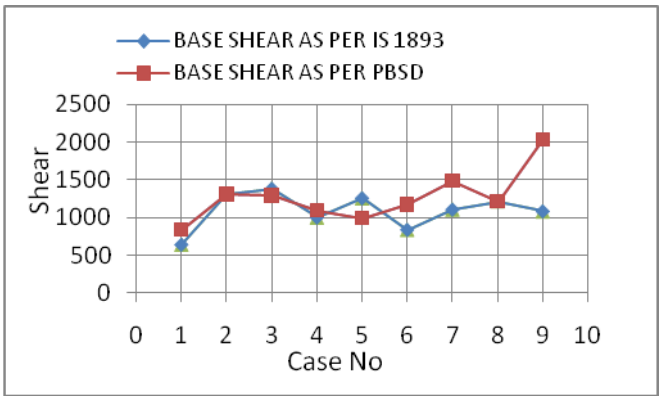

Fig 3.7 Comparison of Roof drift ratio w.r.t IS1893-2002 & PBSD method

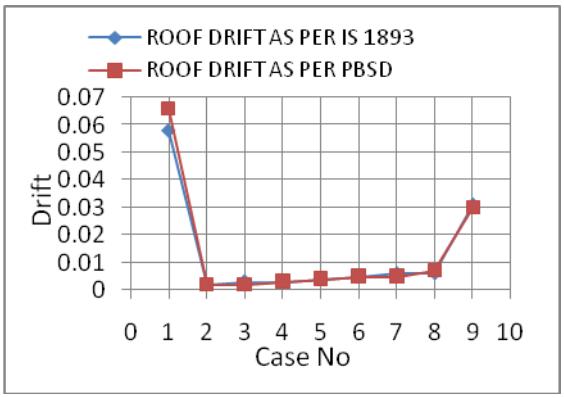

Fig 3.8 Comparison of Base Shear wrt IS1893-2002 & PBSD method

Static Over-strength Ratio : All pushover curves show that even though the design base shear for each baseline frame is smaller than that of corresponding PBSD frame, the ultimate strength of conventional frame .This is due to fact that the design of baseline frame was governed by drift which required major revision of member sizes after having been designed for strength. The iteration is not needed in PBSD method. The static over strength ratio of ultimate strength to design base shear for all frames is summarized in following table.

Table 3.5 Comparison of static over-strength ratio w.r.t is1893 & PBSD method

Case no.	Static Over-strength as per I.S1893 ;2002	Static Over-strength as per PBSD
09	1.5	1
08	1.3	1.3
07	1.4	1
06	1.8	1.3
05	1.1	1.4
04	1.4	1.2
03	1.01	1.08
02	1.03	1.01
01	1	1.02

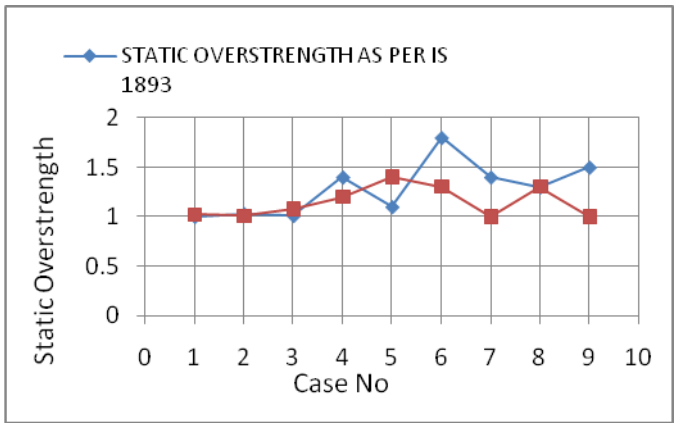

V. DISCUSSION

- Performance point in PBSD and I.S 1893 2002 is near same for all 10 cases .For Soft story to ninth floor varies maximum with 72.08 % increment.
- Displacement in first model is 0.012m less than conventional model so this elates performance point.
- Spectral acceleration is greater only in 9th case is increased up to 50% (0.06) in PBSD method and (0.04) in conventional method.
- Hinges developed in both cases have individual significance; however numbers of hinges developed are same in both cases for all 10 models.
- Base shear in both methods does not show much difference except in last case .The difference is 600KN
- Storey drift for model with ninth floor soft storey is less 0.04mm and largest for storey for which value is 0.4mm for first floor.
- Roof drift ratio (PBSD: I.S method) for ninth storey is maximum i.e1and least for model having soft storey at third floor i.e. 0.857.
- Base shear in all models in both methods is gradual and does not vary much except in ninth model it varies by 1000 KN.

VI. CONCLUSION

Performance Based Seismic Design involves distribution of lateral forces according to new distribution factor which is defined on basis of real ground motion. Initial design process includes utilization of optimum sections which sustain the earthquake loads hence iterative trials are avoided and this method proves to be practical than current practice of designing earthquake resistant structures. Non Linear static analysis for frames gives comparison of performance of buildings even if they are irregular with respect to soft storey. Performance point of the frames (vertical irregularity of soft storey) designed by PBSD method is enhanced than for all frames designed by conventional method. Time period is one of the effective means to check the reliability of PBSD method. Time period for all vertical irregular frames with soft story is lowest than the frames designed by conventional method. These results will help design engineers in fast and reliable assessment of the effects of soft storeys.

REFERENCES

Journal Papers:

[1] Newmark, N.M. and Hall, W.J. Proceedings and Criteria for Earthquake Resistant Design. Building Practice for Disaster Mitigation, Building Science Series 46, National Bureau of Standards, Washington, D.C., 209-23646,

[2] Athanassiadou C.J, Seismic performance of R/C plane frames irregular in elevation. Engineering Structures,30 ,2008,1250–126..

[3] Mo Y.L., Chang Y.F. Application of base isolation concept to soft first storey buildings; Computers & Structures, Volume 55, Issue 5,1995,Pages 883-896.

[4] Vipul Prakash, Whither Performance-Based Engineering in India, ISET Journal of Earthquake Technology, 41(1),2004, pp. 201-222.

[5] Goel, S. C., Stojadinovic.B., and Leelataviwat SEnergy-based Seismic Design of Structures using Yield Mechanism and Target Drift, Journal of Structural Engineering 2009

[6] Gaurav Joshi, K.K. Pathak & Saleem Akhtar Seismic analysis of soft storey building considering structural & geometric parameterst", Journal on today's idas tomorrows technologies volume1,no2, dec2013, pp73-84

Books:

[7] Chopra .A.K. Dynamics of Structures, (Prentice Hall Pvt Ltd , 2006).

[8] Kappos A.J, Penelis G. G, Earthquake-resistant Concrete Structures. (London: E & FN SPON Chapman & Hall 1997).

[9] ASCE Standard Methodology for Seismic Evaluation of Buildings. Standard No. ASCE-31. American Society of Civil Engineers, Reston, Virginia. . 2006

[10] ATC), NEHRP Commentary on the Guidelines for the Seismic Rehabilitation of Buildings, FEMA 274 Report, prepared by the Applied Technology Council, for the Building Seismic Safety Council, published by the Federal Emergency Management Agency, Washington, D.C.1997

Theses:

[11] Chopra A.K, Goel R.K; Chintanapakdee C). Evaluation of a modified MPA procedure assuming higher modes as elastic to estimate seismic demands. Earthquake Spectra,20(3), 2004,757-778.

Proceedings Papers:

[12] Liao W.C. and Goel S. C .Performance-Based Plastic Design (PBPD) of Reinforced Concrete Special Moment Frame Structures. The 3rd Congress of the International Federation for Structural Concrete (fib), Washington DC. 2010

[13] Goel, S. C., Liao, W. C., Mohammad R. B., and Leelataviwat S An Energy Spectrum Method for Seismic Evaluation of Structures. Conference on improving the seismic performance of existing buildings and other structures, ATC & SEI Conference, San Francisco, CA.2009

American Journal of Engineering Research (AJER)
e-ISSN : 2320-0847 p-ISSN : 2320-0936
Volume-03, Issue-12, pp-62-68
www.ajer.org

Research Paper Open Access

Investigation on Effluent Characteristics of Organic Cotton Fabric Dyeing With Eco-Friendly Remazol Reactive Dyes

Md. Mashiur Rahman Khan[1], Md. Mazedul Islam[2], Elias Khalil[3]
[1]*Associate Professor & Head, Department of Apparel Manufacturing Engineering, Bangladesh University of Textiles, Tejgaon, Dhaka-1208, Bangladesh*
[2]*Lecturer, Department of Textile Engineering, Dhaka University of Engineering & Technology, Gazipur-1700, Bangladesh*
[3]*Lecturer, Department of Textile Engineering, World University of Bangladesh, Dhaka-1205, Bangladesh*

ABSTRACT : *Environmental sustainability is the major concern in the age of modern world. For textile and apparel sector, this has been a burning issue for many related concerned bodies. The pretreatment and dyeing process of greige fabrics results in large volume of effluents that has harmful effect on environment. In this study, the ecological parameters of the effluents obtained from scouring and dyeing of 100% organic cotton single jersey knitted fabrics with environmentally low impact Remazol series reactive dyes adopting exhaust dyeing method was investigated. The effluents collected for investigating the ecological parameters include chemical oxygen demand (COD), biological oxygen demand (BOD), total dissolved solids (TDS), total suspended solids (TSS), dissolved oxygen (DO) and alkalinity. The results show that the use of the low impact reactive dyes has greater ecological advantages as it reduces the COD, BOD, TDS, TSS, p^H values and increases the DO values of effluents. Organic cotton itself being eco-friendly along with Remazol series sustainable dyes provides the better ecological results. Hence, the results indicated that wet processing of organic cotton knitted fabric with eco-friendly and low impact reactive dyes provide better ecological advantages.*

KEYWORDS : *Organic cotton, Eco-friendly dyes, Knitted fabrics, Effluents, Wet processing.*

I. INTRODUCTION

The textile industry plays an important role in the economy of Bangladesh. Textile industry involves wide range of raw materials and processes to engineer the required shape and properties of the final product. Out of various activities in textile industry, chemical processing contributes about 70% of pollution [1]. Waste stream generated in this industry is essentially based on water-based effluent generated in the various activities of wet processing of textiles. The main cause of generation of this effluent is the use of huge volume of water either in the actual chemical processing or during re-processing in preparatory, dyeing, printing and finishing [2]. Gray fabrics, after its manufacturing, are subjected to several wet processes such as pretreatment process involving demineralization, scouring, bleaching and mercerization etc. The pretreated fabric is then dyed using textile dyes and finished by softener padding. The pretreatment and dying process results in large volume of effluent that has harmful effect on environment [3]. Generally, textile effluent is colored with high pH, temperature, biological oxygen demand (BOD), chemical oxygen demand (COD), total dissolve solid (TDS) and total suspended solid (TSS) along with low dissolved oxygen (DO) [4]. Color is imparted to textile effluents because of the various dyes and pigments used to color the fabric. The presence of dyes in the waste waters will cause severe damage to the aquatic biology [12]. This is because dyes have a synthetic origin and a complex molecular structure which makes them more stable and difficult to be biodegraded [5]. It is well known that cotton mills consume large volume of water for various processes such as sizing, desizing, and scouring, bleaching, mercerization, dyeing, printing, finishing and ultimately washing. Due to the nature of various chemical processing of textiles, large volumes of waste water with numerous pollutants are discharged. But where is the real problem?

The fact is that the effluent generated in different steps is well beyond the standard and thus it is highly polluted and dangerous [6]. Thus a study on different measures which can be adopted to minimize the environmental impact of effluents discharged from textile chemical processing industries to protect and safeguard our surroundings from possible pollution problem which has been the focus point of many recent investigations [7]. In recent years, different approaches have been discussed to tackle man made environmental hazards. Clean technology, eco-mark and green chemistry are some of the most highlighted practices in preventing and or reducing the adverse effect on our surroundings [8]. Thus, the present study aim to investigate the ecological parameters of effluents obtained from scouring and dyeing the 100% organic cotton single jersey knitted fabric with eco-friendly Remazol series low impact reactive dyes of DySter. The effluent parameters studied includes COD, BOD, TDS, TSS, DO and Alkalinity.

II. MATERIALS AND METHODOLOGY

2.1 Dyeing Organic Cotton Knitted Fabrics: For the study, the selected samples were fixed with standard procedure and dye recipe. The selected sample were discussed with Dystar executive, to obtain recipe based on low impact reactive dyes such as Remazol, Remazol ultra RGB series of dyes. The lab dyeing trails were done using HTHP lab dyeing machine with 10 gm single jersey organic cotton RFD knitted fabric samples. Dyeing method in this study uses low impact reactive dyes, along with others various eco-friendly dyes & chemicals. The Parameters and recipe for dyeing is presented in Tables 1 and Table 2 respectively.

Table 1: Parameters for scouring, dyeing and aftertreatment of organic cotton S/J knitted fabric

Materials Details	Process name	L:R/pH	Req. Temp ×Time
Fabric type: S/J Greige GSM: 160 Color: Black Materials weight: 1 kg	Scouring	1:6/6.0-10.5	60°C ×1hr 50 min (30+20+15+45)
	Dyeing	1:7/9.5-11	50°C x 30 min
	After Treatment	1:6	After Treatment

During the lab dyeing process, effluent from scouring and dyeing process was collected and investigated for ecological parameters such as Chemical Oxygen Demand (COD), Biological Oxygen Demand (BOD), Total Dissolved Solids (TDS), Total Suspended Solids (TSS), Dissolved Oxygen (DO) and Alkalinity with the help of COD Reactor, COD Vial, UV Spectrophotometer, BOD Oxitop are shown in Figure 1.

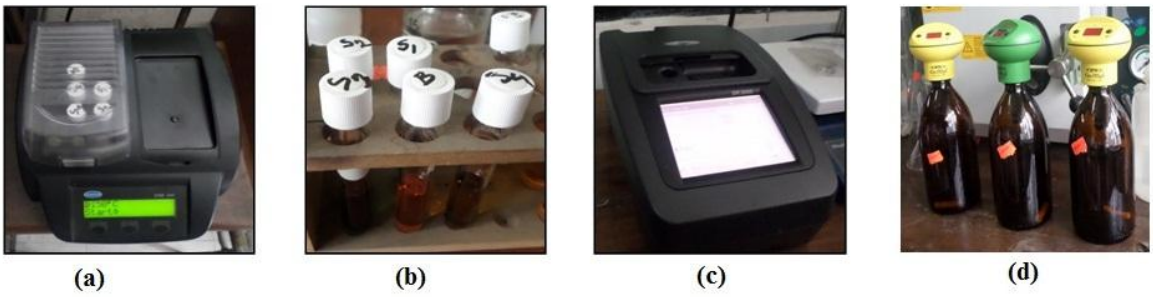

(a) (b) (c) (d)

Figure 1: (a) COD Reactor, (b) COD Vial, (c) UV Spectrophotometer, (d) BOD Oxitop

Table 2: Recipe for Pretreatment, dyeing and aftertreatment of organic cotton S/J knitted fabric

	Amount in g/l or %	Dyes/Chemicals
Pretreatment	0.7	ALO (Wetting Agent/Detergent)
	0.25	ST-700 (Peroxide Stabilizer)
	1.5	ALBA C (Anti-creasing Agent)
	2	CAUSTIC
	2.5	H_2O_2
	1.5	A.ACID
	0.08	T-100 (Peroxide Killer)
	0.40%	Prima Green Eco scour
	0.40%	Prima Fast Gold RSL
Dyeing	0.5	SECURON-540 (Sequestering Agent)
	1	SECURON (Sequestering Agent)
	0.5	ALBA C (Anti-creasing Agent)
	0.5	RDLB (Leveling Agent)
	1.719250%	Remazol Ultra yellow RGBN
	1.326000%	Remazol Ultra Red RGB
	4.550000%	Remazol Deep Black RGBN
	90	SALT
	5	SODA
	1.75	CAUSTIC
After treatment	1.5	A.ACID
	1.5	CS (Softener Cationic)

2.2 Determination of Chemical Oxygen Demand (COD): The COD is used as a measure of oxygen equivalent of organic matter content of sample that is susceptible to oxidation by strong chemical oxidant for sample from a specific source. It is the measure of both biologically oxidizable and biologically inert organic matter [9]. The apparatus used in COD measurement were COD Reactor (Figure 1, a); Micro pipette, Beaker, COD Vial (Figure 1, b); UV Spectrophotometer (Figure 1, c). First effluents were taken in COD vial. Then the vial was kept in COD reactor at 150^0C for 2 hours. Then the vial was put off from COD reactor and cooled in normal temperature. After that the sample was tested in UV spectrophotometer with respect to the fresh COD vial to get COD value.

2.3 Determination of Biological Oxygen Demand (BOD): The BOD is a measure of the quantity of oxygen used by microorganisms in the oxidation of organic matter [10]. The basic principle involves the estimation of dissolved oxygen uptake of sample and blank initially and after incubation for 3 days at 270C. To standardize the measurement of BOD the incubation period and temperature were as period: 5 days and temperature 20ºC respectively. Firstly pure distilled water saturated with oxygen was taken in BOD Oxitop (Figure 1, d). 5ml of polluted water+25ml of pure water were taken in another BOD Oxitop. Then the both oxitop was kept for five days in BOD incubator at 20ºC. Next dissolved oxygen of pure water and dilute impure water were measured after 5 days to get BOD values.

2.4 Determination of Total dissolved Solid (TDS) and Total Suspended Solid (TSS): Total solid (TS) refers to the matter that remains as residue upon evaporation and drying at 103-105^0C [11].The total solid includes total suspended solid (TSS)-the portion of the total solid retained by filter (Figure 2, a) and total dissolved solid (TDS)-the portion that passes through the filter. A clean glass beaker was taken (which was kept at 103ºC in an oven for 1 hour) of 150 ml capacity and also the weight of the beaker was taken. Then 100 ml of the sample was poured into the beaker. After that the beaker was placed in an oven maintained at 103ºC for 24 hours. Then cooling the beaker weight of the beaker was taken. Weight of the solid (Figure 2, b) was found by subtracting this value from the weight of clean beaker.

Total Solids, TS (mg/l) = (mg of solids in the beaker×1000)/volume of sample
TDS (mg/l) = (mg of solids in the beaker×1000)/volume of sample
Total suspended solid, TSS (mg/Lt) = TS (mg/L) – TDS (mg/L)

2.5 Determination of Dissolved Oxygen and P^H: Waste water is taken in a beaker, DO port, and pH ports were set to multi meter (Figure 2, c) for determining pH, DO and Conductivity respectively. Then the port was dipped into the waste water and kept for few seconds until the result was shown in the display. DO (mg/L) and conductivity (mS/cm) values were found directly from multi meter.

(a) (b) (c)

Figure 2: (a) Funnel & Filter Paper, (b) Dried Sample, (c) Multi-meter

III. RESULTS AND DISCUSSIONS

It is easily noticeable from various data, for almost all processes the effluent parameters exceeded the Bangladesh standards to a great extent. The ecological parameters of the effluent obtained from dyeing of bio-scoured and dyeing of organic cotton single jersey fabrics with environmentally low impact textile reactive dyes was investigated. The dyes used include low impact (Remazol RGB series) reactive dyes of DyStar branded along with others non RSL chemicals and auxiliaries certified by Oeko-Tex. The results show that the use of the low impact reactive dyes has greater ecological advantages as it reduces the COD, BOD, TSS, TDS and pH of the effluent considerably. It also shows higher amount of DO and balanced pH values with a tolerable pH limit. Further, the use of good branded and Oeko-Tex certified chemicals and auxiliaries also provide better results for effluents whereas these ecological parameters are of highly environment pollutant for others for regular dyeing process available in most of the industries. Physico-chemical characteristics of effluents of organic cotton fabric after bio-scouring and after dyeing are represented at Table 3 and 4 respectively.

3.1 Chemical Oxygen Demand (COD): The COD (mg O/l) values of the effluent for dyeing of the scoured and dyed fabrics are presented in Figure 3. The results show that the COD of the effluent does from scouring and dyeing stages of fabrics is combatively less and only 3 to 4 times higher than the standard limit by DOE where as these values are many times higher in case of regular dyeing. Hence, the dyeing of organic cotton fabric with the low impact dyes can reduce the COD of the effluent compared to that of dyeing with the regular dyes.

3.2 Biological Oxygen demand (BOD): The BOD (mg O/l) values for dyeing process of the scoured and dyed fabrics are presented in Figure 4. The results show that the BOD of the dye bath effluent for the dyeing process with low impact reactive dyes is less i.e. 200 mg/L & 582 mg/L for dyeing and scouring respectively. Hence, dyeing of organic cotton fabric with low impact reactive dyes can reduce the BOD of effluent to a large extent as comparatively.

3.3 Total Dissolved Solids (TDS) and Total Suspended Solids (TSS): The TDS (mg/l) and TSS (mg/l) values for the dyeing and scouring of fabrics of organic cotton are presented in Figure 5 and Figure 6. The results show that the TDS and TSS values of the effluents obtained less compared to that of others regular dyeing process. This is due to low impact and eco-friendly dyes used in the dyeing process. In general, it is observed that TSS of the effluents obtained from the dyeing and scouring process of the fabrics with eco-friendly dyes chemicals is 1.72 and 2.56 times higher and for TDS this value for dyeing is 1710 mg/L which is within the limit and 3130 mg/L i.e. only 2 times higher compared to that of DOE standard.

3.4 Dissolved Oxygen (DO) and pH: The dissolved oxygen (DO) and pH values are presented in figure 7 and 8 respectively which shows that the DO values are increased for dying and within the limit by Bangladesh standard with a balanced pH for both scouring and dying process with eco-friendly dyes and chemicals.

Table 3: Physico-chemical characteristics of effluents of organic cotton fabric after bio-scouring

Effluents Content	Pollutant Nature	Tested Results	DoE Standard
ALO (Wetting Agent) ST-700 (Peroxide Stabilizer) ALBA C (Anti-creasing Agent) CAUSTIC, H_2O_2, A.ACID T-100 (Peroxide Killer) Prima Green Eco scour (Enzyme) Prima Fast Gold RSL (Enzyme) SECURON (Sequestering Agent)	BOD in mg/L	582	50
	COD in mg/L	965	200
	DO in mg/L	4.34	4.4-8.0
	TDS in mg/L	3130	2100
	TSS in mg/L	384	150
	pH	11.14	6-9

Table 4: Physico-chemical characteristics of effluents of organic cotton fabric after dyeing

Effluents Content in Dyeing stages	Pollutant Nature	Tested Results	DOE Standard
SECURON (Sequestering Agent) ALBA C (Anti-creasing Agent) RDLB (Leveling Agent) Reactive Dyes: Remazol Ultra yellow RGBN Remazol Ultra yellow RGBN Remazol Ultra yellow RGBN SALT, SODA, CAUSTIC	BOD in mg/L	200	50
	COD in mg/L	650	200
	DO in mg/L	5.15	4.4-8.0
	TDS in mg/L	1710	2100
	TSS in mg/L	258	150
	pH	9.5	6-9

3.5 Graphical Presentation of Effluents Tested Results

Figure 3: COD values of effluents after scouring & dyeing of organic cotton

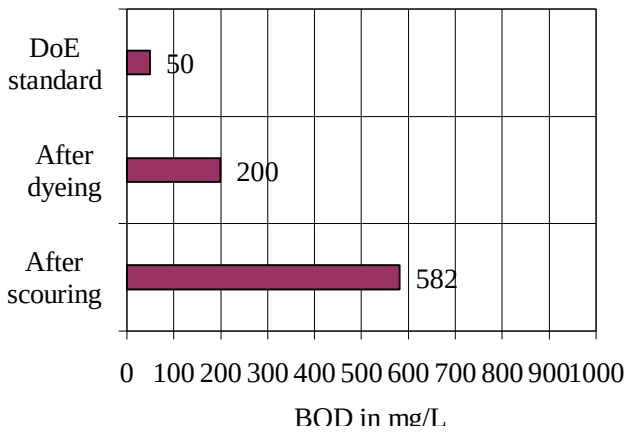

Figure 4: BOD values of effluents after scouring & dyeing of organic cotton fabric

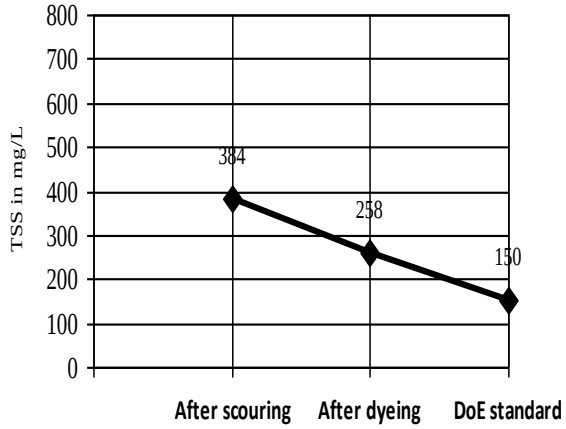

Figure 5: TSS values of effluents after scouring & dyeing of organic cotton

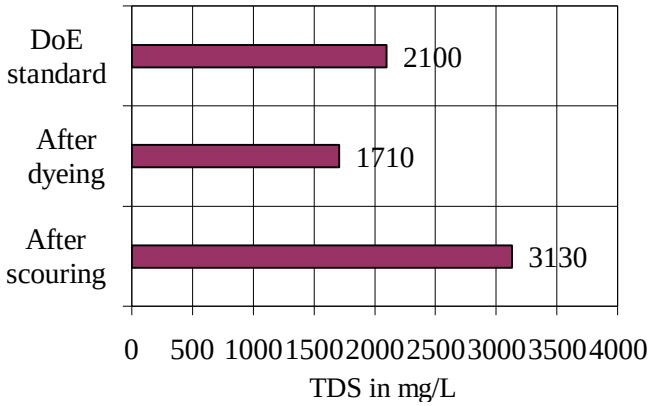

Figure 6: TDS values of effluents after scouring & dyeing of organic cotton

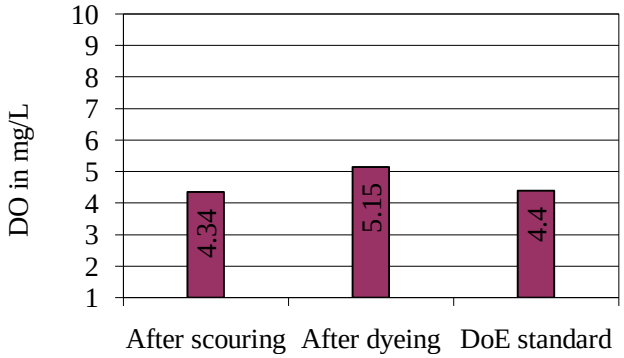

Figure 7: DO values of effluents after scouring & dyeing of organic cotton

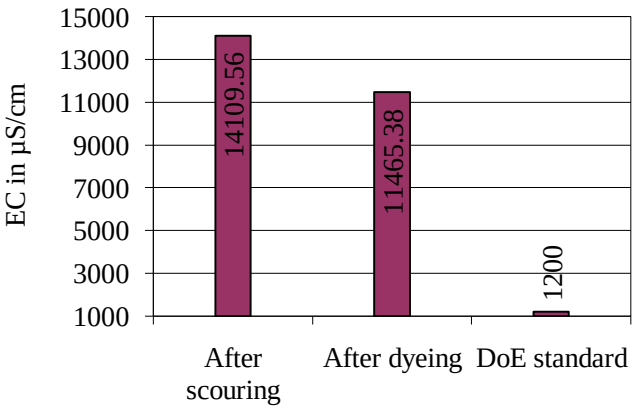

Figure 8: EC values of effluents after scouring & dyeing of organic cotton

IV. CONCLUSION

The textile industry is highly water intensive and one of the major contributor in environment pollution especially water in Bangladesh. In general, the results show that the use of the low impact reactive dyes has greater ecological advantages as it reduces the COD, BOD, TDS, TSS, and increase the DO and balanced pH values of the effluent considerably. Further, the fabric made from organic cotton itself also reduces the COD, BOD, TSS and TDS values. Besides, significantly increases the DO values maintaining tolerable pH values of the effluents. Finally it can be concluded that if various verified eco-friendly dyes and chemicals are used widely in wet processing, the environment pollution could be minimized to a greater extent.

REFERENCES

[1] S.N. Jayanth, R. Karthik, S. Logesh, R.K. Srinivas, & K. Vijayanand, Environmental issues and its impacts associated with the textile processing units in Tiruppur, Tamilnadu. *2nd International Conferences on Environmental Science and Development, IPCBEE*, 2011, 4, 120-124

[2] B.G. Ridoutt, & S.A. Pfister revised approach to water footprinting to make transparent the impacts of consumption and production on global freshwater scarcity. *Global Environmental Change*, 2010, 20, 113–120

[3] V.M. Correia, T.Stephenson, S.J. Judd, Characterization of textile wastewater – a review. *Environ Technol*. 1994,15, 917–929

[4] S.S. Noor, & H. Rohasliney, A Preliminary Study on Batik Effluent in Kelantan State: A Water Quality Perspective. *International Conference on Chemical, Biological and Environment Sciences, Bangkok*, 2011, 274-276.

[5] P.A. Desai, & V.S. Kore, Performance Evaluation of Effluent Treatment Plant for Textile Industry in Kolhapur of Maharashtra. *Universal Journal of Environmental Research and Technology, 2011, 1*, 560-565.

[6] T.S. Nese, Nuket, & T. Ismail, Pollutants of Textile Industry Wastewater and Assessment of its Discharge Limits by Water Quality Standards. *Turkish Journal of Fisheries and Aquatic Sciences, 2007, 7*, 97-103.

[7] V. Lav, & S. Jyoti, Analysis of Physical and Chemical Parameters of Textile Waste Water. *Journal of International Academy of*

Physical Sciences, 2011,15, 269-276
[8] I.A.E. Bisschops, & H. Spanjers, Literature review on textile wastewater characterization. *Environmental Technology, 2003, 24,* 1399-1411.
[9] V.J. Joshi, & D.D. Santani, Literature review on textile wastewater characterization. *Environmental Technology, 2012, 24,*1399-1411
[10] M.D. Roy, Textile industry: beneficiary of environmental management system. *2nd International Conference on Environmental Science and Technology, IPCBEE, Singapore.* 2011
[11] N.H.N. Sofia, Physico-Chemical Characterization of Effluents of Local Textile Industries of Faisalabad–Pakistan. *International journal of agriculture & biology , 2000, 2 (1),* 232-233

American Journal of Engineering Research (AJER)
e-ISSN : 2320-0847 p-ISSN : 2320-0936
Volume-03, Issue-12, pp-69-75
www.ajer.org

Research Paper Open Access

Improved Grid Synchronization Algorithm for DG System using and UH PLL under Grid disturbances

R.Godha[1,] Ch.V.S.S.Sailaja[2,] K.V.Ramana Murthy[3]
[1,]PG Scholor, [2,]Associate Professor , [3,]Professor

ABSTRACT : *Distributed Generation (DG) System is a small scale electric power generation at or near the user's facility as opposed to the normal mode of centralized power generation. In order to ensure safe and reliable operation of power system based on DS, grid synchronization algorithm plays a very important role. Unbalanced Harmonic (UH) based phase locked loop (PLL) aimed to provide an estimation of the angular frequency and both the positive and negative sequences of the fundamental component of an unbalanced three-phase signal. The UH PLL does not require transformation of variables into synchronous reference frame coordinates. Therefore, the proposed scheme is not based on the phase angle detection. Instead the angular frequency is detected and used for synchronization purposes. The design of this PLL is based on a complete description of the source voltage involving both positive and negative sequences in stationary coordinates and considering the angular frequency as an uncertain parameter. Therefore UHPLL is intended to perform properly under severe unbalanced conditions and to be robust against angular frequency variations, sags and swells in the three-phase utility voltage signal.*

INDEX TERMS: *Grid synchronization, phase locked loop, power quality, grid disturbances, positive and negative sequence detection, synthesis circuit, adaptive control, frequency estimation.*

I. INTRODUCTION

The power generation systems based on renewable energy systems are distributed near the user's facility. These Distributed Generation (DG) systems need to be controlled properly in order to ensure sinusoidal current injection into the grid. However, they have a poor controllability due to their intermittent characteristics [3]. The major issue associated with DG system is their synchronization with utility voltage vector [4]. Henceforth the study of grid synchronization algorithms is essential. Few of the earliest known synchronization algorithms Include Zero Crossing Detectors (ZCDs). The performance of ZCDs is badly affected by power quality problems, especially in the case of weak grid. The use of Phase Locked Loops (PLLs) for grid synchronization has shown much better results as it has been discussed in [5]. The Linear PLL is mainly used to detect phase for single phase supply. For balanced three phase supply, Synchronous Reference Frame (SRF) PLL is used. But it is found that this PLL fails to detect the phase for unbalanced supply [6]. Hence Decoupled Double Synchronous Reference Frame (DDSRF) PLL was proposed to deal with unbalanced grid conditions like voltage unbalance [7]. DDSRF PLL can detect the positive sequence phase angle in such conditions. Double Synchronous Reference PLL based on synthesis circuit was proposed in [6] which is more frequency adaptive and can be easily implemented.This paper also presents an algorithm to implement a PLL, which is able to provide an estimation of the angular frequency and both the positive and negative sequences of the fundamental component of an unbalanced three-phase signal. These sequences are provided in fixed-reference-frame coordinates. The synchronization process in the UH-PLL is based on the detection of the fundamental frequency [17]–[20]. The overall design of the UH-PLL does not assume a linearization process as in most conventional PLLs, which are based on the assumption sin x = x for x that is arbitrarily small. Instead, the design and analysis follow the Lyapunov approach. Therefore, the UH-PLL is aimed to perform properly under unbalanced conditions, voltage sags, swells, and angular frequency variations, among others, providing a fast and precise response. Moreover, due to the selective nature of the scheme, it owns certain robustness against harmonic distortion that is present in the source voltage signal. The rejection of low harmonics, however, is an issue that has not been explicitly considered in the present work.

II. ANALYSIS OF UNBALANCED AND HARMONIC BASED PLL

This section presents the model for the grid voltage, which is essential for the design of the UH-PLL. For a clear presentation, only the unbalance operation case is treated first, without harmonics, from which a basic scheme referred as U-PLL is presented [13]. Then, the effects of the harmonic distortion are included, which results in the addition of the UHCM to the basic model. This more complete scheme is thus referred as the UH-PLL.

A. Grid voltage under unbalanced condition: A model describing the grid voltage signal is presented [13]. This signal is originally described in three-phase coordinates v123 = $[v1, v2\ v3]^T$. The grid voltage signal is transformed to (fixed-frame) αβ-coordinates using Clarke's transformation. Moreover, both positive and negative sequences are considered to deal with the unbalanced case.

$$V_{\alpha\beta}=V^{p}_{\alpha\beta}+V^{n}_{\alpha\beta}=e^{J\theta}V^{p}{}_{dq}+e^{-J\theta}V^{n}{}_{dq} \quad (1)$$

$$e^{J\theta}=\begin{bmatrix}\cos\theta_0 & \sin\theta_0\\ -\sin\theta_0 & \cos\theta_0\end{bmatrix} J=\begin{bmatrix}0 & -1\\ 1 & 0\end{bmatrix} \quad (2)$$

Where $V^{p}_{\alpha\beta}$ and $V^{n}_{\alpha\beta}$ represent the positive and negative symmetric components of $V_{\alpha\beta}$ respectively. Based on this, the following model that completely describes the unbalanced sinusoidal signal generator $V_{\alpha\beta}$ is obtained as

$$\dot{V}_{\alpha\beta}=\omega_0 J\varphi_{\alpha\beta}$$

$$\dot{\varphi}_{\alpha\beta}=\omega_0 J V_{\alpha\beta}$$

Where ω_0 represents the fundamental frequency of the grid voltage

and the following auxiliary variable has been defined, which is necessary to complete the model.

$$\varphi_{\alpha\beta} \cong V^{p}_{\alpha\beta} - V^{n}_{\alpha\beta}$$

Based on definitions of $v_{\alpha\beta}$ and of $\phi_{\alpha\beta}$, it is possible to establish the following relationship

$$\begin{bmatrix}V_{\alpha\beta}\\ \varphi_{\alpha\beta}\end{bmatrix}=\begin{bmatrix}I_2 & I_2\\ I_2 & -I_2\end{bmatrix}\begin{bmatrix}V^{p}_{\alpha\beta}\\ V^{n}_{\alpha\beta}\end{bmatrix} \quad (3)$$

Where I_2 is the 2X2 Identity matrix.

B. Model of the grid voltage considering Harmonic distortion: In the case of the presence of harmonic distortion in the grid voltage, can be represented as follows

$$V_{\alpha\beta} = \sum_{K\in\{H\}}(V^{p}_{\alpha\beta,k}+V^{n}_{\alpha\beta,k})=\sum_{K\in\{H\}}(e^{JK\theta}V^{p}_{dq,k}+e^{-JK\theta}V^{n}_{dq,k}) \quad (4)$$

$$e^{JK\theta}=\begin{bmatrix}\cos k\theta_0 & \sin k\theta_0\\ -\sin k\theta_0 & \cos k\theta_0\end{bmatrix}$$

As before it is possible to establish the following relationship for the fundamental component

$$\begin{bmatrix}V_{\alpha\beta,1}\\ \varphi_{\alpha\beta,1}\end{bmatrix}=\begin{bmatrix}I_2 & I_2\\ I_2 & -I_2\end{bmatrix}\begin{bmatrix}V^{p}_{\alpha\beta,1}\\ V^{n}_{\alpha\beta,1}\end{bmatrix} \quad (5)$$

C. Basic U-PLL for unbalanced operation: The objective of the proposed scheme is to deliver estimates for positive and negative sequences of the grid voltage, as well as an estimate of the fundamental frequencyω_0. An adaptive estimator for state variables $V_{\alpha\beta}$ and $\varphi_{\alpha\beta}$ is designed for this purpose. The adaptive estimator generates two pairs of quadrature signals, and thus, it will be referred as the adaptive quadrature signals generator under unbalanced conditions (U-AQSG) [13].

(i) ***Adaptive quadrature signals generator U-AQSG:*** The estimator U-AQSG is proposed for the estimation of the fundamental component of state variables $V_{\alpha\beta}$ and $\varphi_{\alpha\beta}$ Where γ is a positive design parameter used to get the required damping, and $\widehat{\omega_0}$ is the estimate of the unknown parameter ω_0 [13].

$$\dot{\hat{V}}_{\alpha\beta}=\widehat{\omega_0} J\,\hat{\varphi}_{\alpha\beta} + \gamma_1\tilde{V}_{\alpha\beta} \quad (6)$$

$$\dot{\hat{\varphi}}_{\alpha\beta} = \widehat{\omega_0} J\,\hat{V}_{\alpha\beta}$$

(ii) ***Fundamental frequency estimator – U-FFE :*** The reconstruction of $\widehat{\omega_0}$ is performed by means of the following adaptive law referred as the fundamental frequency estimator (U-FFE).

$$\dot{\hat{\omega}} = \lambda\tilde{V}_{\alpha\beta}{}^{T} J\hat{\varphi}_{\alpha\beta} \quad (7)$$

Where λ >0 is the adaptation gain. The design of this estimator follows the estimation by using Lyapunov's approach.

(iii) ***Positive and negative sequences generator – PNSG:***

Having the estimates $\hat{V}_{\alpha\beta}$ and $\hat{\varphi}_{\alpha\beta}$ the positive and negative sequences of the grid voltage can now be reconstructed as follows

$$V^{p}_{\alpha\beta} = \frac{1}{2}(\hat{V}_{\alpha\beta} + \hat{\varphi}_{\alpha\beta}) \qquad (8)$$

$$V^{n}_{\alpha\beta} = \frac{1}{2}(\hat{V}_{\alpha\beta} - \hat{\varphi}_{\alpha\beta})$$

this is referred as the positive and negative sequences generator (PNSG)

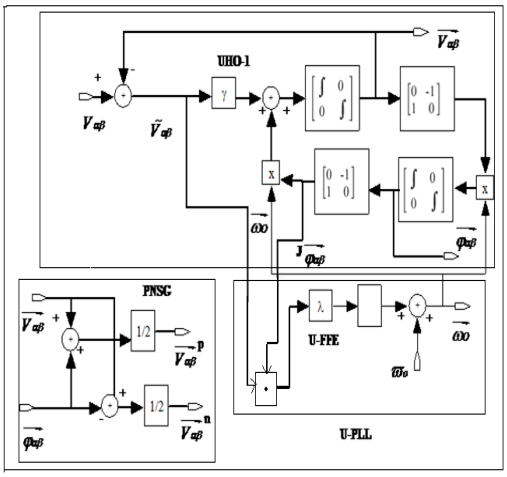

Fig 1: Block diagram of the proposed U-PLL algorithm considering a sinusoidal unbalanced reference signal $V_{\alpha\beta}$

***D. Proposed UH-PLL considering unbalance and harmonic distortion*:** The previous scheme U-PLL is extended to consider harmonic distortion present in the grid voltage. For this purpose it is proposed to introduce a harmonic compensation mechanism (UHCM) .The scheme is referred as UH-PLL as it considers the operation under unbalanced and harmonic distortion. Previous algorithms in [13] and [20] did not include any explicit mechanism for harmonic cancelation. And thus a slight ripple was present in the responses. This effect could be alleviated by limiting the bandwidth of the overall scheme; however, the speed of response is reduced. Hence a trade off between the speed of response and the harmonic compensation properties was established. In the UH-PLL scheme this trade-off is relaxed by the introduction of the UHCM, which allows fast and clean responses.

***E. Unbalanced harmonic compensation mechanism – UHCM* :** The UHCM can be seen as plug-in block that can be easily added to the basic scheme U-PLL. This scheme represents an alternative to the harmonic compensation scheme reported in [15].

The estimator for the kth harmonic component (k ∈ H) can be proposed as follows

$$\dot{\hat{V}}_{\alpha\beta,k} = k\widehat{\omega_0}\,\mathrm{J}\,\hat{\varphi}_{\alpha\beta,k} + \gamma_k \tilde{V}_{\alpha\beta} \qquad (9)$$

$$\dot{\hat{\varphi}}_{\alpha\beta,k} = k\widehat{\omega_0}\,\mathrm{J}\,\hat{V}_{\alpha\beta,k}$$

Where γ_k is a positive design parameter used to introduce the required damping.

$\widehat{\omega_0}$ is the estimate of parameter ω_0 to be defined later; and $\tilde{V}_{\alpha\beta} \cong V_{\alpha\beta} - \hat{V}_{\alpha\beta}$, with $\hat{V}_{\alpha\beta}$ representing the estimated voltage .In fact, the estimated voltage signal $\hat{V}_{\alpha\beta}$can be decomposed as follows

$$\hat{V}_{\alpha\beta} = \hat{V}_{\alpha\beta,1} + \hat{V}_{\alpha\beta,h} \qquad (10)$$

Where $\hat{V}_{\alpha\beta,1}$ represents the estimate of the fundamental component and $\hat{V}_{\alpha\beta,h}$ represents the estimate of the harmonic distortion components of the grid voltage. The fundamental component $\hat{V}_{\alpha\beta,1}$is reconstructed according to

$$\dot{\hat{V}}_{\alpha\beta,1} = \widehat{\omega_0}\,\mathrm{J}\,\hat{\varphi}_{\alpha\beta,1} + \gamma_1 \tilde{V}_{\alpha\beta} \qquad (11)$$

$$\dot{\hat{\varphi}}_{\alpha\beta,1} = k\widehat{\omega_0}\,\mathrm{J}\;\hat{V}_{\alpha\beta,1}$$

The harmonic distortion component $\hat{V}_{\alpha\beta,h}$ computed in block UHCM is performed as follows [13]. First, each harmonic component is reconstructed for k ∈{3, 5, ...}. Second, all harmonic components are accumulated in a single signal as follows.

$\hat{V}_{\alpha\beta,h}=\sum_{K\in\{3,5\ldots\}}\hat{V}_{\alpha\beta,k}$

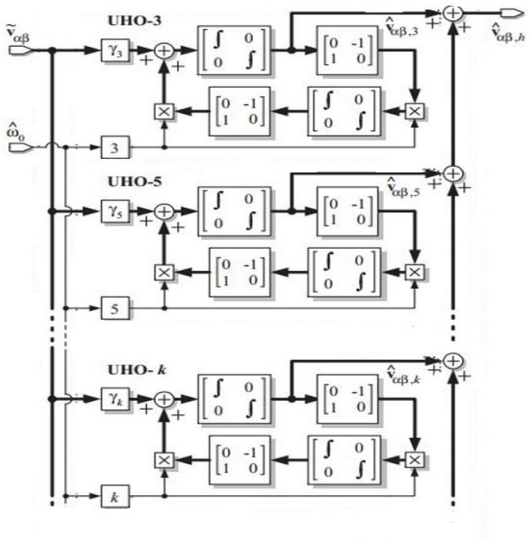

Fig 2 Block diagram of the unbalanced harmonic compensation mechanism UHCM including unbalanced harmonic oscillators tuned at 3th, 5th and k_{th} harmonic

Reconstruction of signal $\widehat{\omega_0}$ is performed by the following adaptive law

$$\dot{\widehat{\omega}}_0 = \lambda \tilde{V}_{\alpha\beta}{}^{T} J \hat{\varphi}_{\alpha\beta,1}$$

Whereas before, λ > 0 represents the adaptation gain,

$$V^{p}_{\alpha\beta,1} = \frac{1}{2}(\hat{V}_{\alpha\beta,1}+\hat{\varphi}_{\alpha\beta,1})$$

$$V^{n}_{\alpha\beta,1} = \frac{1}{2}(\hat{V}_{\alpha\beta,1}-\hat{\varphi}_{\alpha\beta,1})$$

***F. Tuning of the UH-PLL algorithm*:** Some rules for a tuning of control parameters λ and γ_k (k ∈ H) are presented [13]. For this purpose, some simplifications are considered. First, Non distorted case is considered, i.e., no UHCM block is included. Second, it is considered that the system is in balanced operation, that is, ϕαβ~= vαβ. Finally, a linearization process is considered. These simplifications yield a LTI system which coincides with the one studied in [16], where they propose to tune the parameters according to the following expressions.

$\lambda \cong \sqrt{2}\omega_{BW}$

$$\gamma_1 = \left(\frac{\omega_{BW}}{|v_{\alpha\beta}|}\right)^2$$

Where ω_{BW} is basically the desired bandwidth of the fundamental frequency estimator, which is recommended to be selected in the range $\frac{\omega_0}{5} \leq \omega_{BW} \leq \frac{\omega_0}{2}$. For the rest of the gains γ_k (k ∈ {3, 5, ...}) a first tuning rule can be stated as follows.

The influence of the second order system frequency response, each gain γ_k can be fixed at

$\gamma_k = \left(\frac{2.2}{T_{sk}}\right)$, k ∈ {3, 5, ...}

Where T_{sk} is the response time of each harmonic component (evaluated between 10%-90% of a step response of the amplitude of the corresponding sinusoidal perturbation).

III. RESULTS AND DISCUSSIONS

A. Response of UH PLL during unbalanced grid voltages:

The following parameters have been selected λ = 300 and γ1= 1.5, which correspond approximately for a bandwidth of ω_{BW} =150 rad/s (24 Hz). It is assumed that the grid voltage signal contains 3rd and 5th harmonics, and thus the UHCM contains UHOs tuned at these harmonics. The grid voltage has a nominal frequency of ω_0=314.16 rad/s (50 Hz), and an approximate amplitude of |vαβ| = 100 V.

The following cases have been considered for the utility voltage:
(i) **Unbalanced condition:**. The voltage source includes both a positive and negative sequence components. The positive sequence has 100 V of amplitude at 314.16 rad/s (50 Hz) and zero phase shift. For the negative sequence amplitude of 10V approximately and zero phase shift are considered.
(ii) **Harmonic distortion:** Harmonics 3rd and 5th are added to the previous unbalanced signal to create a periodic distortion. Both harmonics have also a negative sequence component to allow unbalance in harmonics as well. Both positive and negative sequences of these harmonics have 10 V of amplitude and zero phase shift.

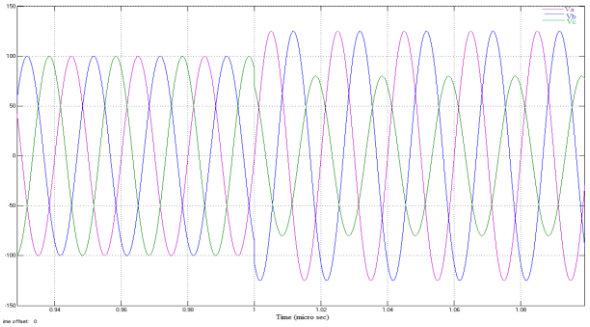

(a)

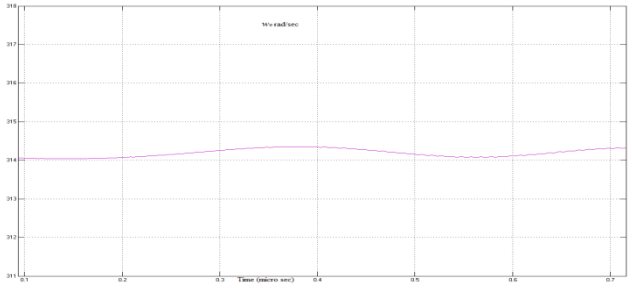

(b)

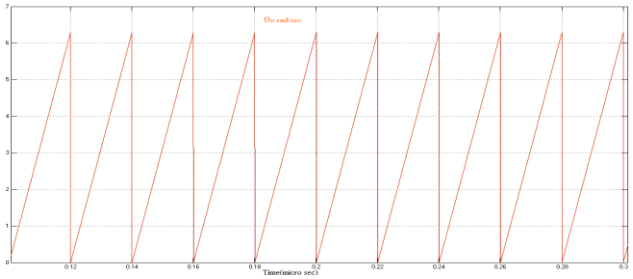

(c)

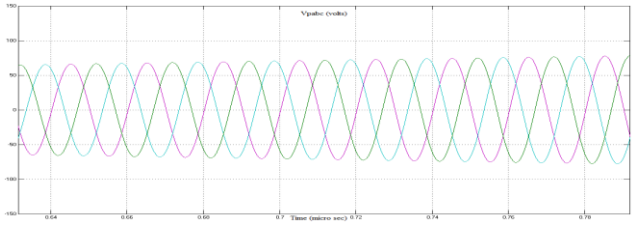

(d)

Fig.3 Response of UH PLL during unbalanced grid voltages
(a) Unbalanced Supply Voltage (b) ω_0 estimate (rad/sec)
(c) θ_0 Estimate (rad) (d) estimated positive sequence voltage in three-phase coordinates.

Fig 3(a) shows the transient response obtained with the pro-posed UH-PLL when the utility voltage goes from a

balanced to an unbalanced operation condition at time t=1s.In Fig 3(b) notice that, after a relatively short transient the signal returns to their desired value of 100π.In Fig 3(c) the phase angle which is the time integration of angular frequency is perfectly triangular as there were only small transients in the angular frequency.

B. Response of UHPLL during distorted harmonic grid condition

Figure 4 shows the transient response of the proposed UH-PLL when harmonic distortion is added to the already unbalanced grid voltage at t = 1.8s.

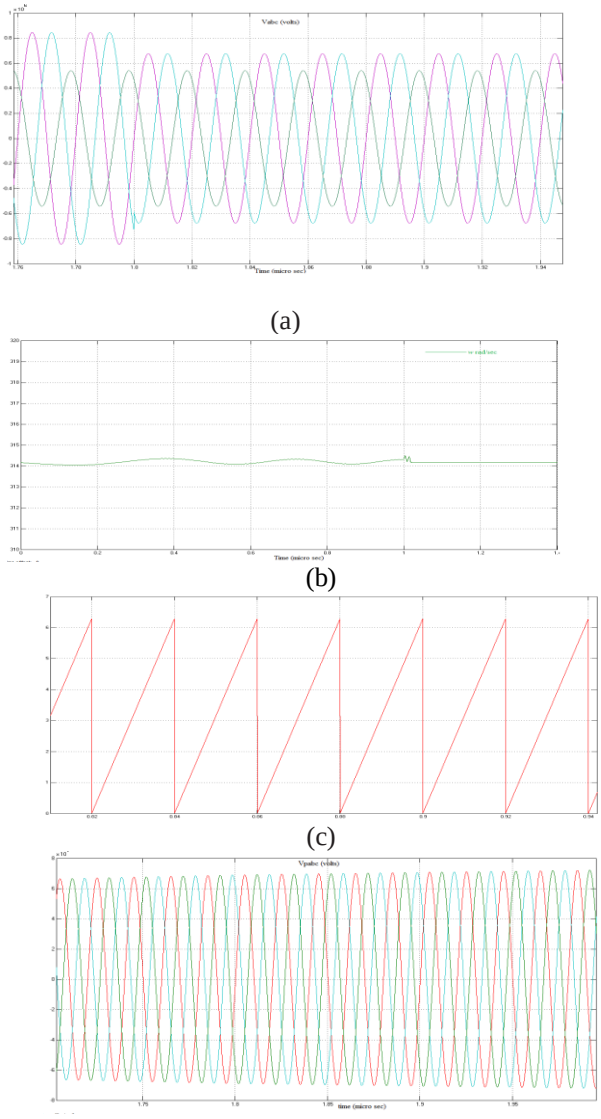

(a)

(b)

(c)

(d)

Fig.4 Response of UH PLL during distorted harmonic grid condition (a) Unbalanced Supply Voltage (b) ω_0 estimate (rad/sec)(c) θ_0 estimate (rad) (d) estimated positive-sequence voltage in three-phase coordinate

In Fig 4(a) it is noticed that, after a relatively short transient, all signals return to their desired values From Fig 4(b) in particular, notice that the estimated frequency is also maintained in its reference fixed to 314.14 rad /s after a small transient, without further fluctuations. In Fig 4(c) the phase angle which is the time integration of angular frequency is perfectly triangular as there were only small transients in the angular frequency. It can be observed that in Fig 4(d) the estimated positive-sequence voltages have an almost imperceptible transient.

IV. CONCLUSIONS

It was observed that in spite of an unbalanced and distorted reference signal the UH-PLL was able to deliver pure balanced sinusoidal signal represented by the positive sequence component of the reference signal, plus a ripple free fundamental frequency estimated signal. As the UH-PLL includes an explicit mechanism to compensate harmonics, it reduced considerably the effect of disturbances without compromising the speed of response of the overall scheme. In cases of low distortion, this mechanism can be easily disconnected and rely on the selective nature of a basic method, which can be enhanced at the expenses of reducing the speed of response of the overall scheme.

REFERENCES

[1] R. Teodorescu and F. Blaabjerg, "Flexible control of small wind turbines with grid failure detection operating in stand-alone and grid-connected mode," IEEE Trans. Power Electron., vol. 19, no. 5, pp.1323–1332, Sep. 2004.

[2] Z. Chen, "Compensation schemes for a SCR converter in variable speed wind power systems," IEEE Trans. Power Delivery, vol. 19, pp. 813-821, Apr. 2004.

[3] F. Blaabjerg, Z. Chen and S. Kjaer, "Power Electronics as Efficient Interface in Dispersed Power Generation Systems," *IEEE Trans. PowerElectron.*, vol. 19, no. 5, pp. 1184-1194, Sep. 2004.

[4] Timbus, R. Teodorescu, F. Blaabjerg and M. Liserre, "Synchronization Methods for Three Phase Distributed Power Generation Systems. An Overview and Evaluation," in Proc. 2005 Power Electronics Specialists Conference, 2005. PESC '05. IEEE 36,pp. 2474-2481.

[5] Francisco D. Freijedo, Jesus Doval-Gandoy, Oscar Lopez, Carlos Martinez-Penalver, Alejandro G. Yepes, Pablo Fernandez-Comesana, Andres Nogueiras, JanoMalvar, Nogueiras, Jorge Marcos and AlfonsoLago, "Grid-Synchronization Methods for Power Converters," Proc. Of IEEE, pp. 522 – 529, 2009.

[6] FANG Xiong, WANG Yue, LI Ming, WANG Ke and LEI Wanjun, "A Novel PLL for Grid Synchronization of Power Electronic Converters inUnbalanced and Variable-Frequency Environment," Proc. of IEEE International Symposium on Power Electronics for Distributed Generation Systems: pp. 466-471, 2010.

[7] P. Rodriguez, J. Pou, J. Bergas, J. I. Candela, R. P. Burgos and D. Boroyevich, "Decoupled Double Synchronous Reference Frame PLL for Power Converters Control," *IEEE Transactions on, PowerElectronics,* vol. 22, pp. 584-592, 2007.

[8] J. Svensson, "Synchronisation methods for grid-connected voltage source converters," Proc. Inst. Electr. Eng.—Gener. Transm. Distrib., vol. 148, no. 3, pp. 229–235, May 2001.

[9] M. Karimi-Ghartemani and M. Iravani, "A method for synchronization of power electronic converters in polluted and variable-frequency environments," IEEE Trans. Power Syst., vol. 19, no. 3, pp. 1263–1270, Aug. 2004.

[10] L.R. Limongi, R. Bojoi, C. Pica, F. Profumo, A. Tenconi, "Analysis and Comparison of Phase Locked Loop Techniques for Grid Utility Applications" Proc. IEEE Power Conversion Conference PCC, 2007, pp. 674-681.

[11] R. M. Santos Filho, P. F. Seixas, P. C. Cortizo, L. A. B. Torres, and A. F. Souza, "Comparison of three single-phase PLL algorithms for UPS applications" IEEE Trans. on Industrial Electronics, Vol. 55, No. 8, pp. 2923-2932, August 2008.

[12] P. Rodriguez, J. Pou, J. Bergas, J. I. Candela, R. P. Burgos and D. Boroyevich, "Decoupled Double Synchronous Reference Frame PLL for Power Converters Control," Power Electronics, IEEE Transactions on, vol.22, pp. 584-592, 2007.

[13] G. Escobar, M.F. Martinez-Montejano, A.A. Valdez, P.R. Martinez and M. Hernandez-Gomez, "Fixed-Reference-Frame Phase-Locked Loop for Grid Synchronization Under Unbalanced Operation," IEEE Trans. on Ind.Electron., Vol. 58, Issue 5, pp. 1943-1951, May 2011.

[14] D. Yazdani, M. Mojiri, A. Bakhshai and G. Joos, "A Fast and Accurate Synchronization Technique for Extraction of Symmetrical Components, "IEEE Trans. on Power Electron., Vol. 24, Issue 3, pp. 674-684, March2009.

[15] P. Rodriguez, A. Luna, I. Candela, R. Teodorescu and F. Blaabjerg,"Grid synchronization of power converters using multiple second order generalized integrators," in Proc. 34th IEEE Ind. Electron. Conf. IECON08, 10-13 Nov. 2008, pp. 755-760.

[16] Francisco D. Freijedo, Jesus Doval-Gandoy, Oscar Lopez, Carlos Martinez-Penalver, Alejandro G. Yepes, Pablo Fernandez-Comesana, Andres Nogueiras, JanoMalvar, Nogueiras,Jorge Marcos and Alfonso Lago, "Grid-Synchronizat ion Methods for Power Converters,"Proc. of IEEE 35th Annual Conference on Industrial Electronics, IECON 2009, pp. 522 – 529

[17] M. Mojiri and A. R. Bakhshai, "An adaptive notch filter for frequency estimation of a periodic signal," *IEEE Trans. Autom. Control*, vol. 49, no. 2, pp. 314–318, Feb. 2004.

[18] [16] D. Yazdani, M. Mojiri, A. Bakhshai, and G. Joos, "A fast and accurate synchronization technique for extraction of symmetrical components," *IEEE Trans. Power Electron.*, vol. 24, no. 3, pp. 674–684, Mar. 2009.

[19] [17] P. Rodriguez, A. Luna, M. Ciobotaru, R. Teodorescu, and F. Blaabjerg, "Advanced grid synchronization system for power converters under un-balance and distorted operation conditions," in *Proc. 32nd IEEE IECON*, Nov. 2006, pp. 5173–5178.

American Journal of Engineering Research (AJER)
e-ISSN : 2320-0847 p-ISSN : 2320-0936
Volume-03, Issue-12, pp-76-81
www.ajer.org

Research Paper Open Access

Renewal and Improvement of the Urban Rusty Areas with Using Of Sustainable Development Approach

Mohammad Hadi Hosseini Sarcheshmeh
MS of Geography & Urban Planning

ABSTRACT : *Today, sustainable development have been the cornerstone of many official forums of international countries and cities in the world. Its roots can be defined as in the problems that caused by the negative effects of the growing industrial towns and cities sought. On the other hand, the deterioration of tissues in the informal settlement areas that biological evolution is a regional industrial and lack of proper planning, struggled most of the metropolises of the world, and especially Iran country. In the this study, initially it has been apply to definition of urban distressed and sustainable development, then it has been clarified guidance's of modernization about distressed areas and indicators of sustainable development. Then to attention of the need to achieve sustainable development in the all urban areas, urban distressed areas should also follow this approach. After the adaptation of sustainable development indicators in the renovation and improvement urban distressed areas conclude that empowerment and indirect involvement in the tissue repair and replace a physical intervention, undermines the realization of sustainable development. Those indicators renovation and improvement of compliance with the indicators of sustainable development are directly and indirectly, by the summation and finally, the conclusion was that in the topics such as the development of inter-mixing of land uses, density increases, the social and economic networks, creating profit-generating functions and... Should be more emphasis on the urban distressed areas with minimal interference to the body and at the same time to increase the desirability and development.*

KEY WORDS: *Urban Distressed Areas, Sustainable Development, Renewal and Improvement*

I. INTRODUCTION & BACKGROUND

Considering that land is a scarce resource, it is thus essential that land especially urban land needs to be properly, efficiently, profitably, feasibly and professionally invested, developed, administered and managed. The objective is to ensure that urban land is used efficiently and effectively in relation to the national development objectives which call for growth with equity (Brebbia, 2000). Whilst it is considered easier and cheaper to look for 'Greenfields' to solve development pressure resulting from rapid urbanization, efficient land use management dictates that there is the need to adapt to external as well as internal pressures within the existing urban area and look at these brownfield as potential sites for re-development that can accommodate the increase in demand for more and better housing accommodation as well as other usage, thus the need for urban renewal or regeneration intervention and policy, through a plethora of initiatives, funding streams, and agencies, using the principles of New Urbanism(or through Urban Renaissance, its UK/European equivalent). Early government policies included "urban renewal "and building of large scale housing projects for the poor. Today with many people interested in moving back to the inner cities, new urbanism has renewed and restored some of these neighborhoods. Due to higher population densities in Europe, economics dictate that extremely low-density housing would be impractical.

According to Roberts & Sykes (2008), termed urban regeneration as a global phenomenon. It is an outcome of the interplay between the many internal forces that are present within the urban areas itself and the external forces that dictate the need for the urban areas to adapt. Within an urban area, a rational pattern of land use will evolve and this tendency is exhibited in all cities irrespective of size, origin or geographical location.

Principle factors that determine the pattern of land use in a particular urban area include competition for sites, accessibility and complementary factor in the sense that once a number of sites in a given area have been developed, this will have a strong bearing on the use of the remaining sites. Urban regeneration can be defined as a social and technical partnership based on the unification of the vision of politicians and designers and on the wide acceptance by the community. It is thus a multi-faceted and complex process which should not be viewed merely as a physical and financial proposition, but as a sociological, cultural, economic and political matter as well (Couch, 1990). Past experience has demonstrated the need to view neighborhood regeneration as comprehensive and integrated process. A realistic renewal program must approach regeneration in a holistic way and be based upon a multi-disciplinary understanding of the social and economic forces affecting urban areas and the physical nature of towns and cities (Roberts & Sykes, 2008). Estimates by the National Association of Home Builders (NAHB 2001) suggest that one in four households in our nation face a serious housing affordability crisis, others argue that our civil society is at risk as a result of a serious civic paralysis resulting in social isolation and a loss of "community"(Murphy and Cunningham 2003), still others suggest that 2/3's of the Michigan's residents living outside of central cities are living in communities struggling with social and fiscal stress thus jeopardizing the public sector's capacity to mobilize the necessary resources essential to a comprehensive revitalization agenda. Regardless of how one describes the scope of the challenges or prescribes the nature of potential solutions, communities in Michigan find themselves at a serious crossroads. They must, in a time of severely constrained economic resources, devise new and creative ways of rebuilding their distressed communities while also reinvigorating their civic society.

II. SUSTAINABLE DEVELOPMENT

Sustainable development is a road-map, an action plan, for achieving sustainability in any activity that uses resources and where immediate and intergenerational replication is demanded. As such, sustainable development is the organizing principle for sustaining finite resources necessary to provide for the needs of future generations of life on the planet. It is a process that envisions a desirable future state for human societies in which living conditions and resource-use continue to meet human needs without undermining the "integrity, The United Nations World Commission on Environment and Development (WCED) in its 1987 report Our Common Future defines sustainable development: "Development that meets the needs of the present without compromising the ability of future generations to meet their own needs (Lee, 2013)." Under the principles of the United Nations Charter the Millennium Declaration identified principles and treaties on sustainable development, including economic development, social development and environmental protection. Broadly defined, sustainable development is a systems approach to growth and development and to manage natural, produced, and social capital for the welfare of their own and future generations. The concepts of sustainable development and sustainability derive from the older forestry term "sustained yield", which, in turn, is a translation of the German term "nachhaltiger Ertrag" dating from 1713 (UN, 2014). Sustainability science is the study of the concepts of sustainable development and environmental science. There is an additional focus on the present generations' responsibility to regenerate, maintain and improve planetary resources for use by future generations.

Sustainable Development Indicators

 Economic considerations

1. Identify and define the technologies, materials and products and Preventing unsustainable production and consumption in the future;
2. Encourage the decentralization of industry;
3. Encourage small businesses and self-employment in urban;
4. The prevention of irregular migration;
5. Changing patterns of production, distribution and consumption of materials;
6. Supply growth and economic development.
7. Supply of goods required in order to reduce the distance and reduce energy
8. Reducing per capita costs of municipal services to enhance the economic viability of the city.

 Social and cultural considerations

1. Axis of the human being and his needs;
2. Deal with the explosion in urban population and reduce the population growth rate to near zero;
3. The identity and specific cultural features of the sustaining and strengthening local cultural value;
4. Alleviating poverty and reducing class differences changes in behavior to changes in consumption patterns;
5. Mobilize women, youth and children to participate in the environmental education and promotion of culture;
6. Balanced and equitable distribution of resources between urban areas.

Physical consideration:

[1] Precise positioning and optimal design and planning of new towns;
[2] Ecosystems that surround the city with the manufacturer or absorbent;
[3] Encourage local scientific knowledge and ingenuity in the field of construction;
[4] Distribution of the urban space based on hierarchical and fits the context of the ecological carrying capacity of the city (land use planning);
[5] In considering the specific situation of the environment as a key factor in development planning;
[6] Designing buildings based on the use of clean energy and promoting their use;
[7] Design of Buildings Based on Energy Saving;
[8] Using the Integrated Public Transport System;
[9] Planning and design standards to increase performance more profitable areas of biological;
[10] Lighting, water supply and public facilities with minimum cost;
[11] balanced spatial distribution of public facilities;
[12] Recycling and reusing space or unused space in the destruction;
[13] Revision of the rules and regulations of the building in terms of consumption building material;
[14] Careful attention to the problem of survival for several consecutive generations' buildings;
[15] Regarding the issue of mixed use and multi-functional use of space;
[16] The increased density based on detailed studies of the diagnosis and define the extent and distribution of density in urban areas;
[17] Given the considerable importance of pedestrian pathways and spaces;
[18] Detailed studies to define and introduce "Urban Sustainability Index" as a tool to measure the movement towards "sustainability" in the process of urban development.

Environmental considerations

[1] Linear flow of materials (data) input to the municipal system should be close as possible to a cyclic flow;
[2] An evaluation of the environmental studies strictly and Urban Development;
[3] The definition of ecological thresholds and capacity to withstand;
[4] Reduction of air pollution, noise, waste, sewage;
[5] Healthy Urban Environment and Health;
[6] Securing the City to prevent accidents and to minimize the effects of damage;

Considerations in decision-making and urban management

[1] The reform of the common practices of urban planning and studies;
[2] Participation of urban institutions, scientists and urban planners, designers and society in open discussion;
[3] To promote and encourage the use of public information public participation;
[4] The use of advanced computer technology for data analysis, evaluation and presentation of solutions;
[5] Urban development strategies should be selected from the top 5 Paym apply but must be designed and implemented by people and experts;
[6] Sustainability information exchange between communities working on a comparative study (Loghayee and Mahmoodzadeh Titkanlou, 1998).

Distressed areas : Accurate sense of old or worn not only in public but also among professionals has extensive barrier is not true. Different and sometimes competing interpretations of those words is raised misunderstandings abuse. Appear before any action is necessary to state the relevant rules, the assignment of all kinds of tissues, the nature and the manner and extent of involvement with the institution of the general ledger (Andalib, 2008). Result of natural wear and urban wear in small communities and individuals to prevent or repair and upgrade aging is a natural process. Economic and social factors that are present, they fuel urban wear rate (Mousavi, 2009). Corrosion or the "body" or "work" or the "body of work" together to penetrate. The equations can be formed that represent the types of wear and tear. One group of these equations can be represented as follows:

Physical Distressed : This is placed in the path of building quality loss caused by the passage of time, the effects of weather, ground movement, vibrations from traffic or improper maintenance or improper occur. Building and maintaining such a definition, more than what we currently provide regular maintenance needs.

Functional Distressed : It can also be caused by deterioration of the quality of the function. The tissue may be designed for functional, and it isn't suitable for current use. So in this case the standards or conditions of a

potential tenant or proprietor not matching. Functional deterioration of a building may be affected by a technical disadvantage. Functional Distressed may also be caused by a variety of features.

Distressed in mental image : Distressed and self-concept of mind based on the product mental image or the range. Over time, the change in the human environment, social, economic or natural, historical context without changing your fitness needs of people today and serve it occurs loss. This approach is a value judgment and may in fact be no real substance.

Distressed in legal and official : This type of physical deterioration and functional aspects relevant to the claim. It is supposed to foster new standards of health and safety, fire or building regulations, a building may be condemned to depression. Similarly, a building may be legally "worn out".

Local Rusty : Local rusty is affected by features functional activities within the scope (Hedaiatnia, 2007). Indicators of old texture:

1. At least 50% of its passages have a width of less than 6 meters .
2. At least 50% of homes have an area less than 200 meters.
3. 50% of homes have at least 3 seismic resistance . (Civil and subsets East, 2008: p 20)

Table (1)

The conclusion of the modernization, rehabilitation and reconstruction Distressed city can be seen in the following table:

Intervention method	Intervention goal	Suggestion principles	Apply method
Protection-health	Improve the quality of urban environment protection	•The urban transformation of the change, according to environmental compatibility, anatomical, functional &... •Improving the social-psychological cities with valuing art evidence nor historical requirement • Contemporary urban spaces for the promotion of tourism	•Improvements • Renovation
Decorative	•preservation of cultural assets •Contemporary frame building •aesthetic landscape Socio-economic development with regard to the preservation of cultural and historical wealth	•conduct individual interests in order to fulfill the public interest •Construction of a new building to preserve the collective memory and cultural •Maintain facial appearance and overall perspective of historic buildings and collections • Encourage owners to maintain historic buildings and collections through: tax breaks, financial aid, legislation and technical support	•Improvements • Renovation
Local-thematic	•Development of the •Contemporary Old Town with the creation of civic life and urban life •protection, monitoring, sustainability • regulate the cultural and historical heritage	•Increased sense of responsibility of state officials and residents of the old city to maintain the positive aspects of the old values of •Avoid moving the native inhabitants of the ancient city of and respect for the legitimate demands of the local population • community awareness of the value of vernacular architecture with sustainability and preservation of original content	•Improvements •Renovation • Restructuring

Comprehensive	•Development physical space •regulate the development and protection • enhance the dynamics of the old town of the city	•flexible and consistent with the protection and participation of all social forces •Comprehensive pre-intervention study • Protection of traditional patterns of old texture	•Improvements •Renovation • Restructuring
Urban Restoration	Contemporary with the promotion of civic life	•damage to surrounding buildings and monuments Remembrance • reconstruction of, buildings and spaces as LSAT	•Improvements •Renovation • Restructuring

Source: Habibi & Maghsoudi, 2009.

Adaptation measures and sustainable development of urban distressed areas : The standards, criteria and guidelines for sustainable development and urban renewal and improvement of the previously mentioned, renovation and refurbishment of worn those approaches that realize sustainable development of urban history or facilitate full compliance with the principles of sustainable development. The criteria considered are two general categories:

Measures consistent with the principles of sustainable development: Participation in the restructure and integrate concept of sustainable development is directly involved in the issue of social sustainability which it has been proposed.

- Guided by personal interests in order to fulfill the public interest: all the principles of sustainable development have been founded on the basis of public interest.
- Increasing urban density and the density incentive grant for the restoration worn out buildings of no value and historical identity.
- Subject increase in urban density and compactness of urban sustainability debate.
- - Protection of traditional patterns of old texture.
- Create a network of economic transactions, and an emphasis on basic employment and employment-related.
- It contributes to economic sustainability in the urban areas encouraged small businesses and self-employment, and reduce poverty and inequality.

Table (2)

Criteria & strategies of Regeneration and Sustainable development:

Criteria & strategies	Criteria & Sustainable development strategies	Match kind
Public participation in the reconstruction and integration	Public participation in the reconstruction and integration	Direct
Guided by personal interests in order to fulfill the public interest	All the principles of sustainable development have been founded on the basis of public interest.	Direct
Increasing urban density and the density incentive grant for the restoration worn out buildings of no value and historical identity	Increasing urban density and compact urban sustainability issues raised in the urinary discussion	Direct
Prevent displacement of the indigenous inhabitants of the ancient city	Prevent irregular migration	Facilitator
Intensive development and maximize land use in the tissue	Mix land use	Facilitator
Increased demand for construction and increased population control	Inside Development, a sustainable development approaches in the problematic context	Facilitator

III. CONCLUSION

Sustainable development is a road-map, an action plan, for achieving sustainability in any activity that uses resources and where immediate and intergenerational replication is demanded. As such, sustainable development is the organizing principle for sustaining finite resources necessary to provide for the needs of future generations of life on the planet. It is a process that envisions a desirable future state for human societies in which living conditions and resource-use continue to meet human needs without undermining the "integrity, The United Nations World Commission on Environment and Development (WCED) in its 1987 report Our Common Future defines sustainable development: "Development that meets the needs of the present without compromising the ability of future generations to meet their own needs. For this reason, guidelines for sustainable development is economic growth and prosperity by creating profit-generating functions that areas of small business, job creation and income growth will also add value to the land market.

REFERENCES

[1] **Andalib, A. Mosavi, S**. (2008). Urban for Chinese Compact, American scientific Journals, Indian research.
[2] **Bebbi, F.** (2000). Government and growth, translation, peggi,P & M.
[3] **Couch, Y.** (1990). Income expectations, urban migration and employment in Africa.International Labor Review, 104(5), 23.
[4] **Habibi, M. Maghsoudi, M.** (2009). Urban Regeneration. Tehran University press.
[5] **Lee, U**. (2013). Urbanization and old texture area, AJSCS, Vol 52.
[6] **Mosavi, S.** (2009). Urban rusty and its fields. Shora Journal.
[7] **NAHB** (2001). Public Affairs with assistance from the. NAHB Economics Group.
[8] **Roberts, J. Sykes, T.** (2008). Regional Development Theory. Canada: Mouton & Co.
[9] **UN**, (2014). Urban regeneration in the world.
[10] **Watkins Murphy and James V. Cunningham**. (2003). organizing for Community Controlled Development: Renewing Civil Society.

American Journal of Engineering Research (AJER)
e-ISSN : 2320-0847 p-ISSN : 2320-0936
Volume-03, Issue-12, pp-82-86
www.ajer.org

Research Paper Open Access

Performance Analysis of GSM System Using SUI Channel

Christin Nabonita Halder Jui[1], Kazi Firoz Ahmed[2]
(Department of Electrical and Electronic Engineering, American International University-Bangladesh, Bangladesh)

ABSTRACT: *GSM (Global System for Mobile Communications) is a standard developed by the European Telecommunications Standards Institute (ETSI) to describe protocols for second generation (2G) digital cellular networks used by mobile phones. A channel is used to convey the information signals. SUI channel model are an extension of the previously work by AT&T Wireless and Ercegetal. The main objective of this paper is to get better performance of GSM system using SUI channel model. Considering this goal, the simulation has been done. The performance is analyzed, which shows satisfactory BER for higher SNR. This result is compared with the performance of GSM system using AWGN channel. BER is affected by a number of factors. By modifying the variables that can be controlled, it is possible to optimize a system to provide the performance levels that are required. This article shows the better performance of GSM system using SUI channel than AWGN channel.*

Keywords – *GSM, SUI, BER, GMSK, AWGN*

I. INTRODUCTION

In telecommunications and computer networking, a communication channel refers either to a physical transmission medium such as a wire or to a logical connection over a multiplexed medium such as a radio channel. A channel has a certain capacity for transmitting information, often measured by its bandwidth in Hz or its data rate in bits per second. Channel models of fixed wireless applications and which contains the definition of a set of six specific channel implementations known as SUI channel.

GSM is a cellular network, which means that cell phones connect to it by searching for cells in the immediate vicinity. There are five different cell sizes in a GSM network- macro, micro, pico, femto and umbrella cells. The coverage area of each cell varies according to the implementation environment. GMSK is a modulation system used in GSM. GMSK (Gaussian Minimum Shift Keying) is a form of modulation used in a verity of digital radio communications system. It has advantages of being able to carry digital modulation while still using the spectrum efficiently. In this paper, the performance of GSM system using SUI channel is analyzed. GMSK modulation system has been followed to perform the analysis and for the simulation purpose, MATLAB software has been used as the simulation tool. The paper is organized as followed. The section II gives the historical backgrounds of GSM system, SUI channel and GMSK modulation. In section III, the modulation techniques have been discussed with necessary figures, which are specially focused on the techniques used in GSM. In section IV, SUI channel models are discussed with the proper information, tables and figures. In section V, the simulation results and comparison between the performances of AWGN channel and SUI channel are shown and discussed and section VI draws the conclusion. Theses information and analysis are useful for the telecommunication system all over the world.

II. BACKGROUNDS

In [1], GSM is the global standard mobile communications with over 90% market share, and is available in over 219 countries and territories. GSM networks operates in a number of different carrier frequency ranges (separated into GSM frequency ranges for 2G and UMTS frequency bands for 3G), with most 2G GSM networks operating in the 900 MHz or 1800 MHz bands. GSM has used a verity of voice codec to squeeze 3.1 KHz audio into between 6.5 and 13 Kbit/s. Originally , two codec, named after the types of data

channel they were allocated, were used, called Half Rate (6.5 Kbit/s) and Full Rate (13 Kbit/s). These used a system based on linear predictive coding (LPC). In addition to being efficient with bit rate, these codec also made it easier to identify more important parts of the audio, allowing the air interface layer to prioritize and better protect these parts of the signal. GSM was further enhanced in 1997 with the Enhanced Full Rate (EFR) codec, a 12.2 Kbit/s codec that uses a full rate channel. So far, it is known that AWGN channel has shown good performance in GSM system.

In SUI channel model, a set of six channels was chosen to address three different terrain types that are typical of the continental US [2]. This model can be used for simulation, design, and development and testing of technologies suitable for fixed broadband wireless applications [3]. The parameters for the model were selected based on some statistical models. The tables below depict the parametric view of the six SUI channels.

Table 1: The terrain types of SUI channel.

Terrain type	**SUI channels**
C (Mostly flat terrain with light tree densities)	SUI-1. SUI-2
B (Hilly terrain with light tree density or flat terrain with moderate to heavy tree density)	SUI-3. SUI-4
A (Hilly terrain with moderate to heavy tree density)	SUI-5. SUI-6

Table 2: General characteristics of SUI channel.

Doppler	**Low delay spread**	**Moderate delay spread**	**High delay spread**
Low	SUI-1,2 (High K Factor) SUI3		SUI-5
High		SUI-4	SUI-6

Gaussian Minimum Shift Keying or Gaussian filtered Minimum Shift Keying, GMSK, the form of modulation with no phase discontinuities used to provide data transmission with efficient spectrum usage. GMSK modulation is based on MSK, which is itself a form of continuous-phase frequency-shift keying. One of the problems with standard forms of PSK is that sidebands extend out from the carrier [4]. To overcome this, MSK and its derivative GMSK can be used. Here there are no phase discontinuities because the frequency changes occur at the carrier zero crossing points.

III. MODULATION TECHNIQUES OF GSM

GSM uses a form of modulation known as GMSK. MSK and also GMSK modulation are what is known as a continuous phase scheme. This arises as a result of the unique factor of MSK that the frequency difference between the logical one and logical zero state is always equal to half the data rate [5].

GMSK can be generated through two methods:

a) Through filtering of signals using Gaussian filter with a modulation index of 0.5. This method is not widely used because it is difficult to obtain a modulation index of exactly 0.5.

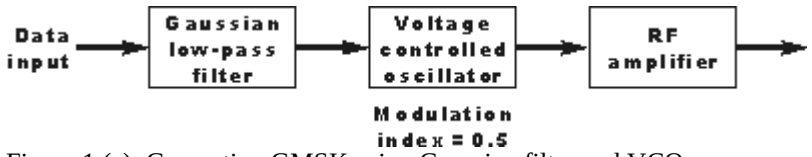

Figure 1 (a): Generating GMSK using Gaussian filter and VCO

b) Another method is where the quadrature modulator is used (phase of the angle is 90^0 to another). This form is also known as I-Q Modulator since it is dependent on the in phase and quadrature of the signals. This enables the modulation index to be set to 0.5 exact. The signal thus cannot be distorted since it is not carried in terms of amplitude elements.

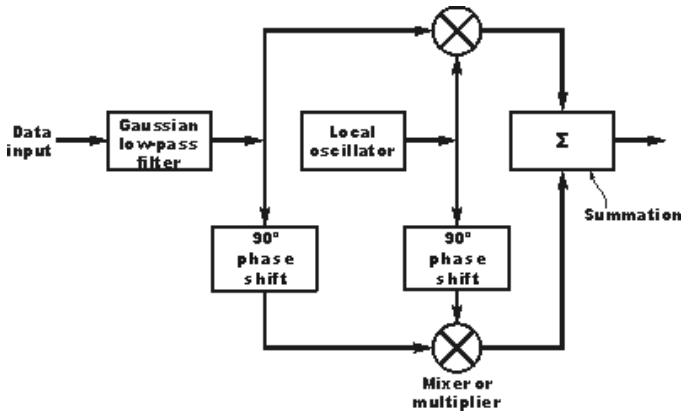

Figure 1 (b): Block diagram of I-Q modulator used to create GMSK

ADVANTAGES OF GMSK MODULATION

There are several advantages to the use of GMSK modulation for a radio communication system. One is obviously the improved spectral efficiency when compared to other phase shift keyed modes. A further advantage of GMSK is that it can be amplified by a non-linear amplifier and remain undistorted. This is because there are no elements of the signal that are carried as amplitude variations [5]. A further advantage of GMSK modulation again arises from the fact that none of the information is carried as amplitude variations.

IV. STANFORD UNIVERSITY INTERIM (SUI) CHANNEL MODEL

In [6], Channel models for fixed wireless applications which contain the definition of six specific channel implementations are known as Standard University Interim (SUI) channels. The general structure for the SUI channel model is shown below in Fig. 2. This structure is for Multi Input Multi Output (MIMO) and includes other configurations like Single Input Single Output (SISO) and Single Input Multiple Output (SIMO) as subset. The SUI channel structure is the same for the primary and interfering signals.

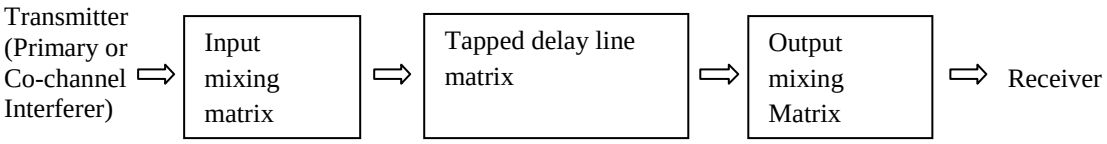

Figure 2: Generic structure of SUI channel model

In [7], there are channel models for SUI-1, SUI-2, SUI-3, SUI-4, SUI-5 and SUI-6. The channel model for SUI-1 is defined below.

Table 3: SUI-1 channel model definition

SUI – 1 Channel				
	Tap 1	**Tap 2**	**Tap 3**	**Units**
Delay	0	0.4	0.9	µs
Power (Omni ant.)	0	-15	-20	dB
K Factor (Omni ant.)	4	0	0	
Power (30^0 ant.)	0	-21	-32	dB
K Factor (30^0 ant.)	16	0	0	
Doppler	0.4	0.3	0.5	Hz
Antenna Correlation:	P_{ENV} = 0.7		Terrain type: C	
Gain Reduction Factor:	GRF = 0 dB			
Normalization Factor:	F_{omni} = -0.1771dB, $F_{30°}$ = -0.0371 dB			

Using this definition of SUI-1, MATLAB codes have been generated to perform a simulation to analyze its performance. The set of SUI channel model specify statistical parameters of microscopic effects (tarred delay line, fading and antenna directivity). To complete the channel model, these statistics have to be combined with microscopic channel effects such as path loss and shadowing (also known as excess path loss) which are common to all six models in the set. Each set models also defines an antenna correlation [8]. The gain reduction factor (GRF) has also been included in the tables to indicate the connection with the K-factor.

POWER DISTRIBUTION

The total power P of each tap:

$$P = |m|^2 + \sigma^2 \quad (1)$$

Where m is the complex constant and σ^2 the variance of the complex Gaussian set. Now, the ratio of power is,

$$K = \frac{|m|^2}{\sigma^2} \quad (2)$$

From equation (2), we can find the power of the complex Gaussian and the power of the constant part as

$$\sigma^2 = P\frac{1}{K+1} \quad and \quad |m|^2 = P\frac{K}{K+1} \quad (3)$$

Here we can see that, for $K=0$, the variance becomes P and the constant part power diminishes, as expected. Note that we choose a phase angle of 0^0 for m in the implementation [9].

V. SIMULATION RESULT AND COMPARISON

The block diagram of the model configuration that has been used for the simulation using MATLAB is given below.

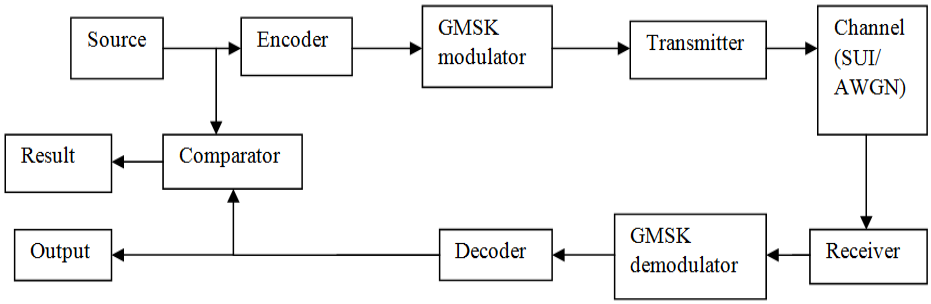

Figure 3: Block diagram of the model configuration for the simulation

For comparing the performance, the AWGN (Additive White Gaussian Noise) channel has been chosen. Here, Fig. 4 shows the BER (Bit Error Rate) Vs. SNR (Signal to Noise Ratio) graphs.

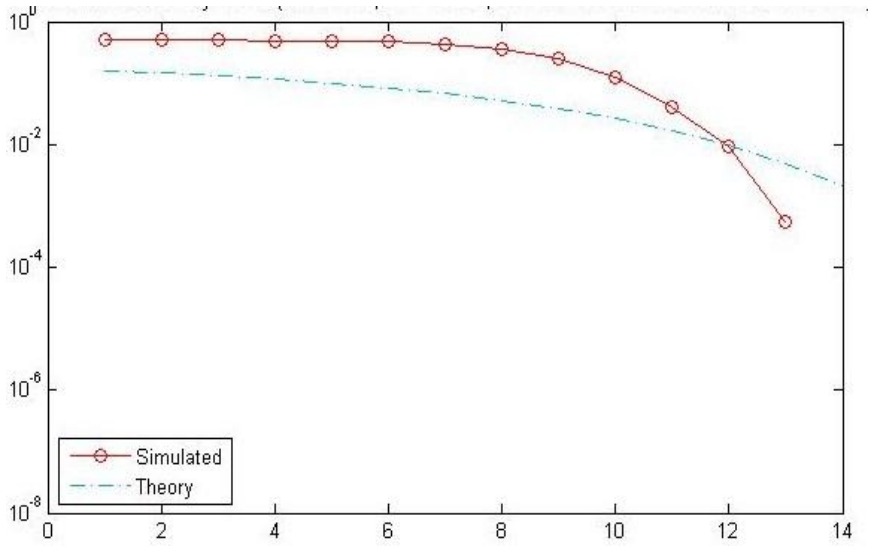

(a)

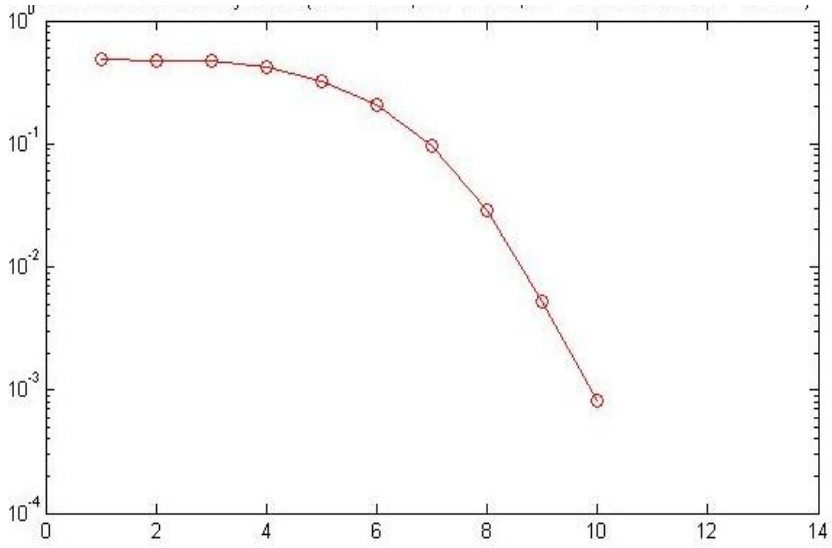

(b)

Figure 4: Comparison between the performances in GSM system of (a) AWGN channel model and (b) SUI-1 Channel model (simulation result).

Fig. 4 shows that, the BER of SUI-1 channel model is lower than AWGN channel model for the higher SNR. BER is a parameter which gives an excellent indication of the performance of a data link such as ratio or fiber optic system. Since SUI-1 channel model shows lower BER, so it's coding gain is higher. By manipulating the variables that can be controlled, it is possible to optimize a system to provide the performance levels that are expected. This is normally undertaken in the design stages of a data transmission system so that the performance parameters can be adjusted at the design concept stages.

VI. CONCLUSION

In this paper, it is deduced that the bit error rate of SUI-1 channel model in GSM system is lower than the AWGN channel model for higher SNR. This means the coding gain is also higher for SUI-1 channel model. Up to SUI-4, the performances are almost same. For the simulation, GMSK modulation has been used. Reducing the bandwidth and increasing the transmitter power, it is possible to get improved BER. If BER rises to high then the system performance will noticeably degrade. If it is within the limits then the system will operate satisfactorily. With SUI channel modeling, it is possible to get the better performance compared to other channels since it has come up with latest technologies and improved capacity.

REFERENCES

[1] W. Mariusz, L. David and D. Patrick, "GSM technology as a communication media for an autonomous unmanned aerial vehicle", 21th Bristol UAV Systems Conference, Vol. 1.0, pp. 1-10, April 2006
[2] S. B. Daniel, "Simulating the SUI channel models", IEEE 802.16.3c-01/53, vol. 1.0, pp. 1-8, April 2001
[3] J. Raj, "Channel Models a tutorial", Vol. 1.0, pp. 5-18, February 2007
[4] P. Ian, "Radio frequency, RF, Technology and design", Radio-Electronics.com, May 2008
[5] R. S. David, "Modulation technique used in GSM", Telecom knowledge blog, February 2013
[6] K. Mohammad, A. Hazim and H. Tahseen, "Design of fixed WiMAX transceiver on SUI channel based on wavelet signals", International journal of engineering and advanced technology (IJEAT), Vol. 3.0, ISSN: 2249-8958, ISSUE-2, December 2013
[7] V. Erceg, K. V. S. Haris, M. S smith and D. S. Baum et al, "Channel models for fixed wireless applications", IEEE 802.16.3c-01/29rt, February 2001
[8] V. Erceg et al, "Channel models for fixed wireless applications", IEEE 802.16.3c-01/29r4, July 2001
[9] M. Mohammad, F. Saleim, G. Mather, "Design and performance of the 3GPP long term evolution transceiver physical layer in SUI channels., International journal of soft computing and engineering (IJSCE), Vol. 3.0, ISSN: 2231-2307, Issue-6, January 2014

American Journal of Engineering Research (AJER)
e-ISSN : 2320-0847 p-ISSN : 2320-0936
Volume-03, Issue-12, pp-87-92
www.ajer.org

Research Paper Open Access

A Novel Design of Half Subtractor using Reversible Feynman Gate in Quantum Dot cellular Automata

Rubina Akter[1],Nasrin Jahan[2], Md. Mamunur Rashid Shanta[3], Anik Barua[4]
[1, 4](Department of ICT, MawlanaBhasani Science and Technology University, Bangladesh)
[2](Department of TE, University of South Asia, Bangladesh)
[3](Department of EEE, East West University, Bangladesh)

Received Manuscript: XX-XX-XXXX
Accept Manuscript: XX-XX-XXXX
Published Manuscript: XX-XX-XXXX

ABSTRACT: *Quantum Dot cellular Automata (QCA) is an emerging, promising alternative to CMOS technology that performs its task by encoding binary information on electronic charge configuration of a cell. All circuit based on QCA has an advantages of high speed, high parallel processing, high integrityand low power consumption. Reversible logic gates are the leading part in Quantum Dot cellular Automata. Reversible logic gates have an extensive feature that does not lose information. In this paper, we present a novel architecture of half subtractor gate design by reversible Feynman gate. This circuit is designedbased on QCA logic gates such as QCA majority voter gate, majority AND gate, majority OR gate and inverter gate. This circuit will provide an effective working efficiency on computational units of the digital circuit system.*

Keywords -*And-Or-Inverter (AOI), Basic QCA, Majority Voter (MV), QCA Logic Gate, Reversible Feynman Gate.*

I. INTRODUCTION

The paradigm of Quantum Dot cellular Automata is a revolutionary approach to molecular-scale computing. Using the charge configuration of nano structures Quantum Dot cellular Automata presents binary information on the current switching devices. For several decades the size of electronics semiconductor device and operating currents has been reduced. Fundamental problems arising from scaling such as quantum mechanical effects and severe power dissipations assist the continued development toward devices on the nanometer scale [1].

Logic design with quantum dots is one of the most recent technologies being researched which allows scaling to continue to atomistic dimensions. Using the current switching Quantum Dot cellular Automata uses the charge configuration of a set of quantum dots to present binary information on molecular scale computing [2]. QCA cell is the basic building block of QCA devices. A QCA cell consists of several quantum dots with two mobile electrons [3, 4]. The charge that takes place on which corner of the cell, the place is known as the quantum dot. Coulombic repulsion between like charge forces electrons in the same cell to occupy dots which maximize their separation. In QCA the electron of a cell can tunnel between a dot to dot. The two mobile electrons in a cell take place as a diagonal pattern of the coulombic interaction between them [5]. Hence the four dotted QCA cells can be used represent the binary information. Due to the electrostatic repulsion the two extra electrons take their position in the four dots. These two free electrons create only two stable positions. These

two stables positions known as -1 and +1 polarity or boolean values 0 and 1 respectively [6]. The presence of clocking zones is a unique feature of QCA based circuits. There are four phases of clocking zones such as the switch, hold, release and relax [7].

Now a day nanotechnology is one of the most wanted research field and Quantum Dot Cellular Automata offers a revolutionary approach to computing at nano level. Parallely, reversible logic is getting more and more conspicuous technology which offers better working performance in QCA technology. Previously researchers have addresseda number of studies on reversible logic gates and their implementation such as described in [8, 9, 10]. H. cho and j. Earl Swartzlander described adder and multiplier design that are optimized in terms of quantum cost, delay and garbage output [11]. A revolutionary design of a shift register and its operation is described in [5]. H. Thapliyal and N. Ranganathan proposed the design of binary and bcd adder circuits based on reversible logic gates. These designs are very effective in terms of reversible gates, garbage output and quantum cost [12]. I. Hanninen and J. Takala emphasis a binary adders design on QCA which is very important in arithmetic logic unit. The main parts is the implementation of logical devices and the reversible logic using QCA is shown in [13, 14].

There are many reversible logic gates and these gate are important for their reversibility characteristics. Among them Feynman gate is one of the most important reversible logic gates. In this paper using the reversible Feynman gate we design a Half Subtractor circuit. This design is very useful for digital signal processing (DSP), optical computing, cryptography etc.

This paper is apportioned into five sections. Section I describes about QCA, reversible logic gate and their implementation in various logical circuits. Section II provides a brief overview about the QCA fundamental logic units. Section III presents our proposed circuit using QCA technology. Section IV shows the simulated waveform and discuss about the simulation results of the proposed circuit. Finally, section V summed up the beneficial perspective of the presented circuit.

II. QCA REVIEW

Quantum Dot cellular Automata is an outstanding nanotechnology which is used for its better performance than CMOS technology. We describe the basic building block of QCA cells in the previous section. A QCA cell is shown in figure 1. This figure is considered as a square with four dots as its corners. The cell is to consist of two extra electrons which can tunnel between cell dots [1, 15].

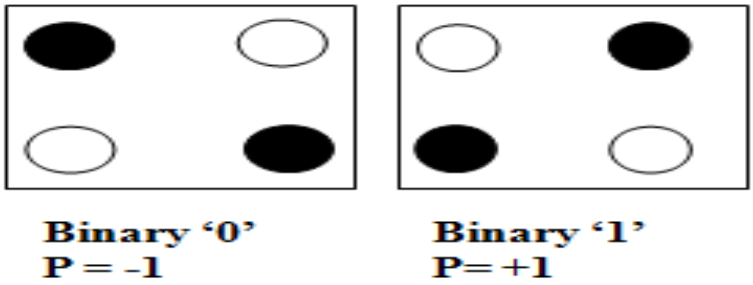

Figure 1: Structure of a QCA cell and its binary logic

The QCA wire is basic QCA logic element which is consist of a set of QCA cells. Due to the electrostatic repulsion signal propagates from input to output through the QCA wire. The QCA wire is a horizontal row of QCA cells [16]. A normal QCA wire is shown in figure 2.

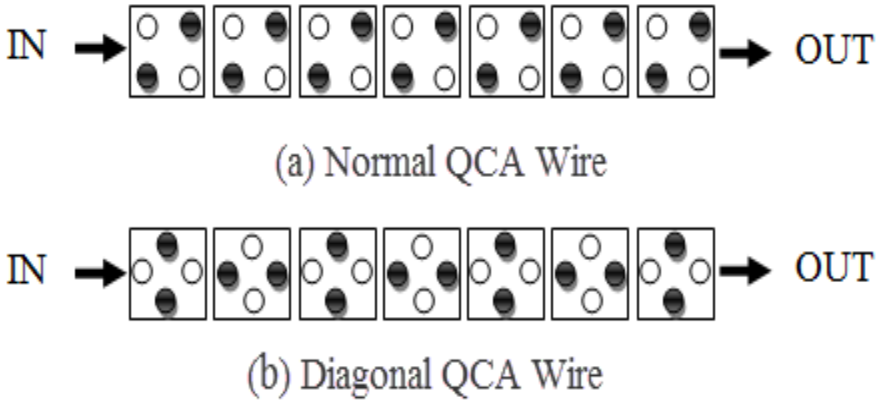

Figure 2: QCA Wire

Another basic QCA logic elementis QCA majority Voter (MV) gate. The 3-input majority gate is composed of five cells. The three cells act as input cell, the center cell is known as device cell and the remaining cell is known as output cell. The center cell performs the calculations. Figure 3 shows a three input majority gates where the input cells are labeled as A,B,C and the output cell labeled as OUT. The Boolean function of this three input majority gate is,

OUT (A, B, C)=Maj (A, B, C)= AB+BC+CA.

The three input majority gate works as 2-input AND gate having a fixed polarity of zero and its output is ab. The three input majority gate works as 2-input OR gate having a fixed polarity of 1 and its output is a+b.

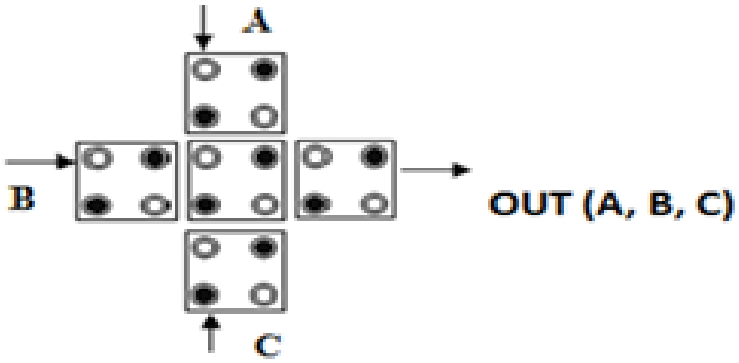

Figure 3: QCA Majority Voter (MV) gate

Inverter gate is a basic building logic element in QCA. For making a complete logical set is needed the inverter gate. Combinational logic circuits need a complete logical set which is fully depends on the Majority Voter gate and the inverter gate. In the inverter gate the input polarization splits and converts to the opposite polarization at the inverter output [17]. Figure 4 shows a QCA inverter gate.

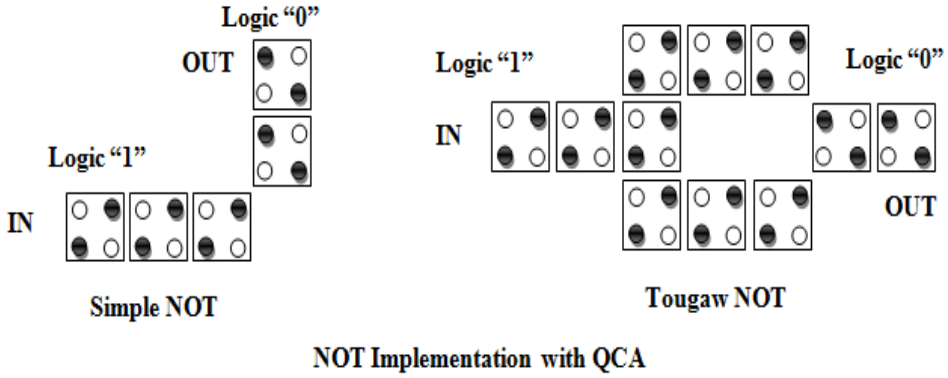

Figure 4: QCA Inverter gate

III. PROPOSED CIRCUIT AND PRESENTATION

There are many reversible logic gates and these are extensively important to QCA technology. In this section we will present our proposed Halfsubtractor circuit which is implemented by reversible Feynman gate.

1. Feynman gate (FG)

Figure 5 shows a 2 x 2 Feynman gate. The input vector is I (A, B) and the output vector is O (P, Q) and the relation between input and output is given by P=A, Q =A⊕B.

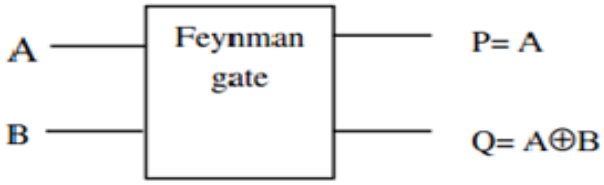

Figure 5: Feynman gate

In this paper we design a reversible Half Subtractor circuit by Feynman gate using QCA Technology. Let A and B are two binary numbers. The half subtractor performs A-B operation. Table 2 shows the truth table of the half subtractor. The output of the XOR gate produces the difference between A and B. The output of the AND gate A'B produces a Borrow. Thus, the output function will be Borr = A'B, Diff = A⊕B.

Table 1: Truth Table of Half Subtractor

Input		Output	
A	**B**	**Borr**	**Diff**
0	0	0	0
0	1	1	1
1	0	0	1
1	1	0	0

Figure 6 shows QCA layout structure of the Halfsubtractor design using reversible Feynman Gate. In this figure the input cells are labeled with A and B and the outputs are labeled as Y2 and Y3. The circuit performs the Boolean functions Y3 = Borr = A'B, Y2 = Diff = A⊕B.

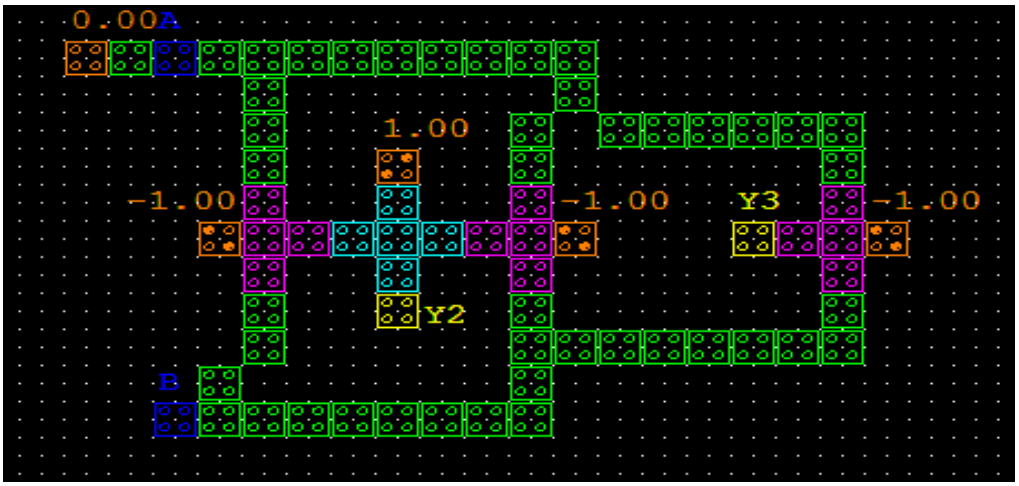

Figure 6: Simulated waveforms for Half Subtractor gate by Feynman gate

IV. RESULT AND DISCUSSION

Our proposed Halfsubtractor circuit functionally simulated using the QCA Designer 2.0.3. The following parameters are used for a Bistable Approximation: cell size=18nm, number of samples=12800, convergence tolerance=0.0000100, radius of effect=65.000000nm, relative permittivity=12.900000, clock high=9.800000e-022J, clock low=3.800000e–023J, clock shift=0, clock amplitude factor=2.000000, layer separation=11.500000, Temperature=1.000000,Reluxation time=1.000000e-015, Time step 1.000000e-016 and Dot Diameter=5.0000. Most of the above mentioned parameters are default values in QCA Designer. Figure 7 shows the input output waveforms of our proposed circuit. In this Figure, the input signals are A, B and the output signals are Y3 and Y2. The input is mapping to output as Y2 =A⊕B and borrow Y3= A'B.

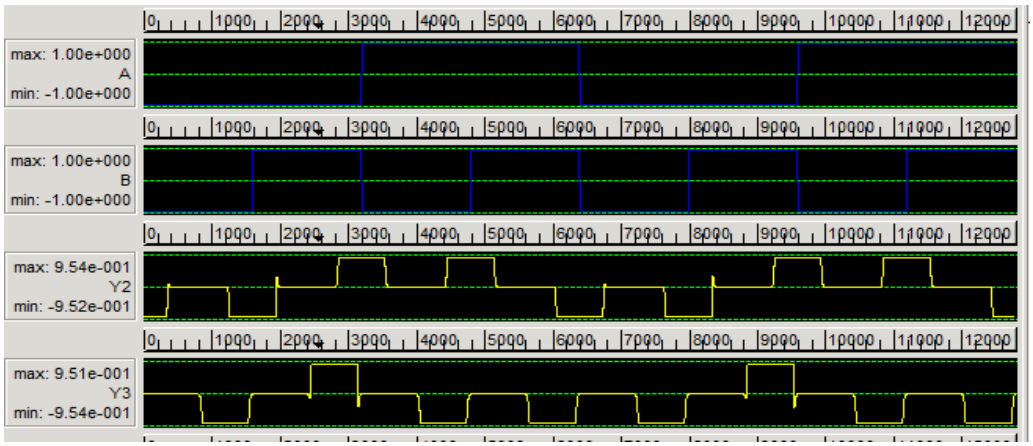

Figure 7: Simulated waveforms for HalfSubtractor gate by Feynman gate

The table 2 shows a data table of Half Subtractor gate designingby Feynman gate.

Table 2:Result analysis of proposed half subtractor circuit in QCA

Parameter	Value
Number of cell	114
Covered area (μm^2)	0.20
Clock used	3
Time delay (Clock cycle)	0.75

The above tables show that, the Half Subtractor gate designing by Feynman gate consists of 114 cells and it covers 0.20 μm^2 areas with time delay 0.75.

V. CONCLUSION

This paper explores a novel design of Half-Subtractor circuit based on the reversible Feynman gate using QCA technology. This proposed circuit has been simulated by QCADesigner. The simulation result shows that the proposed circuit produces the exact output and it performs well. The proposed design is more efficient in terms of cell counts, area and the time delay. This QCA circuit design presents a new functional paradigm for quantum computing, optical computing, digital signal processing and nanotechnology. Hence, we summarize that the proposed design architecture must be take a promising step towards the goal of low power dissipation circuit in QCA technology.

REFERENCES

[1] C. S. Lent, P. D. Taugaw, W. Porod and G. H. Berstein, "Quantum Cellular Automata", *Nanotechnology*, vol. 4, no. 1, January 1993, pp 49-57.

[2] Enrique P. Blair and Craig S. Lent, "Quantum-Dot Cellular Automata: An Architecture for Molecular Computing, " 0-7803-7826-1/03/$17.00 © 2003, IEEE.

[3] J. R. Zhang, K. Walus, W. Wang, and G. .Jullien, "A method of majority logic reduction for quantum cellular automata," *IEEE Transactions on Nanotechnology*, vol. 3, no. 4, pp. 443–450, Dec. 2004.

[4] I. Hänninen and J. Takala, "Binary Adders on Quantum-Dot Cellular Automata," *J. Signal Process. Syst.*, vol. 58, no. 1, pp. 87–103, Jan. 2010.

[5] R. Kummamuru, A. Orlov, R. Ramasubramaniam, C. Lent, G. Bernstein, and G. Snider, "Op-eration of a quantum-dot cellular automata (qca) shift register and analysis of errors," IEEE Transactions on Apllied Physics, vol. 50, pp. 1906–1913, September 2003.

[6] C. S. Lent and P. D. Tougaw, Proceedings of the IEEE 85, p. 541 (1997).

[7] Mohammad RafiqBeigh*, Mohammad Mustafa, Firdous Ahmad, "Performance Evaluation of Efficient XOR Structures in Quantum-Dot Cellular Automata (QCA), " Circuits and Systems, 2013, 4, 147-156 .

[8] J. W. Bruce, M. A. Thornton, L. Shivakumaraiah, P. S. Kokate, and X. Li, "Efficient adder circuits based on a conservative reversible logic gate," in *Proc. IEEE Symposium on VLSI, 2002*, 2002, pp. 83–88.

[9] M. Haghparast, S. Jassbi, K. Navi, and O.Hashemipour, "Design of a novel reversible multiplier circuit using hng gate in nanotechnology," *World App. Sci. J.*, vol. 3, no. 6, pp. 974–978, 2008.

[10] H. Thapliyal and M.B. Srinivas, "Novel reversible multiplier using novel reversible TSG gate," in *Proc.the 4th ACS/IEEE InternationalConference on Computer Systems and Applications*, Dubai , UAE, 2006, pp. 100–103.

[11] H. Cho and J. Earl E. Swartzlander, "Adder and Multiplier Design in Quantum-Dot Cellular Automata," *IEEE Transactions on Computers*, vol. 58, no. 6, pp. 721–727, 2009.

[12] H. Thapliyal and N. Ranganathan, "Design of efficient reversible logic based binary and bcd adder circuits," *To appear ACM Journal ofEmerging Technologies in Computing Systems*, 2011.

[13] C.S Lent and B. Isaksen, "Clocked molecular quantum-dot cellular automata," IEEE Trans. Electronic Devices, vol. 50, no. 9, pp. 1890-1896, Sept. 2003.

[14] P. D. Tougaw and C. S. Lent, "Logical devices implemented using quantum cellular automata," *Journal of Applied Physics*, vol. 75, no. 3, pp. 1818–1825, Feb. 1994.

[15] RaghavaGaripelly, P.MadhuKiran, A.Santhosh Kumar, "A Review on Reversible Logic Gates and their Implementation," ISSN 2250-2459, ISO 9001:2008 Certified Journal, Volume 3, Issue 3, March 2013.

[16] Lent, Craig S., Tougaw, P. Douglas: Lines of interacting quantum-dot cells: A binary wire. Journal of Applied Physics. vol. 74 (1993), pp. 6227 – 6233.

[17] F. Ahmad, G. M. Bhat, and P. Z. Ahmad, "Novel Adder Circuits Based On Quantum-Dot Cellular Automata (QCA)," *Circuits and Systems*, vol. 05, no. 06, pp. 142–152, 2014.

American Journal of Engineering Research (AJER)
e-ISSN : 2320-0847 p-ISSN : 2320-0936
Volume-03, Issue-12, pp-93-101
www.ajer.org

Research Paper Open Access

Effect of Chipped Rubber Aggregates on Performance of Concrete

Sunil N. Shah[1], Pradip D. Jadhao[1], S. M. Dumne[2]

[1]*Department of Civil Engineering, K K Wagh Institute of Engineering Education & Research , Nashik, 422 203 India*

[2]*Department of Applied Mechanics, Government Polytechnic Aurangabad, 433 005, India*

ABSTRACT **:** *Due to rapid growth in automobile industry, use of tyre increases day to day and there is no reuse of the same to decrease the environmental pollution. The decomposition and disposing of waste tyre rubber is harmful to environment. This research reflects the reuse of waste tyre rubber into concrete after observing their properties. In that experimental work chipped rubber aggregates replaced to the natural coarse aggregates by varying percentage of 3, 6, 9 and 12 with comparison of 0% replacement. Silica fume is replaced in 10% with cement for improving the bond properties between cement paste and rubber. In evaluation, test has been carried out to determine the properties of concrete such as workability, unit weight, flexural strength and split tensile strength. The workability of fresh concrete is observed with the help of compaction factor test. From the test of compaction factor, workability is decrease with increasing percentage of chipped rubber. The specific gravity of chipped rubber aggregates is lower as compared to natural aggregates therefore decrease the unit weight of rubber mix concrete. Increasing chipped rubber aggregates as partial replacement into concrete reduces compressive strength. So these can use in non-primary structural applications of medium to low strength requirements. The overall results of study show that it is possible to use recycled rubber tyre aggregates in concrete construction as partial replacement to natural coarse aggregates.*

KEYWORDS: *chipped rubber aggregates, Flexural strength, Natural aggregates, Silica fume, Split tensile strength. unit weight, Workability,*

I. INTRODUCTION

Rapid growth in automobile industry and increasing use of vehicles, production of tyre is also increased which generate waste tyre rubber. Management of waste tyre rubber is challenging to municipalities and burning or biodegradation of waste tyre rubber is harmful to environment. On the other hand, demand of concrete as construction material from society, it is needed to preserve natural coarse aggregate by using alternative material. In this research, reuse of waste tyre chipped rubber in concrete as partial replacement as coarse aggregates. Over the two decades, researchers have underscored to use waste tyre rubbers in concrete and carried out the test on various concrete mixes using rubber aggregate as partial replacement of mineral aggregates [1].

The researchers have studied the Crumb rubber is a material produced by shredding and commutating used tyres and there is no doubt that increasing piles of tyres create environmental concerns [2]. Author studied the product of shredding used rubber tyres as a partial sand replacement in foamed concrete, and investigates the effect of it on some properties of foamed concrete such as, density, water absorption, compressive strength, tensile strength, flexural strength and impact resistance [3]. Recently the flexural strength of normal beam by replacing tension reinforcement as waste tyre is also carried out [4]. Different partial replacements of crumb rubber by volume of fine aggregate are cast and test for compressive strength, flexural strength, split tensile strength and stress strain behavior [5]. An experimental work using recycled rubber tyre aggregates as partial replacement to the coarse aggregates in concrete mix and carried out using tests such as slump, unit weight and compressive strength on different concrete mixes in order to determine properties of concrete [6]. Density and

compressive strength of concrete utilizing waster tyre rubber has been investigated by replacing fine and coarse aggregate with waste rubber tyre by weight along with super-plasticizer using different percentages [7].In this paper, general objective of study is to evaluate some fresh and hardened properties of concrete produced by replacing part of natural coarse aggregates with rubber aggregates collected from locally available waste tyre rubber. The specific objectives of study are i) Observing the physical properties of normal and chipped rubber mix concrete. ii) Study regarding performance of workability of concrete by compaction factor test. iii) Comparison and discussion on results obtained from unit weight, flexural strength and split tensile strength for normal concrete and chipped rubber mix concrete.

II. OUTLINE OF EVALUATION

From the results of physical properties of ingredients, Mix design of M_{25} grade of concrete mixes having water cement ratio 0.5 is prepared. Beam and cylinder specimen is casted in standard size for coarse aggregate replaced by 0, 3, 6, 9 and 12 % of chipped rubber aggregates. The tables and graphs reflect comparisons between normal concrete and rubberized concrete for the various test carried out such as workability by compaction factor, unit weight, flexural test and split tensile test. Tables and graphs are presenting the conclusions and recommendations for the future.

Material properties

Cement : Cement used in this work O.P.C of 53 grades and its properties of cement are determined as per IS 12269:1987.

Silica fume : Silica Fume is densified from smoke gray Elkem India Private Limited, Mumbai which is based Micro Silica Grade 920-D is used which is in dry fine powder form. It was available in weight of 25kg bags. The various properties of silica fume is Sio_2 content-85%, Specific Gravity-2.2-2.3, Moisture content-2.8%, Loss in ignition as per mass- 3.6%, Density- 500-700 kg/m^3, Oversize percentage retained on 45 micron IS sieve- 8.56, Compressive strength of 7 day as percent of controlled sample-88.

Coarse and Fine aggregates : Coarse aggregate from a local commercial quarry with a maximum nominal size of 20 mm was used and natural sand of river bed is used confirming to grading Zone –II of table 4 of IS-383-1970 were procured from Nashik city in Maharashtra. For investigation its properties the various tests are performed as (1) Sieve analysis and fineness modulus (2) Specific gravity (3) Moisture content (4) Density. Whereas for coarse aggregates, fineness modulus= 7.51, specific gravity = 2.80, moisture content= 0.39 % and density=1560 kg/m^3.The test results obtained for fine aggregates are, fineness modulus= 2.31, specific gravity= 2.75, moisture content= 0.69 % and density = 1800 kg/m^3

Chipped rubber aggregates : In this research, Scrap truck tyre rubber is collected from remolding shops available at Nashik city in Maharashtra. These scrap tyre rubbers are cut into aggregates with help of shoemaker and cutting to maximum nominal sizes equal to 20mm.

FIGURE 1. Prepared sample of chipped rubber aggregates

To investigate the properties of chipped aggregates, the procedure has been adopted as same as procedure of coarse aggregates. Therefore the test results obtained for chipped rubber aggregates are fineness modulus= 2.39, specific gravity = 1.10, moisture content= 0.0 % and mass density= 778 kg/m^3.

III. EXPERIMENTAL WORK

The various experimental work and test are carried out in the material testing laboratory of K. K. Wagh

Institute of Engineering Education & Research Nashik**.** Concrete mix design are prepared using IS method and total 60 specimens were casted with replacement of chipped rubber in concrete. The specimens were prepared with percentage replacements of the coarse aggregate by 3, 6, 9 and 12 chipped rubber aggregate. For comparative analysis, M_{25} grade concrete mix is prepared with no replacement of chipped rubber aggregate. Replacing the 10 percent cement by silica fume into normal concrete and chipped rubber mix concrete. The mixing process carried out by using machine mixer and after casting of specimens employed tamping rod and table vibrator. In this evaluation, tests are performed as workability by compaction factor test, unit weight, flexural strength, split tensile strength at 7^{th} and 28^{th} days on various concrete mixes.

IV. TEST RESULT AND DISCUSSION

Workability by compaction factor test : The Compaction factor test is carried out to measuring the workability of concrete which is an important aspect of workability. This test works on the principal of measuring the amount of compaction achieved by a standard amount of workdone by allowing the concrete fall through a standard height. This test is more accurate than slump test,especially for concrete to fall through a standard height.The compaction factor test is more popular to determine the workabilty of concrete mix in laboratories. The compaction factor is the weight of partially compacted concrete to the weight fully compacted concrete.IS 5515-1983 is used for the procedure of compaction factor test.

FIGURE 2.Concrete fills in upper hopper

FIGURE 3.Concrete drop in lower hopper

TABLE 1: Test results of compaction factor

Specimen	% rubber	Compaction factor
CR-0	0	0.92
CR-3	3	0.91
CR-6	6	0.90
CR-9	9	0.86
CR-12	12	0.85

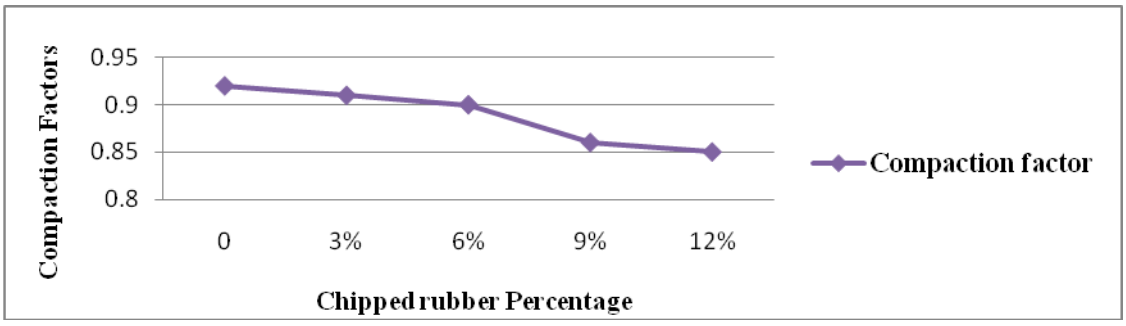

FIGURE 4. Comparison of compaction factor for normal and rubberized concrete

Degree of workability is medium as per IS 456:2000 for normal concrete mix. It is observed the graph, for 0% to 12 % the values of compacting factor are slightly reduce upto 0.9 for the percentage of 6 then after the graphs instantly reduced upto 0.86 for the 9% and again slightly reduce the factor 0.85 for the 12 %. It has to be noted that increasing the percentage of chipped rubber the value of compaction factor is reduce. From

above observation which was also noticed that while casting the rubberized concrete rubber aggregates have a high tendency to come out to the top surface when vibrated by a table vibrator which is due to low specific gravity of rubber aggregate.

Unit weight : Unit weight can be defined as the weight of a given volume of concrete specimen. The specific gravity of the rubber chips are 1.1 which is low as compared to the mineral coarse aggregates is 2.84. From the above observation it has to be noted that increasing the reduction in unit weights of rubberized concrete with increasing chipped rubber percentage into concrete. The loss of unit weight is 9.75 % for 12% replacement of chipped rubber into concrete.

TABLE 2: Unit weights of the normal and rubberized concretes for beams

Specimen	% Rubber aggregates	Av. Unit weight (kg/m^3)	% Unit weight Loss
CHR-0	0	2626	0
CHR-3	3	2540	3.27
CHR-6	6	2510	4.42
CHR-9	9	2428	7.54
CHR-12	12	2370	9.75

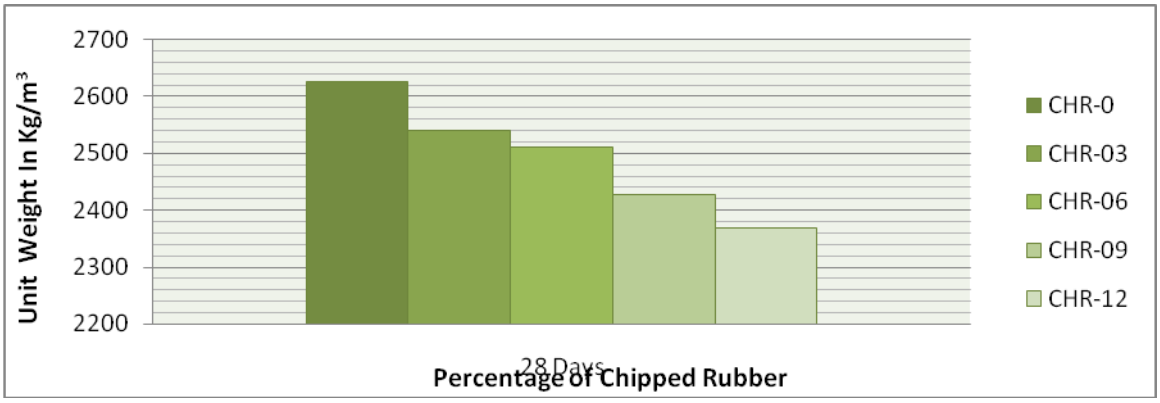

FIGURE 5. Comparisons of unit weight for beam specimens at 7 days

TABLE 3: Unit weights of normal and rubberized concretes for beam cylinders

Specimen	% Rubber aggregates	Av. Unit Weight (kg/m^3)	% Unit Weight Loss
CHR-0	0	2558.5	0
CHR-3	3	2462.3	3.80
CHR-6	6	2424.5	5.24
CHR-9	9	2383	6.83
CHR-12	12	2332.1	8.50

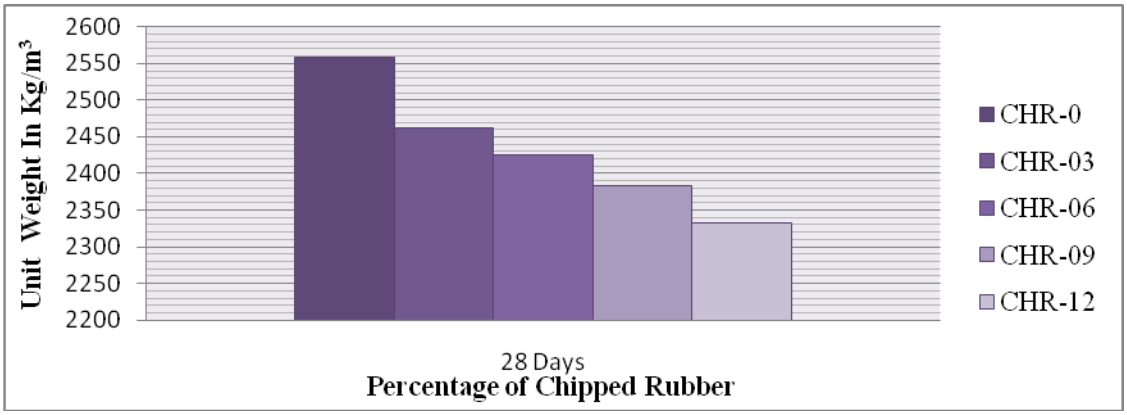

FIGURE 6. Comparisons of unit weights for beam specimens at 28 days

When increasing the percentage of rubber into concrete then reduction in unit weight of cylinder specimen. It is concluded that due to low specific gravity of rubber chips compared with specific gravity of mineral aggregates decrease in the unit weight of the rubberized concrete.

Flexural Strength Test :The test could be performed in accordance with as per code IS: 516 –1959. If the flexural strength would be same as tensile strength then material becomes homogeneous. In fact, most materials have small or large defects in them which act to concentrate the stresses locally, effectively causing a localized weakness. A simple plain concrete beam is loaded at one third span points. For the test span of beam is three times its depth and for determine strength of specimen of size 100 × 100 × 500 mm are supported. Symmetrically over a span of 400mm and two points load was applied at middle third of span.

FIGURE 7.Flexural test on concrete beams

TABLE 4: Flexural strength test results for concrete mixes

Specimen	% Rubber aggregates	Actual flexural strength (MPa)		Av. flexural strength (MPa)		% Strength loss	
		7 days	28 days	7 days	28 days	7 days	28 days
CHR-0	0	4.00	4.75	4.00	4.88	0	0
		4.25	5.00				
		3.75	4.90				
CHR-3	3	3.00	4.50	3.00	4.55	25	6.76
		2.88	4.65				
		3.10	4.50				
CHR-6	6	2.50	4.25	2.55	4.25	19.5	12.90
		2.00	4.15				
		3.15	4.35				

CHR-9	9	1.38	2.75	1.26	3.10	68.5	36.47
		1.00	3.00				
		1.40	3.50				
CHR-12	12	1.10	2.00	1.00	2.50	75	48.77
		0.90	2.25				
		1.00	3.25				

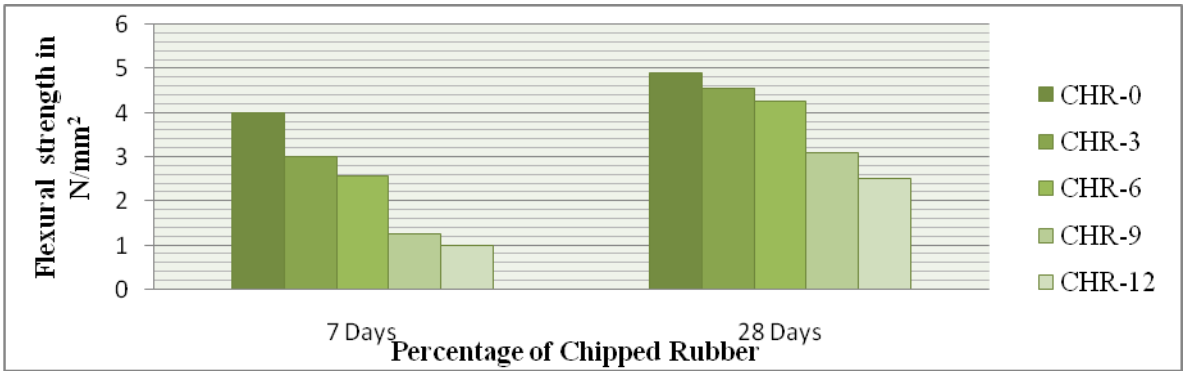

FIGURE 8. Comparison of flexural Strength of various concrete at 7 and 28 days

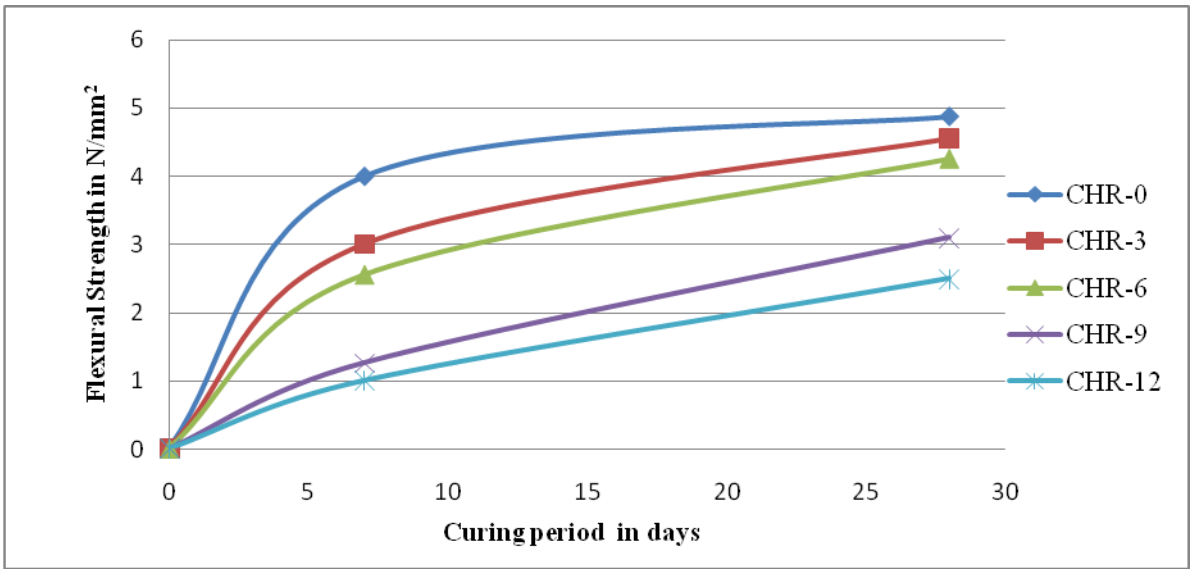

FIGURE 9. Flexural strength of various percentage of crumb rubber containing concrete

The results and graphs shows, when the percentage of chipped rubber aggregates increases into concrete then flexural strength of beam decreases. Soft nature of rubber particles creates the maximum voids into concrete and crushing strength of rubber aggregates is low as compared to mineral aggregates.

Split tensile strength test : It is the standard test; to determine the tensile strength of concrete in a direct way and test has been performed in accordance with IS 5816-1999. A standard test cylinder of concrete specimen (300mmx150mm) is placed horizontally between loading surfaces of compression testing machine. The compression load is applied uniformly along the length of cylinder until the failure of cylinder along the vertical diameter. The concrete cylinders split into two halves along vertical plane due to indirect tensile stresses generated by poison's effect.

FIGURE10. Beam cylinder before failure **FIGURE 11. Beam cylinder after failure**

TABLE 5: Test results of split tensile strength of various concrete mixes

Specimen	% Rubber aggregates	Actual Flexural Strength (MPa)		Av. Flexural Strength (MPa)		% Strength Loss	
		7 days	28 days	7 days	28 days	7 days	28 days
CHR-0	0	2.34	2.66	2.11	2.39	0	0
		2.07	2.15				
		1.92	2.35				
CHR-3	3	1.44	2.16	1.47	2.31	30.33	3.35
		1.46	2.46				
		1.50	2.30				
CHR-6	6	1.45	2.15	1.42	2.19	28.91	8.37
		1.39	2.23				
		1.43	2.20				
CHR-9	9	1.11	1.74	1.19	1.83	43.60	23.43
		1.26	1.84				
		1.21	1.91				
CHR-12	12	1.24	1.87	1.14	1.67	45.97	30.13
		1.15	1.63				
		1.03	1.56				

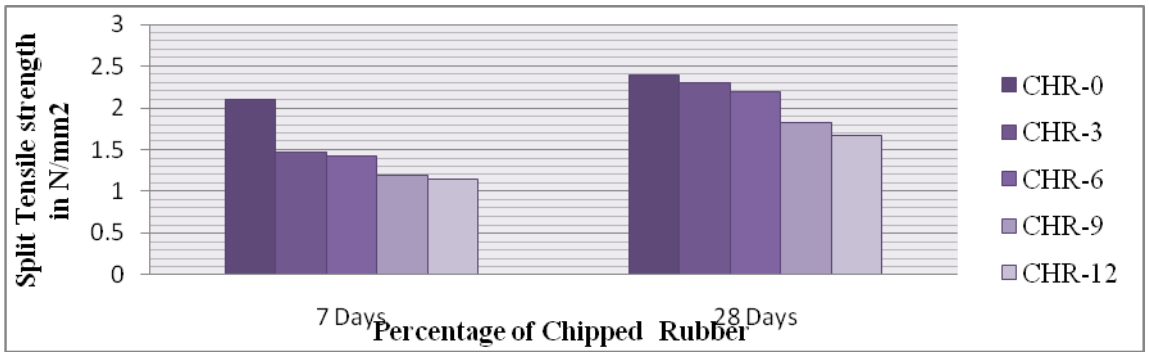

FIGURE 12. Comparison of split tensile strength of diff. concrete mixes at 7 and 28 days

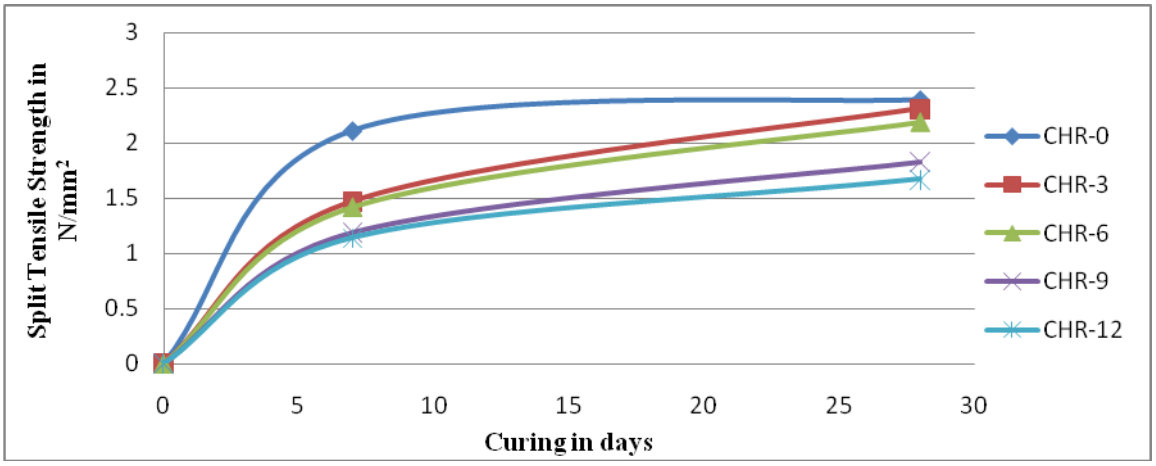

FIGURE 13. Split tensile strengths for various percentage of chipped rubber concrete

Observing from the above results, percentage of chipped rubber increased then split tensile strength is reduced. Bond Strength between cement paste and rubber tire is poor then splitting tensile strength of the chipped rubber mix concrete is lower than normal concrete.

V. CONCLUSIONS

From the test results of various mix samples, the following conclusions are drawn

[1] From the practical evaluation, replacement of chipped rubber at varying proportion in concrete, then workability of fresh concrete is decreasing with increase in percentage of chipped rubber.

[2] From the observations, it is noted that unit weight of beam and cylindrical specimen's has been reduced upto increasing the percentage of chipped rubber into concrete. From this test it has to be concluded that rubberized concrete is used in the light weight structures and restricted to the structural application.

[3] Reduction of solid load carrying material in rubberized concrete is directly affects to reducing the strength of concrete. It can be concluded that as the amount of rubber content increases then there is reduction in flexural strength.

[4] The results of splitting tensile strength test shows that, there is a decrease in strength with increase in rubber aggregate content like reduction observed in the flexural strength tests. One of the reasons that split tensile strength of rubberized concrete is lower than the normal concrete is that the bond strength between cement paste and chipped rubber aggregates is poor.

[5] The crack patterns observed during test on rubberized concrete which does not exhibit typical compression failure behavior. The normal concrete shows a clean split of sample into two halves, whereas rubber aggregate tends to produce a less well defined failure. This may be an indication more ductility in rubberized concrete than the normal concrete.

Acknowledgements : The author would like to the principal and head of the civil engineering department, K.K.Wagh Institute of engineering education and research center, Nashik, Maharashtra for the facility to avail the laboratories for this experimental work

REFERENCES

[1] Abrham Kebede Seyfu., "The use of recycled rubber tires as a partial replacement for coarse aggregates in concrete construction," *The School of Graduate Studies of the Addis Ababa University*, June 2010

[2] Kamil E. Kaloush, George B. Way, Han Zhu., "Properties of Crumb Rubber Concrete," Submitted for Presentation and Publication at the *2005 Annual Meeting of the Transportation Research Board*.

[3] Ameer Abdul Rahaman Hilal., "Effect of Crumb Tyres Rubber on Some Properties of Foamed Concrete," *Anbar Journal for Engineering Sciences(AJES), vol. 4 no 2. 2011*

[4] A.V. Hankare , A. N. Patil, A. R. Deshmukh., "Flexural Strength of Normal Beam by Replacing Tension Reinforcement as Waste Tyre," *International Journal of Engineering Research. (IJER 2014).* Volume No.3, Issue No.5, pp: 330-332.

[5] Parveen, Sachin Dass, Ankit Sharma (2013). "Rubberized Concrete: Needs of Good Environment," *International Journal of Emerging Technology and Advanced Engineering (ISSN 2250-2459, ISO 9001:2008 Certified Journal), Volume 3, Issue 3, March 2013.*

[6] S. M. Dumne (2013). "An Experimental Study on Performance of Recycled Tyre Rubber-Filled Concrete", *International Journal of Engineering Research & Technology (IJERT) ISSN: 2278-081, Vol.2, Issue 12, December 2013.*

[7] El-Gammal, A., A. K. Abdel-Gawad, Y. El-Sherbini, and A. Shalaby., "Compressive Strength of Concrete Utilizing Waste Tyre Rubber, " *Journal of Emerging Trends in Engineering and Applied Sciences (JETEAS) 1,Page No 96-99*

American Journal of Engineering Research (AJER)
e-ISSN : 2320-0847 p-ISSN : 2320-0936
Volume-03, Issue-12, pp-102-108
www.ajer.org

Research Paper Open Access

Simulation Of Annular Gap Effect On Performance Of Solar Parabolic-Trough Collector Model TE38 In Bauchi

[1,]G. Egbo , [2,]I. S. Sintali and [3,]H. Dandakouta
[1,2,3,]Department of Mechanical/Production Engineering,
Abubakar Tafawa Balewa University, Bauchi, Nigeria

ABSTRACT: *Annular gaps of 0.010m, 0.015m, 0.020m, 0.025m, 0.030m, 0.035m, 0.040m, 0.045m, 0.050m and 0.055m are used to simulate the performance of the solar parabolic-trough collector, while maintaining the same geometric dimension of the reflector, the same absorber-tube design features, as well as the same meteorological and radiation data, employing developed thermal energy equations. The higher the annular gap between the absorber-tube and the enveloping glass-cover, with corresponding increase in the diameter of the enveloping glass-cover, the more is the total heat loss of the system and therefore, the lower is the thermal efficiency of the system.*

KEYWORDS: *Absorber-tube, Enveloping-glass-cover, Annular-gap, Transmissivity, Reflectivity, Absorptivity and Emissivity.*

I. INTRODUCTION

The sun is an enormous source of heat and the furnace of all solar systems. The sun radiates, through continuous process of thermonuclear fusion, approximately 83.3 million billion-kilowatt hours (8.33 x 10^{25} kWh) of energy into space every day [1]. While the earth's daily receipt of a minute fraction of this energy depends on its distance from the sun, as well as sunspot activity on the solar surface, it always amounts to very close to 4.14 million billion-kilowatt hours (4.14x10^5 kWh) each day [2]. Based on recent measurements in space, the currently accepted value of the solar constant is 1377 W/m^2 [3]. The extraterrestrial radiation striking the earth varies throughout the year primarily because of the change in the sun-earth distance, due to sunspots, flares and other random activity on the surface of the sun. The earth's outer atmosphere intercepts about one two-billionth of the energy generated by the sun, or about 1500 quadrillion (1.5 x 10 E18) kWh/year. The sun generates an enormous amount of energy - approximately 1.1 x 10 E20 kilowatt-hours every second. A kilowatt-hour is the amount of energy needed to power a 100 Watt light bulb for ten hours. The earth's outer atmosphere intercepts about one two-billionth of the energy generated by the sun, or about 1500 quadrillion (1.5 x 10 E18) kilowatt-hours per year [4]. Because of reflection, scattering, and absorption by gases and aerosols in the atmosphere, as schematically represented in Fig. 1, however, only 47% of this, or approximately 700 quadrillion (7 x 10 E17) kilowatt-hours, reaches the surface of the earth.

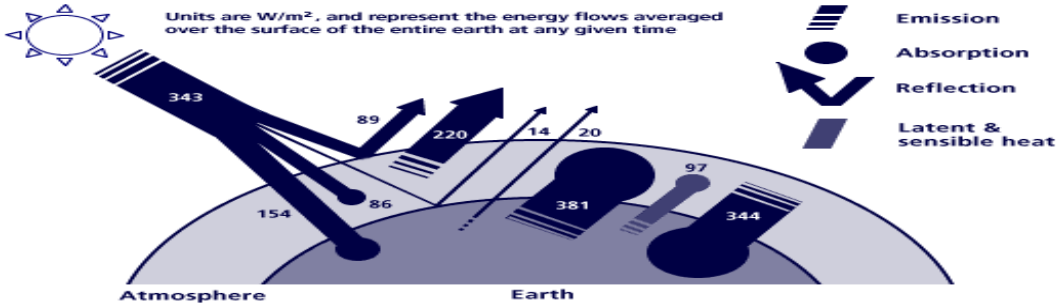

Fig. 1: The Sun radiation reaching the surface of the earth

At the earth's surface, the sum of the incident solar radiation from all directions is called the global insolation. The portion that comes directly from the sun without a change in direction (not scattered) is called the beam or direct insolation. Its value ranges from about 90% of the global insolation on extremely clear day to practically zero on an overcast day. The diffuse or non-direct insolation from all directions except directly from the sun makes up the remainder of the global insolation [1]. Therefore, there are two different components of solar radiation that strike any solar collector surface; these are direct and diffuse (deflected by atmospheric scattering effects and reflected rebound from surrounding terrain) as shown in Fig 2.Harnessing the sun's light and heat is a clean, simple, and natural way to provide all forms of energy we need. The sun's heat can be collected in a variety of different ways. It can be concentrated by parabolic mirrors to provide heat at up to several thousands degrees Celsius. This heat can be used either for heating purposes or to generate electricity. Solar thermal electric power plants generate heat by using lenses and reflectors to concentrate the sun's energy. Because the heat can be stored, these plants can generate power when it is needed, day or night, rain or shine.

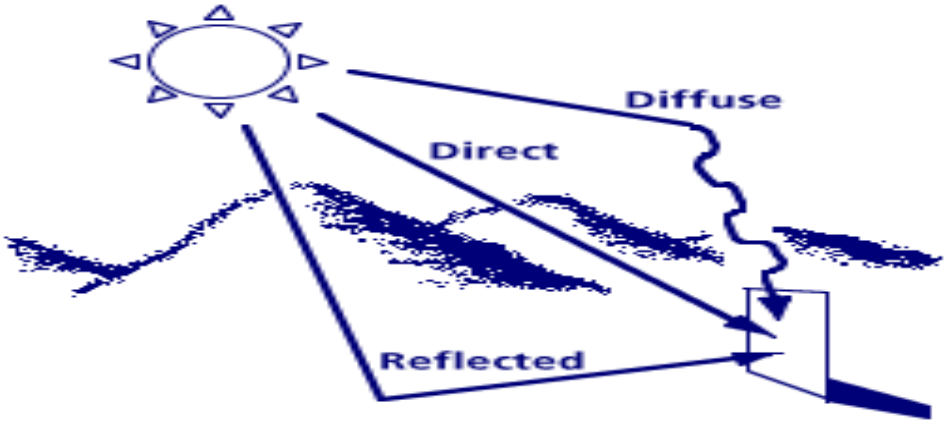

Fig. 2: Solar global radiation

Solar parabolic trough collector (SPTC) is a reflecting surface made of highly polished stainless steel reflector, fixed on a parabolic contour, supported by steel framework and mounted on reflector's support structure as shown in Fig. 3. The reflector is used to concentrate sunlight onto a receiver tube that is positioned along the focal line of the parabolic-trough. A transparent glass-tube envelops the receiver tube to reduce heat loss. Solar parabolic-troughs often use single-axis or dual-axis tracking [5]. In rare instances, they may be stationary. Temperatures at the receiver can reach 400 °C and produce steam for generating electricity [6].

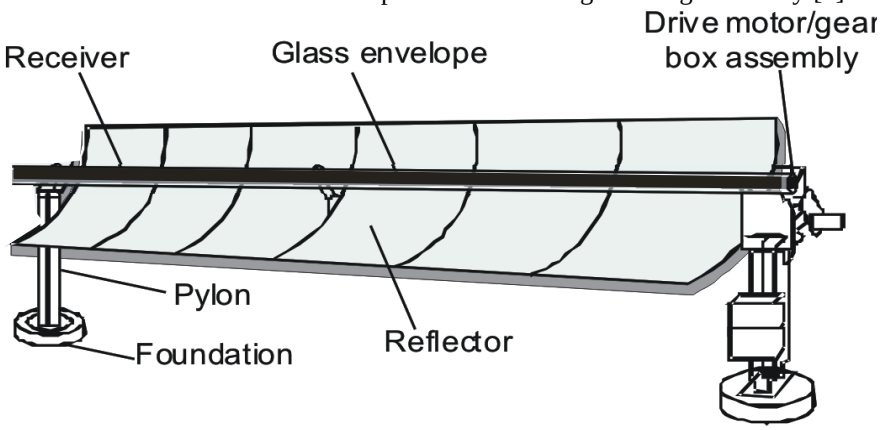

Fig. 3: Solar Parabolic-trough Collector

The mathematical property of a parabola makes it advantageous for steam production using the parabolic trough concentrator [7]. Rays of light that reaches the reflecting surface are reflected onto the focal line of the trough where the receiver assembly which consists of a transparent enveloping glass-tube and an absorber-tube is placed. Working fluid flow inside the absorber-tube and carries away the heat either trapped to the load directly as in active systems or initially stored as in passive systems.

II. METHODS

Energy balance equations for SPTC have been developed [8]. The equations considered the heat-energy-gain, the heat-energy-loss and the heat-energy-transfer between the components, i.e. the reflecting surface, the glass-cover and the absorber-tube, the thermal properties of the materials of the components and geometric dimensions of the SPTC. The equation for the enveloping glass-cover heat energy transfer is given as follows;

$$\alpha_g 2RL\left((I_{beam}R_b)+I_{diff}\right) + \rho_c\alpha_g\left(\frac{(W-D)L}{\pi}\right)(I_{beam}R_b) + \frac{A_t\sigma\left(T_t^4-T_g^4\right)}{\frac{1}{\varepsilon_t}+\frac{A_t}{A_g}\left(\frac{1}{\varepsilon_g}-1\right)}$$

$$-\sigma\varepsilon_g A_g\left(T_g^4-T_{sky}^4\right) - A_g h\left(T_g-T_{surr}\right) = m_g Cp_g\left(\frac{dT_g}{dt}\right) \quad \ldots 1$$

The equation for the absorber-tube heat energy transfer is given as follows;

$$\alpha_t\tau_g\left(\frac{2RL}{\pi}\right)\left[(I_{beam}R_b)+I_{diff}\right] + \tau_g\rho_c\alpha_t\left[\frac{(W-D)\times L}{\pi^2}\right][I_{beam}R_b]$$

$$-\frac{A_t\sigma\left(T_t^4-T_g^4\right)}{\frac{1}{\varepsilon_t}+\frac{A_t}{A_{g_r}}\left(\frac{1}{\varepsilon_g}-1\right)} - \frac{A_{tin}\left(T_t-T_f\right)}{\left[\frac{1}{h_f}+\frac{\ln\left(\frac{r}{r_1}\right)A_{tin}}{2\pi KL}\right]} = m_t Cp_t\left(\frac{dT_t}{dt}\right) \quad \ldots 2$$

The equation for the fluid heat transfer is given as follows;

$$\frac{A_{tin}\left(T_t-T_f\right)}{\left[\frac{1}{h_f}+\frac{\ln\left(\frac{r}{r_1}\right)A_{tin}}{2\pi KL}\right]} - \frac{2A_c\left(T_f-T_{surr}\right)}{\frac{1}{h_{surr}}+\frac{1}{h_f}} = m_f Cp_f\frac{dT_f}{dt} \quad \ldots 3$$

Employing these equations, a Mat Lab program was used to simulate the effect of annular gap which is the evacuated portion shown in Fig. 4.

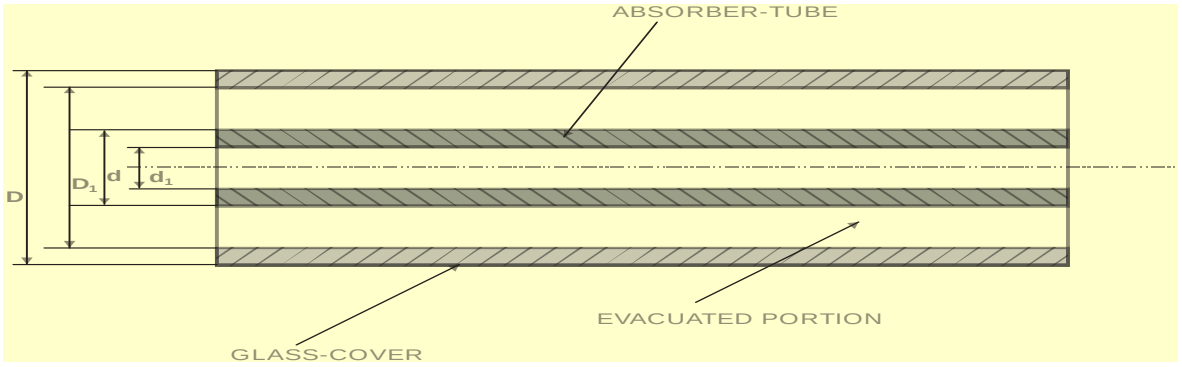

Fig. 4: Receiver assembly dimensions.

The absorber-tube is made of copper tube, coated with black paint. The outer diameter of the absorber tube, d, is given as 0.013 m. With a thickness of the absorber-tube, $x_t = 0.0015$ the inner diameter of the absorber-tube, d_1, can be computed as follows:

$$d_1 = d - 2.x_t \quad \ldots 4$$

With varying annular gap, (a), the inner diameter of the concentric transparent glass-cover, D_1, can be computed as follows:

$D_1 = d + 2a$ ... 5

It therefore follows that the outer diameter of the enveloping glass-cover, (D), with a thickness, (x_g), of 0.002 m, can be computed as follows:

$D = D_1 + 2x_g$ ... 6

Soda lime's transmittance, (τ_g) is 0.83 [9]. The absorptance (α_g) is 0.14. Emittance value of the glass-cover (ε_g) is 0.84 [8]. The Absorptivity of the copper is 0.70, and that of black paint is between 0.90 – 0.97 [3]. The absorptance (α_t) adopted is derived as follows:

$$\alpha_t = \frac{\alpha_c + \alpha_{bp}}{2} = \frac{0.70 + 0.90}{2} = 0.8$$

where α_c = Absorptivity of copper, α_{bp} = Absorptivity of black paint coating material. For the purpose of this work, the emittance of the absorber-tube material; $\varepsilon_t = 0.02$

The reflector is made of stainless steel of length (L) = 300mm, aperture width (W) = 800mm. Emissivity, $\varepsilon = 0.08$ [10]. Therefore, the reflectivity (ρ) can be computed using equation 7 [11].

$\rho_c = 1 - \varepsilon = 1 - 0.08 = 0.92$ ... 7

The fluid is Air and assuming a mean temperature of the fluid to be $77\ ^oC = 350$ K, the following properties are selected from [12]:

Density (ρ_f) $= 1.009\ kg/m^3$, Thermal conductivity (K_f) $= 0.03003\ W/m.K$, Prandtl number ($\Pr$) = 0.697, Specific heat capacity (Cp_f) = $1.0090\ J/kg.K$ and Viscosity (μ_f) = $2.075 \times 10^{-5}\ kg/m.s$, Grashof number ($Gr_d$) can be computed using equation 5 [13].

$$Gr_d = \frac{\rho_f^2 g \beta \Delta T d_1^3}{\mu^2},$$ ... 8

where density of the fluid (ρ_f) $= 1.009\ kg/m^3$, gravitational constant (g) $= 9.81$ m/s, inner diameter of the absorber-tube (d_1) $= 0.0100$ m and coefficient of expansion of the fluid (β) equals the reciprocal of T_f.

Therefore, $\beta = \frac{1}{350}$

Assuming a mean temperature of the absorber-tube (T_t) to be $130\ ^0$C and the mean temperature of the fluid (T_f) to be $80\ ^0$C. Therefore, the mean temperature difference is computed as follows:

$\Delta T = T_t - T_f = 130 - 80 = 50\ ^0C$.

Grashof number, $Gr_d = \frac{(1.009)^2 \times 9.81 \times \frac{1}{350} \times 50 \times (0.0100)^3}{(2.075 \times 10^{-5})^2} = 3313.7$

The expression used for the calculation of Nusselt number is given by [12]. It is written in equation 9 as follows:

$$Nu^{1/2} = 0.60 + 0.387\left\{\frac{Gr_d \Pr}{\left[1+(0.559/\Pr)^{9/16}\right]^{16/9}}\right\}^{1/6} \quad for \quad 10^{-5} < Gr.\Pr < 10^{12} \qquad \ldots 9$$

Therefore ,

$$Nu^{1/2} = 0.60 + 0.387\left\{\frac{(3313.7 \times 0.697)}{\left[1+(0.559/0.697)^{9/16}\right]^{16/9}}\right\}^{1/6} = 3.5374$$

Correspondingly;

$$h_f = \frac{Nu \times K_f}{d_1} = \frac{12.5132 \times 0.03003}{0.0100} = 38.3383 \; W/m^2.K$$

where h_f = Convective heat-transfer coefficient for the inside of the absorber-tube, d_1 = inner diameter of the absorber-tube and K_f = thermal conductivity of the fluid.

The hourly thermal efficiency (□)of the collector is given by:

$$\eta = 1 - \frac{Q_{losses}}{Q_{input}} \qquad \ldots 10$$

The hourly heat-energy supplied to the receiver (Q_{input}) can be computed as follows:

$$Q_{input} = I_g \times A_a = [(I_{beam}.R_b) + I_{diff}][WL] \qquad \ldots 11$$

where I_{beam} R_b = beam radiation on a tilt surface, I_{diff} = diffuse radiation, W = aperture diameter and L = length of the concentrator. The hourly tilt factor ($R_{b_{hr}}$) is the ratio of the beam radiation on a tilted surface to that on a horizontal surface and can be computed using Equation 12 [14].

$$R_b = \frac{\cos(\phi - s)\cos\delta\cos\omega + \sin(\phi - s)\sin\delta}{\cos\phi\cos\delta\cos\omega + \sin\phi\sin\delta} \qquad \ldots 12$$

The latitude of Bauchi is $\phi = 10.33^0$, A slope angle of 2^0 is adopted. Sukhatme [14] has given the following simple relation for calculating the declination:

$$\delta = 23.45\sin\left[\frac{360}{365}(284 + n)\right] \qquad \ldots 13$$

Equation 13 is dependent on n , which is the day of the year.

The hour angle (ω) is the angular measure of time and is equivalent to 15^0 per hour. It is measured from noon based on local apparent time (LAT) being positive in the morning and negative in the afternoon.

The total heat-energy loss in the system (Q_{losses}) is considered as the sum of the radiative heat-loss from the surface of the enveloping glass-cover to the surroundings (q_{r_2}), the convective heat-loss from the surface of the enveloping glass-cover to the surroundings (q_c), the radiative heat-loss from the surface of the absorber-tube (q_{r_1}) and the conductive/convective heat-loss inside the absorber-tube (q_1). This can be expressed as in Equation 14.

$$Q_{losses} = q_{r_2} + q_c + q_{r_1} + q_1 \qquad \ldots 14$$

The hourly radiative heat-loss from the enveloping glass-cover by radiation to the surroundings is given by:

$$q_{r_2} = \sigma\varepsilon_g A_g\left(T_g^4 - T_{sky}^4\right) \qquad \ldots 15$$

where σ = Stefan-Boltzman's constant, ε_g = emittance of the enveloping glass-cover material, A_g = surface

area of the enveloping glass-cover, T_g = temperature of the enveloping glass-cover, and T_{sky} = sky temperature. The sky temperature can be expressed as

$$T_{sky} \approx T_{surr} - 6 \quad \text{...16}$$

where T_{surr} = ambient temperature. The hourly convective heat-loss from the enveloping glass-cover to the surroundings is computed using Equation 17 as follows:

$$q_c = A_g.h(T_g - T_{sky}) \quad \text{...17}$$

where h = the convective heat transfer coefficient given as:

$$h = 3.8V_{wind} + 5.7 \text{ [14]} \quad \text{...18}$$

where V_{wind} = wind velocity.

The hourly radiative heat-loss from the absorber tube to the enveloping glass-cover q_{r_1} can be computed using Equation 19.

$$q_{r_1} = \frac{A_t \sigma \left(T_t^4 - T_g^4\right)}{\frac{1}{\varepsilon_t} + \frac{A_t}{A_g}\left(\frac{1}{\varepsilon_g} - 1\right)}, \quad \text{... 19}$$

where A_t = the surface area of the absorber-tube, T_t = temperature of the absorber-tube and ε_t = *emittance* of the absorber-tube material. The hourly conductive/ convective heat-losses, by the working fluid inside the absorber-tube (q_1) can be computed using Equation 20, as

$$q_1 = \frac{2A_c\left(T_f - T_{sky}\right)}{\frac{1}{h_{surr}} + \frac{1}{h_f}} \quad \text{...20}$$

This work employed the developed energy equations and geometric dimensions of a solar parabolic collector model TE. 38. The meteorological and radiation data were obtained from the work of [15]. The simulation maintained the same thermal properties of the collector materials and Mat lab program was used to simulate hourly thermal efficiency (η) of the system, varying the annular gap between the absorber-tube and the enveloping glass-cover.

III. RESULTS AND DISCUSSION

Table 1: Simulated values of hourly thermal efficiencies of the system for various annular gaps

TIME	SIMULATED THERMAL EFFICIENCIES OF THE SYSTEM FOR VARIOUS ANNULAR GAPS									
	$\eta_{0.010}$	$\eta_{0.015}$	$\eta_{0.020}$	$\eta_{0.025}$	$\eta_{0.030}$	$\eta_{0.035}$	$\eta_{0.040}$	$\eta_{0.045}$	$\eta_{0.050}$	$\eta_{0.055}$
08:00hr	85.648	81.785	77.923	74.060	70.197	66.335	62.472	58.610	54.747	50.884
09:00hr	91.428	89.118	86.810	84.496	82.186	79.876	77.565	75.255	72.944	70.634
10:00hr	94.227	92.669	91.115	89.553	87.996	86.438	84.880	83.323	81.765	80.207
11:00hr	96.110	95.060	94.015	92.962	91.913	90.864	89.815	88.766	87.716	86.667
12:00hr	96.662	95.762	94.866	93.964	93.064	92.165	91.265	90.366	89.467	88.567
13:00hr	97.716	97.103	96.492	95.877	95.264	94.651	94.038	93.425	92.812	92.199
14:00hr	97.431	96.743	96.057	95.368	94.680	93.992	93.304	92.617	91.929	91.241
15:00hr	96.824	95.975	95.125	94.276	93.426	92.577	91.728	90.878	90.029	89.180
16:00hr	94.307	92.785	91.262	89.741	88.219	86.697	85.175	83.653	82.131	80.609
17:00hr	87.837	84.579	81.321	78.063	74.805	71.547	68.288	63.030	61.773	58.514

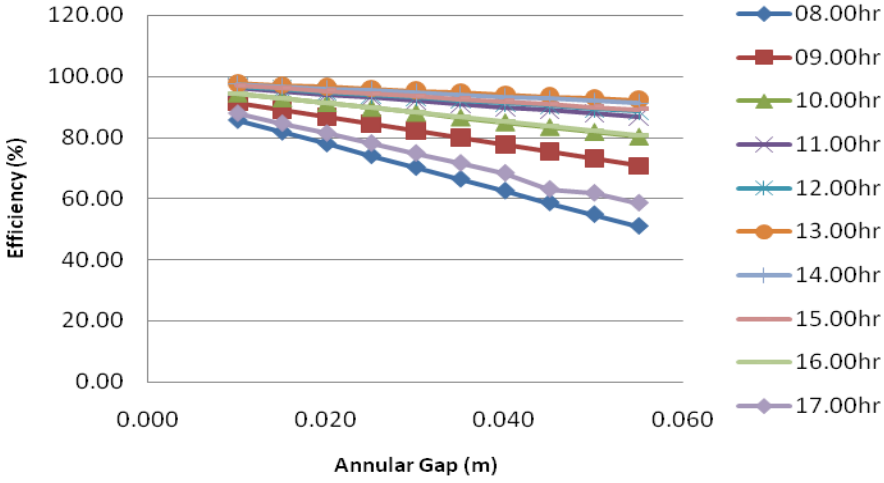

Fig. 5: Simulated Thermal Efficiency for Various Annular Gap

The simulation results in Table 1 and Figure 5 show that increase of annular gap reduces the thermal efficiency of the system. The higher the annular gap between the absorber-tube and the enveloping glass-cover, without corresponding increase in the diameter of the absorber-tube, the more is the total heat loss of the system and therefore, the lower is the thermal efficiency of the system.

IV. CONCLUSION

This paper investigated the annular gap effect on the performance of a solar parabolic-trough collector. The simulation results show that as the annular gap increases the thermal efficiency of the system reduces within the investigation range. The higher the annular gap between the absorber-tube and the enveloping glass-cover, the more is the total heat loss of the system and therefore, the lower is the thermal efficiency of the system.

REFERENCES

[1] Cherimisinoff, P. N., and Thomas, C. R., (1981), Principles and Applications of Solar Energy, Ann Arbor Publishing Company, Inc, U.K., pp. 40-61.
[2] Rose, J. E., and Lawrence, H. A., (March 1996). The chemical composition of the sun, Science, Vol. 191, No. 4233, pp. 1223 to 1229.
[3] Howell, J. R., Richard, B. B., and Gary, C. V., (1982), Solar thermal energy systems: Analysis and Design, McGraw-Hill Book Company, U.S.A., pp. 31-54.
[4] http://www.geocities.com/dieret/re/dieret.html
Thomas, A. (1996), A Design methodology for a small solar steam generation system using flash boiler concept, Energy conversion management, 37.1.
[5] Winter, C. J., Sizman, R. L., and Vaut-Hall, L. L., (1991), Solar Power Plants: Fundamentals. Technology. System Economics, Springe-Verlag Berlin, Heidelberg. pp. 111-123.
[6] William, B. S., and Michael, G., (2003), Power from the sun, http://www.powerfromthesun.net
[7] Egbo, G., Sambo, A. S., and Asere, A. A., (2005), Development of Energy Equations for Parabolic-trough solar collector, Nigeria Journal of Engineering Research and Development, NJERD, Vol. 4, No. 1, pp. 28 – 36
[8] http://www.dynapro.com
[9] http://www.electro-optical.com
[10] Scott, C., (2001), ARE: [Solar] Parabolic-trough reflective mirror options, solar-concentrator@cichlid.com.
[11] Churchill, S. W., and Chu, H. H. S., (1995), Correlating Equations for Laminar and Turbulent free convection from a vertical plate, International journal of Heat Mass Transfer, Vol 18, pp. 1323-1333.
[12] Kreida, Jan. F., and Kreith, Frank, (1981), Solar Energy Handbook, McGraw-Hill Book Company, U.S.A., pp. 67-103.
[13] Sukhatme, S. P. (1991). Solar Energy: Principles of Thermal collection and Storage. Tata McGraw-hill Publishing Company Limited. India.
[14] Egbo, G., (2008), Experimental Performance Evaluation of a Solar Parabolic-Trough Concentrating Collector (model TE. 38), International Journal of Pure and Applied Science, Vol. 2(1), pp 55-64.

American Journal of Engineering Research (AJER)
e-ISSN : 2320-0847 p-ISSN : 2320-0936
Volume-03, Issue-12, pp-109-118
www.ajer.org
Research Paper Open Access

Studying Tourism Indicators In Iran (Case Study: Khoramabad City)

[1,]Mahdi Garavand , [2,] Hamid reza Saremi
Department of Architectural and urban planning , college of architecture , Boroujerd Science and Research branch, Islamic Azad University, Boroujerd, Iran

Assistance Professor Department of Art and Architecture, Tarbiyat Modares University, Tehran, Iran

ABSTRACT : *Now tourism industry is one of the greatest World Industries from point of view development and with attention to be use financial sources and involved persons with that. This industry, has third rank in financial and commercial classifications and including more than 7 percent of whole world exports, also it influence gross national product in all countries; so that increase rate of gross national product 2billion $ in all world nations. Tourism industry important to stress tow important ways: first, the dynamic familiarity with other cultures, nations, races, tribes, dialects and …; second, it provides sources of income and foreign exchanges from an economic point of view. The different world countries fallowed attraction of tourists because of that they have various facilities and various attractions.Iran is ranked as one of the 10 top attractive countries in the world but Iran was place 114th ranking of the countries in terms of attracting tourists (World Economic Forum, 2011), tourism receipts is ranked as 77th, and the number of international tourists arrivals ranked as place 70th (UNWTO, 2009).So, the aim of this research is, studying main indicators in tourism location in order to improving their qualify. This research is qualitative. Also was used the "Descriptive/ Explanatory" through contain analysis. The research method are phenomenological, conceptual and constructive theory in field of tourism industry in context of Iran, Which eventually is bound to lead to the development of tourism industry in Iran. The strategy of this research is qualitative method by using case study in the area of tourism industry in fabric of Iran. So, was introduced touristic-historical building. Then according to visitor comments was ranked. At finally was used T-Test method in order to analyzing hypothesis.*

KEY WORD: *Tourism indicators, indicators, Iran, Khoramabad*

I. INTRODUCTION

Nowadays, Tourism industry is considered as one of the most profitable and intensively developing branches of the world economy in the area of services. This is confirmed by the fact that the share of tourism is about 10% of the world's gross national income. Development of tourism plays an important role in social and physical activities. World Tourism Organization (UNWTO) announced that tourism industry grows up and it will get about 25% of worlds gross national income (UNWTO, 2009).According to UNWTO (2009) economic importance of tourism and travel, increasing the vast number of passengers continues 25 million people between the years 1950 to 1.18 billion in 2010. UNWTO (2009) forecasted that the numbers of tourist arrivals continue to growth and on 2020 will 16 be 1.6 billion passengers a year. In the view of tourism potential and opportunities to contribute to the attractiveness of country for the tourists, according to UNWTO (2009), Iran is ranked as one of the 10 top countries in the world in term of tourism attractions but its tourism receipts industry is ranked 77th and the number of international tourists arrivals who have traveled to Iran, was ranked as place 70th (UNWTO, 2009), this evidence shows that in current time Iran's tourist industry is not working with full capacity. Iran is a four season country whole of a year, tourists can travel from hottest place in the world to a very cold place by just a 45 minutes flight (Karimi, 2009).

Tourism is recognized as one of the key sectors of development in all countries and a major source of income, jobs and wealth creation. It also plays a wider role in promoting the image and international perception of a country externally as well as influencing complementary domestic policies. This range of influence and importance creates challenges in measuring competitiveness in tourism.

Understanding country competitiveness in tourism is a major consideration for policy makers and a major challenge for professionals in providing evidence to inform decision making. Various indicators have been developed by different organizations over the years to address particular aspects of competitiveness but there has remained a lack of an overall measurement framework for competitiveness in tourism for the use of governments. The current work by member and partner countries seeks to address this gap and make a positive contribution to the practical measurement of competitiveness.The purpose of this research is, studying tourism indicators at LORESTAN province in Iran. Khoram abad is the center of Lorestan province.

Hypothesis research
This research tries that response main research question & hypothesis. Thus the question and hypothesis is:

- ✓ Question: What is the sample space tourism of Khoramabad according to quality indicators?
- ✓ Hypothesis: it seems, Falak-ol-Aflak castle (The Heaven of Heavens), is important tourism location based on quality indicators.

II. LITERATURE REVIEW

Tourism definition : Up to now tourism has been under study and discussion from view of different science like economics, sociology, and geography and based on any views has raised various definitions that Rezvani (1996) accumulates the collection of them under title as geography and tourism industry. For example Artobruman has defined tourism the fallowing: " tourism contains travels collection that it performs due to rest, fun, experience and other vocational activities or due to take part in the specific ceremonies and it is temporary and passing that tourist don't exist in her/himself address. It is clear that persons, who perform permanent vocational travel between her/himself address and place of work, don't include to this definition" (Rezvani , 1996) .From view of sociology, tourism is a relations collection that person creates with others in her/himself temporary address. According to Honziker-krapph, tourism is relation collection that it creates from travel and residence of one nonnative person without having permanent address and job. The definition was acceptable by international council of science experts in tourism for times. According to Morgan Rout, tourism in literal meaning is travel of persons that go away from themselves address temporary until they granted vital, cultural and personal needs in form of a consumer of economic and cultural goods. In competitions that tourism international union held to gain general definition for tourism, the fallowing definition is selected. According to this definition "tourism is collection of changing place of persons and actions that conclude from it. The changing caused by come true demands that they force person to movement and there are potentially in any person by different intensity and weakness.

Today tourism phenomena is more than simple phenomena of visit and return visit and obtain specific importance that it is called as a huge, producer and main industry. In many advanced countries and some of countries exist many attractions of historical, cultural, natural and facilities of tourism attracted (Tulaii, 2007). The grate portion of nation income supplies with tourism development. It isn't UN due that most of countries, especially countries that have more historical, cultural and natural attractions, try to obtain more options in absorption of different countries tourists and get foreign exchange income for themselves by creating and development of necessary touristic facilities. On the other hand, tourist is foreign person for travel, tourism, and sports .The residence is not less than 24 hours and not more than 2 months. According to a Committee on 22 January 1937, the following definition for tourists can be justified: a person who travels to a country for 24 hours or more and usually has the right to stay there (Moradi, 2007: 9 -14).

Classification of Tourism : Classification of tourism is the important tool to understand the capacity of the country according to get the competitive advantages by focusing in some types of them. According to World Tourism Organization (UNWTO) in 1993 defined the word of tourism as the following: "travel to and stay in places outside their usual environment for more than twenty-four (24) hours and not more than one consecutive year for leisure, business and other purposes not related to the exercise of an activity remunerated from within the place visited."United Nations In 1994 classified three forms of tourism in its Recommendations on Tourism Statistics:

- Domestic tourism, which involving residents of a given country traveling only within this Country.
- Inbound tourism, involving non-residents of a given country that traveling within this country.
- Outbound tourism, which involving residents of a country traveling to the other countries.

In June 1991, the International conference held by organizing the World Tourism Organization and government of Canada about the travel and tourism statistics in Ottawa. Their defining words, phrases and their classification decisions were taken which are as below:

- Tourism, is the things or acts that the person who travelled doing in a place outside of his/her normal environment, the traveling take long not more than a year and its purpose is to fun, business or other activities.

- Traveler or tourist (overnight visitor) is someone who spent at least a night in public or private residence at the site visit.
- Same day visitor or one day tourist is someone who is staying in a place but not for the night.
- Based on the above classification, the governments must focus their forces to promote international tourism by making their strategies base on their capacity to attract travelers.

History of tourism industry in Iran : Tourism shaped in Iran from the second decade of present century and the first time in 1994 year was established office named "attraction of foreign visitors and publicities office" in interior ministry and was assigned to this office do works related to tourism. "Iran tourism association" established for supplying comfort and facilitating travel of tourists in this same year. The association, that record officially in MAY /1939 year, organized different tour for tourists visit. Attraction of visitors office was changed its name to "tourism supreme council" in September of 1942 year. Tourism supreme council was changed to tourism affairs office and was centered in the interior ministry in1333 year. From the office actions during 1955-1959 years, can indicate to doing some services of sub structural and compilation of laws and rules related to tourism as "entry law and residence of foreign national".An organization named "attraction of visitors organization" depended on premiership was established on April /1964. The organization main purpose was presentation of country back ground, encouragement of interior and foreign tourists to traveled and visited ancient relics and natural views and created necessary concentration and coordination in affaires. Attraction visitors organization was combined on information ministry and made new ministry named "information and tourism ministry" in Jun /1975. To fallowing of Islamic revolution victory, information and tourism ministry at firs changed name to ministry of national guidance and then to ministry of Islamic guidance and tourism assistance district of this ministry undertook tourism affairs supervision. Iranology and tourism office established for planning of tourism industry, educating of tourism charges, classification, supervision and evaluation of plants, establishment of international relationship with institutions and organs of foreign tourism and take part in meetings, tourism exhibitions and international gatherings. After a while this office according to ratified in 21/December /1980 of Islamic revolution council was changed its name to "organization of Iranology and tourism centers" that was made by combining four state companies as plants stocks of Iran tourism company, stocks of Iran visiting company, stocks of Iran homes centers company and stocks company of tourism centers tourism for winter sports (Moddaresi, 2000). Despite the fact that government hadn't clearly politic related to tourism industry until first developing plan and also in the private district due to didn't clear politics and laws, there wasn't tendency to make resident and reception centers and plants; but in the course of politics of first, second and third developing plans, tourism district is benefited from special position in planning country and people up to become interested in the investment within making and developing resident and reception plants.

III. RESEARCH METHODOLOGY

This research is a qualitative. Also was used the "Descriptive/ Explanatory" through contain analysis. The research method are phenomenological, conceptual and constructive theory in field of tourism industry in context of Iran, Which eventually is bound to lead to the development of tourism industry in Iran. The strategy of this research is qualitative method by using case study in the area of tourism industry in fabric of Iran. So, was introduced touristic-historical building. Then according to visitor comments was ranked. At finally was used T-Test method in order to analyzing hypothesis. Therefore were proposed strategies in order to promoting tourism space quality.

RESEARCH AREA : "KHORAMABAD "is a city in and capital of Lorestan Province, Iran. At the 2006 census, its population was 328,544, in 75,945 families. Khoramabad is situated in the Zagros Mountains. Khoramabad Airport is 3 km south of the city proper.The city population is predominantly Lur and Lak, although the two groups are closely related. Although not a major tourist destination, it is quite scenic and possesses several attractions, such as 5 Paleolithic cave-dwelling sites. In the city center, a tall citadel called Falak-ol-Aflak (The Heaven of Heavens), a relic of the Sassanid era, is now a nationally popular museum. Economically, it is the regional base of the agricultural industry.

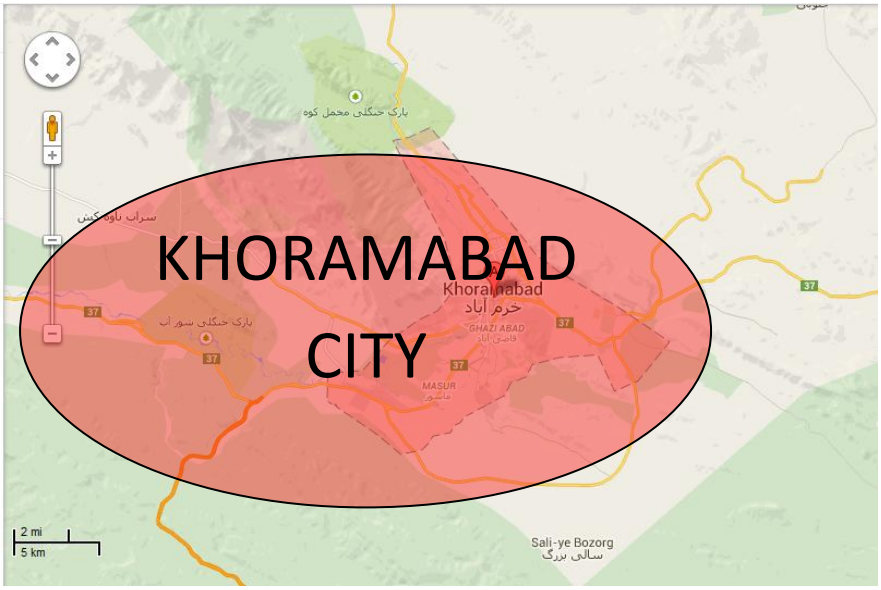

FIGURE 1: STUDIED AREA

TOURISTIC LOCATION OF KHORAMABAD :

Gerdab sangi : Gerdab Sangi is located in Takhti Square in Khorramabad, Lorestan and is made of stones and plaster. It dates back to the Sassanid era (224-651 CE) and is a circular whirlpool built for the purpose of accurate and optimal distribution of water. Encircling several springs, the edifice sits near the prehistoric Qomri Cave. The construction was once used for rationing and distributing potable and agricultural water among local population and farmers. Its surrounding cylindrical stone wall has a height of 10 meters and a diameter of 18 meters. There are a few different-sized outlets in the wall for controlling the flow of water into a canal on the west of the structure. While originally there were 7 of such outlets, however, today only one is functional. This outlet measures 160 x 90 centimeters and opens and closes like a drawer. The water flowing out of this outlet, after a path of approximately 12 kilometers, would eventually make its way to a valley called Baba Abbas. In the vicinity of this valley, and the location of the ancient city of Shapurkhast, the remnants of an old mill, which was run using water from the springs, can be observed. Gerdab Sangi was registered on the National Heritage List in 1976.

Figure 2: GERDAB SANGI

Brick Minaret : Brick Minaret is a 900 years old brick tower located beside the ancient city of Shapur khawst, south of Khorramabad, Lorestan province. It was built as a guidepost for caravans in ancient times. The minaret is about 30 meters tall with a circumference of 17.5 meters. Inside the tower there is a spiral staircase of 99 stairs.

Figure 3: Brick Minaret

Shapoori Bridge : Shapoori Bridge is located in southern KhorramAbad. It has been used to connect the western part of Lorestan (Tarhan) to the east, and then on to Khoozestan province and Taysafun, the capital city of the Sassanian. The bridge is 312 meters long and 10.75 meters high. It has 28 arches and 27 piles. The area of each pile is 61 square meters, and the distance between the two piles is 7.5 meters. Five of its arches are intact; the others have been destroyed by natural factors. The arches of the bridge are made in the form of a wishbone. The piles and breakwaters of the bridge are in the form of six lateral lozenges made of stone. Probably the bridge also was used to distribute water. Materials of the bridge are river stones and stone chips in the arches and truncated stones in the piles. The bridge floor is paved in red block stones that have lost their square shape due to erosion. This attractive, huge bridge belongs to Sassania era, and it is registered as number 1058 in the list of Iranian national monuments.

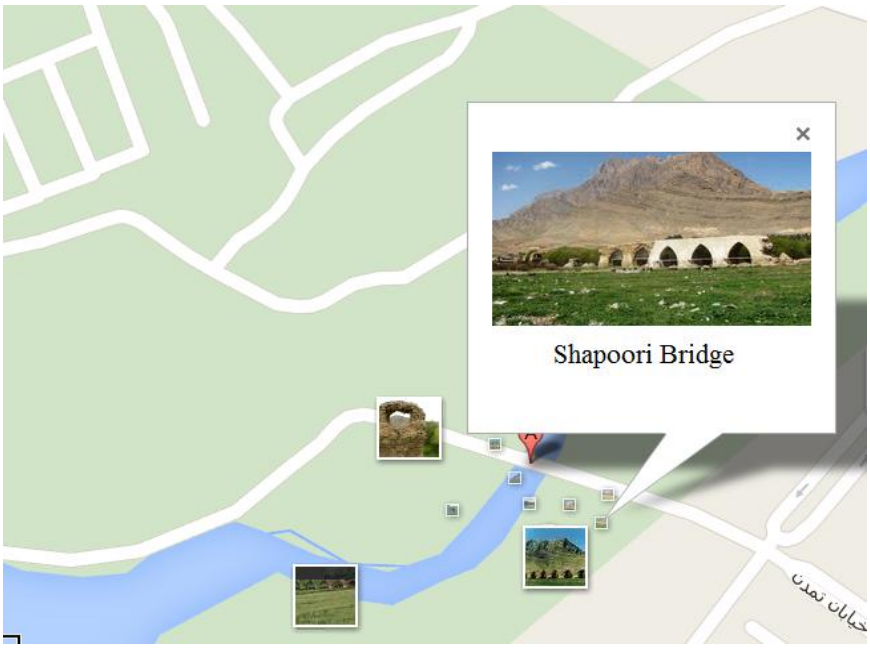

Figure 4: Brick Minaret

Falak-ol-Aflak castle[1] **:**Falak-ol-Aflak Castle, Dež-e Shāpūr-Khwāst, Falak-ol-Aflak Castle, in ancient times was known as Dezbaz as well as Shapur-Khast, is one of the most impressive castles in Iran. It is situated on the top of a large hill with the same name within the city of Khorramabad, the regional capital of Lorestan province. The Khorramabad River runs past the eastern and south-western side of the Falak-ol-Aflak hill providing the fortress with an element of natural protection. Today, the western and northern sides of the hill are bordered by the residential districts of Khorramabad. This gigantic structure was built during the Sassanid era (226–651). It has been known by a number of names since it was built over 1800 years ago. Recorded names have referred to it as Shapur-Khast or Sabr-Khast fortress, Dezbaz, Khorramabad castle, and ultimately the Falak ol-Aflak Castle. The foundations of the actual castle measure approximately 300 meters by 400 meters. The height of the entire structure, including the hill, reaches up to 40 meters above the surrounding area. This space is divided into four large halls, and their associated rooms and corridors. The rooms all surround two courtyards with the following measurements: the first courtyard measures 31×22.50 meters and the second 29x21 meters. . When originally built the castle used to have 12 towers, but only 8 remain standing today. The building's entrance is situated towards the north, within the body of the northwestern tower.

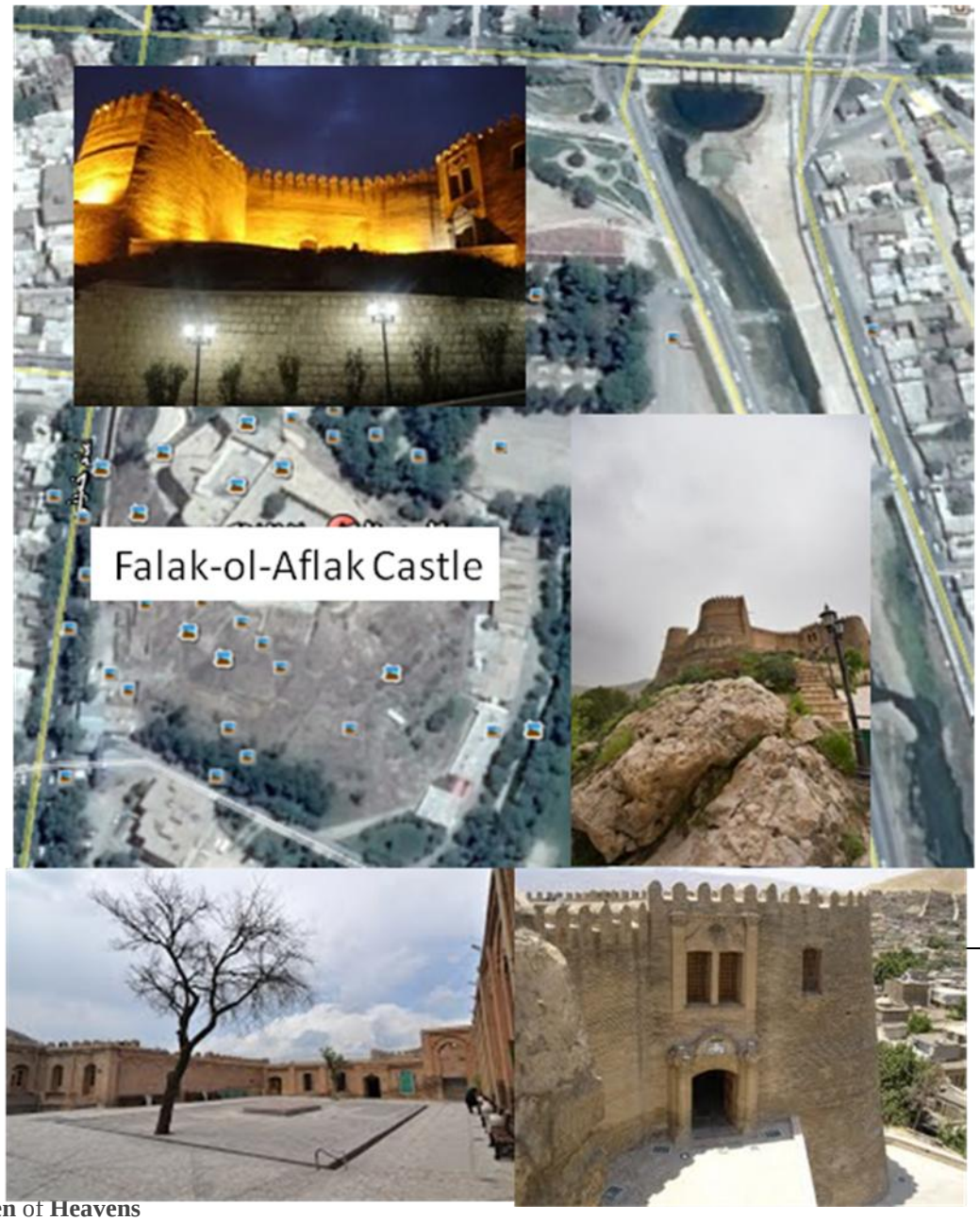

Heaven of **Heavens**

Figure 5: Falak-ol-Aflak castle

IV. DISCUSSION

Descriptive findings : According to introduced attractive tourism locations, it seems khoramabad have important role in order to attracting indoor and outdoor tourists. So, we need planning in order to improving tourism industry many aspects. Thus, was used questionnaire tool. Also, sample size is 240 persons. In order to, were classified main indicators of touristic location.
The indicators were presented in table 1.

Table 1: studied indicators

Indicators of touristic locations qualify	Marker
Qualify of touristic location as cleanliness space	Q1
Landscape	Q2
Building stability	Q3
Satisfaction of native person behavior	Q4
Entertainment space for kids	Q5
Appropriate accessibility to transportation	Q6
Total satisfaction	Q7
Visiting again in future	Q8
Proposing friends in order to visiting this location	Q9
Visual aesthetics of mentioned location	Q10

Gerdab sangi : According to analyzing of questionnaire 75 % of visitor have emphasized on landscape. Also, 31% of visitors haven't satisfied from entertainment spaces. (Table 2 & graph 1).

Table 2: analyzed data from GERDAB SANGI

Indicators of touristic locations qualify	Marker	Score	Percentage
Qualify of touristic location as cleanliness space	Q1	56	75
Landscape	Q2	51	68
Building stability	Q3	51	68
Satisfaction of native person behavior	Q4	52	69
Entertainment space for kids	Q5	23	31
Appropriate accessibility to transportation	Q6	40	53
Total satisfaction	Q7	55	73
Visiting again in future	Q8	50	71
Proposing friends in order to visiting this location	Q9	53	69
Visual aesthetics of mentioned location	Q10	52	71

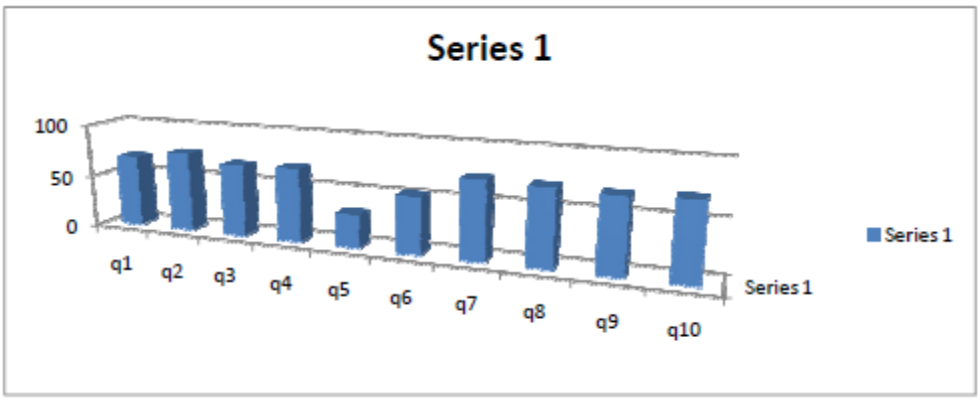

Graph 1: analyzed data from GERDAB SANGI

Brick minaret : One of the negative point in brick minaret is pollution due to 25% of persons believed mentioned location is cleanliness. On the other hand, 84% believed this place have good view (table 3& graph 2).

Table 3: analyzed data from brick minaret

Indicators of touristic locations qualify	Marker	Score	Percentage
Qualify of touristic location as cleanliness space	Q1	19	25
Landscape	Q2	63	84
Building stability	Q3	50	67
Satisfaction of native person behavior	Q4	50	67
Entertainment space for kids	Q5	62	83
Appropriate accessibility to transportation	Q6	37	49
Total satisfaction	Q7	55	73
Visiting again in future	Q8	56	75
Proposing friends in order to visiting this location	Q9	57	76
Visual aesthetics of mentioned location	Q10	57	76

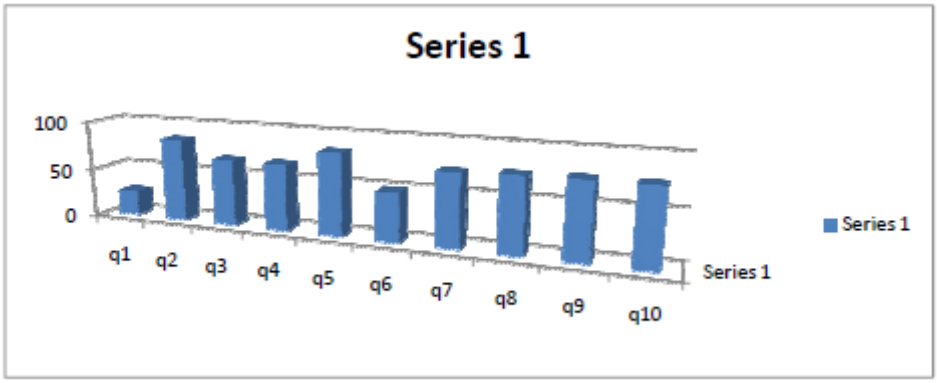

Graph 2: analyzed data from brick minaret

Shapori bridge : Based on table 4, 83% of persons believed landscape is good.

Table 4: analyzed data from Shapori Bridge

Indicators of touristic locations qualify	Marker	Score	Percentage
Qualify of touristic location as cleanliness space	Q1	48	64
Landscape	Q2	62	83
Building stability	Q3	57	76
Satisfaction of native person behavior	Q4	56	75
Entertainment space for kids	Q5	37	49
Appropriate accessibility to transportation	Q6	24	32

Total satisfaction	Q7	56	75
Visiting again in future	Q8	50	67
Proposing friends in order to visiting this location	Q9	54	72
Visual aesthetics of mentioned location	Q10	53	71

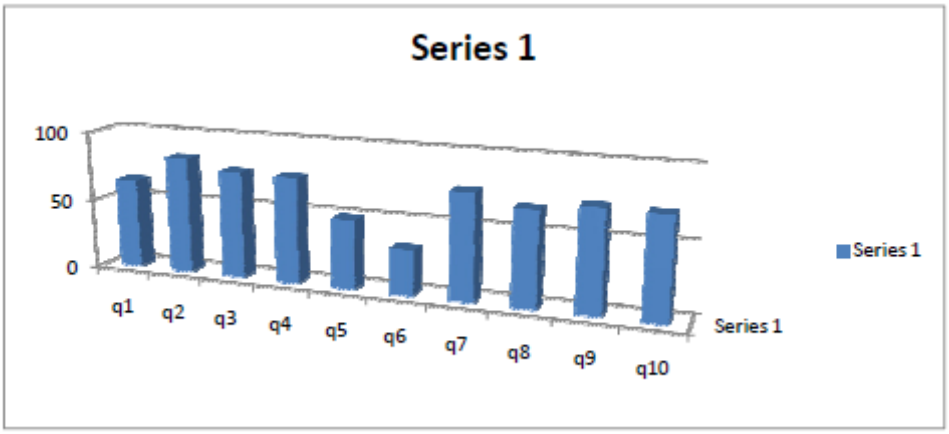

Graph 3: analyzed data from Shapori Bridge

Falak-ol-Aflak castle

Based on analyzed data, 92% of persons believed Visual aesthetics of mentioned location is high. Also, 83% satisfied totally.

Table 5: analyzed data from Falak-ol-Aflak castle

Indicators of touristic locations qualify	Marker	Score	Percentage
Qualify of touristic location as cleanliness space	Q1	56	75
Landscape	Q2	65	87
Building stability	Q3	53	71
Satisfaction of native person behavior	Q4	37	49
Entertainment space for kids	Q5	44	59
Appropriate accessibility to transportation	Q6	63	84
Total satisfaction	Q7	62	83
Visiting again in future	Q8	58	77
Proposing friends in order to visiting this location	Q9	55	73
Visual aesthetics of mentioned location	Q10	69	92

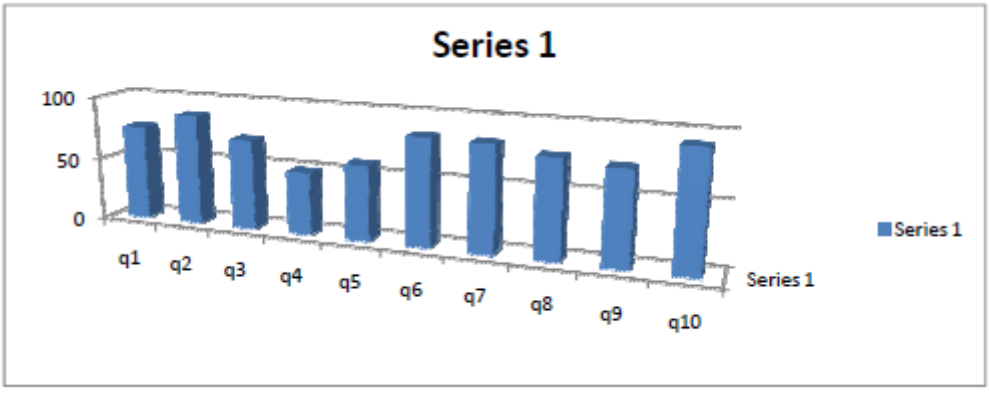

Graph 4: analyzed data from Falak-ol-Aflak castle

Analytical findings : In order to analyzing hypothesis, has been used from SPSS software. Also, in order to meaningful test was used one- sample T-TEST. The t-test is probably the most commonly used Statistical Data Analysis procedure for hypothesis testing. The statistics t-test allows us to answer this question by using the t-test statistic to determine a p-value that indicates how likely we could have gotten these results by chance, if in fact the null hypothesis were true (i.e. no difference in the population). By convention, if there is less than 5% chance of getting the observed differences by chance, we reject the null hypothesis and say we found a statistically significant difference between the two groups (Saberi, 2014:192).

In this research after using mentioned technique were diagnosed main indicators between ten. They are:

[1] Landscape
[2] Visual aesthetics of mentioned location
[3] Building stability
[4] Total satisfaction

On the other hand, were ranked mentioned place. The reports are according to T-TEST. They proposed in table

Table 6: ranked tourist location

Touristic location	Score	Ranke
Falak-ol-Aflak castle	562	1
Brick minaret	506	2
Shapori bridge	497	3
Gerdab sangi	486	4

V. CONCLUSION

As it shown in bellow based on the literature the structure of tourism industry evolve two dimensions; firstly is tourism resources and the second is the tourism infrastructure, understanding the positive points (strengths and opportunities) which are the cultural, nature and human based activities are making and improving the tourism sources, on the other hands the major dominate actors (Media, Education, Government, etc) are the major players on tourism infrastructures. After the result the following Conceptual map came up by author:

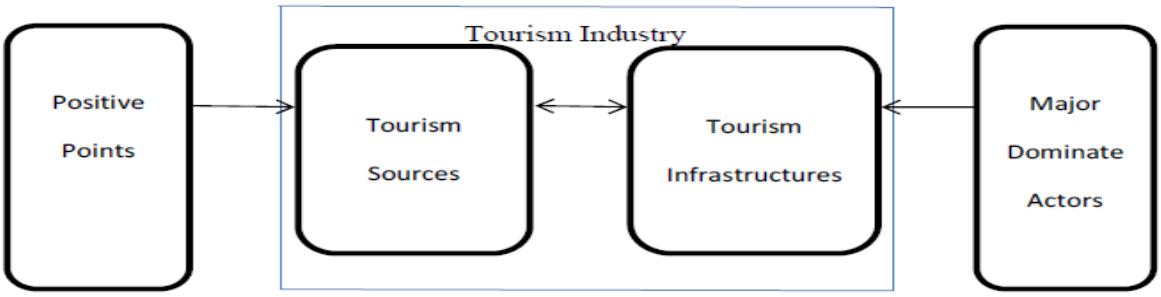

Figure 6: Conceptual map

REFERENCES

[1] Karimi, G. (2009), "Tourism development in the 24 essential public programs", p.156-172.
[2] "UNWTO World Tourism Barometer June 2009". UNWTO World Tourism Barometer (World Tourism Organization) 7 (2). June 2009.
[3] UNWTO technical manual: Collection of Tourism Expenditure Statistics" (PDF). World Tourism Organization. 1995. p. 14.
[4] Modaresi, Mansur. (2000). Way of compilation of development plan of province: Tourism area of Plan and Budget organization, Assistance of economic and culture affaires.
[5] Rezvani, Aliasghar (1996). Plan and Development in Iran
[6] Tulaii, Simin (2007) Review of Industry Tourism, Tarbyat moallem university, Tehran.
[7] Iranology and tourism and development (1999). Tehran: Ministry of Islamic culture and guidance.
[8] Moradi Maryam. Fayyazi Marjan, (1385) Tourism Management, Principles, Principles, and functional concepts: p. 9 -14
[9] http://www.itto.org/tourismattractions/?sight=1238&name=Falakol+Aflak+Castle+Museum#ixzz3GNXoak8e
[10] Reza Saberi Tavalaee (2014) , Assessment effective factors on satisfaction of personals occupation in Rural Municipalities (Dehyari) in Iran (Case study: Kuhsorkh of Kashmar County), American Journal of Engineering Research , Volume-3, Issue-9, pp-185-193
[11] Ministry of Islamic culture and guidance. Assistance of journey and visiting. (1992). summery of foreign Tourism report in Iran. Tehran: Ministry of Islamic culture and guidance.

American Journal of Engineering Research (AJER)
e-ISSN : 2320-0847 p-ISSN : 2320-0936
Volume-03, Issue-12, pp-119-123
www.ajer.org
Research Paper Open Access

Embedded Systems: Security Threats and Solutions

Anik Barua[1], Mohammad Minhazul Hoque[2], Rubina Akter[3]
[1, 2, 3] *(Department of ICT, Mawlana Bhashani Science and Technology University, Bangladesh)*

ABSTRACT : *With the increasing use of embedded devices in our daily life, security threats have also been increasing in a proportional rate. However, ensuring security in the embedded systems has become a great challenge not only for the embedded device experts but also for the manufacturers. The problem especially arises because of the limited hardware and software implementation options for the designers. At the same time, companies are trying to keep the vulnerabilities of the operating system of those embedded devices in secret and they are not relieving any necessary security updates quickly. It has become very urgent to ensure proper security of the embedded systems to save it from any major technological disaster near future. In this paper, we have broadly discussed the structures, characteristics and applications of different embedded devices in our daily life. Beside this, we have also discussed about the different causes of security threats and some of our suggested solutions to protect the systems from the attackers as well that we have found in our research.*

KEYWORDS: *cryptography, firmware, hackers, microcontroller, real-time constraints*

I. INTRODUCTION

An embedded system can be defined as a special type of computer system that performs some specific pre-defined programs which is generally used within a larger scale of electrical or mechanical system. Generally, it is started from small MP3 players to largely complex hybrid vehicle systems. Some other examples of frequently used embedded systems in our daily life are keyboard, mouse, ATM, TV, PDA, cell phone, printer, elevator, smoke detector, DVD player, refrigerator, camera, GPS navigator, radio, TV remote, telephone, game controller, monitor, digital image processor, bar code reader, SD card, washing machine, anti-lock breaking system, blender etc. We use embedded systems especially because of its dependability, efficiency and it meets the real-time constrains.

Examples of the embedded system show that it has become a part and parcel of our daily life in term of use. We are very familiar with the term ‘Smart Home’ because of the deployment of smart embedded system in our home. Now-a-days almost all of the embedded systems are connected with the internet. So security threats have become a major issue at present because most of the embedded systems lack security even more than personal computers. One of the reasons for this lack of security is the very limited hardware and software implementation options for the manufacturers of embedded system companies. Again they have to deal with the competitive market price of the other embedded manufacturer companies because they all have to keep the lowest possible price to maintain the customer satisfaction and at the same time they do not conduct any specific security research of their manufactured embedded products. This leads to the security threats for the embedded devices because ensuring advance security techniques for embedded systems means the higher cost of that embedded products. Customers also don’t want to be more expensive usually when buying an embedded device and they are not concerned also about the probable security threats of their products. Lack of security analysis and low-cost market product mentalities of the manufacturer companies lead the hackers the exact environment they are expecting for. Many embedded systems hacking tools are easily available in the internet. Hacking in the PDAs and modems are very common example of embedded systems hacking.

Recent development trends of the embedded systems protocol are going to be convergence because of its applications in TCP/IP protocol for the purpose of inter-media interfacing. In this case, using IPv6 will cost much more for the development of the embedded applications at least for the next few years. As a result IPv4 is going to dominate in the applications of embedded systems. This IPv4 is much more challenging for its internal security problems in terms of authentication, integrity and confidentiality.

II. STRUCTURE, CHARACTERISTICS AND APPLICATIONS OF EMBEDDED SYSTEMS

Although there are many types of applications, the principle of the embedded device structures is typically the same in terms of system components and design methodologies. Complex applications such as chemical plants may need standard I/O (Input / Output) devices but this is not mandatory for the most of the other embedded systems. At present, most of the embedded systems are microcontroller based that means memory and other specific devices are integrated with the Central Processing Unit (CPU). In general it can be divided into three categories: small, medium and large. Small such as TV remote needs 4-bit microcontrollers. 8-bit or 16-bit microcontrollers are well enough for medium size systems such as automated data acquisition systems and 32-bit or more needed for the high–end large scale computer system such as plant monitoring and central control system.

Embedded systems are not standalone always rather than in the most of the time it is used as a part of a larger complex device. Here performance based real-time constrains must be met for the usability and safety of those devices. Graphical user interface is not always mandatory for the small scale device such as simple button or LED (Light Emitting Diode). But it is a must for the bigger and complex devices such as nuclear power plant systems along with the networks, data bus connections, screen-edge systems etc.

Figure 1: VIA VAB-800 10 cm x 7.2 cm Pico-ITX embedded ARM board

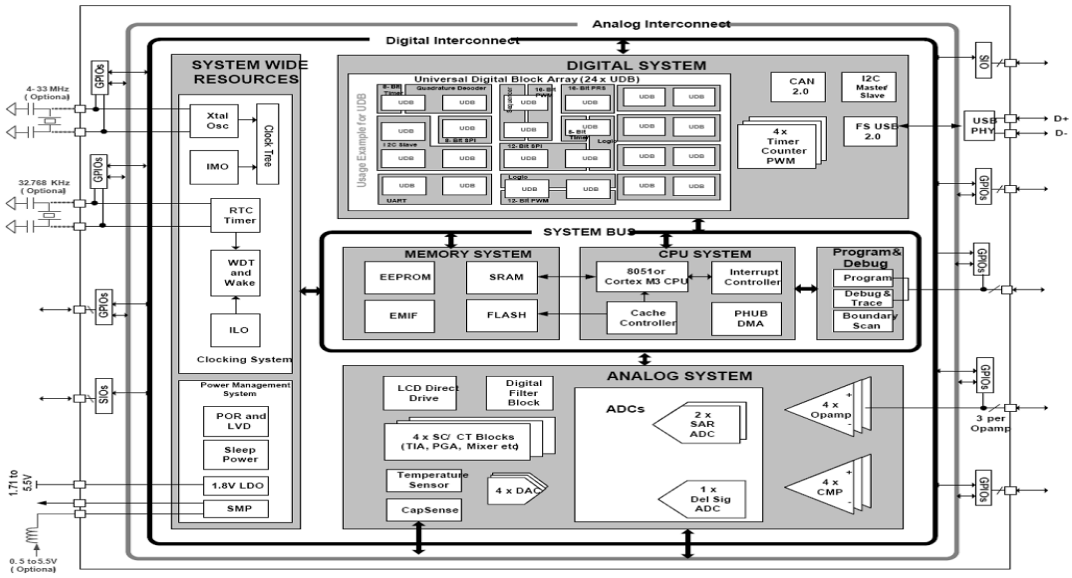

Figure 2: Block diagram of Cypress PSoC 5 (32-bit ARM Cortex-M3 processor) embedded ARM board

The term 'PSoC' stands for Programmable System on Chip. It is a programmable embedded design platform which integrates discrete, analog and programmable logic with a memory and a microcontroller. PSoC 5 is based on 32-bit ARM Cortex-M3 processor. It allows the designer to make flexible changes during design, validation and production. It is easy to reconfigure and implement using fewer system components. A single PSoC device can integrate about 100 peripheral functions. It also offers single-chip integration of multiple buttons, sliders, touch pads and proximity detectors with requiring no external components for sensing.

Characteristics of Embedded Systems:

In general, embedded systems are designed to perform any particular pre-defined task that must meet any real time constraint. The main difference between a computer and an embedded system is a computer is used to perform multiple tasks defined by the user. On the other hand, an embedded system is used to perform a specific task that is pre-defined by the manufacturers. Here, meeting all the real-time constraints is a very important characteristic of an embedded system. A real-time constraint is divided into two parts. One is hard real-time system and the other is soft real-time system. Hard real-time system means it must meet all its deadlines with a zero degree of flexibility and it is acceptable to be little flexible in the soft real-time system. It is not necessary to be standalone always for the embedded devices. Actually most of the embedded systems are integrated within a large computerized device. Devices such as MP3s, cameras and TV remotes are the example of standalone embedded devices. For the example of integrated embedded devices car and nuclear power plant are some good examples. GPS, fuel injection controller, anti-locking brake system, transmission controller, cruise control, active suspension, air- bag system, air-conditioner, display monitor-all the devices are integrated in a modern car system.

The term 'firmware' is used to refer the program instructions written for embedded systems. It is stored in ROM (Read Only Memory) or in a flash memory chip. Resources like computer hardware do not need much to run. Another important characteristic of embedded systems is the dedicated user interface. It may range from no user interface to complex graphical user interface. For simple button and LED system, no user interface is needed. User interface means the task of button can change with the on-screen display and the selection depends on the user. Handheld device such as joystick which needs to be pointed with the screen is a good example user interface system. Size and weight should be less for an embedded device. For that reason, microcontrollers are used in embedded devices to deliver the best performance on demand. Generally, microcontrollers are required to perform repeated functions for long time without any failure. Beside this, it must be reliable and safe in case of some special systems such as car's anti-locking brake system and nuclear power plant controlling systems. Adding to those characteristics, embedded systems must be cost efficient also. Manufacturer companies try to keep the lowest price of their products. Using sensors and actuators it may be also connected with physical environment.

Applications of Embedded Systems:

As we describes earlier, embedded systems have become parts and parcels of our daily life in term of use. From the following table we can easily understand our daily use of embedded systems.

Table 1: Examples of embedded systems used in our daily life

Home Applications	Dishwasher, Washing Machine, Microwave Oven, Top-set Box, Home Security Systems, HVAC system, DVD player, Answering Machine, Garden Sprinkler Systems, Lighting Systems, Remote Controls, Air Conditioners, Sprinklers.
Consumer Electronic Products	Cell phones, Cordless Phones, Digital Cameras, Video recorders, DVD players, TV set, Calculators, MP3 Players, Stereo Systems, Cable TV tuners, Digital watches, Personal PDA, iPhone.
Industrial applications	Personal Smart Phone, Fax Machines, Photo Copy Machines, Printers, Scanners, Assembly Line, Data Collection System, Monitoring Systems on Pressure, Voltage, Current, Temperature, Hazard Detecting System, Industrial Robot.
Business Equipment	ATM, Cash Registers, Alarm Systems, Card Readers, Finger Print Detectors, Automatic Toll Systems, Voice recognizers, Smart Vendor Machine, Cash Register, Bar Code Reader.
Automobile	GPS, Fuel Injection Controller, Anti-locking Brake System, Transmission Controller, Cruise Control, Active Suspension, Air- bag System, Air-Conditioner.
Communication Systems	Router, Hub, Cell Phone, Web Camera, Modem, Network Cards, Tele-conferencing System.
Aerospace	GPS system, Automatic Landing System, Flight Attitude Controller Inertial Guidance System, Space Robotics, RADAR.
Medical Technology	CT scanner, ECG, EEG, EMG, MRI, Glucose Monitor, Blood Pressure Monitor, Diagnostic Device, X-ray machines, Digital Pulse Monitor.
Security Systems	Face Recognition System, Finger Recognition, Irish Recognition, Building Security System, Airport Security System, Alarm System, Digital Access Card, Fingerprint based Smart Card.
Classroom applications	Smart Board, Smart Room, OCR, Calculator, Smart Cord, Stereo Systems, Projector.
Game and Entertainment	Video games, Robot, MP3, Mind Storm, Smart Toy.

III. CAUSES OF SECURITY THREATS OF EMBEDDED SYSTEMS

In this age of advanced technology, almost all of the embedded systems are connected to different network systems such as internet. At one side, these embedded devices are being more connected to our life day by day whereas on the other hand its security threats are also increasing as a proportional rate. Security threats in the embedded systems are not a new concept at all. As an example, in the year of 2001, Peter Shipley and Simson L. Garfinkel claimed that they have found an unprotected modem line to a system that could control a high voltage power transmission line. Internet enabled home applications are very available now. However the problem arises when internet connections expose applications to intrusions and malicious attacks. Some major causes of embedded system security threats are explained below:

One of the major limitations of embedded systems are they are very cost sensitive. A little change in cost can make a big difference in the case of heavy manufacture devices. This cost sensitivity leads manufactures to use4-bit processor or 8-bit processor. Bigger cryptographic key cannot be stored by many of these 8-bit microcontrollers. Embedded devices have to perform same task again and again usually by using loop. Here, speed can easily reach to 100 loops in every 5 seconds with strong real-time constraints. Therefore, a single delay of even 0.01 second can cause a loss of control loop stability which means the system can be vulnerable to attack that is designed to destroy the system timing. In the most of the time, embedded systems have no real administrator by which an internet connected device can be easily launched by distributed denial-of-service (DoS) attacks by the hackers. Many embedded systems are designed and developed by the small development teams even by the single engineer sometime. Organizations that write few kilobytes of code per year usually cannot afford any embedded system security specialist even they do not understand the importance the necessity of the security specialists as well.

There are many embedded systems that have significant battery constraints and powered by battery as well such as PDAs or cell phones. Some embedded systems can get fresh battery charge daily but other must last months or years depending on a single battery only. An attacker can create system failure by seeking to drain the battery especially when the security of the system is very high or almost impossible to break the security system of that particular device. This vulnerability is very much critical and worsens the security of the device. As an example, ensuring enough security in the battery-powered device is not easy at all that uses the power-hungry wireless communication system. Firmware is being completed day by day and will be more completed in near future. This will increase more bugs and other security problems. One reason may be the use of more popular programming languages such as C and C++ as they are very efficient for embedded systems. However they cannot protect against the simple kinds of attacks such as buffer overflows. Although small programs can be theoretically prove as safe but it is about impossible against complex programs.

IV. SOLUTIONS OF SECURITY THREATS IN EMBEDDED SYSTEMS

Security requirements of embedded devices can vary from different aspects. As an example of a cell phone system, end user may be concerned about his private data protection while content provider may be concerned about copy protection of the multimedia contents delivered to the cell phone and manufacturers may be concerned about the proprietary firmware that has been used in that cell phone. Here the system of attack may also vary for users, content providers, manufacturers etc. We have already described different challenges of embedded systems in term of security and in this section we will describe some probable solutions also to get rid of those problems also. Modern cryptography techniques provide strong defiance against the conventional attacks. However, much more effort and care is still required in the software design to make the system more protected from bugs and design flaws. Designers should be emphasizing more on Software Development Life Cycle (SDLC). Different secure level practices should be applied which can be classified into three. They are the design level, the implementation level and the testing level. Tamper-resistance techniques should be strengthening more to protect the system against different software and hardware attacks. These techniques can be used for attack detection, recovery and prevention as well.

To prevent side-channel attacks, different hardware and software level approaches have been proposed to identify symptoms that allow the leak of the system's side-channel information like power dissipation, timing and electromagnetic radiations. Software based countermeasures include randomization instruction sequence, introducing dummy instructions, bit splitting and balancing hamming weights of internal data. Randomization can also be applied on the clock signal or the power consumption. It has been experimented that software based countermeasures are most efficient although they slightly decrease the performance of cryptographic algorithm in terms of memory, energy and execution time.

Security solution in the architectural level should also be improved that means consider the mapping of adopted algorithms and protocols more efficiently. One solution to overcome the limitation of software based efficiency is to implement the resource-greedy cryptographic computations on a dedicated hardware using Application Specific Integrated Circuits (ASICs). Therefore 'hardwired algorithm' approach may be followed for its proven performance although it's costly.

Beside those solutions, some extra added modules such as SSL and SSH may also be implemented. It would be the best solution to protect many attacks such as denial of service (DoS) attack, spooling, hijacking and sniffing although implementation of such value added module is not mandatory because of the lacking of hardware resources available.

V. CONCLUSION

Embedded devices have made our life more easy and comfortable by meeting almost all the real-time constraints. Although it is very popular among the mass people but they are quite unconscious about the probable security threats till now even the manufactures and the engineers associated with embedded devices. Expert hackers from the different parts of the world have already found many security pitfalls of the embedded devices and they are further working on it. So, it is very clear that it could create a huge blow in near future for the technological industry if the engineers and the manufactures do not take the necessary security solutions as proposed in this paper to protect the unauthorized access from the unsecured third party. We heartily believe that more concentration on cryptography, tamper-resistance techniques, advanced microcontroller and algorithms can mostly make the embedded devices secure enough. At the same time, it is also important for the manufacturer companies to design and implement the whole embedded system with much more security concern.

REFERENCES

[1] Sudhakar Singh, Prashant Mor and Gajendra Singh, Application of Embedded Systems in Modern Society, VSRD International Journal of Electrical, Electronics & Communication Engineering, 2 (6), 2012, 373-384

[2] Jesús Lizarraga, Roberto Uribeetxeberria, Urko Zurutuza, Miguel Fernández, Security in Embedded Systems, Computer Science Department, Mondragon University, Spain

[3] Lyes Khelladi, Yacine Challal, Abdelmadjid Bouabdallah, and Nadjib Badache,On Security Issues in Embedded Systems: Challenges and Solutions, International Journal of Information and Computer Security, 2(2), 2008, 140-174

[4] James O. Hamblen, Introduction to Embedded Systems Using Windows Embedded CE, School of Electrical and Computer Engineering, Georgia Institute of Technology, USA, 2007

[5] Philip Koopman, Embedded System Security, Associate Professor,Department of Electrical and Computer Engineering, Carnegie Mellon University, 2004

[6] Bergman, P., Berman, S., The Criminal Law Handbook: Know Your Rights, Survive the System

[7] Paul Kocher, Ruby Lee, Gary McGraw, Anand Raghunathan and Srivaths Ravi, Security as a New Dimension in Embedded System Design, NEC Laboratories America, Princeton, NJ

[8] Bleichenbacher, D., and Nguyen, P. Q. 2000, Noisy polynomial interpolation and noisy Chinese remaindering. Advances in Cryptography, EUROCRYPT 2000

[9] Kaufman, C., Perlman, R., Speciner, M. Network Security: Private Communication in a Public World, Second Edition.

[10] Morrose, F., Reiter, M., and Wetzel, S (1999), Password hardening based on keystroke dynamics. ACM Conference on Computer and Communication Security

[11] National, R. C., (2002), Cyber Security Today and Tomorrow: Pay Now or Pay Later, National Academy Press, Washington, D.C.

[12] Massey, J. L. 1969, Shift register synthesis and bch decoding. IEEE Transactions on Information Theory vol. 15, no. 1, pp. 122-127

[13] Smeulders, AWM 2000, Content based image retrieval at the end of the early years', IEEE Transactions on pattern analysis and machine intelligence, pp. 1349-1380

[14] Phrack Magazine 2014, Hacking with Embedded Systems, www.phrack.org

[15] Embedded Insights Inc. 2012, Security and Encryption, www.embeddedinsights.com

[16] Embedded Systems, www.wikipedia.org

American Journal of Engineering Research (AJER)
e-ISSN : 2320-0847 p-ISSN : 2320-0936
Volume-03, Issue-12, pp-124-133
www.ajer.org
Research Paper Open Access

Evaluation of ultrasonic influence intensities providing formation of cavitation area in liquids with various rheological properties

R.N.Golykh[1], A.V. Shalunova[1], V.A. Nesterov[1], E.V. Ilchenko[1]
[1]*Biysk Technological Institute (branch) of Altai State Technical University named after I.I.Polzunov, Russia*

ABSTRACT: *The model of cavitation area containing cavitation bubbles ensemble in high-viscous and non-Newtonian (usually with a solid dispersed phase) liquids is presented in this article. Proposed model is based on the study of the cavitation bubbles ensemble as a whole but taking into account the main effects and phenomena occurring inside this ensemble. This model takes into account coalescence and breakup of bubbles due to collapsing. According to model, breakup and coalescence effects lead to concentration bubbles dependency on ultrasonic pressure amplitude or intensity. Thus, these effects affect on total energy of shock waves being generated by collapsing cavitation bubbles as well as bubble radius. The analysis of the model allows revealing optimum intensities of the ultrasonic influence, that are necessary to provide maximum total shock wave energy, at which, for example, the maximum degree of solid particle's destruction (maximum interphase surface contact) or maximum free surface "liquid-gas" due to formation and breakage of capillary waves (formed on liquid's free surface) is achieved. The analysis of the model lets evaluating, that optimum intensity of the influence for the most of liquids does not exceed 40 W/cm^2 at the frequency of 22 kHz. However for dilatant liquids intensity of influence can achieve 100 W/cm^2. Obtained results can be applied for the choice of power modes of the ultrasonic technological equipment to increase interphase surface under cavitation influence.*

KEYWORDS: *Cavitation, coalescence, dispersing, ultrasonic, viscosity*

I. INTRODUCTION

One of promising approach to increase interphase contact surface in systems "liquid-solid particles" and "liquid-gas" is an ultrasonic cavitation influence on liquid or liquid-dispersed media. This influence implements ultrasonic dispersing of solid particles in liquids or formation of capillary waves on liquid's free surface bounding between liquid and gas. The uniqueness and efficiency of the ultrasonic influence on liquid or liquid-dispersed media is determined by the formation of cavitation gas-and-steam bubbles, which accumulate energy at their extension during one of half-period of vibrations and generate shock waves and cumulative jets at their collapse during the other half-period of vibrations [1-3]. Cavitation influence helps to change structure and properties of substance and materials, increase interphase surface of the interaction in liquid-dispersed systems or surface "liquid-gas", realize the processes of dissolution, extraction, emulsification, etc.

However, most liquid-dispersed mediums are high-viscous or non-newtonian. Cavitation ultrasonic treatment of such media in practice cannot be realized owing to a number of reasons which are absence of scientific data on the influence of the modes, at which maximum total energy of shock waves causing dispersing of suspensions is achieved; necessity of high intensity of ultrasonic influence (more than 25 W/cm^2) to advance cavitation with maximum total energy of shock waves in high-viscous and non-linear viscous liquid-dispersed media. Stated problems do not allow designing ultrasonic equipment providing the productivity of ultrasonic cavitation dispersing (increasing of interphase surface between liquid and solid) in high-viscous and non-Newtonian liquid media, which is sufficient for industrial applications.

II. PROBLEM STATEMENT

To determine the modes of ultrasonic influence providing the formation of the cavitation area in processed liquids different in their properties it is necessary to develop the model, which takes into account both all the main effects and phenomena occurring inside the area, and allows analyzing cavitation area containing cavitation bubbles ensemble as a whole. The problem became more complicated, as in the most part of theoretical papers [3-6] directed to the development of scientific foundation of efficiency increase of ultrasonic

cavitation treatment of liquid or liquid-dispersed media it is considered the behaviour of single bubble in liquids, which viscosity does not depend on deformation rate (rate of shear). However, obtained results of studies cannot be applied to high-viscous and non-newtonian media, as they do not take into account following important factors:

[1] nonlinear character of the dependence of viscous stress forces on fluid velocity gradient preventing from the extension of cavitation pocket;

[2] changes of mean viscosity of processed medium after a time due to the influence of the processes of mixing and viscosity hysteresis leading to the decrease of threshold intensity, which is necessary for occurring of cavitation shock waves causing dispersing of solid particles.

Moreover the efficiency of cavitation influence defined by total shockwave energy of cavitation bubbles depends not only on the behaviour of single bubbles but also on the concentration of bubbles. This concentration due to the interaction of cavitation bubbles changes with a time and depends on the intensity of ultrasonic effect, that is proved by the results of the experimental studies carried out before.

Thus, complex studies of the process of the cavitation area formation should include:

[1] study of the behavior of single bubble to determine permissible regimes of the influence, at which collapse of cavitation bubble occurs and it does not degenerate into long-lived one. At that for the first time the presence of the dependence of liquid viscosity on the rate of shear and the relaxation of the viscosity as a result of the cycle of radial expansion and collapse of cavitation bubble are taken into consideration;

[2] study of the behavior of all bubbles ensemble taking into account their interaction, which determine energy characteristics of the area as a whole, and revealing of optimum modes of the interaction, at which total energy of bubble collapse is maximum. At this stage new approach based on revealing of stationary concentration of cavitation bubbles as a result of their breaking up and coalescence and determining of ultrasonic absorption coefficient in cavitating medium caused by expenditure of energy on the formation of cavitation can be used [7].

III. ANALYSIS OF THE DYNAMICS OF SINGLE BUBBLE FOR THE EVALUATION OF ALLOWABLE RANGE OF THE INTENSITIES OF ULTRASONIC EFFECT

The analysis of the dynamics of single bubble subject to the properties of liquid is in definition of functional dependence of cavitation bubble radius R on time *t*, amplitude of acoustic pressure *p* and rheological properties of liquid **P**:

$$R = f(t, p, \mathbf{P}).$$

Required functional dependence is defined on the base of the analysis of obtained equation of the dynamics of single bubble taking into account the dependence of liquid viscosity on the rate of shear:

$$R\frac{\partial^2 R}{\partial t^2} + \frac{3}{2}\left(\frac{\partial R}{\partial t}\right)^2 = \frac{p(R) - p_\infty}{\rho} + \frac{R^2}{\rho}\frac{\partial R}{\partial t}\int_R^\infty \frac{1}{r^3}\frac{\partial \varphi}{\partial r}\left(\sqrt{I_2}\right)dr \qquad (1)$$

where R is the instantaneous radius of the cavitation bubble, m; $p(R)$ is the liquid pressure near the walls of the cavitation bubble, Pa; p_∞ is the instantaneous value of the acoustic pressure, Pa; $\sqrt{I_2}$ is the Euclidean norm of deformation rate tensor, s^{-1}; φ is the certain function defined the dependence of liquid viscosity μ on rate of shear, Pa·s, at that $\mu = \frac{\varphi\left(\sqrt{I_2}\right)}{2}$; r is distance from bubble center, m.

Euclidean norm of deformation rate tensor is

$$\sqrt{I_2} = \sqrt{\sum_{i,j=1}^{3}\left(\frac{\frac{\partial u_i}{\partial x_j} + \frac{\partial u_j}{\partial x_i}}{2}\right)^2} = \sqrt{\left(R^2\frac{\partial R}{\partial t}\right)^2\frac{6}{r^6}}$$

where u_i (for $i = 1\ldots3$) are liquid velocity projections to Cartesian axes.

Equation (1) is obtained as a result of integration of the momentum conservation equation in differential form in the volume of liquid flowing around the cavitation bubble. Integrated equation of momentum conservation takes into consideration the presence of arbitrary dependence of the liquid viscosity on the rate of shear, which is Euclidean norm of the deformation rate tensor $\sqrt{I_2}$.

The function φ is defined by three parameters characterizing rheological properties of liquids: starting viscosity μ (Pa·s), consistency index *K* (Pa·s^{N+1}) and nonlinearity index *N*.

$$\phi\left(\sqrt{I_2}\right)=2\mu\left(1+\left(\frac{K}{2\mu}\right)^{\operatorname{sgn} N}\left(\sqrt{I_2}\right)^{|N|}\right)^{\operatorname{sgn} N}$$

This function was obtained by experimental data for liquid and liquid-dispersed mediums with different concentrations of solid particles.

As it is known, that surface tension of liquid lightly influences on the maximum radius of the bubble, it is possible not to take it into account at the analysis of the formation of cavitation area, it equals to 0.072 N/m, [1-3]. The density of the most liquids varies in the narrow range (900…1200 kg/m^3) and it does not influence greatly on the cavitation process. Therefore high emphasis is placed on the studies of the influence of rheological properties of liquid on optimum action modes. At that depending on the rheological properties of liquids they are divided into *linear-viscous* (the viscosity does not depend on the rate of shear), *pseudoplastic* (the viscosity decreases with the growth of the rate of shear) and *dilatant* (the viscosity increases with the growth of the rate of shear). Generally, dilatant liquids are suspensions with high-concentration (more than 30%) of solid particles. Obtained results are given for all three types of liquids. The analysis of the dynamics of single bubble allows determining of permissible range of intensities, in which it is necessary to realize ultrasonic influence depending on starting viscosity, consistency index K and nonlinearity index N of the liquids (see Fig.1).

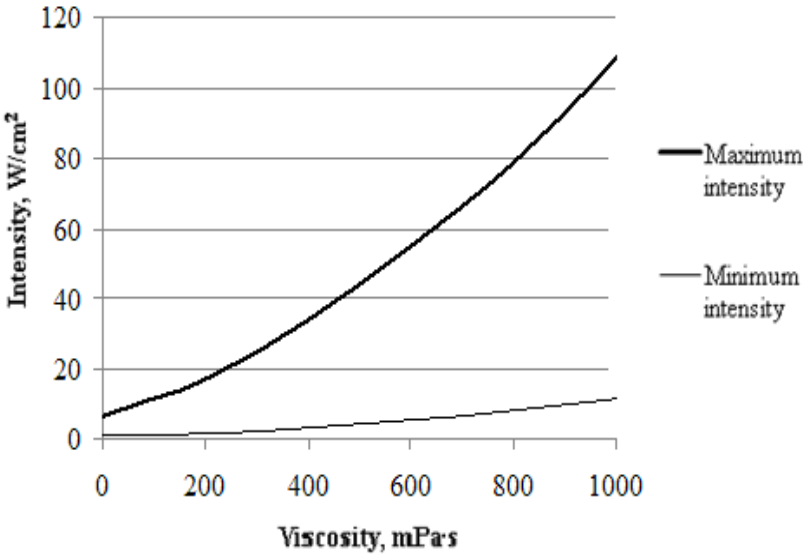

a) linear-viscous

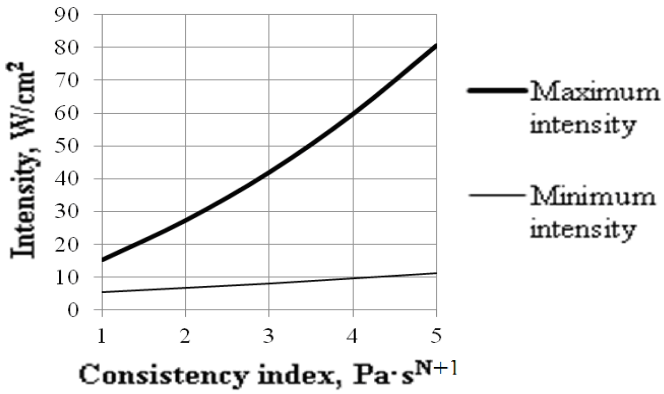

b) pseudoplastic (nonlinearity index N=-0.1, starting viscosity – 1 Pa·s)

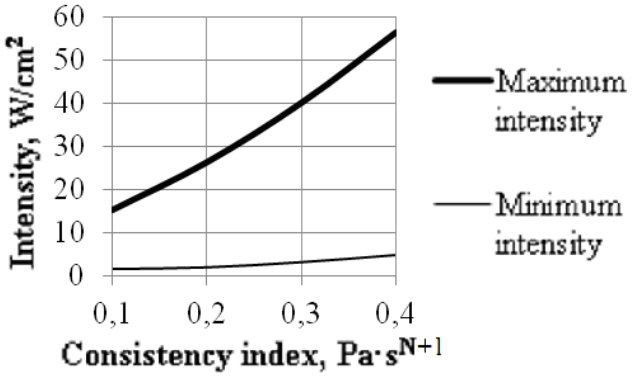

c) dilatant (nonlinearity index N = 0.15, starting viscosity 0.1 Pa·s)

Fig. 1. Dependencies of boundary intensities of influence on rheological properties of liquids

At minimum intensities determined by these dependences cavitation only begins to originate (the speed of bubble collapse achieves speed of sound in pure liquids), at maximum intensities bubble collapse does not occur (the absence of collapse during 3 periods of initial ultrasonic wave and more from the moment of initial expansion of the bubble). As it follows from presented dependences, the range of possible intensities can exceed 100 W/cm^2.Thus, theoretical analysis of the dynamics of the single bubble is insufficient for determination of optimum modes and conditions of the influence, as at boundary intensities the energy of shockwaves generated by the aggregates of bubbles is close to zero and consequently the efficiency of treatment will be insignificant.
It is evident, that in this range there is narrower range of optimum intensities, at which efficiency of cavitation causing dispersing of solid particles will be maximum. To determine this range of intensities it is necessary to study the formation of ensemble of cavitation bubbles, as the energy of cavitation influence is defined by total energy of shockwaves generated by each single cavitation bubble.

IV. ANALYSIS OF THE FORMATION OF BUBBLE ENSEMBLE FOR THE DEFINITION OF OPTIMUM INTENSITIES OF ULTRASONIC INFLUENCE

The analysis of cavitation bubbles ensemble is carried out in the range with characteristic dimensions L, which is much less than the length of the ultrasonic wave λ, but much more than the radius of the cavitation bubble R:

$$\lambda >> L >> R$$

It helps to define the dependence of the concentration $n(m^{-3})$ of the cavitation bubbles on the amplitude of acoustic pressure, time and rheological properties of the liquid **P**.

The dependences of the concentration of cavitation bubbles are determined on the base of the equation of the kinetics of breaking and coalescence of the bubbles given in [8]:

$$\frac{\partial n}{\partial t} = \frac{n(j-1)}{iT_0} - k_B n^2 \qquad (2)$$

where n is concentration of cavitation bubbles being depended on time t(s), m^{-3}; i is average count of cavitation bubble oscillations before its breakup; k_B is coalescence rate, м^3/с; T_0 is ultrasonic oscillations period, s; j is average number of nuclei formed after breakup of alone bubble.
Coalescence rate is defined by following expression:

$$k_B = \frac{S_{eff}\langle u \rangle}{2}$$

where S_{eff} is square of effective collision cross-section which is $S_{eff}=25\pi R_{MAX}^2$ (R_{MAX} is maximum bubble radius, m), m^2; $\langle u \rangle$ is average velocity of bubbles proximity, m/s.

$\langle u \rangle$ is defined by differential equations of bubbles motion given in [4].

Average number of nuclei (j) formed after breakup of alone bubble is defined by experimental data given in [3].Obtained bubbles concentration dependences on intensity and rheological properties of the liquid are shown in Fig. 2.

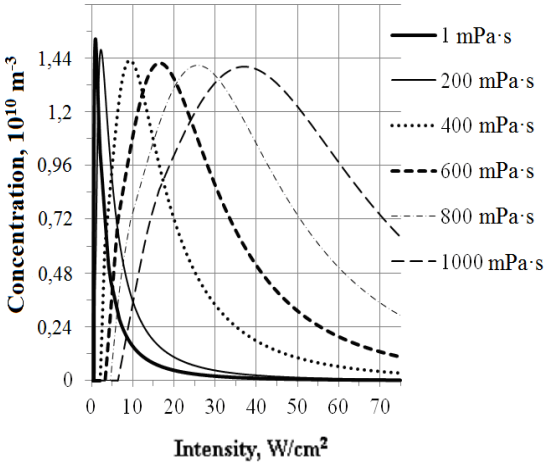

a) linear-viscous liquids

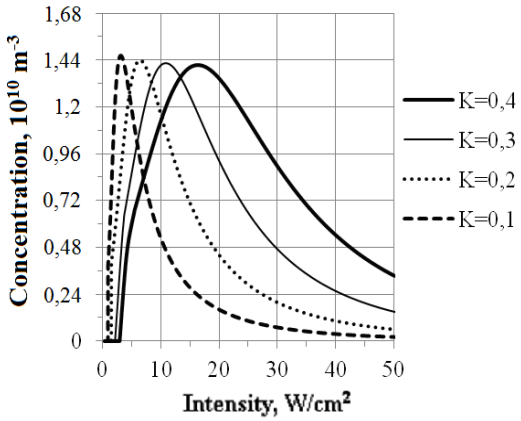

b) pseudoplastic with different consistency indices K, $Pa \cdot s^{N+1}$ (nonlinearity index N = 0.1, starting viscosity is 0.1 Pa·s)

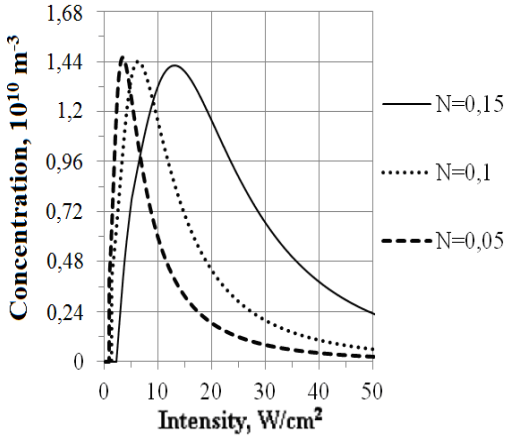

c) pseudoplastic with different nonlinearity indices N (consistency index K = 0.2 $Pa \cdot s^{N+1}$, starting viscosity is 0.1 Pa·s)

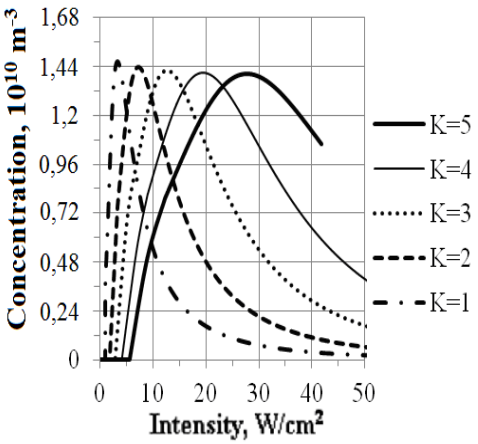

d) dilatant with different consistency indices K, $Pa \cdot s^{N+1}$ (nonlinearity index N = -0.1, starting viscosity is 1 Pa·s)

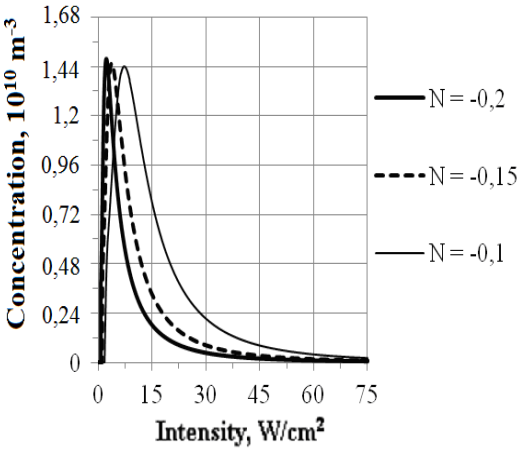

e) dilatant with different nonlinearity indices N (consistency index K = 2 $Pa \cdot s^{N+1}$, starting viscosity is 1 Pa·s)

Fig. 2. Dependences of bubbles concentration on the intensity of influence for the liquids with different rheological properties

These dependences were used for further definition absorption coefficient, which is in proportion to the total energy of shock waves and it is a measure of the efficiency of cavitation influence [9].At that the absorption coefficient in cavitating liquid is defined on the base of following obtained expression:

$$K_* = -\frac{\omega}{c_0}\,\mathrm{Im}\,\frac{\rho_0 c_0^{\,2}}{\overline{p_1}}\,\frac{\omega}{2\pi}\int_0^{\frac{2\pi}{\omega}}\frac{4}{3}\pi R^3(t)ne^{-i\omega t}\partial t$$

where $\overline{p_1}$ is complex amplitude of the 1st harmonics of the pressure (Pa), ω is the vibration frequency of the acoustic radiator in liquid medium, s^{-1}, ρ_0 is the steady-state density of liquid phase, kg/m^3, c_0 is the velocity of sound in pure liquid, m/sec; *n* is previously determined bubbles concentration, m^{-3}; *R(t)* is bubble momentum radius determined equation (1) for alone bubble dynamics. The dependences of the absorption coefficient on intensity of influence for the liquids with different rheological properties are given in Fig. 3.

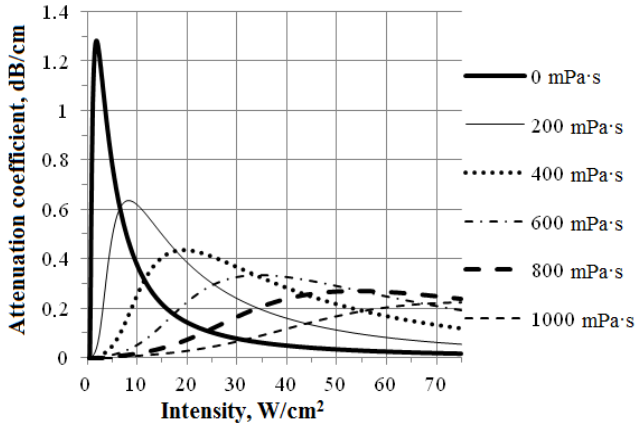

a) linear-viscous

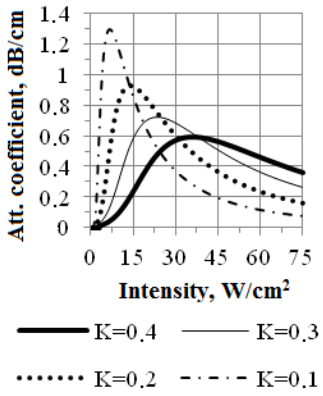

b) pseudoplastic with different consistency indices K, $Pa{\cdot}s^{N+1}$ (nonlinearity index N = 0.1, starting viscosity is 0.1 Pa·s)

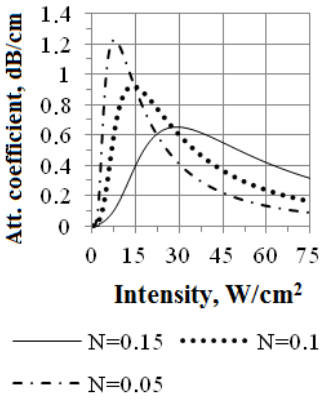

c) pseudoplastic with different nonlinearity indices N (consistency index K = 0.2 $Pa{\cdot}s^{N+1}$, starting viscosity is 0.1 Pa·s)

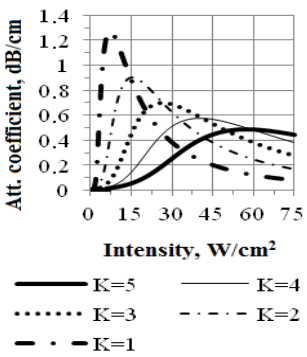

d) dilatant with different consistency indices K, Pa·s^{N+1} (nonlinearity index N = -0.1, starting viscosity is 1 Pa·s)

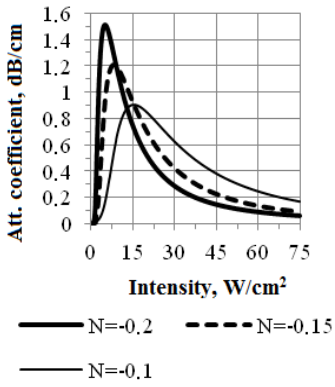

e) dilatant with different nonlinearity indices N (consistency index K = 2 Pa·s^{N+1}, starting viscosity is 1 Pa·s)

Fig. 3. Dependences of absorption coefficient on the intensity of influence for the liquids with different rheological properties

The dependence of the absorption coefficient on the intensity of influence has extreme character and maximum position determines optimum intensity of ultrasonic influence, as in this case maximum degree of energy transformation of initial ultrasonic wave into the energy of shock waves generated by cavitation bubbles is achieved. Thus, at optimum intensity maximum efficiency of ultrasonic cavitation influence is achieved. Dependences of minimum, maximum and optimum intensities of influence for linear-viscous liquids are shown in Fig.4.

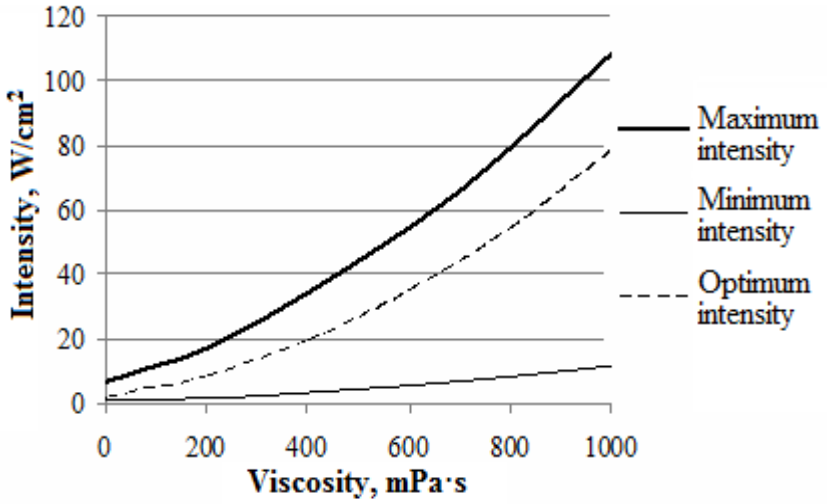

Fig. 4. Dependences of maximum, minimum and optimum intensities of influence for linear-viscous liquids

It should be noted, that in the case of nonlinear-viscous liquids the dependence of optimum intensity on the parameters characterizing their rheological properties lies in the certain range. It can be caused by the changes of their rheological properties due to the viscosity relaxation during the processing. The dependences of the range of optimum intensities for non-Newtonian liquids are shown in Fig. 5, 6. In Fig. 5 dependences for pseudoplastic liquids are shown.

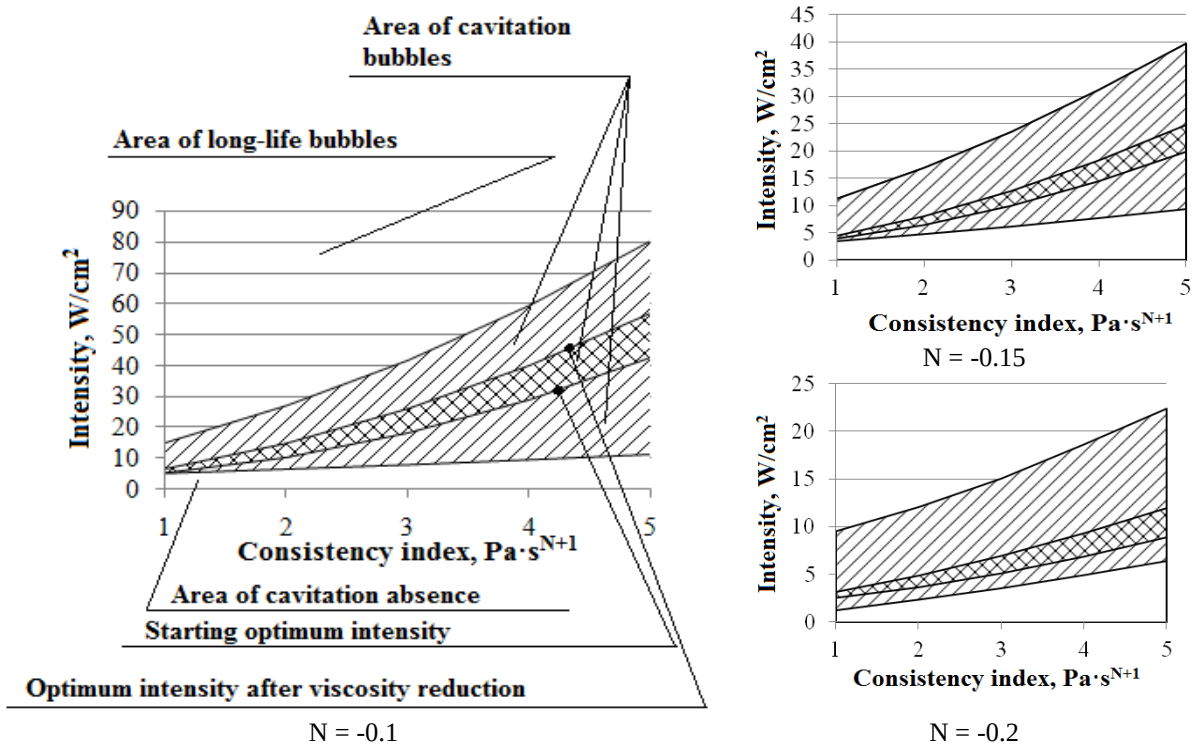

Fig. 5. Dependences of boundary intensities of influence on rheological properties of pseudoplastic liquids with different non-linearity indices

In Fig. 6 dependences for dilatant liquids are shown.

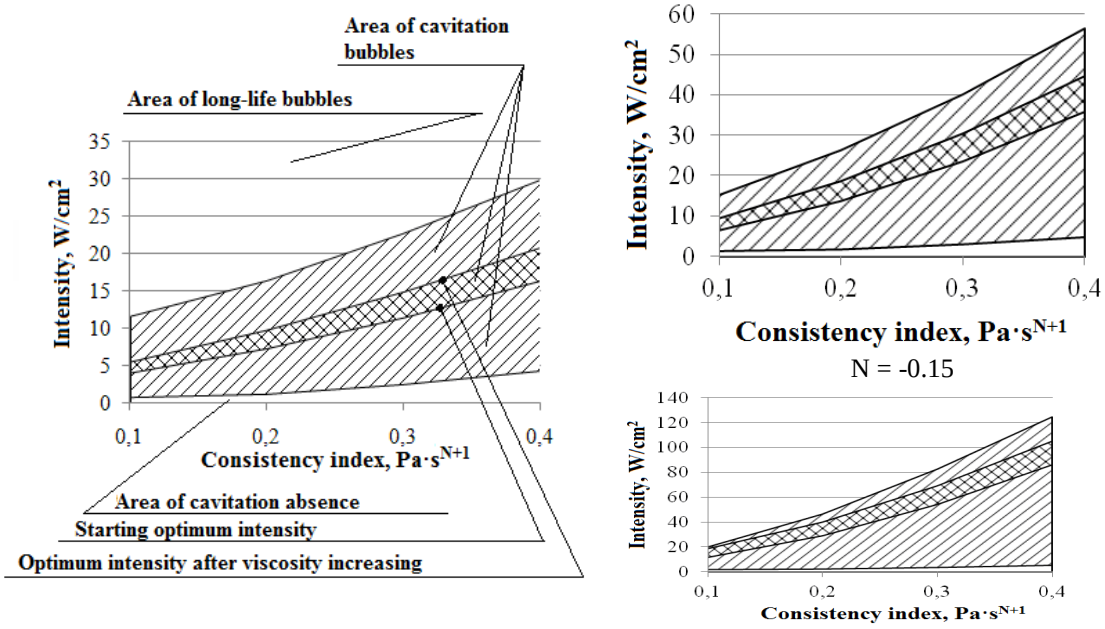

Fig. 6. Dependences of boundary intensities of influence on rheological properties of dilatant liquids with different non-linearity indices

As it follows from Fig.5 during the processing optimum intensity decreases in 5…20 W/cm^2 for pseudoplastic liquids, while for dilatant liquids (Fig. 6) intensity increases in 5…15 W/cm^2 due to the rise of their viscosity under the influence of ultrasound. It causes the necessity of adjustment of output power of the ultrasonic apparaus during the processing.

Table I shows the values of optimum intensities of influence and optimum amplitudes of radiator's vibrations for different liquids used in practice. The values given in the table were obtained with the application of the dependences presented in Fig.4-6.

Table I. The values of optimum intensities of influence for the liquids used in practice

Name of liquid	Starting viscosity, Pa·s	K, Pa·s^{N+1}	N	Optimum intensity, W/cm^2	Optimum amplitude, μm
Water	0.00082	0	0	1.73	0.7
Olive oil	0.085	0	0	4.51	1.7
Motor oil PMS-400	0.4	0	0	19.25	7.4
Glycerin	0.6	0	0	34.4	13.3
Epoxy resin ED-5	3	5	-0.15	19.95…24.77	7.7…9.6
Trifunctional oligoestercyclocarbonates on the base of propylene oxide	4	5	-0.2	11.92…23.4	4.6…9.03
Water-coal suspension (mass concentration 20%)	0.1	0.1	0.1	13.74…18.74	5.3…7.2

Presented results can be directly used for the choice of power operation modes of the ultrasonic equipment at known rheological properties of processed liquid or and liquid-dispersed medium.

V. CONCLUSION

During carried out researches for the first time we proposed the approach for the determination of optimum modes of ultrasonic influence based on the formation of cavitation area as a whole. At that developed model of the formation of cavitation area takes into consideration the main effects and phenomena occurring inside the area:

[1] coalescence of the bubbles at radial vibrations and breaking up at collapse;
[2] influence of the dependence of liquid viscosity on the rate of shear on the dynamics of the single bubble; viscosity relaxation of liquid with time under the action of cavitation.

It is shown that coalescence and breaking up of bubbles cause concentration bubbles dependency on ultrasonic intensity. This dependency may be explanation that optimum intensity at total collapse bubbles energy achieving maximum is exist. The analysis of the model allows revealing optimum intensities of ultrasonic influence, which is necessary for achieving of maximum total microscopic shock waves energy being generated in liquids with different rheological properties. It is determined, that optimum intensities of influence for the most of liquids used in practice do not exceed 40 W/cm^2. However, for dilatant liquids with the nonlinearity index of 0.15 and more the intensity of influence can achieve 100 W/cm^2. It is evident, that due to the viscosity relaxation the change of optimum intensity for non-newtonian liquids occurs in the course of time. The width of change range of the intensity achieves 20 W/cm^2. Obtained results can be applied for the definition of the intensity of ultrasonic influence providing maximum efficiency of liquid or liquid-dispersed medium treatment to increase interphase surface (for examples, dispersing of suspensions with solid particles or formation of capillary waves being broken into droplets on free surface "liquid-gas") with known rheological properties.

ACKNOWLEDGEMENTS

The reported study was supported by RFBR (Russian Foundation for Basic Research). Research Project No. 14-08-31716 mol_a.

REFERENCES

[1] V.N. Khmelev, R.N. Golykh, S.S. Khmelev, R.V. Barsukov, A.V. Shalunov, Modeling of cavitation area formation process in viscous liquids for evaluation of optimum treated volume and influence modes, *Tidings of high-educational institutions of Chernozem region, 4(22),* 2010. In Russian.

[2] V.N. Khmelev, R.N. Golykh, S.S. Khmelev, R.V. Barsukov, Method for Calculation of Optimum Intensity of Cavitation Influence on Viscous and Fine-dispersed Liquid Media, *Proc. 12th International Conference and Seminar on Micro / Nanotechnologies and Electron Devices. EDM'2011*, Novosibirsk, RU, 2011, 245-250.

[3] L.D. Rozenberg, *Powerful ultrasonic fields* (Moscow, RU: Science, 1968). In Russian.

[4] M.A. Margulis, *Sonochemical reactions and sonoluminescence* (Moscow, RU: Chemistry, 1986). In Russian.

[5] G. Flynn, Physics of acoustic cavitation in liquids, *Physical acoustics*, vol. 1, 1967. In Russian.

[6] R.W. Time, A. H. Rabenjafimanantsoa, Cavitation Bubble Regimes in Polymers and Viscous Fluids, *Annual transactions of the Nordic rheology society*, vol. 19, 2011.

[7] R.N. Golykh, V.N. Khmelev, S.S. Khmelev, Process Modeling of Cavitation Zone in Process Vessels with High-viscous and Fine-dispersed Liquid Media, *Proc. 12th International Conference and Seminar on Micro / Nanotechnologies and Electron Devices. EDM'2011*, Novosibirsk, RU, 2011, 251-256.

[8] M.A. Margulis, I.M. Margulis, Dynamics of bubbles ensemble in cavitating liquid, *Physical chemistry journal*, vol. 81, 12, 2007, 2290-2295. In Russian.

American Journal of Engineering Research (AJER)
e-ISSN : 2320-0847 p-ISSN : 2320-0936
Volume-03, Issue-12, pp-134-138
www.ajer.org
Research Paper Open Access

Analysis of Zr, Pb and Zn in Soil and Cereal Grown Around Birnin Gwari Artisanal Goldmine, Kaduna State- Nigeria

Abdullahi , M.A., Mohammed , S.S. and Aliu, S. O
Department of Applied science, College of Science and Technology, Kaduna Polytechnic, Kaduna- Nigeria.

ABSTRACT: *Energy Dispersive X-ray Fluorescence technique was used to Analysis the concentration of Zr, Pb and Zn in soil an cereal grown in farm lands around Birnin Gwari Artisanal Goldmine. The mean concentrations of Zr, Pb and Zn in soil are 446.33±5.94mg/kg, 20.83±3.31mg/kg and 61.82±4.88mg/kg respectively while the mean concentrations in maize are 6.51±0.69mg/kg, 11.61±1.14mg/kg and 102.34±3.94mg/kg for Zr, Pb and Zn respectively. The concentration of Zr in soil is higher across all sampling locations while for Pb and Zn the concentration is higher in soil in some locations and higher in maize in other locations. The results indicated that Pb and Zn have elevated concentration in maize which may cause health problem.*

KEYWORDS*: Soil, maize, X-ray fluorescence, concentration Zr, Pb and Zn.*

I. INTRODUCTION

In many developing countries like Nigeria, soils are affected by mine waste disposal, acid deposition, sewage sludge and other anthropogenic and agricultural activities. Heavy metal contamination of arable soils through industrial and anthropogenic activities is a serious problem in Nigeria. The impact of contamination on the environment should be of scientific concern in order to minimize the threat of soil and ground water contamination[1]. Studies have shown that the heavy metals are potentially toxic to crops, animals and humans when contaminated soils are used for crop production[2]. For example, Lead (Pb) affects every organ system in the body. It is absorbed into the body and distributed to the body soft tissue and bones. The central nervous system is the most vulnerable to lead toxicity particularly in developing children [3,4]. A case study is the lead poisoning that killed over 400 children in Zamfara State as a result of illegal mining activities[5]. The total heavy metal content in the soils provide a convenient means of expressing a measure of pollution.

Mining and industrial processing are among the main sources of heavy metal contamination in the environment. Mining activities, through milling operations coupled with grinding, concentrating ores and disposal of tailings, along with mill wastewater provide obvious sources of heavy metal contamination of the environment [6,7]. It is, therefore, not surprising that the degree and extent of heavy-metal pollution as a result of human activities has been one of the main topics studied in environmental geochemistry. Heavy metals can cause health problems at higher exposures and destroy aquatic organism when leached into water bodies [8,9]. Metals contamination in aquatic environmental has received huge concern due to their toxicity, abundance and persistence in the environmental and subsequent accumulation in the aquatic habitats [10] . Heavy metal residues in contaminated habitats may accumulate in microorganisms, aquatic flora and fauna, which in turn may enter the human food chain and result in health problems like the lead poisoning problems In this research, the concentration of heavy metals in cereals and soil samples were determined using Energy Dispersive X-Ray Fluorescence (EDXRF) spectrometric technique. The relation between the cereal and soil metal contents was also investigated.

II. MATERIALS AND METHOD

Sampling Location : A total of 80 samples were collected comprising of 40 soil samples and 40 maize samples from 3 mining communities of the study area which comprised of Kakani, Farin Ruwa and Tsoho Gwari. Global Positioning System (GPS) was used to determine the location of each farm where samples were collected. The position of each farm is shown in table 1 below.

Table 1: Sampling Coodinate

S.No	Place	No. sample	No.sample	N	E
1	Kakani				
	a.BG1	4	4		
	b.BG2	4	4	$11^0\ 11^{11}\ 23^1$	$06^0\ 59^{11}\ 15^1$
	c.BG3	4	4		
	d.BG4	4	4		
2	Farin Ruwa				
	Farin Ruwa1	4	4		
	BG5	4	4		
	Farin Ruwa2	4	4		
	BG6	4	4	$11^0\ 04^{11}\ 14^1$	$06^0\ 47^{11}\ 34^1$
	Farin Ruwa 3BG7				
	Farin Ruwa 4BG8				
3	Abuja				
	Abuja 1BG9	4	4	$10^0\ 59^{11}\ 19^1$	$06^0\ 48^{11}\ 31^1$
	Abuja 2BG10	4	4		

Samples Preparations : The soil samples collected were taken to the Laboratory of Mineral Resources Engineering Department of Kaduna Polytechnic where they were crushed and sieved separately to a tiny bits of 38µm (Kogo *et al.*, 2009). The crushed samples were then oven dried at about 100^0C to a constant weight. While the maize samples were taken to chemistry laboratory Kaduna Polytechnic where they were oven dried at 50^0C and also crushed to tiny bits. All the prepared samples were then taken to Nigerian Institute of Mining and Geosciences Jos Plateau State for XRF analysis using FXL-83358 model of XRF machine.

III. RESULTS AND DISCUSSION

The result of X-ray fluorescence analysis showing the concentrations in mg/kg of Zr, Pb and Zn in both soil and cereal (maize) are indicated in table 2-4 below.

Table 2: Concentration of Zr in Soil and Maize Samples

S/N	Locations	Concentration in (mg/kg)	
		Zr	
		Soil	Maize
1	BG 1	1408.53± 7.40	5.97 ± 0.67
2	BG 2	1332.75± 7.48	5.04 ± 0.66
3	BG 3	903.08± 6.63	7.09 ± 0.68
4	BG 4	707.43 ±5.40	6.28 ± 0.67
5	BG 5	805.01 ± 5.48	5.41 ± 0.69
6	BG 6	906.66 ± 5.91	6.09 ± 0.67
7	BG 7	580.78 ± 4.54	6.63 ± 0.69
8	BG 8	1083.14 ± 5.79	7.84 ± 0.73
9	BG 9	444.50 ± 4.08	7.88 ± 0.70
10	BG 10	1291.44± 6.64	6.86 ± 0.70
	Mean	446.33±5.94	6.51±0.69

Table 3: Concentration of Pb in Soil and Maize Samples

S/N	Locations	Concentration in (mg/kg)	
		Pb	
		Soil	Maize
1	BG 1	19.68 ± 3.33	5.90 ± 1.32
2	BG 2	16.00 ± 3.40	11.65 ± 1.51
3	BG 3	29.05 ± 4.51	ND
4	BG 4	36.39 ± 4.09	2.61 ±1.21
5	BG 5	23.47 ± 3.37	40.18 ± 2.28

6	BG 6	16.68 ± 3.10	ND
7	BG 7	11.35 ± 2.64	5.85 ± 1.36
8	BG 8	11.83 ± 2.49	ND
9	BG 9	22.36 ± 3.11	10.46 ± 1.51
10	BG 10	21.45 ± 3.10	39.46 ± 2.25
	Mean	20.83±3.31	11.61±1.14

Table 4. Concentration of Zn in Soil and Maize Samples

S/N	Locations	Concentration in (mg/kg)	
		Zn	
		Soil	Maize
1	BG 1	57.79 ± 5.29	17.99 ± 3.96
2	BG 2	66.12 ± 5.75	109.43± 3.94
3	BG 3	117.02 ± 7.52	45.19 ± 2.89
4	BG 4	116.03 ± 6.84	82.51 ± 3.56
5	BG 5	52.33 ± 4.97	297.90 ± 6.24
6	BG 6	44.41 ± 4.81	54.74 ± 3.07
7	BG 7	25.06 ± 3.99	54.74 ± 3.07
8	BG 8	44.83 ± 4.29	90.07 ± 3.88
9	BG 9	46.78 ± 4.67	100.39 ± 3.93
10	BG 10	47.82 ± 4.67	170.42 ± 4.89
	Mean	61.82±4.88	102.34±3.94

Zirconium (Zr) : Zr is a transition metal and was found in both the soil and maize samples in all the locations. The mean concentration of Zr in soil is 946.33±5.94mg/kg while the mean concentration in maize is 6.15±0.69mg/kg. The 95% confidence interval for the mean concentration of Zr was between(444.50±4.08 to 1408.53±7.40)mg/kg in soil and was between (5.97±0.67 to 7.88±0.70)mg/kg in maize. The concentration of Zr is more in soil than in maize in all locations as shown in Fig.1.

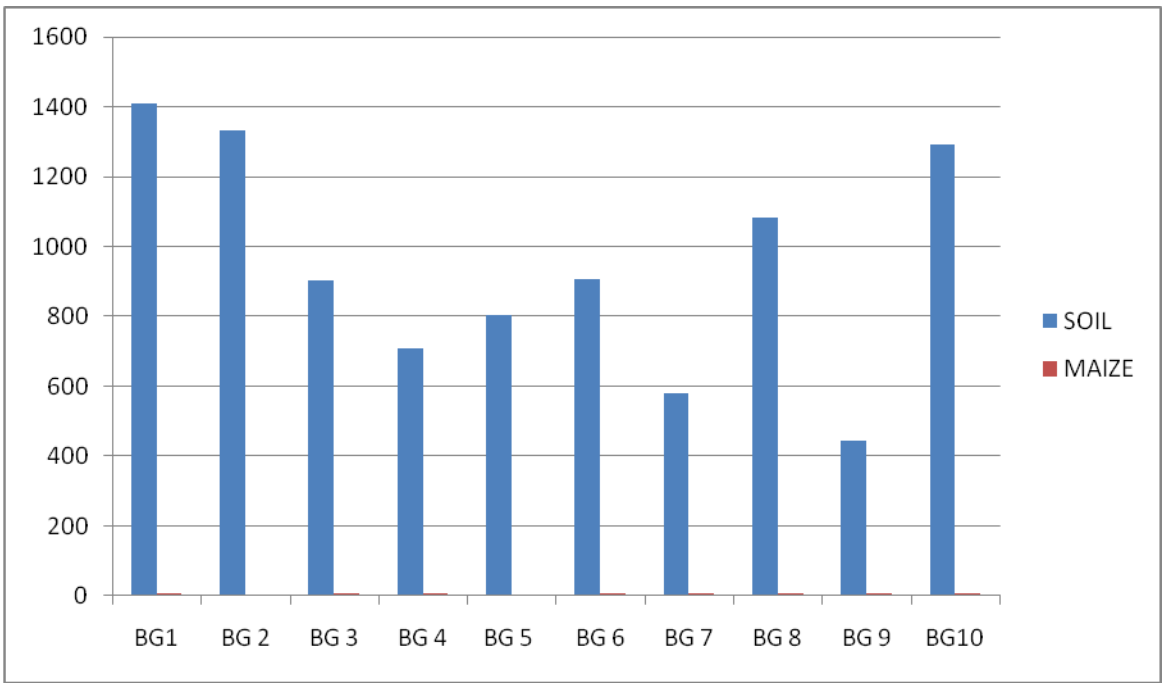

Fig 1 Plot of Concentration of Zr by location

Lead (Pb) : The result of analysis show that Pb is present in soil in all location while in 3 location Pb was not detected in maize. The mean concentration of Pb in soil sample is 20.83±3.31mg/kg while in maize the mean concentration is 11.61±1.14mg/kg. The 95% confidence interval indicated that the mean concentration of Pb in soil and maize lies between (11.35±2.64 to 36.39±4.09)mg/kg and(2.61±1.21 to39.46±2.25)mg/kg respectively. The concentration of Pb in soil is higher in8 locations while it is higher in maize in only 2 locations as shown in Fig.2.

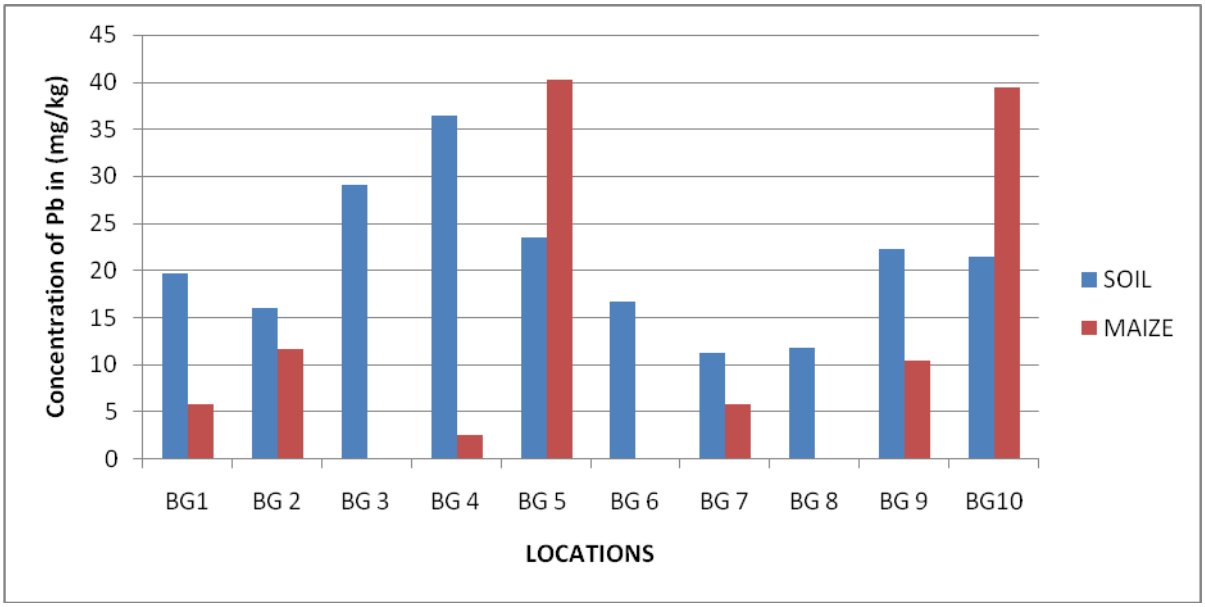

Fig 2 Plot of Concentration of Pb by location

Zinc (Zn)

The results show that Zn is present in both soil and maize. The mean concentration of Zn in soil is 61.82±4.88mg/kg while in maize the mean concentration is 102.34 ± 3.94mg/kg. The 95% confidence interval indicated that the mean concentration of Zn in soil and maize lies between (25.06±3.99 to 117.02±7.52mg/kg and (17.99 ± 3.96 to 297.90±6.24) mg/kg respectively. The concentration o Zn is higher in soil in only 3 locations while in the remaining 7 locations the concentration of Zn is higher in the maize samples as shown in Fig. 3.

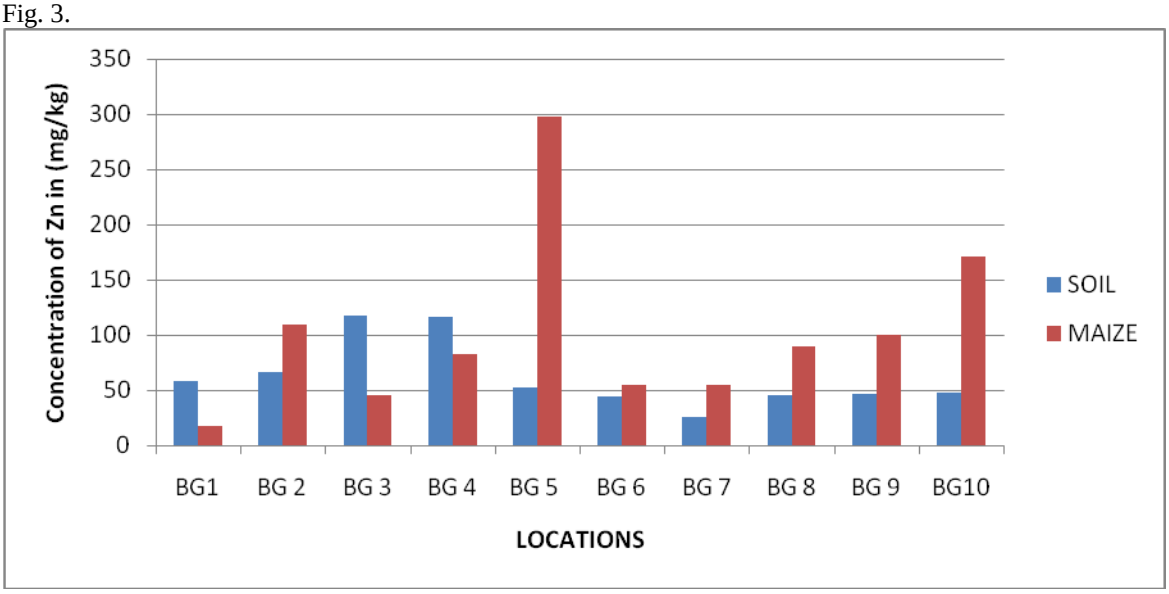

Fig. 3 Plot of Concentration of Zn by location

IV CONCLUSION

The concentration of Zr is higher in soil in all locations with mean values of 446.33±5.94mg/kg and 6.51±0.69mg/kg in soil an maize respectively. This shows that the accumulation of Zr by maize from the soil is only 1.45%. The mean concentration of Pb in soil and maize are 20.83±3.31mg/kg and 11.61±1.14mg/kg respectively with the concentration in soil being higher than in maize in 8 locations while the mean concentration of Zn in soil an maize are 61.82±4.88mg/kg an 102.34±3.94 mg/kg respectively unlike Zr and Pb the concentrations of Zn is higher in maize samples across 7 locations. The mean values obtained in this work for Zr is within the world average values in both soil and maize[11]. However, the mean values of Pb and Zn in soil are within the world average value but maize has elevated values of Pb and Zn which may cause health problem.

V ACKNOWLEDGEMENT

We sincerely wish to express our profound appreciation to Tertiary Education Trust Fund TETFUND for sponsoring this work.

REFERENCES

[1] Matos, A. T., M.P.F. Fontes, L.M. Costa and M.A. Martinez, 2001. Mobility of heavy metals as related to soil chemical and mineralogical characteristics of Brazilian soils. Environ. Pollut., 111: 429-435

[2] Xian, X., 1989. Response of Kidney bean to concentration and chemical from cadmium, zinc and lead polluted soils. Environ. Pollut., 57: 127-137.

[3] Berthelson, B.O, E. Steinnes, W. Solberg and L. Jingsen, 1995. Heavy-metal concentrations in plants in relation to atmospheric heavy-metal deposition. J. Environ. Qual., 24(5): 1018-1026.

[4] Yaman, M. and D. Yusuf, 2002. AAS Determination of cadmium in fruits and soils. Atom. Spectrosc., 23(2): 59-63.

[5] Galadima A and Garba Z N (2012). Heavy metal pollution in Nigeria; Causes and Consequences. *Elixir Pollution* **45** 7917-7922.

[6] Ayodele J.T and Mohammed, S.S. 2011.Zinc Speciation in maize and soils *Res. J. Chem. Sci.1(4), 98 – 108.*

[7] Kabala C and Singh B.R. 2001 Fractional mobility of copper, lead and zinc in soil profiles in the vicinity of a copper smelters. *J. Environ. Qual. 30 485 – 492.*

[8] Chroma T.M Ebewele, R.O and Hymore F.K. 2012 Level of Heavy metals (Cu, Zu, Pb Fe and Cr) in Bush green and Roselle irrigated with treated and untreated sewage water. *Int. Res. J. Envrionment Sci. 1(4), 50 – 55.*

[9] Abdullahi M.A Mohammed, S.S. and Mshelia M.S 2013. Distribution of Cr Zn and Pb in soil along the bank of River Kaduna Nigeria. *Int. Res. J. Environmental Sci. 2(7) 64 – 68.*

[10] Kogo, B.E. Gajere, E.N. Ogunmola J.K and Ogbole J.O (2009), Neutron Activation Analysis of Soil samples from different parts of Abuja metropolis *Middle -East J. Scientific Research* 4 (4) 254 - 262.

[11] U.S Environmental Protection Agency 1992 Ground\water issue. EPA/540/5-92/018

American Journal of Engineering Research (AJER)
e-ISSN : 2320-0847 p-ISSN : 2320-0936
Volume-03, Issue-12, pp-139-149
www.ajer.org
Research Paper Open Access

Theoretical Study Of The Interaction Of Cavitation Bubbles With The Interface "Liquid-Gas" Determining Optimum Modes Of Ultrasonic Effect To Increase The Surface Of The Phase Contact

R.N.Golykh[1], V.A. Nesterov[1], A.V. Shalunova[1], E.V. Ilchenko[1]
[1]*Biysk Technological Institute (branch) of Altai State Technical University named after I.I.Polzunov, Russia*

ABSTRACT: *The article describes the model of the interaction of the cavitation area formed upon influence of ultrasonic vibrations with the interface of gas and liquid phases. In the system "liquid-gas" studied in the frameworks of the model liquid spreads on some solid surface in the form of the film and it is in contact with gas medium. It is shown, that the interaction of cavitation bubbles with the interface of liquid and gas leads to the generation capillary waves and consequently to the increase of the surface of phase contact. The model analysis allows determining the modes of ultrasonic effect, which are necessary for maximum enlargement of interphase boundary area. It leads in turn to the increase of the rate of physic-chemical processes based on the surface interaction of dissimilar substances (absorption of gas mixtures both for cleaning and for separation of specific-purpose components, drying, wet cleaning of gases from dispersed admixtures, etc.). As a result of model analysis we determined threshold vibration amplitudes of solid surface covered with the film of liquid phase, which excess resulted in stability failure of capillary waves and their decomposition to liquid drops. It was shown, that the most efficient frequency of ultrasonic effect was 60 kHz, at which phase contact surface increased in more than 3 times.*

KEYWORDS : *Absorption, capillary waves, cavitation, liquid, ultrasonic*

I. INTRODUCTION

The rate of the most of physicochemical processes is limited by the interface of interacted substances or phases and also by the rate of agent introducing to this boundary. The most part of such processes occurs in two-phase system "liquid-gas". For instance in the systems "liquid-gas" following process such as wet gas cleaning from different dispersed admixtures, absorption of gas mixtures both for their cleaning and for separation of specific-purpose components, drying of the materials and others can be realized. It is evident, that for maximum efficiency of mentioned above processes first of all it is necessary to provide large area of contact surface of liquid and gas phases. In existing chemical engineering apparatuses (absorbers, wet dust collectors, dryers) specific interface area (for the mass unit) required for the industrial realization of physic-chemical processes at the interface can be achieved by the following ways:

a. liquid is sprayed during gas phase in the form of small drops;
b. liquid spreads on the surface of the solids as a film (the thickness is no more than 5 mm) and contacts gas medium.

The first variant has limited application, as for its realization there is a need in good reciprocal solubility of interacted phases (for instance, solubility of gas in the absorbent). In this paper we mainly consider the second variant.However the second method is characterized by insufficient interface area for industrial realization of physic-chemical processes, which is required higher power inputs. One of the promising method of the increase of phase contact surface is the influence by microscopic shock waves leading to the generation of the profile disturbance of interface "liquid-gas" (capillary waves) of small length (no more than 200 μm). The appearance of shock waves can be provided due to the generation of periodically expanding and collapsing cavitation bubbles in liquid phase.

It is known, that the most advantageous method [1, 2] of creation of cavitation bubbles is the introduction ultrasonic vibrations into liquid phase with the frequency of 20…60 kHz. Ultrasonic influence can be carried out by excitation of mechanical vibrations of the solid surface, on which liquid film spreads. It is necessary to develop theoretical model allowing to determine optimum modes of ultra-sonic effect (amplitude and vibration frequency of the solid surface), which provides maximum interface area "liquid-gas". There is a need to study in details the interaction of shock waves of cavitation bubbles with the surface of phase contact.

For a long time the development of the theories of the interaction of shock waves of cavitation bubbles with the interface had some mathematical difficulties, as there was no correct solution of the equations of the hydrodynamics of supersonic liquid flow streaming cavitation bubble. At the beginning of 20th century foreign scientists (B.E. Nolting, E.A. Neppiras, H.G. Flynn, J.G. Kirkwood, H.A. Bethe) [3-5] gave basic theoretical descriptions of the growth and pulsation of the cavitation cavity (bubble). These descriptions are equations of radial vibrations of the bubble, which take into account possible factors influencing the dynamics of the cavitation cavity including compressibility of liquid and change of its wave properties at the supersonic flow. These equations are non-linear differential equations of second order relative to the radius of the bubble, which is a function on time. It was stated, that the bubble retained its spherical form during the cycle of expanding and collapsing, and it was assumed, that shock wave had spherically divergent character. Such assumption does not allow explaining experimentally observed the generation of capillary waves of small length (no more than 200 μm) at the interface "liquid-gas".

However, as it was mentioned above in these processes, liquid spread on solid surface as a film. The thickness of the film does not exceed 5 mm [6], solid surface reflects shock waves. Reflecting phenomena break the sphericity of cavitation bubbles at their collapse [7]. This sphericity failure narrows the diagram of shock wave directivity, and this fact explains the generation of capillary waves of small length (no more than 200 μm). Stated factor should be taken into consideration at theoretical studies of the interaction of cavitation bubbles with the interface "liquid-gas". Thus, the aim of the paper is to develop the mathematical model of the interaction of cavitation bubbles with the interface "liquid-gas" for the determination of the modes of ultrasonic effect providing maximum surface area of phase contact. The model includes following stages of the generation of capillary waves on the interface "liquid-gas" under the action of ultrasonic cavitation:

[1] expansion of cavitation bubble up to maximum radius, which is spherically symmetric due to the low speed of its walls (no more than 15 m/s);
[2] asymmetric collapse of the cavitation bubble from maximum radius to minimum size;
[3] generation and propagation of narrow directional shock wave in the thin liquid film at the collapse of the cavitation bubble;
[4] formation of capillary waves on interface "liquid-gas". In this stage capillary waves profile is determined and square of the interface "liquid-gas" is calculated.

Further proposed model is described.

II. MODEL OF INTERACTION BETWEEN CAVITATION BUBBLES

Theoretical study of the process is carried out according to the scheme shown in Fig. 1.

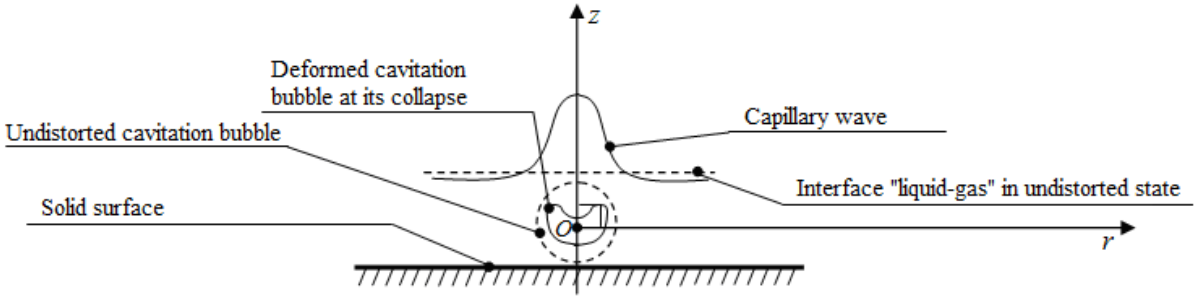

Fig. 1. Scheme of theoretical study of the interaction between cavitation bubbles and interface "liquid-gas"

At the *stage of cavitation bubble expansion* its maximum radius R_{MAX} and center z location relative to the solid surface are determined. At this stage it is assumed that:

[1] expansion of the bubble is spherically symmetric, which is caused by low speed of walls motion, however the bubble center vertically moves relative to the solid surface in the course of time;
[2] in initial time the center of the cavitation bubble is located near the solid surface, as such bubbles mostly influence on the formation of capillary wave.

Maximum radius of the bubble R_{MAX} is defined on the base of Nolting-Neppiras equation [3]:

$$\rho\left(\frac{3}{2}\left(\frac{\partial R}{\partial t}\right)^2+R\frac{\partial^2 R}{\partial t^2}\right)=-4\mu\frac{\frac{\partial R}{\partial t}}{R}+p_V+\left(p_0+\frac{2\sigma}{R_0}\right)\left(\frac{R_0}{R}\right)^{3\gamma}-p_0+4\pi^2 f^2\rho Ah\sin(2\pi ft)$$

where R is the instantaneous radius of the cavitation bubble, m; R_0 is the radius of cavitation nucleus, m; σ is the liquid surface tension, N/m; ρ is the density of liquid, kg/m^3; p_0 is the static pressure in liquid, Pa; f is the frequency of ultrasonic action, Hz; h is the thickness of liquid film, m; A is the amplitude of ultrasonic action, m; p_V is the pressure of saturated vapor of liquid, Pa; t is the time, s; μ is the dynamic viscosity of liquid, Pa·s.

The distance between the center of the cavitation bubble (at the moment of maximum expansion) and the solid surface is defined from the equation given in Rozhdestvenskiy's paper [8]:

$$6b^2\frac{\partial b}{\partial t}\frac{\partial R}{\partial t}+2b^2R\frac{\partial^2 b}{\partial t^2}+3R^2\left(\frac{\partial R}{\partial t}\right)^2=0$$

where b is the distance between the center of the cavitation bubble and the solid surface, m.

Obtained values of maximum bubble radius and the distance between its center and the solid surface are used for theoretical studies of further stages of the capillary wave formation.
During the study of the stage of cavitation bubble collapse its form in the moment of the minimum size is determined.
The form of the cavitation bubble is defined from the integral equation (1) with boundary conditions (2, 3) on the wall of the cavitation bubble for liquid velocity potential and entry conditions (4, 5) on cavitation bubble wall:

$$\frac{\varphi(\mathbf{r}_0)}{2}=\int\limits_{S_A\cup S_B}\left(E_{\mathbf{r}_0}V_{\mathbf{n}}-\frac{\partial E_{\mathbf{r}_0}}{\partial\mathbf{n}}\varphi\right)\partial S \tag{1}$$

$$\frac{\partial\varphi}{\partial t}+\frac{|V_{\mathbf{n}}|^2+|V_{\boldsymbol{\tau}}|^2}{2}=\frac{2\sigma K}{\rho}-\frac{p_{\text{п}}}{\rho}\left(\frac{3V}{4\pi R_{MAX}{}^3}\right)^{\gamma} \tag{2}$$

$$\nabla\varphi=\frac{\partial\mathbf{r}}{\partial t} \tag{3}$$

$$\varphi\big|_{t=0}=0 \tag{4}$$

$$|\mathbf{r}|\big|_{t=0}=R_{MAX} \tag{5}$$

where $\mathbf{r}_0$, $\mathbf{r}$ are the vectors of the coordinates of the points of the wall of the cavitation bubble or solid surface, m; φ is the fluid velocity potential on the wall of the cavitation bubble or solid surface, m^2/s; $V_{\mathbf{n}}$ and $V_{\boldsymbol{\tau}}$ are the normal and tangential components of fluid velocity, m/s; $E_{r_0}(\mathbf{r})$ is the fundamental solution of Laplace's equation; V is the volume of the cavitation bubble, m^3; p_n is the pressure of saturated vapor of fluid, ρ and σ are the density (kg/m^3) and surface tension (N/m) of fluid, respectively; K is the mean curvature of the walls of the cavitation bubble, m^{-1}; S_A is the wall of the cavitation bubble; S_B is the solid surface on which V_n is equal 0.

With the help of system of equations (1-5) we calculate deformation of the walls of the cavitation bubble in the course of time. Entry conditions (3-5) being a part of the system (1-5) is determined by the bubble radius and the position of its center at the moment of maximum expansion, which were found at the previous stage of the model study. Integral equation (1) aimed at the determination of distribution of fluid velocity potential on the walls of the cavitation bubble is solved by the boundary element method. For this purpose the discretization of the cavitation bubble wall into ring elements is carried out, as it is shown in Fig. 2.

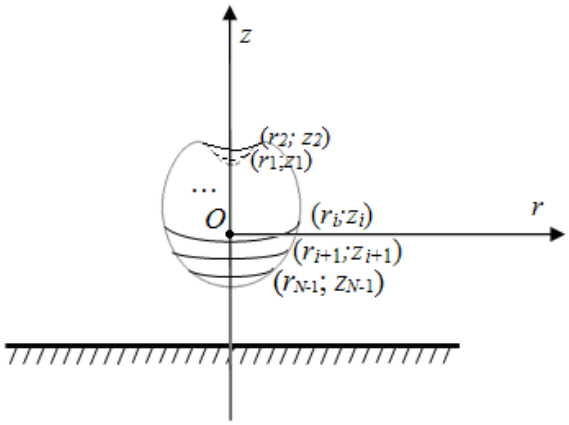

Fig. 2. Discretization of the cavitation bubble wall into ring boundary elements

It is assumed, that in the frameworks of each ring element the velocity potential is constant. It allows solving boundary integral equation (1) as a system of linear equations (6). This system is obtained by using method of "images" (replacing solid surface by symmetrically placed cavitation bubble).

$$\{A_{ij}\}_{i,\,j=1\ldots 2N}\begin{Bmatrix} V_n^{(1)} \\ V_n^{(2)} \\ \ldots \\ V_n^{(N-1)} \\ V_n^{(N)} \\ V_n^{(1)} \\ V_n^{(2)} \\ \ldots \\ V_n^{(N-1)} \\ V_n^{(N)} \end{Bmatrix} = \{b_i\}_{i=1\ldots 2N} \tag{6}$$

where $\{A_{ij}\}$ is the matrix of linear system; $V_n^{(i)}$ is normal velocity on i-th bubble wall boundary item with coordinates $(r_i; z_i)$ and $(r_{i+1}; z_{i+1})$; $\{b_i\}$ is right part of system; N is count of boundary items;

The coefficients of the system of linear equations (A_{ij} and b_i) are defined by the following obtained expressions:

$$b_{i+pN} = \frac{\varphi_{\max(i-1;1)} + \varphi_{\min(i,N-1)}}{4} + \\ + \sum_{q=0}^{1}\sum_{j=1}^{N}\frac{\varphi_{\max(j-1;1)} + \varphi_{\min(j,N-1)}}{2} J\left(\begin{pmatrix} r_{j-1} \\ (1-2q)z_{j-1} - 2qb_0 \end{pmatrix}, \begin{pmatrix} r_j \\ (1-2q)z_j - 2qb_0 \end{pmatrix}, \right. \\ \left. \frac{\begin{pmatrix} r_i + r_{i-1} \\ (1-2p)(z_i + z_{i-1}) - 2pb_0 \end{pmatrix}}{2}, \frac{\begin{pmatrix} z_j - z_{j-1} \\ (1-2q)(r_j - r_{j-1}) \end{pmatrix}}{\sqrt{(r_j - r_{j-1})^2 + (z_j - z_{j-1})^2}}\right) \tag{7}$$

$$\{A_{(i+pN)(j+qN)}\} = \delta_{ij}\delta_{pq} I_0\left(\begin{pmatrix} r_{j-1} \\ (1-2q)z_{j-1} - 2qb_0 \end{pmatrix}, \begin{pmatrix} r_j \\ (1-2q)z_j - 2qb_0 \end{pmatrix}\right) + (1 - \delta_{ij}\delta_{pq}) \times \\ \times I\left(\begin{pmatrix} r_{j-1} \\ (1-2q)z_{j-1} - 2qb_0 \end{pmatrix}, \begin{pmatrix} r_j \\ (1-2q)z_j - 2qb_0 \end{pmatrix}, \frac{1}{2}\begin{pmatrix} r_i + r_{i-1} \\ (1-2p)(z_i + z_{i-1}) - 2pb_0 \end{pmatrix}\right) \tag{8}$$

where I_0, J, I are integrals over on each boundary item; b_0 is starting distance (at maximum bubble expansion) between bubble center and solid surface, m.

In expressions (7-8) it is mentioned that following equalities are true:

$$\begin{pmatrix} r_0 \\ z_0 \end{pmatrix} = \begin{pmatrix} r_1 \\ z_1 \end{pmatrix}$$

$$\begin{pmatrix} r_N \\ z_N \end{pmatrix} = \begin{pmatrix} r_{N-1} \\ z_{N-1} \end{pmatrix}$$

Integrals I_0, J, I are defined as follows (9-11):

$$J(\mathbf{r}_1,\mathbf{r}_2,\mathbf{r}_0,\mathbf{n}) = v.p.\int_0^{2\pi}\left([r_1 - r_0\cos\varphi]n_r + (z_1 - z_0)n_z\right)\times$$

$$\times\left(-\frac{r_2 - r_1}{4\pi l^2}\frac{1}{\sqrt{t^2 - \frac{(\mathbf{r}_1 - \mathbf{l}_\varphi,\mathbf{l})^2}{l^4} + \frac{l_1^2 + l_0^2 - 2(\mathbf{r}_1,\mathbf{l}_\varphi)}{l^2}}}\right|_{t=\frac{(\mathbf{r}_1-\mathbf{l}_\varphi,\mathbf{l})}{l^2}}^{t=1+\frac{(\mathbf{r}_1-\mathbf{l}_\varphi,\mathbf{l})}{l^2}} +$$

$$+\frac{r_1 - \frac{(\mathbf{r}_1 - \mathbf{l}_\varphi,\mathbf{l})}{l^2}(r_2 - r_1)}{4\pi l^2\left(-\frac{(\mathbf{r}_1 - \mathbf{l}_\varphi,\mathbf{l})^2}{l^4} + \frac{l_1^2 + l_0^2 - 2(\mathbf{r}_1,\mathbf{l}_\varphi)}{l^2}\right)}\times \tag{9}$$

$$\times\frac{t}{\sqrt{t^2 - \frac{(\mathbf{r}_1 - \mathbf{l}_\varphi,\mathbf{l})^2}{l^4} + \frac{l_1^2 + l_0^2 - 2(\mathbf{r}_1,\mathbf{l}_\varphi)}{l^2}}}\Bigg|_{t=\frac{(\mathbf{r}_1-\mathbf{l}_\varphi,\mathbf{l})}{l^2}}^{t=1+\frac{(\mathbf{r}_1-\mathbf{l}_\varphi,\mathbf{l})}{l^2}}\Bigg)\partial\varphi$$

$$I(\mathbf{r}_1,\mathbf{r}_2,\mathbf{r}_0) = -\frac{1}{4\pi}\int_0^{2\pi}\left(\ln\left|\frac{\sqrt{l^2 + 2(\mathbf{r}_1 - \mathbf{l}_\varphi,\mathbf{l}) + l_1^2 + l_0^2 - 2(\mathbf{r}_1,\mathbf{l}_\varphi)} + l + \left(\mathbf{r}_1 - \mathbf{l}_\varphi,\frac{\mathbf{l}}{l}\right)}{\sqrt{l_1^2 + l_0^2 - 2(\mathbf{r}_1,\mathbf{l}_\varphi)} + \left(\mathbf{r}_1 - \mathbf{l}_\varphi,\frac{\mathbf{l}}{l}\right)}\right|\times\right.$$

$$\left.\times\left(r_1 - (r_2 - r_1)\frac{(\mathbf{r}_1 - \mathbf{l}_\varphi,\mathbf{l})}{l^2}\right) + \right. \tag{10}$$

$$\left. + (r_2 - r_1)\left(\sqrt{1 + 2\frac{(\mathbf{r}_1 - \mathbf{l}_\varphi,\mathbf{l})}{l^2} + \frac{l_1^2 + l_0^2 - 2(\mathbf{r}_1,\mathbf{l}_\varphi)}{l^2}} - \sqrt{\frac{l_1^2 + l_0^2 - 2(\mathbf{r}_1,\mathbf{l}_\varphi)}{l^2}}\right)\right)\partial\varphi$$

$$I_0(\mathbf{r}_1,\mathbf{r}_2) = -\frac{1}{2\pi}\lim_{\varepsilon\to 0+}\int_\varepsilon^\pi\left(\ln\left|\frac{\sqrt{l^2 + 2(\mathbf{r}_1 - \mathbf{l}_{0\varphi},\mathbf{l}) + l_1^2 + \frac{(r_1 + r_2)^2 + (z_1 + z_2)^2}{4} - 2(\mathbf{r}_1,\mathbf{l}_{0\varphi})} + l + \left(\mathbf{r}_1 - \mathbf{l}_{0\varphi},\frac{\mathbf{l}}{l}\right)}{\sqrt{l_1^2 + \frac{(r_1 + r_2)^2 + (z_1 + z_2)^2}{4} - 2(\mathbf{r}_1,\mathbf{l}_{0\varphi})} + \left(\mathbf{r}_1 - \mathbf{l}_{0\varphi},\frac{\mathbf{l}}{l}\right)}\right|\times\right.$$

$$\left.\times\left(r_1 - (r_2 - r_1)\frac{(\mathbf{r}_1 - \mathbf{l}_{0\varphi},\mathbf{l})}{l^2}\right) + \right. \tag{11}$$

$$\left. + (r_2 - r_1)\left(\sqrt{2\frac{(\mathbf{r}_1 - \mathbf{l}_{0\varphi},\mathbf{l})}{l^2} + \frac{l^2 + l_1^2 + \frac{(r_1 + r_2)^2 + (z_1 + z_2)^2}{4} - 2(\mathbf{r}_1,\mathbf{l}_{0\varphi})}{l^2}} - \right.\right.$$

$$\left.\left. - \sqrt{\frac{l_1^2 + \frac{(r_1 + r_2)^2 + (z_1 + z_2)^2}{4} - 2(\mathbf{r}_1,\mathbf{l}_{0\varphi})}{l^2}}\right)\right)\partial\varphi$$

where r_1, r_2, r_0 are vectors of coordinates $\mathbf{r}_1 = \begin{pmatrix} r_1 \\ z_1 \end{pmatrix}; \mathbf{r}_2 = \begin{pmatrix} r_2 \\ z_2 \end{pmatrix}; \mathbf{r}_0 = \begin{pmatrix} r_0 \\ z_0 \end{pmatrix}$; $\mathbf{n}$ is vector of normal $\mathbf{n} = \begin{pmatrix} n_r \\ n_z \end{pmatrix}$;

$\mathbf{l}_\varphi = \begin{pmatrix} r_0 \cos\varphi \\ z_0 \end{pmatrix}; \mathbf{l}_{0\varphi} = \frac{1}{2}\begin{pmatrix} (r_1 + r_2)\cos\varphi \\ z_1 + z_2 \end{pmatrix}$; $l = \sqrt{(r_2 - r_1)^2 + (z_2 - z_1)^2}$; $l_1 = \sqrt{r_1^{\,2} + z_1^{\,2}}$; $l_0 = \sqrt{r_0^{\,2} + z_0^{\,2}}$.

Obtained system of linear equations (6) is solved by iterative Seidel method.

Obtained forms of cavitation bubble walls (by equations (1-5) at the collapse in different moments of time are shown in Fig. 3. The initial moment of time (0 μs) is the moment of the maximum bubble expansion.

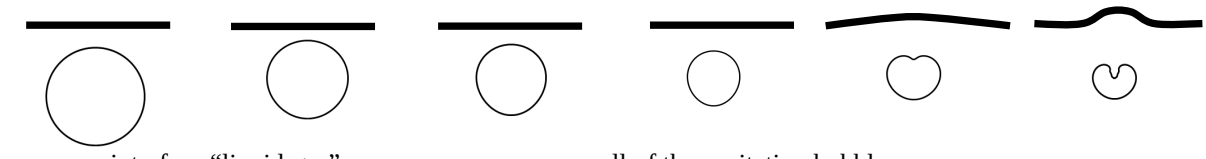

– interface "liquid-gas"; ——— – wall of the cavitation bubble

a) 0 μs b) 0,38 μs c) 0,75 μs d) 1,13 μs e) 1,24 μs f) 1,35 μs

Fig. 3. Evolution of the form of asymmetrically collapsing cavitation bubble in the course of time at different initial distances (at the moment of maximum expansion) between its center and solid surface

As it is shown in Fig. 3, cavitation bubble is a hemispherical radiator of shock wave.

At the study of *the stages of generation and propagation of shock wave* it allows approximating its pressure profile at different distances from the bubble by the following obtained expression (12).

$$p(\mathbf{r},t) = \sum_{n=-\infty}^{\infty} \frac{\omega a^2}{2\pi\sqrt{r^2+z^2}} \operatorname{Re}\int_0^{\frac{\pi}{2}}\int_0^{\frac{2\pi}{\omega}} \left[p_c(t_1)\sin\psi \times e^{in\frac{\omega}{c}\left(c(t-t_1)+\sqrt{r^2+z^2}-\frac{\eta n\omega}{2\rho c^2}+\frac{za\cos\psi}{\sqrt{r^2+z^2}}\right)} J_0\left(n\frac{\omega r a\sin\psi}{c\sqrt{r^2+z^2}}\right)\partial t_1 \partial\psi \right]; \quad (12)$$

where (r; z) are the coordinates of the points, m; ω is the circular vibration frequency of solid surface, s^{-1}; t and t_1 are the moments of time, s; η is the viscosity of liquid, Pa·s; ρ and c is the velocity of sound in liquid, m/s; $p_c(t_1)$ is the pressure in the nucleus of the cavitation bubble, Pa; a is the radius of the cavitation bubble at maximum pressure in the nucleus, m.

The function of shock wave pressure in the nucleus of the cavitation bubble $p_c(t_1)$ being a part of the expression (12) is defined as:

$$p_c(t_1) = p_V\left(\frac{4\pi R_{MAX}^{\,3}}{3V}\right)^{\gamma};$$

p_V is pressure of saturated liquid vapor; R_{MAX} is bubble radius at maximum expansion; V is bubble volume at time t_1; γ is a adiabatic index of gas.

Given profile of shock wave pressure is used further for the definition of capillary wave form and finally interphase boundary area.

The form of the capillary wave is defined from the expression (13):

$$\xi(r,t) = -\frac{1}{\rho}\int_0^t\int_0^{t_2}\frac{\partial p}{\partial z}\partial t_1 \partial t_2 \quad (13)$$

where $\xi(r,t)$ is the value of displacement of the interface "liquid-gas" along the axis z.

Thus mathematical description presented above allows determining the profile of single capillary wave generated by separate bubble.

However at the realization of the technological process it is impossible to obtain separate bubble that is

why it is necessary to consider the interaction between the aggregate of cavitation bubbles and the interface generating set of capillary waves.

The specific area of the interface "liquid-gas" per unit volume of liquid phase at the generation of the set of capillary waves is defined by the expression:

$$S = 2\pi\langle n\rangle \int_0^{0,5\lambda} r\sqrt{1+\left(\frac{\partial\xi}{\partial r}\right)^2}\,\partial r + \frac{1}{h}$$

where S is the specific area of the interface, m^2/m^3; λ is the length of the capillary wave (m) defined from the condition $\frac{\partial\xi}{\partial r}\left(\frac{\lambda}{2},t\right)=0$.; *n* is the concentration of cavitation bubbles, m^{-3}; < > is sign of averaging by liquid film thickness; *h* is thickness of liquid film, m.

The term $2\pi\langle n\rangle \int_0^{0,5\lambda} r\sqrt{1+\left(\frac{\partial\xi}{\partial r}\right)^2}\,\partial r$ characterizes a shock wave energy being generated at bubble collapse.

For the concentration of cavitation bubbles kinetic equation (14) obtained from Smolukhovskiy's equation [9] for the processes of coalescence and breakage of disperse particles (liquid drops, gas and solid particles) is true [10]:

$$\frac{\partial n}{\partial t} = \frac{n(j-1)}{iT_0} - k_B n^2 \qquad (14)$$

where *n* is the calculating concentration of cavitation bubbles depending on time *t*, m^{-3}, *i* is the average number of cavitation bubble pulsation before its collapse, k_B is the constant of coalescence rate of the bubbles, m^3/s, T_0 is the period of ultrasonic vibrations, s, *j* is the mean amount of the nuclei generated at the breakage of the separate bubble.

By solving the equation (14) following analytic expression is obtained:

$$n = \frac{n_\infty n_0}{n_0 + (n_\infty - n_0)e^{-n_\infty k_B t}}; \qquad (15)$$

where n_0 is the initial unknown concentration of cavitation bubbles, m^{-3}, n_∞ is the stationary concentration of cavitation bubbles, m^{-3}.

According to the expression (15) the concentration of the bubbles *n* in time, which equals tens periods of ultrasonic vibrations, achieves stable value and equals to n_∞, which is defined by the expression (16):

$$n_\infty = \frac{j-1}{ik_B T_0}; \qquad (16)$$

Variable *j* being in expression for stable concentration (16) is calculated from experimental data given in Rozenberg's book [3].

The constant of coalescence is defined as follows:

$$k_B = \frac{S_{eff}\langle u\rangle}{2}$$

where S_{eff} is square of effective bubbles collision's cross-section which is proportional to R_{MAX}^2, m^2; <u> is approach velocity of the cavitation bubbles, m/s.

To define approach velocity of the cavitation bubbles <*u*> the model of bubble interaction caused by the forces of the second order is used.The interaction model is based on the 2nd Newton's Law for the separate cavitation bubble taking into consideration Bjerknes force acting from the neighbor bubbles and caused by radial vibrations of the last ones. According to this model the position of the center of each cavitation bubble making the ensemble can be described by the following equation [10]:

$$\frac{4\pi R_{0i}^{\ 3}}{3}\rho_G\frac{\partial^2\mathbf{r}_i}{\partial t^2}=\frac{4\pi R_i^{\ 3}}{3}\rho_L\frac{\partial\mathbf{v}_L}{\partial t}(\mathbf{r}_i,t)+\sum_{j=1,n,j\neq i}\frac{4\pi R_i^{\ 3}}{3|\mathbf{d}_{ij}|^3}\rho_L\frac{\partial\left(R_j^{\ 2}\frac{\partial R_j}{\partial t}\right)}{\partial t}\mathbf{d}_{ij}+ \quad ; \quad (17)$$

$$+\frac{1}{2}\frac{\partial}{\partial t}\left(\frac{4\pi R_i^{\ 3}}{3}\rho_L\left(\mathbf{v}_L(\mathbf{r}_i,t)-\frac{\partial\mathbf{r}_i}{\partial t}\right)\right)+4\pi\eta R_i\left(\mathbf{v}_L(\mathbf{r}_i,t)-\frac{\partial\mathbf{r}_i}{\partial t}\right)$$

where i is the ordinal number of the bubble in zone of liquid phase; R_i is the instantaneous radius of i-th bubble, m; c is the local velocity of sound in liquid phase, m/s; p_{wi} is the gas pressure near the walls of i-th bubble, Pa; p is the instantaneous value of pressure of liquid phase without cavitation bubbles, Pa; ρ_L is the density of liquid phase, kg/m^3; v_L is the instantaneous vibrational speed of liquid phase without cavitation bubbles, m/s; R_{0i} is the radius of i-th bubble nucleus, m; ρ_G is the equilibrium density of gas inside the bubble, kg/m^3; t is the time, s; η is the viscosity of liquid phase, Pa·s; $\mathbf{r}_i$ is the coordinate vector of the center of i- bubble, м; $\mathbf{d}_{ij}=\mathbf{r}_j-\mathbf{r}_i$ is the vector of center line of i-th and j-th bubbles couple, m.

On the base of the results of equation solution (17) approach velocity of cavitation bubbles is defined by the following expression:

$$\langle u\rangle=\frac{|\mathbf{d}_{12}(T_0)-\mathbf{d}_{12}(0)|}{T_0}.$$

Thus proposed model allows defining dependence surface area of interphase boundary on the modes of ultrasonic action (frequency and vibration amplitude of solid surface covered with liquid film, which borders on gas phase) and liquid properties.

III. RESULTS AND DISCUSSION

Obtained dependences of relative increase of the interface area on the modes of ultrasonic action are shown in Fig. 4.Relative increase K of interface area is the ratio of the interface area upon ultrasonic action (S_{US}) to the area without ultrasonic action ($S_{\text{without US}}$):

$$K=\frac{S_{US}}{S_{Without\ US}}$$

Fig. 4 shows the breakage of the graph corresponds to the fact, that capillary wave loses its stability and breaks into drops [11]. The dependence of frequency (Fig 4b) is built up at threshold amplitudes, when capillary wave remains stable.

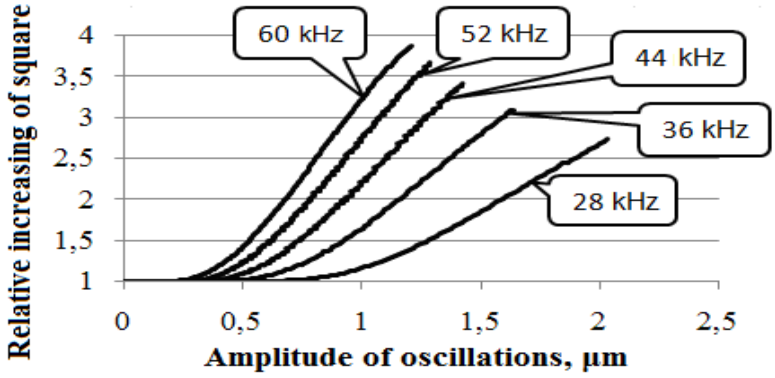

a)

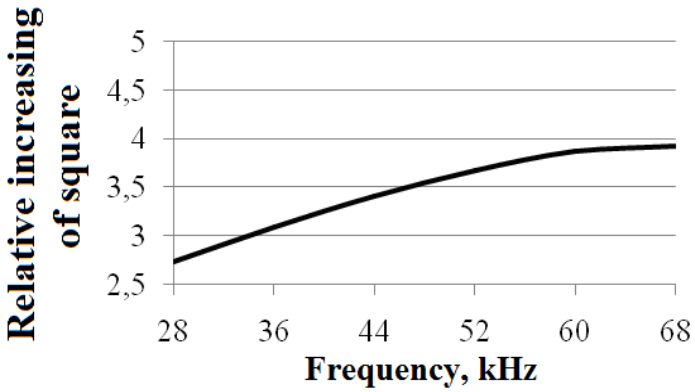

b)

Fig. 4. Dependences of specific area of the interface on the modes of ultrasonic action: (a) on amplitude at different frequencies; (b) on frequency at maximum amplitude

From presented dependences it is evident, that with the increase of amplitude interface area grows. If frequency rises, surface area grows (up to more than 3 times) due to the increase of cavitation bubble concentration [3]. However starting with the frequency of 60 kHz the growth of the area essentially becomes slower, and energy loss of the ultrasonic radiator increases quadratically. That is why; the application of frequencies of more than 60 kHz is unpractical. Fig. 5 shows the dependence of threshold vibration amplitude, at which capillary wave remains stable, on the frequency of action.

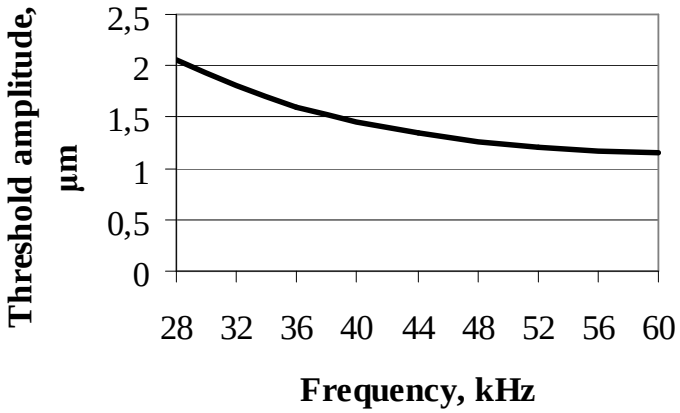

Fig. 5. Dependence of threshold amplitude, at which capillary wave remains stable, on the frequency of action

According to presented dependence the asymptotic amplitude reduces with the rise of frequency. In particular at the frequency of 28 kHz the threshold amplitude exceeds 2 μm, and at the frequency of 60 kHz it is 1…1.2 μm. Fig. 6 shows the dependences of specific interface area on amplitude at the change of physical properties of liquid – viscosity (a) and surface tension (b), which influence on the profile of contact surface together with the modes of ultrasonic action.

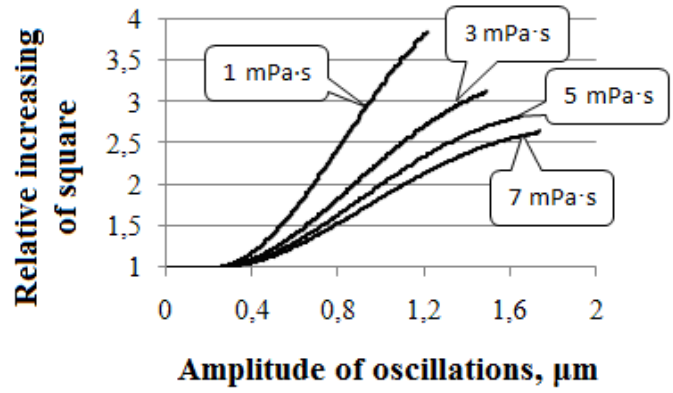

a)

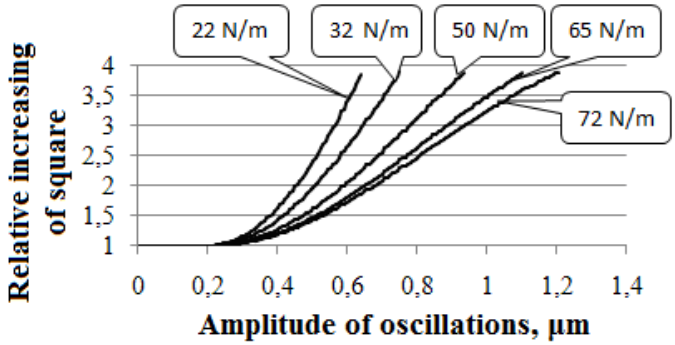

b)

Fig. 6. Dependence of specific area of interphase boundary on amplitude at different properties of liquid (frequency of 60 kHz): viscosity (a) and surface tension (b)

Presented dependences (Fig. 6) can be used for the determination of the area change caused by change of the liquid type and change of its properties. In particular it is stated, that growth of viscosity leads to the decrease specific area of the interface. It is caused by the absorption of energy of shock waves in liquid phase due to forces of viscous friction. At that decrease of surface tension leads to the growth of the area, as surface energy of a liquid directly depends on its surface tension.

IV. CONCLUSION

Thus model of the interaction of cavitation zone generated under the action of ultrasonic vibrations with interface of gas and liquid phases is developed. It is shown, that this interaction leads to the generation of capillary wave and consequently to the growth of surface of phase con-tact. Analysis of the model allows determining the modes of ultrasonic action, which are necessary for maximum increase of interphase boundary area. As a result of the analysis we determine threshold vibration amplitudes of solid surface covered with thin film of liquid phase, which excess leads to stability failure of capillary waves and their breakage into liquid drops. It is shown, that the most appropriate frequency of ultrasonic vibrations is 60 kHz, at which more than 3 times increase of contact surface. Obtained new scientific results have fundamental interest for the understanding of physical mechanism of the interaction of cavitation bubbles with the interface “liquid-gas”. They can be used for the practical realization of physic-chemical processes at the boundary “liquid-gas” (absorption, drying, evaporation, etc.). In particular ultrasonic action in the packed absorbers lets applying in more than 3 times less number of the nozzles at the same productivity of absorption.

V. ACKNOWLEDGEMENTS

The reported study was supported by RFBR. Research Project No. 14-08-31716 mol_a.

REFERENCES

[1] L.D. Rozenberg, *Physical principles of ultrasonic technology* (Moscow, RU: Science, 1969). In Russian.

[2] V.N. Khmelev, R.N. Golykh, S.S. Khmelev, R.V. Barsukov, Method for Calculation of Optimum Intensity of Cavitation Influence on Viscous and Fine-dispersed Liquid Media, *Proc. 12th International Conference and Seminar on Micro / Nanotechnologies and Electron Devices, EDM'2011*, Novosibirsk, RU, 2011, 245-250.

[3] L.D. Rozenberg, *Powerful ultrasonic fields* (Moscow, RU: Science, 1968). In Russian.

[4] G. Flynn, *Physics of acoustic cavitation in liquids* (Physical acoustics, vol. 1, 1967. In Russian.

[5] V.K. Kedrinsky, *Hydrodynamics of explosion. Experiment and models* (Novosibrisk, RU: Publisher of SB RAS, 2000). In Russian.

[6] Edited by G.M. Ostrovsky, *New handbook for chemist and technologist. Part I* (Saint Petersburg, RU: Publisher "Professional", 2004). In Russian.

[7] H. Ishida, C. Nuntadusit, H. Kimoto, T. Nakagawa, T. Yamamoto, Cavitation bubble behaviour near solid boundaries, *Proc. Fourth International Symposium on Cavitation*, California Institute of Technology, US, 2001.

[8] V.V. Rozhdestvensky, *Cavitation* (Leningrad, RU: Shipbuilding, 1977). In Russian.

[9] C. Sheng, X. Shen, Modelling of acoustic agglomeration processes using the direct simulation Monte Carlo method, *Journal of Aerosol Science*, 37, 1, 2006, 16-36.

[10] M.A. Margulis, I.M. Margulis, Dynamics of bubbles ensemble in cavitating liquid, *Physical chemistry journal*, vol. 81, 12, 2007, 2290-2295. In Russian.

[11] V.N. Khmelev, R.N. Golykh, A.V .Shalunov, A.V. Shalunova, D.V. Genne, Revelation of optimum modes of ultrasonic influence for atomization of viscous liquids by mathematical modeling, *Proc. 13th International Conference and Seminar on Micro / Nanotechnologies and Electron Devices, EDM'2012*, Novosibirsk, RU, 2012, 114-123.

American Journal of Engineering Research (AJER)
e-ISSN : 2320-0847 p-ISSN : 2320-0936
Volume-03, Issue-12, pp-150-154
www.ajer.org

Research Paper Open Access

Iron ore Development and supplies from Third world: A Potential for Sustainable Development.

Abdurrauf A. Ibrahim, Murtala A. Garba and Hussaini Abdulkareem
Department of Mechanical Engineering, Kaduna Polytechnic, Kaduna, Nigeria.

ABSTRACT: *This paper discuss the qualitative leaching of iron ore in hydrochloric acid and multi gravity separation method as new strategies for reducing lost of iron during production. The focus of the paper is on the potential of iron ore development and supplies from Third world for Sustainable Development and to enter and sustain in the export global competitive Market..*

KEY WORDS*: Sustainable Development, Iron ore, Potential, Strategies.*

I. INTRDUCTION:

The occurrence of mineral resources in commercial quantities alone does not however guarantee optimum benefit, factors such as technological capacity, finance and market are also equally important. Nigeria for example is blessed with abundant mineral resources and human resources capable of tapping these resources for industrial growth, however, what is witnessed today is that most of the mineral development, especially the exploitation is done by informal and in most cases illegal miners using very crude techniques with no consideration for the environment or human health. The Ministry of Mines and Steel Development has identified, and is promoting the development of 34 mineral resources in Nigeria which include iron ore, gold, coal, tantalite, bitumen, limestone, barite, gypsum, kaolin etc. Some Third world countries are endowed with enormous mineral resources which when properly harnessed can lead to industrial development and prospects. It is a known fact that countries abundantly endowed with mineral resources become great industrial nations [1]. While on the other hand, the level of greatness of a nation is often a reflection of how its resources have been planned, managed and utilized [2] The importance of mineral development of any nation cannot be overemphasized as it is one of the sources of industrial raw material supply, what must however, be emphasized is the manner in which the resources are developed. Iron ore deposits have been found in various locations in Nigeria, but mainly in the north-central, north-east and south-east regions. Iron ore deposits in Nigeria typically occur in the following forms: hematite, magnetite, metasedimentary, bands of ferruginos quartzites, sedimentary ores, limonite, maghemite, goethite and siderite. [3]
Below are some of the notable iron ore deposited in central Nigeria.

S/N	Deposit Area	Estimated Reserves (million tones)
1	Itakpe	310
2	Ajabanoko	60
3	Agbado-okudu	60
4	Tajimi	20
5	Anomaly K-3	30
6	Anomaly K-2	20
7	Ochokochoko	12
8	Agbaja	370.5

The most notable iron ore occurrence in this region include Itakpe,Ajabanoko, Ochokochko, Tajimi, Agbado-Okudu, Ebiya, Ero, Echakaraku, Ozenyi, Udiarehu and some others. They occur as bands and lenses of banded (and sometimes massive) iron formation dipping between 21 and 85 and mostly conformable to the host rocks (gneisses and amphibolities). The tabular ore bodies, up to 45m thick, and extending for distances from hundreds of meters to over 5km, are developed to a depth of over 300m, and are often displaced by small to large faults, The ore are mostly magnetite and/or hematite with quartz, biotite and amphiboles in the groundmass, iron content ranges between 15% and 65%, averaging 30-36.

(i) Rich ores with more than 50% Fe, and constitutes about 4.5% of the total reserves.
(ii) Medium grade ores, with 30-50% Fe, and constitutes about 85.4% of the reserve.
(iii) Lean ore, with 25-30% Fe, which constitutes 13.1% of the reserve.

The numerous occurrence of banded iron formation associated with the metasediments of the schist belt areas occur sporadically in minor bands and lenses These locations extend from Tsofon Birni Gwari -Farinruwa to south of Birni goga, and west of Kaura-Namoda, Baraba hills , 5km west of Maru, Koriga river, kalangai and Jamare areas. Magnetite and hematite are the major ore constituents in variable percentages. Average ore grade is usually between 38.9 -57.4% Fe2 03 . Three occurrences of iron bodies at Oko, Gbede, Ajashe have been mapped around Ogbomosho area as narrow lenses and bands. They are mostly hematite, magnetite iron formation with an Fe grade of 34.4% at Oko, 42.7% at Gbege and 39.0% at Ajashe. They are extensively laterally enough to attract detailed economic evaluation. Although the thickness of occurrence have not yet been ascertained.

II. EMERGING INVESTMENT OPPORTUNITIES

While the Itakpe iron ore deposits are being mined as raw material feeds for Ajaokuta smelting facilities, opportunities for investment in the iron ore resources of Nigeria exist for the deposits in the Northwestern and Southwestern Nigeria. Investors are invited to explore the possibilities of either wholly owning the mineral titles or partnering with existing title holders in exploiting the resources for economic development of Nigeria. Investment opportunities abound in the following areas:

1. Applying for mineral titles with a view of wholly owning the mining rights for the iron deposit
2. Partnering with existing title holders for detailed exploration as consultants and specialists
3. Partnering with existing title holders in joint venture agreement to explore, mine and market the iron ore resources of areas of interest [4]
4. Legal transaction in iron ore won in quarries and operations for export.

III. IRON ORE WORLD TRADE

Developing countries accounted for 57.7 % of world iron ore production (down from 58.6 % in 2010), the CIS countries for 10.6 % (slightly down from last year) and the industrialized economies for almost 31.7 %. The decrease in the share of the developing countries was due mainly to growth of production in Australia - up over 55 Mt. Chinese production, on a comparable grade basis, was 321.9 Mt, or 16.6 % of total world production in 2011, down from 17.3 % in 2010 but below the top level of 20 % in 2007. In more general terms, for the long run, Australia and Brazil will be the dominating forces in iron ore production. India, which has large and good quality resources of iron ore, will be hampered by red tape and an on-going internal struggle of use. Over time, as the Indian steel industry grows, most of the iron ore will be used domestically. We also foresee a slow decline in Chinese output. If prices fall, it will decline more rapidly and a major “Great Chinese shake-out” will begin. In 2011, international iron ore trade reached a new record level as exports increased for the tenth year in a row and reached 1117.0 Mt, up 6.7 %. The increase was the result of higher demand from mainly China while most other countries in the world had trade levels similar to the year before and most of them have not reached their import levels of 2008. These figures include all export trade including intra-CIS trade, while re-exports figures have been deleted as far as possible. World total iron ore exports have increased by 109.7 % since 2002. Developing countries accounted for 49.0 % of total in 2011, and their exports have grown by 100.2 % since 2002. Developed countries accounted for 51 %, including CIS republics (with about 6.6 % of total world exports). Australia’s exports increased by 8.9 % to 438.8 Mt in 2011 compared to 2010. With important markets in Europe and the Americas picking up pace, Brazilian exports, which fell sharply in 2009, had definitely turned around by 2011 with an increase of 12.1 % in 2011, compared to 2010, up to 348.6 Mt up from 310.9 Mt. Exports from India fell for the second consecutive year, 2010 was the first time in twelve years with falling exports but the country, at its 78.4 Mt down 18.2 % from 95.9 Mt, is still the third most important exporter.

In 2011 the Ukraine, Kazakhstan and Russian Federation increased their exports. China has become an important market for all three countries. Transport capacity has been a limiting factor for further expansion.
In 2003, China outstripped Japan to become the world's largest iron ore importer. In 2011, its imports were 686.7 Mt, an increase by 11.0 % compared to 2010. In 2010, China accounted for almost 59 % of total wor1ld imports. In 2011, this figure had increased to 61.5 %. Almost everywhere else, imports fell: in Japan by 4.4 % to 128.4 Mt, and in the Republic of Korea by 15.3 % to 64.9 Mt. European imports (excluding the CIS countries), decreased by 1.4 %, reaching 132.1 Mt down from 133.9 Mt and corresponding to just under 12 % of world imports. In Europe, Germany, France, Italy and the United Kingdom are the largest importers. Though these countries were hit by the crisis in 2009 with falling imports, all four have saw increases in 2010. However imports in Europe have fallen in 2011 for all countries except Italy, and are still lower than 2008 levels. As a group, developing countries accounted for almost 68.1 % of total iron ore imports in 2011 (66 % in 2010). Due to a strong growth in imports of China, the developing world's share of total imports increased from only 31 % in 2002 to 46 % in 2005, 50 % in 2006 and 55 % in 2008. The CIS republics do not yet import iron ore from outside the CIS, and their internal trade in 2011 was only 1.2 % of the world total. Developed economy countries accounted for about 30.7 % of world imports in 2011.

Challenges of Mining Industry
The major challenges faced by the industry can be categorized into the following heads:
• **Project funding**

Due to the long period of inactivity and the slow implementation of the Federal Government's reform agenda in the sector, multinational corporations have been reluctant to fund major mining projects in the country. However, the progress made in the regulatory reform, so far, is expected to stimulate activities by new investors in the sector.

• **Infrastructure development**

A major challenge to the development of the sector is the infrastructural imbalance within a country, particularly, adequate electricity supply, and access roads to sites of mineral deposits.
However, the ongoing privatization of the national utility and reform of the power sector started in 2005 are stimuli for private investment in the sector. As capacity increases with new investments in the generation, transmission and distribution sectors, the shortages currently being experienced will be overcome. Meanwhile, mining investors can meet their power needs by engaging independent power producers for captive generation and supply of energy to the mines. Furthermore, access roads will ultimately improve with ongoing investments by the Federal and State Governments in road infrastructure. The ongoing rehabilitation of the rail lines will also facilitate product evacuation across the country for export. [4]

• **Security**

Militancy and insurgency in Developing countries has pose a threat to communities where mining ndustries are located, Security concerns are of the magnitude that discourage investors in some third world countries mining sector. However, investors are well advised to have a robust corporate social responsibility programme to address the needs of their host communities. Therefore Government security agencies should be equipped to respond appropriately to social conflicts as and when they arise.

• Illegal mining and community challenges

There are pockets of Illegal mining activities in some of the regions, with the attendant risks and community challenges. However, with the enactment of the Mining Act, foreign investors with the necessary permits and licenses are guaranteed unfettered operation of their legitimate business in the country.

IV. METHODS OF OBTAINING HIGHER PERCENTAGE OF IRON FROM IT'S ORE

(1) **Quantitative Leaching of Iron Ore in Hydrochloric Acid**

Metallurgy of iron is a process of extracting iron from ores and preparing it for use. These extraction and preparation processes involve the conversion of naturally occurring iron-bearing minerals into metallic iron. The major process for the production of iron is the smelting process in blast furnace. It entails two major procedures: ore preparation and reduction of oxide concentrates, and the overall reaction for the reduction of say hematite to metallic iron with carbon monoxide is:

$$\tfrac{1}{2}\ Fe2O3(s) + \tfrac{3}{2}\ CO(g) \rightarrow Fe(s) + \tfrac{3}{2}\ CO2(g) \quad (1)$$

Iron may be efficiently extracted from its principal ores with hot conc. HCl, but not with conc. H2SO4 or

HNO3. The efficiency of HCl extraction is ascribed to the formation of ferric chloride complexes (Encycl. Sc. & Tech., 1997). Ore also contain Si and SiO2 and silicates. Iron may be extracted from some kinds of silicates, rovided that the sample is finely ground, but the process is slow. SnCl2 increases the rate of extraction by reducing Fe(III) to Fe(II), and is particularly effective for haematites and magnetites [7]. The kinetics of dissolution of sulphidic inerals or the related form in chloride media has received considerable attention recently. There are several justifications for this interest. Among them is the ability of materials of construction with improved resistance to chloride attack. More importantly, however, are the substantially faster dissolution rates exhibited by most sulfides in chloride media and the potential application of such electrolytes in the treatment of complex sulphide [8]. They reported and proposed results of the overall leaching reaction which are consistent with the following stoichiometry [9],relating to pressure oxidation of the base metal sulphides:

Chalcophyrite: $CuFeS2 + 2HsSO4 + O2 \rightarrow CuSO4 + 2S0 + H2O$ (2)

Pyrite: $FeS2 + H2SO4 + ½O2 \rightarrow FeSO4 + S0 + H2O$ (3)

Furthermore, the leaching of the iron-ore in different media has been studied by many investigators [10]. To the best of our knowledge, there is no reported works viz a viz the quantitative leaching of a Nigerian iron ore. Therefore, this strategy has provided data on the quantitative leaching and the kinetics of dissolution behavior of the iron ore in hydrochloric acid solutions. This strategy is interesting from the industrial perspective, as it could provide optimum conditions for the commercial production of ferric chloride from the indigenous iron ore [5]. Ferric chloride is an important material for water and industrial liquid effluents treatment [11].

(2) **The Multi Gravity Separator Method**

The Multi Gravity Separator (MGS) is reported to be promising equipment for the separation of particles in fine size range. The MGS is suitable for the treatment of fines with a maximum particle size of approximately 0.5 mm. Maximum concentrate grade and maximum recovery is of today's demand with MGS concentration as it is with many concentration processes [12]. The equipment is based on a concept developed by M/s Richard Mozley Limited, U.K. [13]. The principle of MGS may be visualized by rolling the horizontal surface of a conventional shaking table into a drum and rotating the same along the horizontal axis. This causes application of an enhanced gravitational force, many fold higher than the normal one, on the mineral particle flowing across the surface. This leads to improvement in the treatment of fine particles in comparison to conventional separator like shaking table. Conventional gravity separation process of iron mineral fines is not very effective. In present work Multi Gravity Separation (MGS) process has been studied. This study was performed on a low-grade iron ore namely goethiticlateritic ore (GLO) from Eastern India. Detailed mineralogical, physical and chemical characteristics of a goethiticlateritic iron ore showed that the sample contained porous and friable oxides and hydroxides of iron. The ore sample had a feed grade of 54.43% total Fe, 9.27% SiO2 and 8.02% Al2O3. Hematite and goethite are main iron-bearing minerals while kaolinite and gibbsite are the major gangue mineral constituents. Considering the characterization data, these ores were ground separately to three size fractions, namely -300 µm, -250 µm and -150 µm sizes and subjected to flowing film concentration in Wilfley Table. As revealed by the liberation study, higher concentration was obtained by the processing of -150 µm crushed sample. The grade of the ore was improved from 54.43% Fe to 65.71% Fe. However, significant amount of fine iron ore particles were lost during the processing of -150 µm size ore, because it is not very effective for particles less than 15 µm. Thus, fine hematite and goethite particles are usually not recovered resulting in the loss of valuable iron ore fines. To recover this fine, Multi Gravity Separator was used in place of Wilfley Table and was found to be effective in reducing loss of fine iron particles and increasing the grade of the concentrate.[6] The MGS process improved the Fe from 54.43% to 66.5% along with decreasing the alumina from 8.02% to1.17%..

IV. CONCLUSION

Some Developing Countries are well endowed with metallic minerals which include iron ore, However the minerals are not fully harnessed for industrial development, also the mineral development is so slow because of inadequate funding and also lack of awareness on the importance of the minerals in industrial development. If this trend continues then there is little hope of fully harnessing the mineral resources fully for industrial and technological development. This paper has discussed the possibility of Developing countries to produce up to 80% of world iron if the strategies of obtaining pure iron are well applied.

REFERENCES:

[1] Okpanachi, U.M.(2004).*The Economics of the Solid Minerals Market*. Paper presented at the Nigeria Shippers Council seminar on "Solid Mineral Exploration and Exploitation", Jos, Nigeria, 22nd July, 2004

[2] Gotan, B.J (2004). *Solid Minerals Exploration in Plateau State(Legislation, Difficulties and Framework Involved)*. A paper presented at a Seminar by the Nigeria Shippers Council, Jos, Nigeria, 22nd July, 2004.

[3] KPMG)February 2012,The Nigerian mining Sector.

[4] Ministry of Mines and Steel Development

[5] ALAFARA, A. BABA; ADEKOLA, F A; FOLASHADE, A O(2005) *Department of Chemistry, University of Ilorin*

[6] Subrata Roy(*2005)MNP Division, National Metallurgical Laboratory, Jamshedpur 831 007, India*

[7] Blaede, W.J. and Meloche, V.M. (1985) Elementary Quantitative Analysis. John Willey & Sons,London, 2nd Ed., pp. 104 – 111.

[8] Zuo-Mei Jin, Warren W. and Henein, H. (1984)Metall. Trans. B.Vol. 15B, pp 5 – 12.

[9] Harvey, T.J. and Yen, W.T (1998) Minerals Engineering vol. II part 1, pp. 1 – 21.

[10 DHugues, P., Foucher, S., Galle-Cavalloni, P. and Morin D. (2002) Minerals Engineering vol.66 part 1, pp 131 – 139]

[11] Morris, J.C. (1990) Advanced Waste Water Treatment manual IHE, Delft, Netherlands, pp.3

[12] N. Aslan, "Multi-objective optimization of some process parameters of a multi-gravity separator for chromite concentration", *Separation and Purification Technology*, vol. 64, pp. 237-241, 2008.

[13] B. S. K. Chan, R.H. Mozley, and G.T.C. Childs, "The Multigravity separator (MGS),- A mine scale machine", in *Mineral Processing in the United Kingdom*, London, P.A. Dowd Ed., London: IIM Publishers., 1989, p.107.

American Journal of Engineering Research (AJER)
e-ISSN : 2320-0847 p-ISSN : 2320-0936
Volume-03, Issue-12, pp-155-159
www.ajer.org
Research Paper Open Access

Based on Preventive Maintenance Strategy Analysis cold standby system reliability optimization design

CHEN YanLi

(Yinchuan Energy Institute , 750105, China)

Fund: Fund research of Yinchuan Energy Institute (2012-KY-P-31)

ABSTRACT: *In order to make the system meeting the two requirements: (1) the designed system have maximize reliability;(2) the designed system have a lowest cost. In this paper, we use the methods of linear programming and Lagrange multiplier method, in view of the above two requirements, we discuss the optimization scheme which is reliability of the system.*

KEYWORDS: *Preventive maintenance, cold standby systems, reliability, optimal design*

I. INTRODUCTION

We considered the cold redundant system, which was composited by two same type components and a repair equipment. the distribution of parts is general distributed distribution whose averages is $1/\lambda$ .After malfunction, the time obeys the general distributed, which is from average μ_1 .

We considered the cold redundant system, which was composited by two same type components and a repair equipment. the distribution of parts is general distributed distribution whose averages is $1/\lambda$ .After malfunction, the time obeys the general distributed, which is from average μ_1 .

Assumption：(1) moment t_0 , the parts is working. The other part is cold redundant. When working parts happen malfunction, we repair it immediately, at the same time, supply parts begin to work.
(2) When the working time whose the working parts, reach the specified time, the parts have not yet been failure. The working parts are maintained preventive. Stocking parts switch to the working state. Parts of preventive maintenance time obey the general distribution $G_2(t)$, whose average is μ_2.
Because there is only one repairing equipment. When the age of working part reach the specified time, the part have not been failure. If the other part is malfunction repairing or preventive repairing, the working parts are not preventive maintenanced and repaired. It continue to work. If the parts which is repairing or preventive repair, have been repaired. Then it begin to work immediately. While the working part switch to prevent repair.
Until a component repair or preventive maintenance have completed. If the other is still working, and the working time is less than T , then the repair parts are reserved.
(3)Assume <1>All of the component can been repaired,<2> The switch is completely reliable, <3> instantaneous is completed instantaneously, <4> The life of two components, the time of repair, the time of preventive repair are independent of each other.
The definition of system state are as follows:
0: One of component is working, the other component is cold standby, component new.

1: One of component is working, the other component is repaired.
2: One of component is working, the other component is preventive repaired,
3: One of component is repaired or preventive repaired, working, the other component is waiting for repaired.

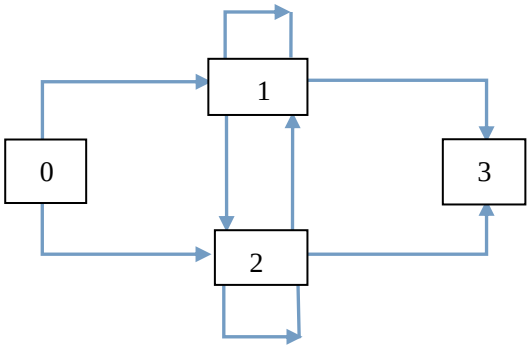

Fig. Because we consider the time before the fault only, so the fault state 3 is the absorbing state, the state transition diagram of figure 1:

Moment $X(t) = j$, if the time is t, the system status is j, $j = 0, 1, 2, 3$. $\{X(t), t \geq 0\}$ is a half Markov process, whose absorbing state is 3 state.

The Y_1 is repair time, the Y_2 is preventive maintenance time, and the specify time T is regarded as fixed-length random variables X_T .The distributed is $U(t) = P\{X(t) \leq t\} = \begin{cases} 0, t < T \\ 1, t \geq T \end{cases}$.

The semi Markov nuclear system is:

$$Q_{01}(t) = P\{X \leq t, X < X_T\} = \int_0^t \overline{U}(u) dF(u)$$

$$Q_{02}(t) = P\{X_T \leq t, X > X_T\} = \int_0^t \overline{F}(u) dU(u)$$

$$Q_{i1}(t) = P\{X \leq t, Y_i < X \leq X_T\} = \int_0^t G_i(u)\overline{U}(u) dF(u)$$

$$Q_{i2}(t) = P\{Y_i \leq t, X > Y_i > X_T\} + P\{X_T \leq t, Y_i \leq X_T < X\}$$

$$= \int_0^t \overline{F}(u) U(u)\, dG_i(u) + \int_0^t F(u) G_i(u) dU(u), i = 1, 2$$

$$Q_{i3}(t) = P\{X \leq t, Y_i > X\} = \int_0^t \overline{G}_i(u) dF(u), i = 1, 2$$

transform the above equations do Laplace-Stieltjes

$$\hat{Q}_{01}(s) = \int_0^T e^{-st} dF(t)$$

$$\hat{Q}_{02}(s) = e^{-st}\overline{F}(t)$$

$$\hat{Q}_{i1}(s) = \int_0^T e^{-st} G_i(t) dF(t) \qquad i = 1, 2$$

$$\hat{Q}_{i2}(s) = \int_T^\infty e^{-st} \overline{F}(t)\, dG_i(t) + e^{-st} \overline{F}(T)\, G_i(T) \qquad i = 1, 2$$

$$\hat{Q}_{i3}(s) = \int_0^\infty e^{-st} \overline{G}_i(t) dF(t) \qquad i = 1, 2$$

Let $\Phi_i(t)$ is 0 time, The system starts into the state distribution system MTTFF, r_j Is the mean,

j = 0, 1, 2. Markov updates the equation

$$\begin{cases} \Phi_0(t) = Q_{01}(t) * \Phi_1(t) + Q_{02}(t) * \Phi_2(t) \\ \Phi_i(t) = Q_{i3}(t) + Q_{i1}(t) * \Phi_1(t) + Q_{i2}(t) * \Phi_2(t), i = 1, 2 \end{cases} \quad (1)$$

transform the above equations do Laplace-Stieltjes

$$\begin{cases} \hat{Q}_0(s) = \hat{Q}_{01}(s) * \hat{\Phi}_1(s) + \hat{Q}_{02}(s) * \hat{\Phi}_2(s) \\ \hat{\Phi}_i(s) = \hat{Q}_{i3}(s) + \hat{Q}_{i1}(s) * \hat{\Phi}_{i1}(s) + \hat{Q}_{i2}(s) * \hat{\Phi}_2(s) \quad i = 1, 2 \end{cases} \quad (2)$$

slove $\Phi_0(s)$,

MTTFF is $r_i = -\frac{d}{ds}\hat{\Phi}_i(s)\Big|_{s=0}$

above（2）, About s derivation，and let $s = 0$

$$\begin{cases} r_0 = \hat{Q}_{01}(0) * r_1 + \hat{Q}_{02}(0) * r_2 + \varepsilon_0 \quad i = 1, 2 \\ r_i = \hat{Q}_{i1}(0) * r_1 + \hat{Q}_{i2}(0) * r_2 + \varepsilon_i \quad i = 1, 2 \end{cases} \quad (3)$$

$$\begin{cases} \varepsilon_0 = -[\hat{Q}_{01}'(0) + \hat{Q}_{02}'(0)] \quad i = 1, 2 \\ \varepsilon_i = -[\hat{Q}_{i1}'(0) + \hat{Q}_{i2}'(0) + \hat{Q}_{i3}'(0)] \quad i = 1, 2 \end{cases}$$

Model assumptions:

(1) assumes a life of two parts, repair and preventive maintenance time independent of time, followed a normal distribution.

(2) $C(\overline{X})$ represents the stress in the mean cost function of $\overline{X}$, $C(D_X)$ represents the stress variances D of the cost function of $\overline{Y}$.

(3) Let $C(\overline{Y})$ represents the mean intensity, $C(D_Y)$ represents the intensity of D_Y the variance of the cost function.

Due to the high intensity of the mean must rely on the use of fine materials, and in the process strictly control various processes and take appropriate measures to achieve, which is bound to increase the cost. So, $C(\overline{Y})$ is a monotonically increasing function of $\overline{Y}$.

From a reliability point of view, under symmetrical conditions require a lower variance, and therefore, $C(D_Y)$ is a monotone decreasing function of D_Y.

Here are two cases to discuss the reliability of the optimization problem:

1. at the level of reliability required, so that the total cost TC (Total Cost) minimum.

In this case, the constraint conditions $\frac{\overline{Y} - \overline{X}}{\sqrt{D_Y + D_X}} \geq z$: here set $z \geq 0$.

The objective function is: $\min \quad TC = C(\overline{X}) + C(D_X) + C(\overline{Y}) + C(D_Y)$

Application of Lagrange function

$$L(\overline{X}, D_X, \overline{Y}, D_Y, \lambda) = C(\overline{X}) + C(D_X) + C(\overline{Y}) + C(D_Y) + \lambda[\overline{Y} - \overline{X} - z(D_X + D_Y)^{1/2}]$$

For each variable were partial derivative, and make it equal to zero,

$$\left.\begin{aligned}
&\frac{\partial L}{\partial X} = \frac{\partial C(\overline{X})}{\partial \overline{X}} - \lambda = 0 \\
&\frac{\partial L}{\partial Y} = \frac{\partial C(\overline{Y})}{\partial \overline{Y}} + \lambda = 0 \\
&\frac{\partial L}{\partial D_X} = \frac{\partial C(D_X)}{\partial D_X} - \frac{\lambda z}{2}(D_X + D_Y)^{1/2} = 0 \\
&\frac{\partial L}{\partial D_Y} = \frac{\partial C(D_Y)}{\partial D_Y} - \frac{\lambda z}{2}(D_X + D_Y)^{1/2} = 0 \\
&\frac{\partial L}{\partial \lambda} = \overline{Y} - \overline{X} - z(D_X + D_Y)^{1/2} = 0
\end{aligned}\right\}$$

If all cost functions are convex, that there is a positive second derivative, the above optimization problem locally optimal solution that is global solution.

This can be used to solve the optimization problem of Mathematical software.

1. under the condition of constant total cost, reliability maximized.

Time constraints for: $C(\overline{X}) + C(D_X) + C(\overline{Y}) + C(D_Y) \le r$ (the total cost limit)

The objective function: $\max \quad z = (\overline{Y} - \overline{X})(D_Y + D_X)^{-1/2}$

Application of Lagrange function:

$$L(\overline{X}, D_X, \overline{Y}, D_Y, \lambda) = (\overline{Y} - \overline{X})(D_X + D_Y)^{-1/2} + \lambda[C(\overline{X}) + C(D_X) + C(\overline{Y}) + C(D_Y) - r]$$

For each variable were partial derivative, and make it equal to zero

$$\left.\begin{aligned}
&\frac{\partial L}{\partial X} = -(D_X + D_Y)^{-1/2} + \lambda \frac{\partial C(\overline{X})}{\partial \overline{X}} = 0 \\
&\frac{\partial L}{\partial Y} = -(D_X + D_Y)^{-1/2} + \lambda \frac{\partial C(\overline{Y})}{\partial \overline{Y}} = 0 \\
&\frac{\partial L}{\partial D_X} = -\frac{1}{2}(\overline{Y} - \overline{X})(D_X + D_Y)^{-3/2} + \lambda \frac{\partial C(D_X)}{\partial D_X} = 0 \\
&\frac{\partial L}{\partial D_Y} = -\frac{1}{2}(\overline{Y} - \overline{X})(D_X + D_Y)^{-3/2} + \lambda \frac{\partial C(D_Y)}{\partial D_Y} = 0 \\
&\frac{\partial L}{\partial \lambda} = C(\overline{X}) + C(D_X) + C(\overline{Y}) + C(D_Y) - r = 0
\end{aligned}\right\}$$

Under the conditions of $D_X / D_Y \ge 1/2$ local solution above optimization problem is a global optimal solution. Again, this can also be adopted to solve the optimization problem of Mathematical software.

REFERENCES:

[1] J. M. Kontoleon. Reliability Determination of a r-successive–out- of-n：F system. IEEE Trans. on Reliability,1980，29(3)：437-411.

[2] D. T. Chiang, S. C. Niu. Reliability of a Consecutive-k-out-of-n System. IEEE Trans on Reliability,1981. 30(1)：87-89.

[3] M. Lambiris, S. Papastavrisis. Exact Reliability Formula for Linear and Circular Consecutive-k-out-of-n：F System. IEEE Trans on Reliability,1985，34(2)：124-127.

[4] J.C. Sha. Recursive Algorithm on Evaluate the Reliability of Consecutive-k-out-of-n：F system. IEEE Trans n

Reliability,1982，31(4)：442-443.

[5] Y .Lam, Y．L．Zhang．Analysis of Repairable Consecutive-2-out -of-n：F Repairable System with Priority in Repair．International Journal of Systems Science，1999，30：799-809.

[6] Y. L．Zhang, M．J． Zuo, Y．Lam．Reliability Analysis for A Cir- cular Consecutive-2-out-of-n：F Repairable System with Priority in Repair. Reliability Engineering and System Safety,2000，68:113 -120.

[7] K．Cheng，Y．L．Zhang．Analysis for a Consecutive-k-out-of-n：F Repairable System with Priority in Repair．International Jour- nal of Systems Science, 2001，32：591-598.